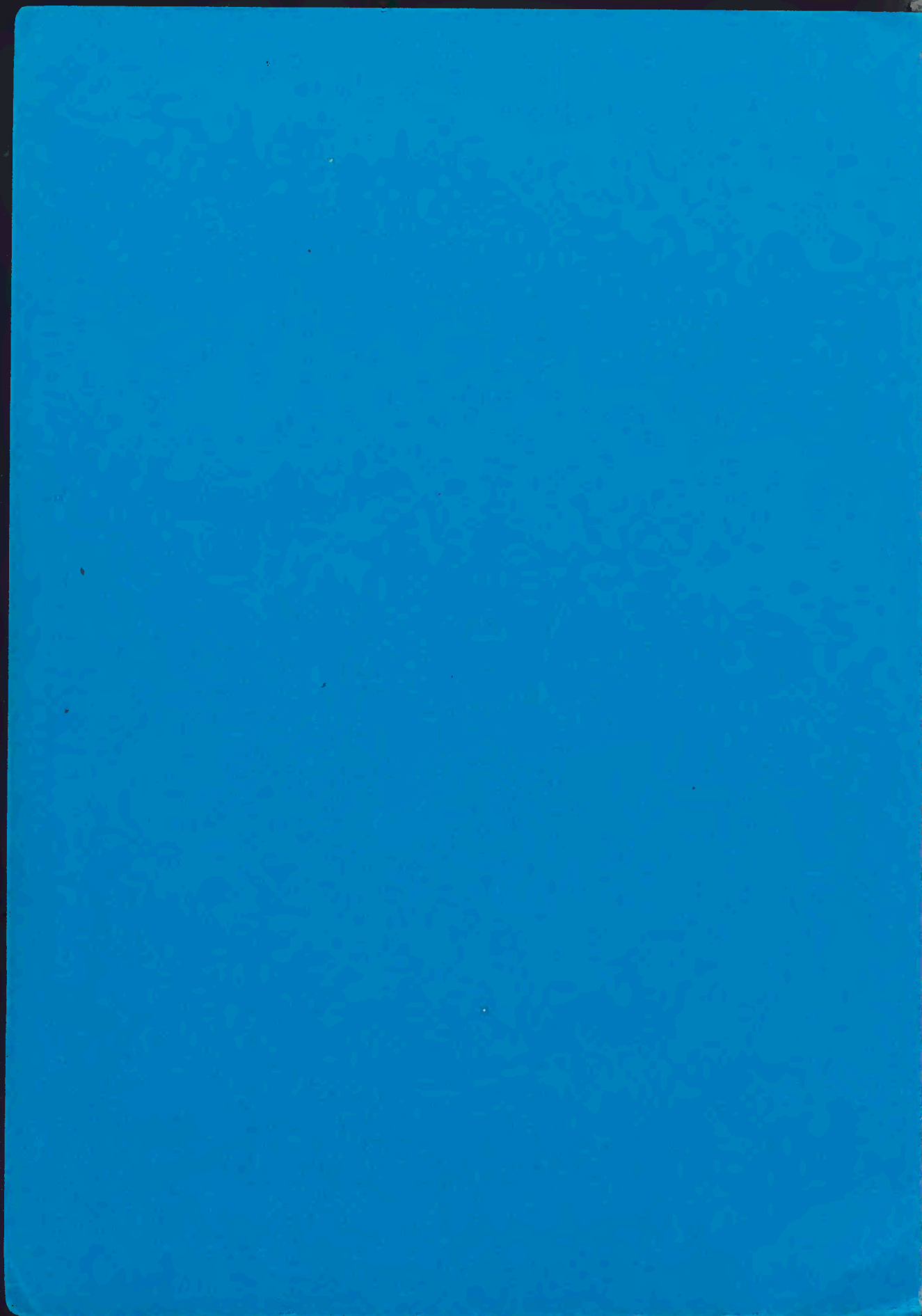


International conference on

**ELECTRIC FUSES
AND THEIR
APPLICATIONS**



Arvid Møller

International conference on

ELECTRIC FUSES AND THEIR APPLICATIONS

Wednesday 13, Thursday 14,
and Friday 15 June 1984

TRONDHEIM, NORWAY

Organisers:

EFI

The Norwegian Research
Institute of Electricity
Supply

NTH

The Technical University
of Norway, Electrical, Eng.
Dept., Power Section

CONTENTS

		page
1	Lipski, T. Review lecture: What next with the H.B.C. fuses?	1
2.	Howe, A.F. de Cogan, D. Webb, P.W. Nurse, N.P.M. Measuring the pre-arcing temperature of high-breaking-capacity fuselinks by thermal imaging	12
3	Wilkins, R. Simulation of fuselink temperature-rise tests	24
4	Rex, H-G. Calculations of models for adiabatic processes	34
5	Lipski, T. Application of the arc-pinch-forces-interaction theory to the calculation of striation modulus of the strip H.B.C. fuses	52
6	Hibner, J. The numbers of arcs initiated during striated disintegration of the uniform strip H.B.C. fuse-elements at A.C. short-circuit current interruption	60
7	Paukert, J. Electric conductivity of arc extinguishing media for low-voltage fuses	70
8	Arai, S. Kawano, Y. Recovery of dielectric strength of expulsion fuses after arc current zero	77
9	Naot, Y. How far is an insulated conductor protected by a fuse	87
10	Czucha, J. On the proper coordination of fuses with semiconductor devices in the heavy short-circuit region	95
11	Barbu, I. Considerations upon the analogy among electrothermal phenomena within fuses and their semiconductor protection	106
12	Jimei, W. Research on power-fuse coordinated with vacuum contactor	116
13	Ofte, A. Rondeel, W. The striker system in the fuse switch combination	124
14	Lindgren, S. Operating times at low short-circuit currents	134
15	Gyan-Son, C. The development of electric fuses in China	139
16	Krasuski, B. Lipski, T. Szymanski, E. Zwiazek, W. New line in the H.B.C. fuses development	143

		page
17	van der Scheer, D. Reith, H.F.J.	High voltage current limiting fuse-links capable of breaking all currents that cause melting of the fuse-element 150
18	Boggavarapu, R.L.	Programmable fuses 160
19	Mulertt, C.	A fuse used as an arc quenching chamber generates a new concept of power circuits protection 171
20	Barbu, I.	Notes on heating of fuses with ordinary substitution elements and standard units 180
21	Ofte, A. Rondeel, W.	Test procedure and arcing phenomena in H.V. fuse links near the minimum breaking current 190
22	Feenan, J.	Harmonisation of IEC & UL requirements for low voltage fuses - Is it possible? 200
23	Daalder, J.E.	The arcing voltage in high voltage fuses 212
24	Leistad, P.O. Kongsjorden, H. Kulsetås, J.	Simulation of short circuit testing of high voltage fuses 220
25	Wilkins, R. Wade, S. Floyd, J.S.	A suite of interactive programs for fuse design and development 227
26	Narancic, V.N. Fecteau, G.	Arc energy and critical tests for HV current-limiting fuses 236
27	Arai, S.	Deteriorations and cycles to failure of H.V. current-limiting fuses subjected to cyclic loading 252
28	Turner, H.W. Turner, C.	Thermal constants of filler and their influence on the metallurgical effects in fuse elements during pulse duty 262
29	Øvland, S. Kulsetås, J. Förster, H. Rondeel, W.	Metallurgical deterioration of copper fuse elements in high voltage fuses 270
30	Hofmann, M. Lindmayer, M.	Fusing and ageing behaviour of fuse elements with "M"-effect at medium- and long-time overload 280

WHAT NEXT WITH THE H.B.C. FUSES?

T.Lipski

PREFACE The word "fuse" derives from the Latin "fundo /fundi, fusum/" meaning "pour", "cast", "melt" but also "become brittle" or "crumble". A step ahead we have the word "fusio" in English "indundation", "outflow". In more recent times the word "fuse" has been used to denote the production of fluids by means of intense heat and that of producing fusion of materials. Clearly these literal interpretations clarify or convey little about the action of or role of electric fuse as a device for preventing damage to electric circuits under fault conditions.

The simplest description of the role of the electric fuse was probably Edison's who envisaged it as "a weak link in a circuit". Although the description fails to adequately convey the many uses and actions of electric fuses in circuits it nevertheless remains admirably clear, simple and true for the majority of fuse applications and is most people's concept of electric fuse protection.

The I.E.C. definition of an electric fuse is: "A device that, by fusion of one or more of its specially designed and proportioned components, opens a circuit in which it is inserted by breaking the current when this exceeds a given value for a sufficient time. The fuse comprises all the parts that form the complete device". The definition is not intended to include fuses other than those which actually interrupt excessive currents in circuits.

The limitation referred to is important as, in common with most fuse definitions, the previous definition interprets the electric fuse as a plain interruptor of fault currents in electric circuits and, in so doing, conveys a restricted role for the fuse to that of solely a current interruptor. But for some electric fuses would need to interpret the protection role as both current interruptor and initiator of events leading to the safe isolation of faulted circuits from supplies. Hence a global definition should embrace all classes and categories of fault protection afforded by fuses and in addition include its roles as an activating device for tripping contactors and circuit-breakers or energising secondary circuits to initiate alternative or complementary current-interrupting devices.

But simple fusion has take place only if a fuse-element operates in the overload or the moderate short-circuit conditions. Whereas under influence of a heavy short-circuit current the plain fuse-element and constictions instead that do explode due to rather sophisticated coincidence of the phenomena among which the Joule heating is only one predicting component. After that the fusion is not only operating principle of fuses. For example are in service fuses in which:
- the liquid transfers into electric arc, say in the mercury fuses /U.S.A./ known in principle from abt a century;

The author is with Gdansk Technical University, Institute of High Voltages and Electrical Apparatus, Gdansk, Poland

- the solid state fuse-element is mechanically interrupted by an electromagnetically driven special knife /U.S.S.R./, when the overcurrent overruns a specified limit, causing arc-initiation and then circuit current interruption;
- the temporary change of the current-carrying path into the non-conducting state has take place due to reaching the critical state of that metallic path /Japan/

what have not so much common with the simple fusion.

The history of fuse technology reaches as far back as 80-th of previous century and was recently briefly introduced by the paper [1].

Since the fuse technology already is so mature one could wonder whether the question posed in the title of this paper is felicitous. The answer undoubtedly is: it is the felicitous one because we have to talk about a rather simple and cheap conventional protective element but which development is incessantly constraint by the improvement of overcurrent protective systems and exertion of the new electric devices. More recent examples illustrating this statement are:

- the rapid extension of the short-circuit current-limiting back-up fuses to cooperation with: load-switches, contactors equipped within thermal relay /a very special case are vacuum contactors/, expulsion fuses /U.S.A./ but above all of moulded case l.v. circuit-breakers;
- the implementation of the semiconductor devices was a challenge to come into existence of the special fuses for the protection of diodes and thyristors /called in this paper semiconductor fuses/.

A correct answer on the question pushed out in the title largely depends upon the circumstances existing in given country. That what is already solved in one state it is a task for today or future in another one. China for instance [2] already has implemented the aluminium fuse-elements whereas the rest of the world,- as far as I know,- rather did not yet, despite there are known some endeavours to do that /e.g. Denmark, U.S.S.R./.

Although the fuses manufacturers are restricted by national and international standards the margin of a freedom existing in course of the designing of new fuses enables to create individual solutions and the designers can still demonstrate their art of the fuse engineering. It is a reason why we do observe on the market a huge number of fuses variations. An opposite example, if I am not wrong, are the conventional electrical machines, in which practically already all is based upon the classical calculations using existing complete programs for digital computations of the whole machine. But of course, the manufacturing processes and the quality control methods of either machines and the fuses are still under intensive improvements.

Normally a paper on the topic like this have to be proceed by a review of the present state-of-art, but in here one can omit it as it is addressed to the people working in the fuses. Moreover an apparent witness of the prior art of the fuse technology is a number of books on fuses, specifically issued over the last 15 years [3+9] and a periodical edition on protective devices [10] in which fuses and their applications are

widely represented.

The question being the contents of this paper let's limit to the h.b.c. fuses only, as in the power electric engineering at present and over the nearest future we will have to do practically mainly with the h.b.c. variety. However frankly speaking the gas-expulsion fuses are and will be also widely used but they do not have involved so many potential possibilities in creation of the new kinds of features needed for a modern protection as compared with the h.b.c. ones.

To be correct understood all the fuses indicating the short-circuit current-limiting ability are recognized here as the h.b.c. fuses. All of them have the arc-quenching filler, preferably a fine quartz sand. So for example the screw-in household D-type fuses very often used throughout the Continental Europe are also considered as the h.b.c. ones.

Obviously it is impossible to touch all of the aspects even of the h.b.c. fuses only due to a limited space of this paper. But those which are selected in the following have, after my mind, a greater importance. I believe the discussion will enrich the scope and deepness of our clearance on the actual fuse problems.

So limiting the contents of this paper we leave untouched a consistent number of the varieties of fuses /e.g. gas-expulsion, miniature, liquid, vacuum a.s.o./ but it enables to concentrate on the several important features of h.b.c. fuses.

POWER-LOSSES AND TEMPERATURE RISES Obviously better the fuses smaller the rated power-losses and the steady-state temperature-rises by unchanged technical data.

From the short-circuit current-limiting ability point of view a typical h.b.c. fuse-element shall fulfil two requirements: 1st is to keep its cross-section as small as possible in order to have the smallest pre-arcing time and the 2nd, - to create as high as possible arc-voltage using to that quite reasonable fuse-link length. That's why in comparison with the gas-expulsion fuses, which are not current-limiting ones, striking is that the h.b.c. fuses do indicate several times larger watt-losses. This is the price paid for the current-limiting ability.

For instance, a 15 kV h.b.c. fuse has the element-length of order 100cm, whereas a 15 kV gas-expulsion one, - few cm only. So the h.b.c. fuses are comparatively very much electrical energy consuming devices. Some general purpose h.b.c. fuses of 10 kV rated voltage and 100 A rated current do indicate abt 200 W rated power-losses. Or a h.b.c. fuse for diodes and thyristors of 1000 V a.c. rated voltage and 100 A rated current shows abt 20 W, but of 500 A rated current, - abt 100 W. This is a waste energy, which shall be artificially removed specifically in the case of large power semiconductor invertors within great number of fuses.

So alarming losses giving in consequence high temperature rises of the h.b.c. fuses do urge us to drastical diminishing of them, what is a beautiful task for fuses designers to cope with.

Some recently suggested new fuses concepts would be in this

respect a challenge to the traditional h.b.c. fuses. A promising example could be so-called "two-path" fuses described in a paper for this Conference [11]. However discovering of the all advantages and imperfections of two-path fuses is a question of time only but already it is safe to say this concept really does indicate much better quality at least as concerns the watt-losses and the temperature rises.

Another a very effective direction of action is to cut down the fuse-element length keeping all remaining parameters unchanged. But it needs to enhance the arcing gradient by this same rated voltage using for example a better arc-quenching means or/and improving the geometric proportions of the fuse element. Some examples are: the quartz-sand kept under an overpressure over the whole period of life of fuses [12], use of the sand-liquid filler [13], but also introducing a thinner strip by this same cross-section which should indicate a higher voltage gradient in the power 0.6 which proceed from a relation given in [14] and empirically was shown already several decades earlier in [15], a.s.o.

A quite different way is to improve the cooling. We obtain as a result the lower temperature rises conservating this same power-losses. But improving the cooling according to the actual practice we rather do the larger rated current keeping invariably these same permissible temperature rises. A good example of this way is the use of a sand-liquid filler [16], but also the use of fuse-elements deposited directly on an insulating substrate and/or glueing the sand-grains in one whole e.g. by a special chemical treatment of sand /TYPOWER fuses of LK-NES Co. Demark/, use of the various cooling sinks a.s.o.

In the context of power-losses and temperature rises there is situated a problem of the thermal cracking of the fuse-link barrel, even in the steady-state conditions, by loads nearly the minimum fusing current. Such sort of cracking surely is known for fuse-designers from several decades, was it also mentioned in the book [3]. But a theoretical approach which does indicate very clear the induced thermal stresses throughout the fuse-link body due to the heat transfer one can study in the rather less known work [17].

CHARACTERISTICS OF OPERATION Among the problems of characteristics of the operation one of the most important it seems is a problem of the interchangeability of fuses of different manufacturers. It is known practice that the fuses of these same basic standart parameters, i.e. dimensions, rated currents and voltages and t-I characteristics can show different operation in similar conditions. From this reason we are never sure whether the protection with the replaced fuse-links agreed with the standarts will remain equal to the originally done. This remark is important practically for such cases like various back-up protection systems, protection of diodes and thyristors and some others. In this respect important are not the standart but rather the actual t-I zones, cut-off currents, pre-arcing and clearing I^2t 's, sometimes also the minimum breaking capacity, overvoltages, rated power losses and temperature rises and several others. A disorganization of the protection becomes here due to the rather too wide permissible standart gates of mentioned parameters.

The problem is well known but to accentuate it we will give the following exemplary comments:

- The standart ratio of time operation say at 6 times of the rated current of a 100 A industrial fuse can reach abt 20 [18]. The choosen exemplary overcurrent is close to the usual take-over current of the contactor-thermal relay-fuses assembly.
- The ratio of cut-off currents of equal fuses of different manufacturers can be say 2.
- The ratios of pre-arcing and clearing I^2t 's can have magnitudes even greater than 10. The actual situation in this respect among the semiconductor fuses do illustrate the data given in [19] which are actual even now.
- The ratio of rated power-losses and temperature-rises of semiconductor fuses in the utmost cases can approach say 10 [19]. And if replacing the original fuses by more hot ones in a large power semiconductor equipment there may arise a question of an overheating of the whole arrangement.
- The minimum breaking capacity defined by the coefficient k_1 [20] of the fuses type a can have an arbitrary magnitude defined by a given manufacturer. So after replacing of fuses there may arise the problem of the incorrect interrupting of moderate overload overcurrents.
- A jeopardy of the use of semiconductor fuses of higher over-voltages than that generated by the originally installed is an evident case.

Above given examples are far to be complete, especially if we consider a proper utilization of semiconductor fuses.

What kind of the conclusions one can push forward from those examples? First of all it seems that a corollary is to tighten up of the standart requirements, as much as it is needed for the correct service. But we shall move in this direction in a very cautious way in order to not limit excessively a desired margin of the freedom of the fuses designers and consequently to not bring to a stop of the progress of development.

A quite different problem also does exist with t-I characteristics of operation in respect of the service safety of the domestic screw-in fuses of 380 V, type D. This is a case important in systems of small prospective short-circuit currents /say few times of the rated current/. It is a typical case rather for the old tonement houses feaded by weak old networks. When a short-circuit has take place in similar cases the mentioned fuses enable of the existance of a failure earth-leakage current during some decades or even hundreds seconds. The failure current existance in similar case means in turn the appearance of a touch voltage on the household electrical conviniences. If this voltage is high enough the service safety therefore can be drastically diminished. In some individul countries described situation can be normal practice over majority of the old dwelling quarters /e.g. in Poland/. Hence it exists the need to create some domestic fuses of 380 V of a rather quick-acting t-I characteristic instead of the time-lag one required by I.E.C. specifications. Here one shall know that the earth-leakage domestic protection as a rule in those countries rather are not available. Situation analogous to described one can observe

in the farms poorly equipped within agricultural electrical conveniences supplied by weak overhead rural high voltage systems and small transformers. In several number of the third world countries are similar situations.

Afore-going exemplary problem is not a lonely exception but it is a rather an illustration of a more general rule that the adaptation of the I.E.C. requirements may push forward the needs to design the fuses having not standardized characteristics of operation.

SEMICONDUCTOR H.B.C. FUSES The development of this specific fuses is still stimulated by the uninterrupted improvement of the power semiconductor devices. They are therefore in the very centre of attention of the fuse makers. That's why a couple of detached words could be said on them behind of some remarks already given above on semiconductor fuses. In following there are summarized the chief ideas on said fuses published already in [22].

The role of semiconductor fuses as an economical means of protection of power semiconductor devices is to remain in the foreseeable future. The problem however still remains how to achieve protection of the newest high power semiconductor devices keeping step with diodes and thyristors in power handling capability also in future.

Already twice in history technology got a violent progress: in the mid-sixties when the beveling-technique the "hokey-nuck"-design has been introduced and second one actually due to extremely homogeneous phosphorus doping of silicon single crystals by nuclear transmutation of ^{28}Si into ^{31}P by means of neutron radiation resulting in increase of the break-down field strength what enables already to manufacture semiconductor devices with maximum continuous current ratings up to abt 4 kA and peak inverse voltage of 6 kV in one piece.

But what we have to do with semiconductor fuses in future in face of expected further development of the semiconductor devices?

First of all, we need to awake ourself the weak points of the present day's semiconductor fuses. One of them is the nonuniformity of the arc-voltage. A comparison made for several products manufactured in Europe, U.S.A. and Japan shows that actually are available semiconductor fuses with the coefficient of the arc-voltage nonuniformity, understood as a relation of the maximum arc-voltage to the average arc-voltage, in the range of abt 1.05+1.4. Only very good products indicate that coefficient close to 1. An eventual improvement of the arc-voltage consisting in doing of a uniform arc-voltage shape /rectangular shape/ in some cases can drastically diminish of the arcing I^2t and in consequence of the clearing I^2t too.

The next problem is the power-losses diminishing which was already touched in afore-mentioned section. The urgent need is a further increasing of the rated current density of restrictions of fuse-elements. The possible improvements are innumerable.

The last but not the least problem which we will to mention

here is the saving of silver and/or complete replacing it by a less expensive metal. In this last respect the competitive are combined Cu-Ag elements but of course also Al-elements.

Looking more ahead it seems that the conventional semiconductor fuses would be unsuitable due to too large length, as the protective device for high voltage semiconductor devices. The length is nearly proportional to the rated voltage. On the other hand the dimensions of semiconductor devices indicate a weak dependence on the rated voltage. Hence utilizing present day's semiconductor fuses the semiconductor invertors designed for high voltages shall have rather large dimensions strongly dependent on the fuses dimensions. That's why the new principle of semiconductor fuses would be warmly welcomed.

On the background of the problems we have to solve in h.b.c. semiconductor fuses the new two-path fuses [11] it seems to be hopeful.

SOME PROBLEMS OF RESEARCH

Generally we may note, the pre-arcing behaviour of fuses was in a very centre of scientific interest during the first 3/4 of period of the fuses existence. But during the last decade or so only, the calculating methods of the steady-state heating and the pre-arcing times, even of the very complicated fuse-element's forms, have been successfully developed by several authors and we do not come back to them here. However one point shall be added. Nearly two years ago I did see in dr Wilkins' laboratory /Liverpool Poly./ a nice and a very needed for designers a computer aided engineering procedure which makes possible in an easy way to select the proper fuse-link dimensions in order to get a desired t-I characteristic, rated power-losses and temperature rises of the specific parts of the fuse-link. It is a true success of the implementation of theoretical considerations into the engineering practice.

On the contrary around the arcing processes we focus our attention practically over the last few decades only, despite there are known individual investigations on arcing in fuses say since 50 years /Kleen, Gantenbein, Lohausen, Kroemer, Schuck a. Boehne, Melkumov, Baxter, Johann and several others/

One can have an opinion that the arcing behaviour shall remain over the nearest period still in the centre of our attention.

A switching arc phenomenon is the most enigmatic one in the switchgear devices. And in the case of h.b.c. fuses the exploration of it is bristling with the difficulties inasmuch this phenomenon takes place inside of a closed volume with a filler. Moreover a period of its duration at short-circuit interruption is very short one. The special diagnostic tools therefrom are necessary such as an ultra-rapid X-ray flash, a rapid spectography, an ultrarapid temperature and pressure measurements a.s.o. That's why only recently more deep laboratory study of an electric arc performance in h.b.c. fuses was developed in several countries.

The temperature distribution along the fuse-element just prior of this element disintegration and the velocity of energy supply to the element are the predicting factors of arc ignition and to some extent of arc-burning and then arc-extinc-

tion.

There are one-arcing and multiple-arcing processes depending upon the fuse-element shape and the velocity of energy supply. Plain wires and strips under heavy overcurrents demonstrate a typical multiple-arcing, i.e. striation. Despite some endeavours of several authors /e.g. Nasiłowski, Lipski [23]/ there is no clear and universal point of view on the physics of striation. But there is an experimental approach [24] which makes possible to calculate the peak arc-voltage in case of striation.

On the other hand we are of a step ahead with calculations of a single arcing process characterized by a burn-back of the fuse-element as compared with the striation. A number of approaches in this respect are known / more recent are Wilkins with co-workers and Daalder's and Schreurs' [24]/. These dynamic approaches do open the door to a full calculation of the h.b.c. clearing ability. But before that, keeping still the one-arcing mechanism under considerations, there are several questions to investigate, among them are:

- generation and propagation of the pressures arising during the arcing and their influence on the arcing behaviour in h.b.c. fuses,
- reciprocal action of the parallel fuse-elements in one cartridge over the arcing period.

Speaking about the pressure, the more recent investigations indicate on the two characters of this pressure generation: one is monotonous connected with the slow burn-back process at rather moderate overcurrents [25] and another one is in form of the pressure shock-wave initiated at the instant of arc-ignition. The last is a very typical one when a plain wire or strip transits explosively into the streaks [26].

But interrupting a heavy overcurrent by a notched fuse-element it seems the both characters should exist abreast: the simultaneous arcs ignition in a number of series equal notches can give a suddenly arising pressure shock-wave and then the burn-back process contributes to the further pressure elevation but over this stage in a monotonous manner. If however the burn-back process would be slow enough then this contribution may not exist.

The mutual influence of the parallel fuse-elements placed after all close to each other in a cartridge is also a problem awaiting for investigations. However there are known some fragmentary investigations in this respect [3,27] but the question still waits for its discoverer. We shall pay more attention to that problem since a considerable number of h.b.c. fuses are designed for rated currents above say 25 A in which as a rule the fuse elements are in parallel. Aforementioned mutual influence is a complex interaction of parallel elements in which an important role shall play also the pressure and the overlapping of spaces occupied by the arc-channels.

In connection with this there is a more general reflection on specifically h.b.c. fuses operation during the arcing period. Such fuse is an interrupting device in which the interaction between the fuse-elements, the arc-quenching medium and the fuse-link body, which does reflect those shock-waves, is an

essential base of the correct action. All three parts shall be selected and coordinated in an appropriate way as a one whole. This statement is not new and the fuse designers surely know that well from their own experience.

Author had not an ambition to exhaust all problems on the arcing in h.b.c. fuses. It would be not possible to do that by one person. But it seems said remarks are sufficient to get the judgement on the tasks awaiting for right solution in the nearest future.

But beyond arcing problems we have also plenty to do with the quite different but how important problems on h.b.c. fuses and their proper selection for applications. Several examples of such problems are given below:

- A number of questions on the ageing due to M-effect, mechanical deterioration, pulsed loading a.s.o.
- We have to investigate a number of problems pertaining to the really full-range-clearing-ability fuses. In this respect we have to note very promising high voltage fuses with the cadmium fuse-elements /Westrom and co-workers, Canada/.
- A number of questions on the proper selection of fuses for various applications. For instance there is not yet solved finally the problem of a correct coordination of h.b.c. fuses with the expulsion fuses in an assembly designed to protection of padmounted and pole-type transformers in U.S.A. H.b.c. fuses are here best applied as back-up fusing devices while the expulsion fuse is used as the first line of defense. H.b.c. fuses in assembly serve also to prevent against a violent rupture of oil filled transformers as result of the arcing inside of the transformers tank.
- Several points are to enlighten in connection with the testing and standardization.

The list could be continued.

FINAL REMARKS Above given superficial observations on the question "what next with the h.b.c. fuses?" it seems to me do indicate that we have still many problems to solve in the research and development. But we have also to improve the manufacturing processes, for h.b.c. fuses shall be produced as far as it is possible independently of the manual ability of workers in order to stabilize the final quality. In this respect for example interesting is a set of manufacturing machinery for the fuse-elements with constrictions in form of the grooves and continuously deposited tin-lead alloy to get time-lag fuses [28,29]. Same machinery for grooves plus another machinery to make the continuous welding of Cu- and Ag-strips [30] enables the mass manufacturing of fuse-elements of semiconductor fuses. Having the consciousness of a not fully exhaustive answer on the question in the title let's say couple of closing words.

The subject of our common interest i.e. the fuses are destined to serve as a protection of the very different objects. That's why we shall be prepared to create in a very limited time quite new fuses operational characteristics sufficient to be a good protector of the not yet existing devices. This menial role of fuses, we believe, will still remain for the long years, despite several suggestions to design

the electrical installations on the fuseless basis.

Now we see that the Latin word "fundo /fundi, fusum/" does cover a vast field of the electrical overcurrent protective devices we have to deal with. And that our activity in this field is needed for society.

REFERENCES

- 1 Newbery P.G., Wright A.: Electric fuses. Proc.IEE. Vol.124. No.11R. Nov.1977. p.909-924.
- 2 Wang Ji-mei: Research of fast acting fuse with aluminium element. Int. Conf. on Gas Discharges and Their Applications. London.1982.Proc.p.393-394.
- 3 Lipski T.: Low voltage fuses./a book in Polish/. WNT Ed. 1968.Warszawa.
- 4 Jacks E.: High rupturing capacity fuses./a book/. London. E. a. F.N. Spon Ltd. 1975.
- 5 Bratinov P.: Low voltage fuses./a book in Bulgarian/. Sofia Technika Ed. 1976.
- 6 Namitokov K.K., Chmelnickij R.S., Anikeeva K.N.: Fuses /a book in Russian/. Moskva. Energija Ed. 1979.
- 7 Wright A., Newbery P.G.: Electric fuses./a book/. Stevenage. Peter Peregrinus Ltd. 1982.
- 8 JohannH.: Fuses for low voltage./a book in German/. Berlin Springer Ed. 1982.
- 9 Barbu I.: Low voltage fuses./a book in Rumanian/. Bucureşti Technica Ed. 1983.
- 10 Turner H.W., Turner C.: Digests of information on protective devices. Leatherhead. ERA 2979 Rep.
- 11 Krasuski et al: New line in the h.b.c. fuses development. Int.Conf. on Fuses and Their Applications. Trondheim. 13-15 June 1984.
- 12 Pastors Y.A.: Some characteristics of electric arc extinguishing in compressed quartz sand. Izvestia AN Latvvijskoj SSR. ser.Fiz. i Techn. Nauk, 1969. No.5. p.55-58. /Russian/
- 13 Cosh J.Q., Wright A.: Fuses for protection of thyristors. Authors are with Nottingham University.
- 14 Daalders J.E., Schreurs E.F.: Arcing phenomena in high voltage fuses. EUT Report 83-E-1937. TU Eindhoven 1983.
- 15 Müller A.O., Paetow H.: Design, mode of operation and service features of new low voltage h.b.c. fuses. Siemens Z. 1951. No.3. p.149./in German/.
- 16 Pastors Y.A.: Liquid-filled fuses for the protection of thyristors. Int. Conf. on Fuses and Their Applications. Liverpool. 7-9 April. 1976. Proc. p.264-269.
- 17 Stenzel H.D.: Action of power-losses of high voltage h.b.c. fuses on the fuse-link body under small overcurrent. Ph.D. Thesis. TU Hannover. 1972. /in German/.
- 18 I.E.C. Publication 269-2. 1973. Low-voltage fuses. Supplementary requirements for fuses for industrial applications.

- 19 Lipski T.: I^2t values of real and ideal semiconductor fuses. Int. Conf. on Fuses and Their Applications. Liverpool. 7-9 April 1976. Proc. p.233-234.
- 21 I.E.C. Publication 269-3. 1973. Low-voltage fuses. Supplementary requirements for fuses for domestic and similar applications.
- 20 I.E.C. Publication 269-1. General requirements. 1968.
- 22 Lipski T.: Some problems of development of semiconductor fuses. SIELA-Symp. Plovdiv. Bulgaria. 19-21 May. 1983. Proc.P.I. p.186-191.
- 23 Lipski T.: Application of the arc-pinch-forces-interaction theory to the calculation striation modulus of the strip h.b.c. fuses. Int. Conf. on Fuses and Their Applications. Trondheim. 13-15 June 1984.
- 24 Hibner J.: Gradient-resistance method of calculation of the overvoltage peak value generated by short-circuit current-limiting fuses. Ph.D. Thesis. TU Gdańsk. 1973 /in Polish/.
- 25 Barrault M.R.: Pressure in enclosed fuses. Int. Conf. on Fuses and Their Applications. Liverpool. 7-9 April. 1976. Proc. p.110-113.
- 26 Lipski T.: On the theory of the striated fuse-wire disintegration. IEEE Trans. Vol. PS-10. No.4. Dec.1982. p.339.
- 27 Rosen P.: Arcing-phenomena in h.r.c. fuses under varying conditions. Int. Conf. on Fuses and Their Applications. 7-9 April. 1976. Proc. 89-100.Liverpool.
- 28 Krasuski B.: A special rolling-mill for mass manufacturing of grooves on the metal tape destined to produce strip fuse-elements. SIELA-Symp. Plovdiv. Bulgaria. 19-21 May. Special edition. /in Russian/.
- 29 Krasuski B., Szymański E.: New process of mass deposition of tin-lead alloy on strip fuse-elements. *ibid.*
- 30 Krasuski B.: A special welding machinery for manufacturing of the tape for strip fuse-elements. *ibid.*

MEASURING THE PRE-ARCING TEMPERATURE OF
HIGH-BREAKING-CAPACITY FUSELINKS BY THERMAL IMAGING

*A.F. Howe, D. de Cogan
+P.W. Webb
+N.P.M. Nurse

SUMMARY The paper describes experiments to measure by thermography the variation in temperature across the surface of fuse elements carrying up to rated current.

1. INTRODUCTION To ensure that fuselinks do not deteriorate when they carry continuously rated current, manufacturers design their elements in such a way that the notch temperatures never reach values where permanent deformation of the element will normally occur. This sets a limit on the notch temperature for semiconductor fuselinks with silver elements at about 250°C and for industrial fuselinks with copper elements around 140°C. There is no easy method to measure these temperatures directly. For example, the use of thermocouples to measure notch temperatures is inappropriate because the masses of notches are so small that heat would be conducted away from the restrictions along the thermocouple wires. Instead, notch temperatures have to be deduced from the measurement of the "hot" fuse resistance and computations based on Fourier's Law [1],[2]. This paper describes a feasibility study to investigate whether a technique called thermography might be used to measure the temperatures of the restrictions in fuse elements.

2. THERMOGRAPHY Thermography is widely used in industrial and medical applications. In this instance a system is being developed to measure the surface temperatures of samples [3]. The operation of the system relies on all black bodies radiating energy which is proportional to the absolute temperature to the fourth power. This phenomenon is called Stefan's Law and is written mathematically thus:

$$\text{Radiated Energy} = \sigma T^4$$

where σ = Stefan-Boltzmann constant = $5.67 \times 10^{-8} \text{ Jm}^{-2} \text{ s}^{-1} \text{ K}^{-4}$, and

T = absolute temperature

For temperatures below approximately 400 to 500°C the emitted radiation is almost entirely within the infra-red spectrum. To measure this radiation experimenters use a scanning thermal (infra-red) imager

*University of Nottingham, U.K.
+University of Birmingham, U.K.
+Brush Fusegear Limited, U.K.

like the Barns RM50 (see Fig. 1) or a fixed position infra-red microscope, like the Barns RM2A in conjunction with a moveable sample table (see Fig. 2) [3]. The instruments which are fitted with liquid-nitrogen cooled indium-antimonide (InSb) detectors, are focussed on a small region of the specimen surface (35 μm , 17 μm or 7 μm diameter) and a measurement is taken. Adjustments are then made to the scanning mirrors in the thermal imager, or the position of the moveable sample table relative to the position of the fixed microscope, to obtain a measurement from an adjacent area. The process continues until the whole surface has been examined. The scanning is automated and the measurement signals are transmitted to a PDP 11/34A computer where they are digitised, converted to temperatures and stored [3]. Quantising the results enables an image, which shows the variations in temperatures across the surface, to be displayed on a cathode ray tube.

3. MEASUREMENTS WITH "GREY" SAMPLES "Grey" bodies emit lower radiation than black bodies at the same temperature, and so Stefan's Law is modified for "grey" bodies thus

$$\text{Radiated energy} = \epsilon \sigma T^4$$

where ϵ = emissivity, which has a value between 0 and 1.

Before thermography can be used to find the surface temperature of a "grey" body the experimenter must know the emissivity or make it unity by some artificial means. If the former is adopted then the sample is heated to known temperatures and the emission is observed. This information is supplied as data to the computer, which then applies software corrections to the data derived during the thermographic measurements of the samples.

4. INVESTIGATIONS WITH FUSE ELEMENT PROFILES Using thermography in its present state of development it is not possible to scan the notch region of a fuse element mounted in a ceramic body and embedded in sand. So for the investigatory tests specimens were made by evaporating silver films on to clear quartz discs. The profiles were similar to a semiconductor fuselink element currently produced by Brush Fusegear Limited.

The emissivity of silver is less than unity. In order to save the time involved in calibrating the emissivity the fuse element was coated with a thin layer of carbon black, which has an emissivity of 1.0. Independent measurements showed that this had little effect on the electrical properties of the fuse element.

4.1 Steady-state Direct Current Test In the first test with the fuse element profile a current of 2A d.c. was passed through the element for several minutes to allow a steady-state temperature distribution to be established within the element. The measurements were then taken and the temperature variations were displayed on a cathode ray tube, as shown in Fig. 3. When a colour monitor is available the regions of intermediate temperatures are shown in different colours to improve the clarity of the display.

The computer stores the temperature for each small region in the surface as a discrete value so it is possible to produce

- a) temperature profiles along (line A) and across (line B) the narrow part of the element (see Figs. 4 and 5),
- b) "close-ups" of the temperature distribution in a small part of the fuselink profile. If this option is selected then the temperature scale is automatically adjusted to shade the hottest points in the chosen area black, the coldest points white and redistribute the grey divisions accordingly. With this facility it is possible to examine closely any irregularities in the temperature pattern.
- c) Three-dimensional representations of the temperature profile, as illustrated in Fig. 6.

To test the accuracy of the measurements the temperature distribution for the fuse element was calculated using the finite-difference method developed by Leach et al [2] (see Fig. 7). Comparison of the isotherms with Fig. 3 will show that there was reasonable agreement between the two methods. One reason for the small discrepancy in the notch region is that the computational method ignored the fact that with the fuse element firmly attached to the quartz glass disc some heat will be conducted from the fuse restriction to the substrate.

4.2 Tests with alternating current

4.2.1 Measurements taken at one point The fixed staring microscope, Barns RM2A, is used in conjunction with the moveable table for these measurements. The instrument records the temperature measurements at set times at a chosen location on the surface of the specimen. The results can be plotted on a transient recorder or sent to the computer for analysis, as shown in Fig. 2. Fig. 8 shows the variation in temperature when an alternating current flows through the fuse element when it is mounted on quartz. This technique can also be used to monitor thermal transients. Fig. 9 shows how the temperature at a discrete point increases during the first few cycles of an alternating current.

4.2.2. Temperature variation over the whole surface To use the thermal imager to measure the temperature variations in the elements when a steady-state alternating current flows through it, the instrument with the scanning mirrors is used. The instrument is focussed on a small area of the specimen. Then at a chosen instant on the voltage waveform, say t ms after a voltage zero, a measurement is taken. The scanning mirrors are then adjusted to look at the adjacent point on the surface and at t ms after the next voltage zero the second measurement is taken. The process continues until the whole of the fuse element has been examined. The timing of the "firing" pulse is illustrated simply by Fig. 10.

The gating delay is selectable so a "family" of thermal plots can be produced to demonstrate how the temperature fluctuates across the whole surface as the current varies with time (see Fig. 11).

5. FUTURE WORK For thermographic measurements of fuse element temperatures to have practical significance the elements must be covered by granular quartz. However, it is impossible to "look" through grains so the next step is to modify the test rig (as illustrated in Fig. 12)

to take measurements through the quartz. Unfortunately, the temperatures measured will not be the element temperatures, but some function of the correct values. As a result software is now being developed so that the measurements from the second phase of the work can be presented in a meaningful way.

It is hoped that the results from the proposed work will prove useful to fuse designers and will aid the future development of fuse element designs.

6. ACKNOWLEDGMENTS The authors wish to thank Mr. I.R. Shelton, the Universities of Birmingham and Nottingham, and Brush Fusegear Limited for the facilities provided.

7. REFERENCES

1. Wright, A. and Newbery, P.G., Electric Fuses, (Peter Peregrinus, 1982).
2. Leach, J.G., Newbery, P.G. and Wright, A., "Analysis of high-rupturing-capacity fuselink pre-arcing phenomena by a finite-difference method", Proc. IEE 120 (9), 1973, pp. 987-993.
3. Webb, P.W., "Measurement of thermal transients in semiconductor power devices and circuits", Proc. IEE, 130, Pt I, (4) pp. 153-159.

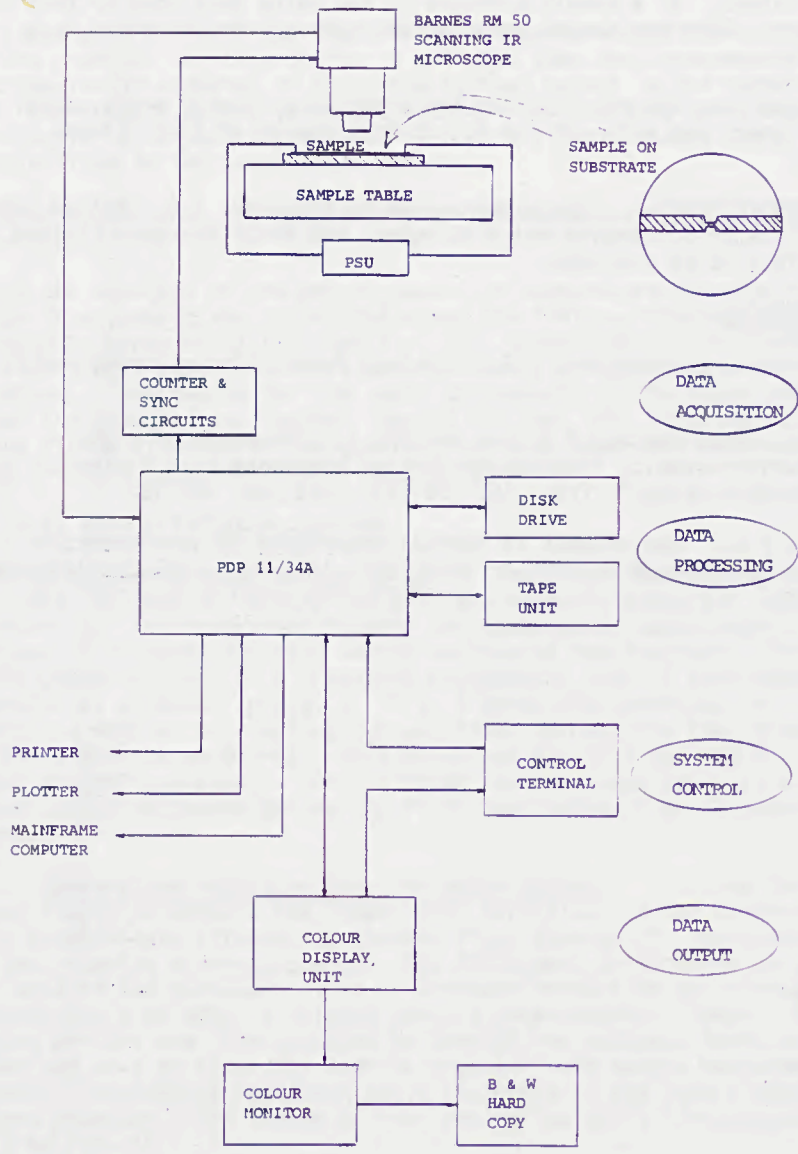


Fig. 1

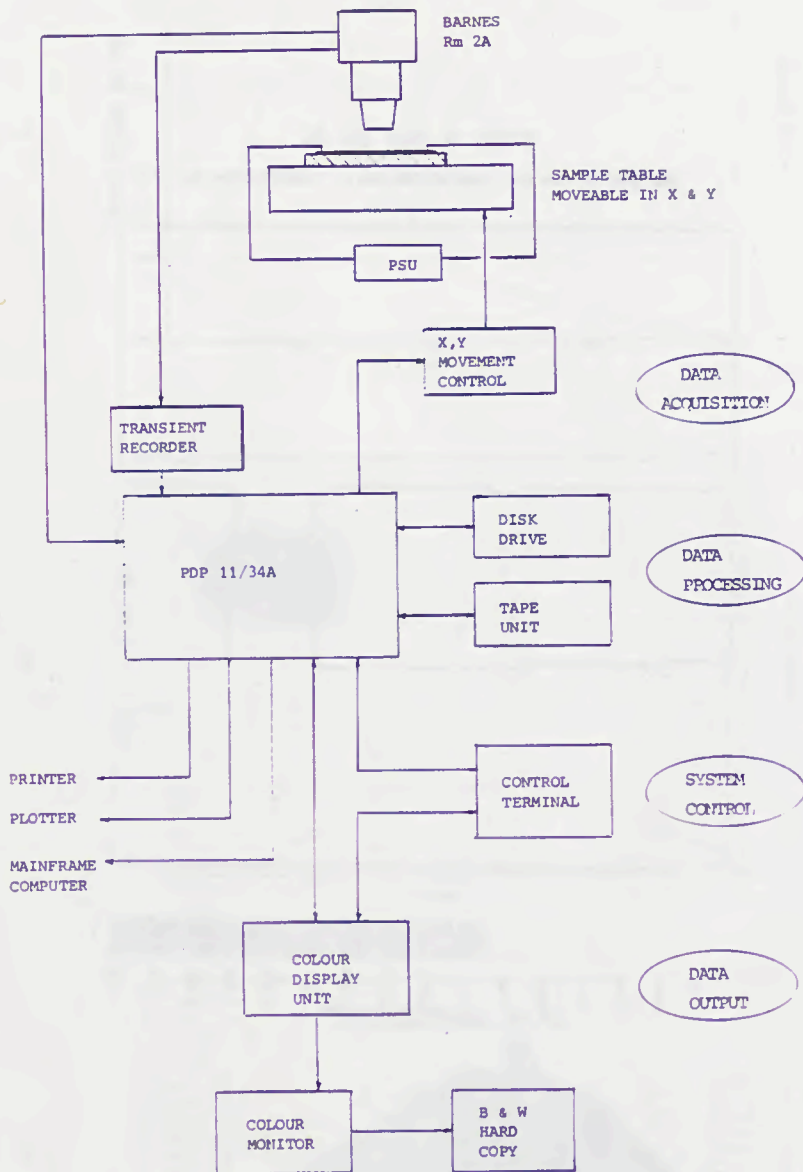


Fig. 2

FUSE GLASS 2A DC

DARK LEVEL SETTING= 48.6 SPAN SETTING= 283.1 MAGNIFICATION= 18

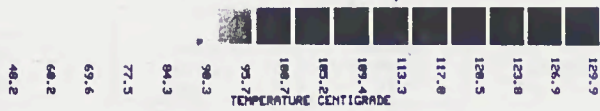
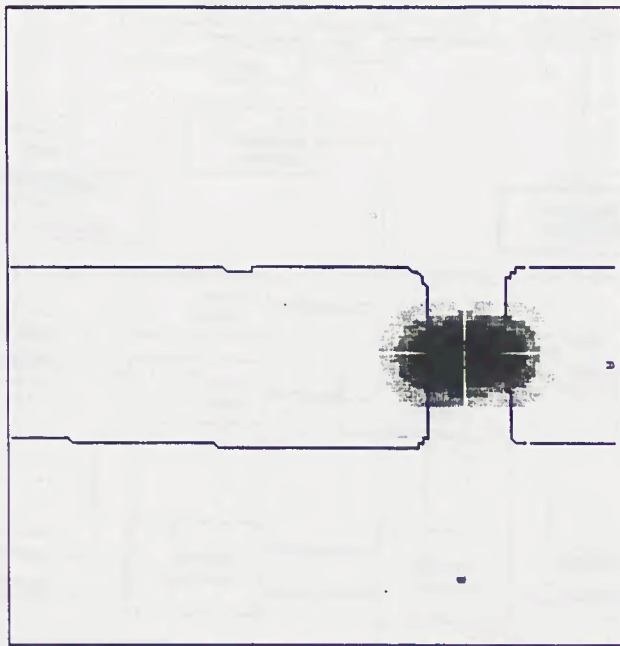


Fig. 3

Fig. 4

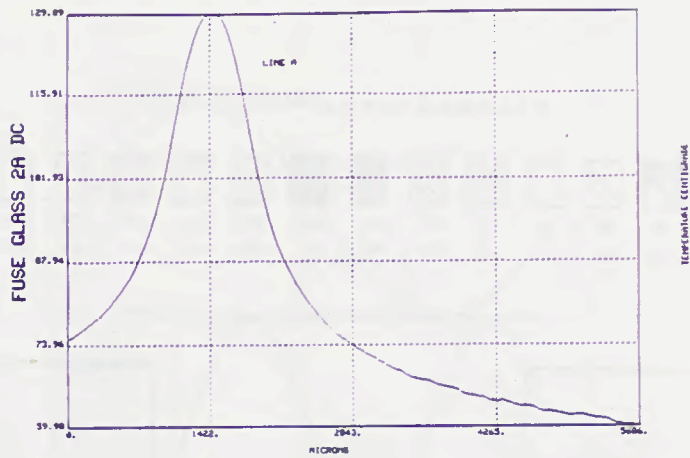


Fig. 5

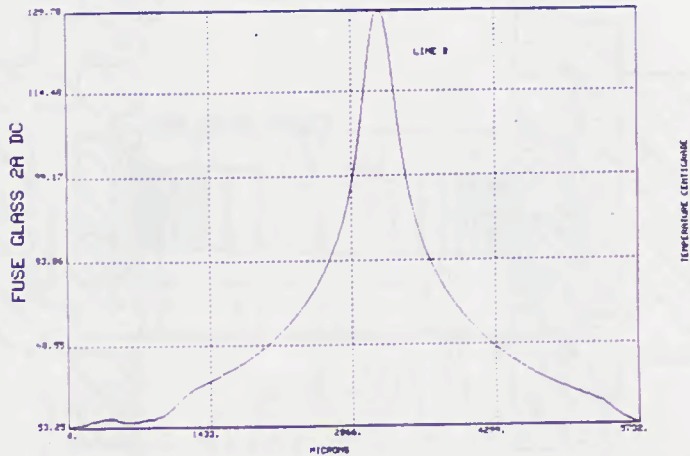
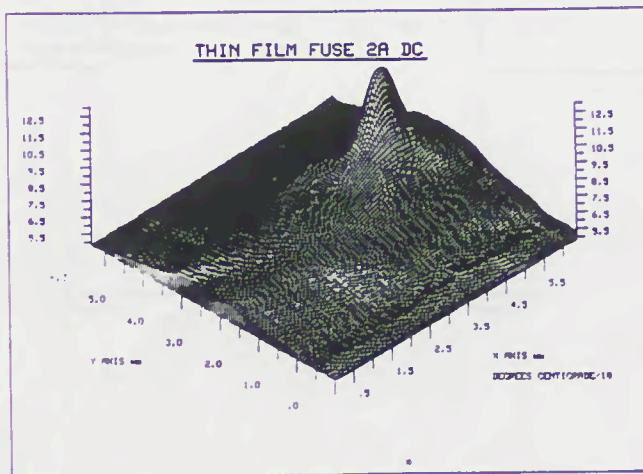


Fig. 6



TEMPERATURES °C

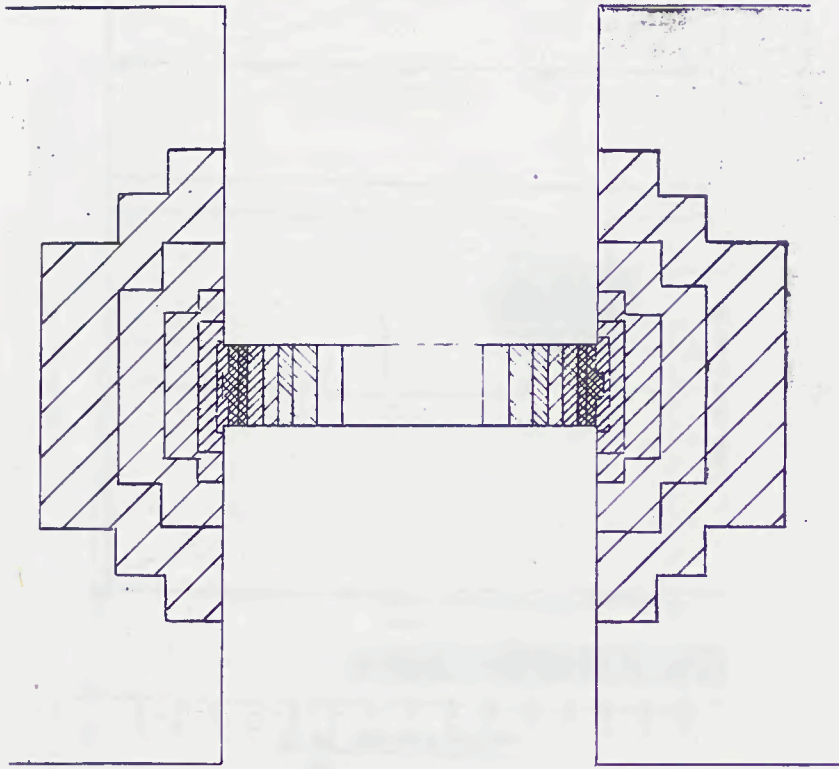
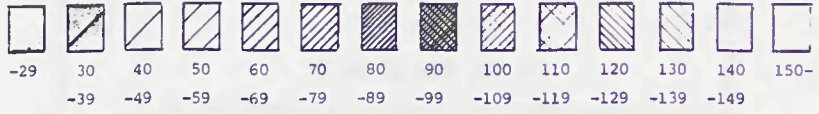


Fig. 7

Fig. 8

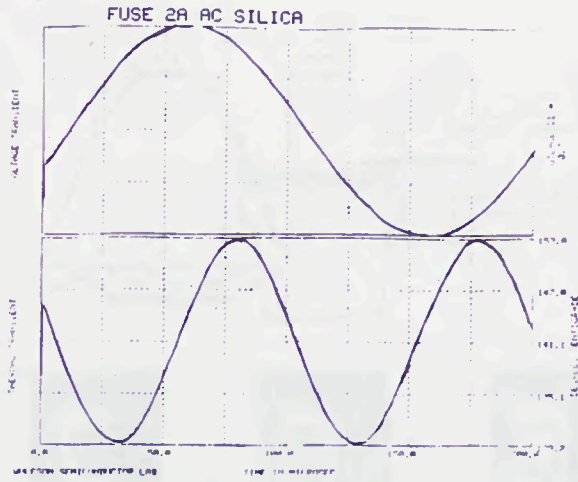


Fig. 9

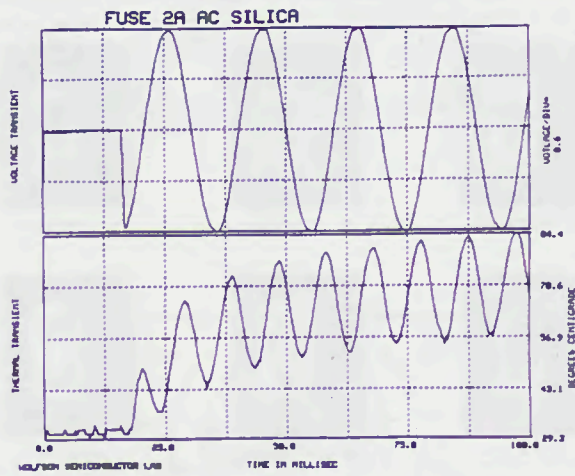
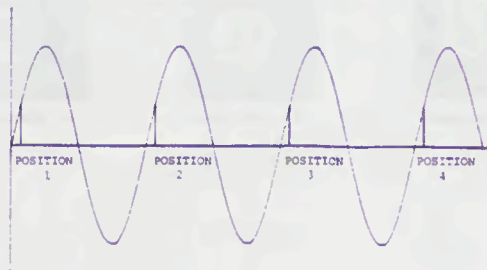


Fig. 10



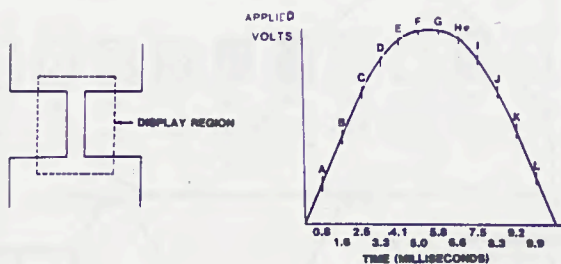


Fig. 11

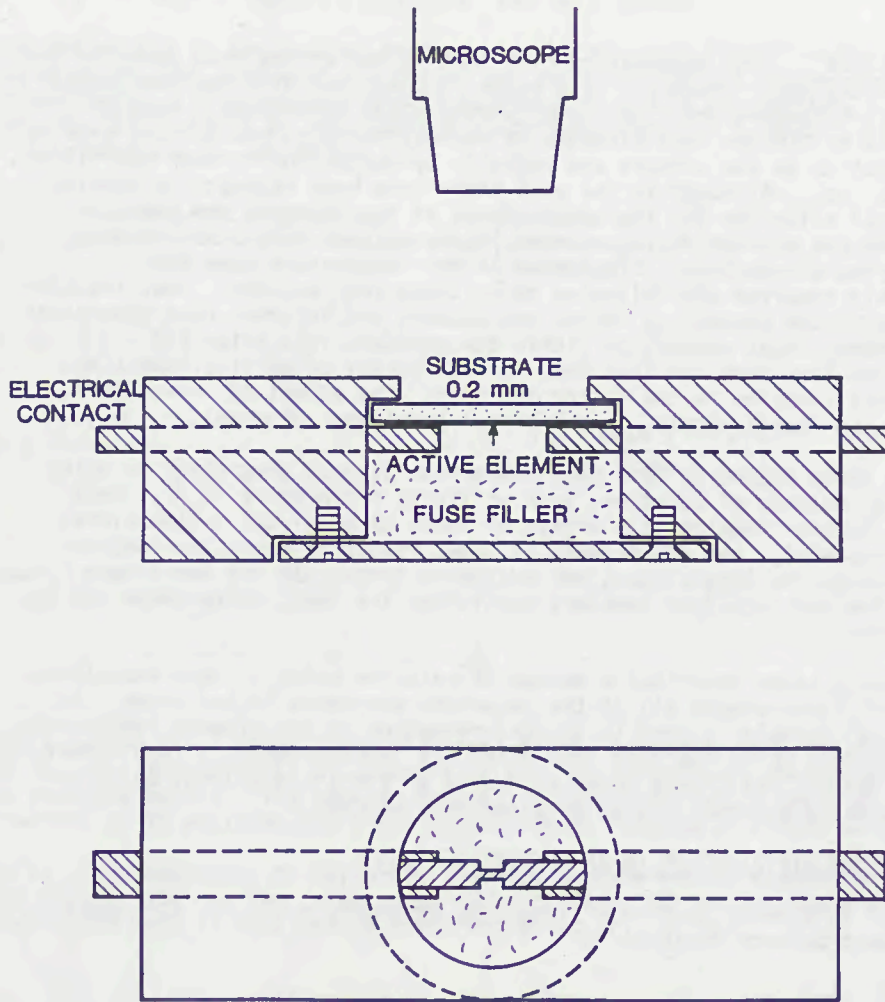


Fig. 12

SIMULATION OF FUSELINK TEMPERATURE-RISE TESTS

R. Wilkins

INTRODUCTION The temperature-rise test is one of the most commonly used tests in the fuse industry. This paper is concerned with the computation of fuselink temperature rises under steady-state conditions. Heat is generated within the fuse elements by Joulean heating, and is lost axially by conduction to the endcaps and radially by conduction through the filler and fuse body. Although in the past there have been attempts to develop analytical solutions for the temperatures of the elements and hence to determine the minimum fusing current, these methods have involved many simplifying assumptions. Simulation of the temperature rise test accurately requires the following to be taken into account; heat transfer to and from the connecting cables and busbars and internal heat generation within them; heat generation within the endcaps; radiation and convection loss from the fuse body for horizontal or vertical mounting; axial heat transfer in the filler and body; the effect of non-uniform flow in the fuse elements; and M-effect processes (if used).

Some of these phenomena have been taken into account previously by using numerical methods of solution, such as finite differences [1,2]. Such methods however require vast arrays of nodes to model the 3-dimensional field accurately, and convergence is slow, requiring excessive computer time even on the largest machines available today. If the non-linear convection and radiation boundary conditions are used, convergence may be impossible.

The present paper describes a method of solution which is semi-analytical and which incorporates all of the important phenomena listed above. An analytical formula is used in the determination of the element temperature distribution, while the heat loss paths are represented by a (non-linear) lumped thermal resistance network. Using an iterative method, solutions of reasonable accuracy can be obtained very quickly.

TEMPERATURE DISTRIBUTION IN AN ELEMENT SECTION

Consider an element section of length 2ℓ as shown in Fig.1. The steady-state heat balance equation is

$$\frac{I^2 \rho_0 (1 + \alpha T)}{S} = \frac{T}{g} - KS \frac{d^2 T}{dx^2} \quad (1)$$

Dr. Wilkins is with Liverpool Polytechnic, Byrom Street, Liverpool, U.K.

Where T = temperature rise (function of x)
 x = axial position ($0 \leq x \leq 2l$)
 I = current
 ρ_0 = resistivity at zero datum temperature
 α = temperature coefficient
 S = cross-sectional area
 K = thermal conductivity
 g = radial thermal resistance, per unit length.

The LHS of (1) is the Joulean heat generation per unit length, while the terms on the RHS represent the radial and axial conduction losses, respectively. It is assumed that g is constant within the section. Solving (1), subject to the boundary conditions that $T = T_L$ when $x = 0$ and $T = T_R$ when $x = 2l$, we obtain [3]

$$T = \frac{T_L \sin a(2l-x) + T_R \sin ax}{\sin 2al} + \frac{k}{a^2} \left[\frac{\cos a(l-x)}{\cos al} - 1 \right] \quad (a^2 > 0)$$

$$T = T_L \left(1 - \frac{x}{2l} \right) + T_R \frac{x}{2l} + \frac{kx}{2} (2l-x) \quad (a^2 = 0)$$

$$T = \frac{T_L \sinh a'(2l-x) + T_R \sinh a'x}{\sinh 2a'l} + \frac{k}{a'^2} \left[1 - \frac{\cosh a'(l-x)}{\cosh a'l} \right] \quad (a^2 < 0)$$

....(2)

where $(a')^2 = -a^2$, and

$$k = \frac{I^2 \rho_0}{S^2 K}; \quad a^2 = \alpha k - \frac{1}{gSK}.$$

The solution for T takes three different forms, depending upon the sign of a^2 . For low currents a^2 is negative and the temperature distribution is governed by the 'flat-topped' hyperbolic functions, while for high currents a^2 is positive and the distribution is related to a sine curve.

It is often necessary to calculate the heat transferred by conduction to the ends of the section. The temperature gradient at the left-hand and right-hand ends is obtained by differentiating (2), to get

$$\left. \begin{aligned} \frac{dT}{dx} \Big|_L &= XT_L + YT_R + Z \\ \frac{dT}{dx} \Big|_R &= -YT_L - XT_R - Z \end{aligned} \right\} \quad (3)$$

where the coefficients X , Y and Z are given in the Table below.

	X	Y	Z
$a^2 > 0$	$-a \cot 2a\ell$	$a \operatorname{cosec} 2a\ell$	$\frac{k}{a} \tan a\ell$
$a^2 = 0$	$-\frac{1}{2\ell}$	$\frac{1}{2\ell}$	$k\ell$
$a^2 < 0$	$-a' \coth 2a'\ell$	$a' \operatorname{cosech} 2a'\ell$	$\frac{k}{a'} \tanh a'\ell$

These formulae refer to a single element section, the whole element being regarded as the series combination of a number of such sections (Fig.1a).

RADIAL THERMAL RESISTANCE

Referring now to Fig.1(b), we will calculate the radial thermal resistance g for a section of width w_i and thickness t_i . If there are n elements in parallel we need to compute g for a sector of angle $(2\pi/n)$. As there is no analytical formula for a strip element we may treat the element as an equivalent round wire. This method, due to Guile [4] gives the radius of the equivalent wire as

$$r_e = \frac{w_i}{2} \cdot \frac{x}{x + \sqrt{x^2 - 1}} \quad (4)$$

where $x = 2r_a/w_i$ (assuming an isothermal at r_a).

Analysis of the thermal field due to a parallel circular array of wires, using the theory of conjugate functions [5], gives the thermal resistance per sector of the filler as

$$g_f = \frac{1}{2\pi k_f} \ln \frac{r_a^n - r_p^n}{(r_p + r_e)^n - r_p^n} \quad (5)$$

where k_f is the filler thermal conductivity and r_p is the pitch circle radius. (5) is quite general, since for $r_p = 0$ and $n = 1$ it reduces to the well-known formula for a single, central wire.

The body thermal resistance is given by

$$g_b = \frac{1}{2\pi k_b} \ln \frac{r_b}{r_a} \quad (6)$$

where k_b = thermal conductivity of the body, and the external thermal resistance is

$$g_{\text{ext}} = \frac{1}{2\pi r_b h_b} \quad (7)$$

where h_b is the effective surface heat loss coefficient, which may be approximated by [6]

$$h_b = C \left(\frac{T_b}{2r_b} \right)^{0.25} + \epsilon \sigma \left(T_b^4 - T_{\text{amb}}^4 \right) \quad (8)$$

where C is a convection constant, ϵ is the body emissivity and σ is Stefan's constant.

The total thermal resistivity is therefore

$$g = g_f + g_b + g_{ext} \quad (9)$$

The problem is that we cannot explicitly calculate g_{ext} , since the convective and radiative losses depend upon the body temperature T_b , which is unknown. Furthermore g_{ext} is a non-linear function of temperature. As will be described later, this problem can be overcome by making an initial guess for T_b , and subsequently correcting this value.

EFFECT OF FIELD DISTORTION The analysis leading to equation (2) assumes that the Joulean heat is generated uniformly throughout the section, but in fact this is not so. Fig.2 shows a sketch of the current-flow field near a typical neck-shoulder transition region of a fuse element. The distortion of the field gives rise to additional heating which would require a full two-dimensional field model to calculate accurately. However, an analytical solution exists for the additional resistance caused by this field distortion [7]. In the case shown in Fig.2, the additional resistance is given by

$$\Delta R = \frac{\rho}{2\pi t} \left[\frac{r^2 + 1}{r} \ln \frac{r + 1}{r - 1} + 2 \ln \frac{r^2 - 1}{4r} \right] \quad (10)$$

where t is the strip thickness and r is the ratio of full section to reduced section. Fig.2 shows that almost all of the distortion occurs in the full-section, the field in the reduced section remaining almost uniform. Thus to a first approximation the effect of field distortion can be allowed for by increasing the effective resistance of the full section by ΔR , and using the analytical formulae given previously (which assumes that the additional heating is uniformly distributed within each section). Thus the use of complex and time-consuming finite-difference solutions is avoided.

HEAT GENERATED IN ENDCAPS For fuses with high current ratings it is not possible to obtain reasonable results without including the effect of the endcap resistance. This varies with construction but typically consists of three components; the resistance of the inner cap, from the element ends to the outside of the cap (obtained using a formula similar to (5)); the resistance of the outer cap (assumed to touch the inner cap only at the periphery); and then the resistance of the tag up to a chosen point where the current is assumed to leave the fuse and at which the volt drop measurements are assumed to be taken.

By this, or a similar process, the cold endcap resistance is found. During computation, when the endcap temperature rises, the resistance is corrected by use of the appropriate temperature coefficient.

HEAT LOST TO END ASSEMBLIES Heat is lost from the end assemblies by radiation and convection from the endcaps, tags, nuts, and busbars to which the fuselink is connected, and also by conduction into the connecting cables. The latter component is lost radially from the surface of the cable until at some large distance from the fuselink a constant

sink temperature is reached. This sink temperature is determined only by the heating of the cable itself. In the present method, all of these processes are represented by a lumped thermal impedance G_{ec} , which is the ratio of the endcap temperature rise to the total heat input to the end assemblies. Like the external body resistance, G_{ec} has a non-linear dependence upon the endcap temperature and therefore an initial estimate is made based upon some assumed temperature value.

SOLUTION METHOD A method will now be described for linking together the various models as described previously. Firstly consider the axial temperature distribution, and the conditions at the junction between the i 'th section and the $(i+1)$ 'th section (see Fig.1). The axial heat balance requires that

$$S_i \left. \frac{dT}{dx} \right|_R^i = S_{i+1} \left. \frac{dT}{dx} \right|_L^{(i+1)} \quad (11)$$

Now using (3), we obtain

$$S_i Y_i T_{i-1} + (S_i X_i + S_{i+1} X_{i+1}) T_i + S_{i+1} Y_{i+1} T_{i+1} = -S_i Z_i - S_{i+1} Z_{i+1} \quad (12)$$

If there are N sections, an equation of this form can be written for each junction point except the ends ($i=1$ and $i=N+1$), where the effect of the end assemblies must be considered. At the ends a heat balance as shown below must be considered.

Heat source

1. Input to endcap from all parallel elements by conduction.
2. Internal Joulean heating in endcap.
3. Axial conduction to endcap through filler and body.
4. Convective input to top cap (vertically-mounted fuses only).

Heat loss

To busbar metalwork and cables via a thermal resistance G_{ec} .

Sources 3 and 4 are allowed for by the following method. A simple lumped thermal resistance network (passive) is established with resistors R_1 , R_2 and R_3 , where

R_1 = total thermal resistance, element-to-body

R_2 = total exterior thermal resistance, body-to ambient

R_3 = body centre-to-endcap thermal resistance.

R_1 and R_3 are constant while R_2 is a function of the body temperature. Using this network, for a given element temperature distribution, a new value of body temperature can be computed. The axial heat input to the end-cap can be then simply calculated and the convective input to the top cap for vertical fuselinks is assumed to be a fraction f of the total loss from the body, due to the upward motion of the air. Applying these conditions to the endcaps gives two further equations, which together with the equations (12) give a matrix equation

$$[Q] [T] = [R] \quad (13)$$

[Q] is a known square matrix of order (N+1)

[R] is a known (N+1) vector

[T] is the unknown (N+1) vector of temperatures.

Solution of (13) gives the temperatures at the section junctions. The temperature at any location within a section can then be found using the analytical expressions (eq.2).

[Q] is a triadiagonal matrix, which permits minimal computer storage and very fast efficient solutions. The elements of [Q] and [R] are given by the following relationships:

major
diagonal
elements
of
[Q]

$$\left\{ \begin{aligned} q_{11} &= S_1 X_1 - \frac{1}{n \cdot n_b K G_{ec}} - \frac{1}{KR_3} \\ &= q_{N+1, N+1} \\ q_{ii} &= S_i X_i + S_{i+1} X_{i+1} \end{aligned} \right.$$

minor
diagonal
elements
of
[Q]

$$\left\{ \begin{aligned} q_{i, i+1} &= S_{i+1} Y_{i+1} \\ q_{i+1, i} &= q_{i, i+1} \\ q_{ij} &= 0, \text{ otherwise} \end{aligned} \right.$$

elements
of
[R]

$$\left\{ \begin{aligned} r_1 &= -S_1 Z_1 - \frac{I^2 R_{ec}}{n n_b K} - \frac{T_b}{KR_3} - \frac{f T_b}{KR_2} \\ r_i &= -S_i Z_i - S_{i+1} Z_{i+1} \\ r_{N+1} &= -S_N Z_N - \frac{I^2 R_{ec}}{n n_b K} - \frac{T_b}{KR_3} \end{aligned} \right.$$

where n_b is the number of fuse bodies in parallel.

Solution is achieved by using the iterative scheme shown in Fig.3. First values of the body and endcap temperatures are assumed, which permits evaluation of all the lumped thermal resistances. Solution of the matrix equation (13) then gives the complete element temperature distribution, which includes a new value of endcap temperature. Use of the thermal resistance network then gives a new estimate of the body temperature. This procedure is repeated until the body and endcap temperatures converge. Convergence, however, is not guaranteed, owing to the basic non-linearity of the problem, and in fact for high applied currents convergence becomes quite difficult with certain fuse designs unless under-relaxation is used. In this method, the new value of, for example, body temperature is calculated as

$$T'_b = T_b^{(old)} + u (T_b^{(new)} - T_b^{(old)}) \quad (14)$$

where $u < 1$, is the underrelaxation factor. Another factor which critically affects convergence is the value chosen for the initial estimate of body temperature. Fig.4 illustrates the effect of these parameters upon the number of iterations to converge for a particular fuse.

Use of an initial body temperature rise of 500°C and an underrelaxation factor of 0.2 has been found to give satisfactory convergence to date for all fuses studied, from zero current up to the minimum fusing current.

M-EFFECT After the element temperature distribution has been calculated the maximum temperature is compared with the melting temperature. For fuses with M-effect the situation is more complicated. It is not sufficient to consider that element rupture will occur if the temperature exceeds the melting point of the M-spot material. Even if this temperature is exceeded, the rate of diffusion may be so slow that rupture does not occur within the conventional time (t_c).

To account for this, a simple model for the diffusion process has been used, in which the depth of penetration of the diffusion interface is assumed to be [8]

$$z = \left[D_0 t \exp(-Q/T) \right]^{1/2} \quad (15)$$

where Q is the activation energy constant and D_0 is a diffusion constant. This permits the calculation of an 'effective melting temperature' which is the temperature which must be sustained in order for the element to rupture in the conventional time. If the element thickness at the M-spot location is z_c , the effective melting temperature is then obtained from (15), as

$$T_m = \frac{Q}{\ln \left(\frac{D_0 t_c}{z_c^2} \right)} \quad (16)$$

T_m is given from (16) in Kelvin. Values of D_0 and Q have been determined for several commonly-used types of M-spot material. This simple model appears to represent accurately the important processes affecting M-spot operation, and to date has given good results.

PROGRAM 'TRISE' AND TYPICAL RESULTS The models described have been incorporated in an interactive computer program TRISE which is one of a suite of programs [9] for fuse simulation. The program computes the temperature distribution for a fuse selected by the user, when tested under standard or non-standard conditions. A simulated test report is then output giving the predicted values of cold resistance, power loss, mV drop, end-cap temperature, body temperature, hotspot temperature plus a series of comments.

The Table below gives a comparison of predicted values at rated current with test values, for fuses selected from a low-voltage industrial range. In each case the first figure is a measured value and the second is the computed value.

Fuse rating (A)	Cold resistance ($\mu\Omega$)	mV drop	endcap rise ($^{\circ}\text{C}$)	body rise ($^{\circ}\text{C}$)
32	2950	110.7	43.0	39.0
	2570	110.7	42.3	44.5
100	610	70.0	32.0	29.0
	561	69.7	37.0	38.4
200	284	77.3	44.7	47.5
	299	77.8	46.9	50.4
315	218	91.6	58.6	64.0
	205	86.8	53.2	60.7
630	90	77.0	62.5	56.5
	90	71.1	56.6	56.7

The results above are typical in that the cold resistance and mV drop values are much more accurate than the temperature-rise values. This is not surprising as the latter values are very sensitive to slight changes in the test environment, such as the presence of draughts. The element temperature distributions are much more accurate and result in predicted minimum fusing currents very close to those which may be estimated from the measured time-current characteristic.

CONCLUSIONS The paper has described a method for simulating a temperature-rise test on a fuselink. The method uses analytical solutions as far as possible together with a linking iterative algorithm. The method has been found to converge for all fuses tried so far. Initial results correspond well with those observed in the test laboratory, but the program remains to be accurately 'calibrated' for all types of fuse by a more precise determination of the convection constants appropriate to the particular fuse geometry.

The structure of the program TRISE is such that improved models of the various processes involved may be substituted for the models described here, so that the accuracy of the predictions may be improved in the future.

REFERENCES

1. Leach, J.G., Newbery, P.G. and Wright, A. "Analysis of high-breaking-capacity fuselink prearcing phenomena by a finite-difference method". Proc IEE, vol. 120, 1973, pp 987-993.
2. McEwan, P.M. Ph.D. Thesis, Liverpool Polytechnic, 1975.
3. Carslaw, H.S. and Jaeger, J.C. "Conduction of heat in solids" (Oxford, 1959).
4. Guile, A.E. "The calculation of complete time-current characteristics of certain cartridge fuses with strip elements". Electrical Energy, 1956, pp 114-119.

5. Bewley, L.V. "Two-dimensional fields in electrical engineering" (Dover, 1963).
6. Incropera, F.P. and De Witt, D.P. "Fundamentals of heat transfer" (Wiley, 1981).
7. Smythe, W.R. "Static and dynamic electricity" (McGraw-Hill, 1950, p 257).
8. Crank, J. "The mathematics of diffusion" (Oxford, 1956).
9. Wilkins, R., Wade, S. and Floyd, J.S. "A suite of interactive programs for fuse design and development". Int. Conf. on Electric Fuses and their Applications, Trondheim, June 1984.

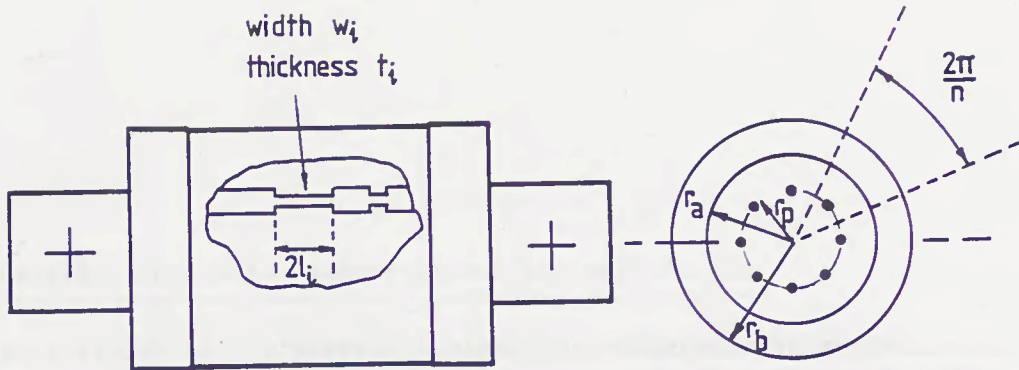


Fig 1. Basic geometry

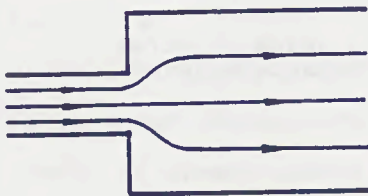


Fig 2. Current-flow field

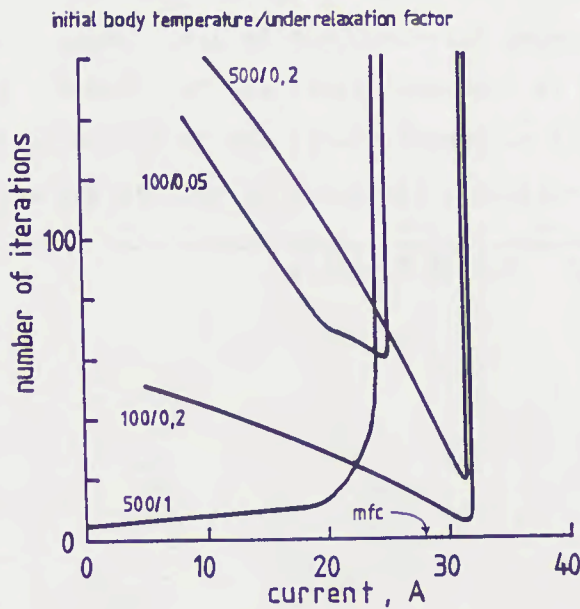


Fig 4. Convergence range

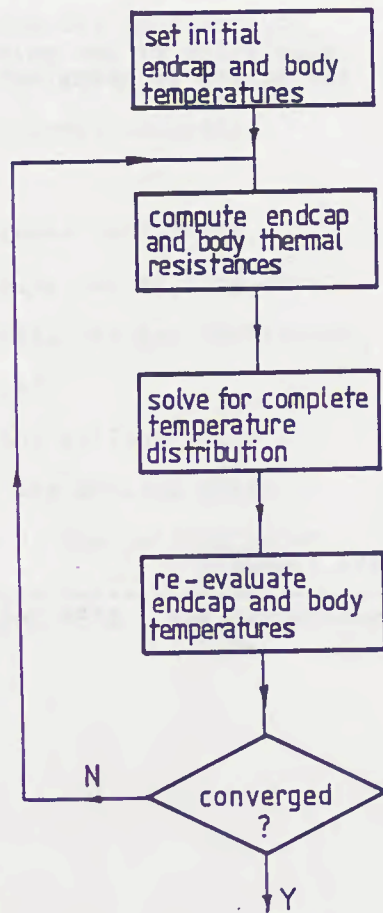


Fig 3. Iterative method

Calculations of models for adiabatic processes

1. calculation of the maximum duration of adiabatic melting
2. calculation of the melting integral value of wires and strips by means of material constants only

1984, February

Hans-Günter Rex , EFEN GmbH , D-6228 Eltville

Material constants: abbreviations and definitions

- A0 = resistivity of the conductor at 20 degrees centigrade
A1 = first order temperature coefficient of resistivity
A2 = second order temperature coefficient of resistivity
A3 = thermal conductivity k at 20 degrees centigrade
A4 = first order temperature coeff. of thermal conductivity
A5 = thermal capacity c at 20 degrees centigrade
A6 = first order temperature coeff. of thermal capacity
A7 = coeff. of linear thermal expansion
A8 = density d of the material at 20 degrees centigrade
A9 = resistivity of the liquid conductor at the melting point
B0 = melting temperature T_s of the material, degrees centigrade
B1 = latent heat of the conductor material
B3 = density of the solid conductor at the melting point
B4 = density of the liquid conductor at the melting point
W9 = resistivity of the solid conductor at the melting point

Material constants: numerical values

	dimension	Ag	Cu	sand
A ₀	$\Omega \cdot \text{mm}^2 / \text{mm}$.000016	.00001	
A ₁	1/K	.00377	.0039	
A ₂	1/K ²	5.7 E-7	6.7 E-7	
A ₃	W*s/(mm*s*K)	.428	.385	.0003
A ₄	1/K	- .00018	- .0008	
A ₅	W*s/(g*K)	.237	.377	.9
A ₆	1/K	.00013	.00024	
A ₇	1/K	.000024	.000020	
A ₈	g/mm ³	.0105	.00895	.002
A ₉	$\Omega \cdot \text{mm}^2 / \text{mm}$.00016	.00022	
B ₀	K	960	1083	
B ₁	W*s/g	105	214	
B ₃	g/mm ³	.00976	.00838	
B ₄	g/mm ³	.0091	.0079	
W ₉	*mm ² /mm	.0000801	.000103	
T ₀	K	20	20	

1. Calculation of the maximum duration of adiabatic melting

The loss of heat by conduction is connected with the temperature equalization by a simple model. As a result of this method maximum melting times for adiabatic melting processes are calculated. The time/current characteristic of wires and strips for a defined range of melting time can be given quickly and accurately.

Ermitteln der maximalen Zeiten für adiabatisches Schmelzen.

Mit einem einfachen Modell werden Wärmeleitung und Temperaturausgleich verbunden. Aus dieser Beziehung werden Schmelzvorgänge und Schmelzzeit für adiabatische Vorgänge bestimmt. Damit können Kennlinien für diesen Bereich sehr genau und schnell ermittelt werden.

Loss of heat and temperature equalization

dt=time interval

dT=deviation of temperature

T=temperature difference

x=length of wire section

d=density of the material

k=thermal conductivity

c=thermal capacity

m=mass of wire section

q=cross section of wire

We use the classical theory of the conduction of heat.

We consider only the conduction of heat along a wire. Heat losses from the wire to the environment, i.e. quartz sand, by conduction or radiation are neglected because they are remarkably smaller.

On a homogenous long wire there is a section 1, equal in length and adjacent to a section 2. The section 1 shall be warmer than the section 2. The temperature difference shall be T degrees.

In a time dt the heat dQ1 is flowing from the section 1 to the section 2. The temperature difference T shall not alter much.

Then we find for the conducted heat

$$1.1 \quad dQ_1 = (k \cdot q / x) \cdot T \cdot dt$$

A deviation dT of the temperature of intercept 1 requires an amount of heat dQ2.

$$1.2 \quad dQ_2 = m \cdot c \cdot dT = d \cdot q \cdot x \cdot c \cdot dT$$

We assume these amounts of heat dQ_1 and dQ_2 have the same value.

$$1.3 \quad dQ_1 = dQ_2 = dQ$$

The deviation dT decreases the temperature difference T . Section 1 will be cooled. Section 2 conducts the heat dQ_2 to the next section. The temperature of section 2 will therefore remain constant. We obtain an expression for the deviation of the temperature of section 1.

$$1.4 \quad dT = -dQ/(m*c) = -k*T*dt/(d*x^2*c)$$

We separate the variables T and t and obtain the differential equation

$$1.5 \quad dT/T = -k*dt/(d*x^2*c)$$

Integration of Eq. 1.5 gives the temperature difference T as a function of the time t :

$$1.6 \quad \ln(T/T_0) = -k*t/(d*x^2*c)$$

$$1.7 \quad T/T_0 = \exp(-k*t/(d*x^2*c))$$

A small table will be more informative. The length of the two sections is $x=0.1$ mm each. When the time t has passed the temperature difference has decreased from the value T_0 to the value T .

table 1

$x=0.1$ mm	$T/T_0(\text{Ag})$	$T/T_0(\text{Cu})$
$t=0.1$ ms	0.18	0.32
$t=0.01$ ms	0.84	0.89

Periods less than .01 ms do not alter very much the temperature difference T for lengths of $x=.1$ mm.

In the example mentioned above we have calculated with material constants of the temperature value 20 degrees centigrade. This limitation does not influence the result very much.

With this simple model maximum melting times for adiabatic processes in wires can be predicted very quickly.

In the following a more handy formula will be given. A wire of the length $2*x$ is heated up by a current. The temperature of the wire will be the highest in the middle and the lowest at both ends. We cut the wire in two sections with the length x .

In order to have maximum time values t_m the length of section 2 is set to zero. We solve the formula 1.6 and obtain the maximum time t_m

$$1.8 \quad t_m = (c*d/k) * x^2 * \ln(T_0/T)$$

$$(Ag) \quad t_m = 5.8 * x^2 * \ln(T_0/T)$$

$$(Cu) \quad t_m = 8.8 * x^2 * \ln(T_0/T)$$

According to Eq. 1.5 the temperature deviation decreases with decreasing temperature difference T . We also find that it is necessary to have a small temperature deviation dT in order to obtain a real value t_m of melting time. We accept $T_0/T=2$ for practical use. That yields the value $\ln(T_0/T)=0.7$.

$$t_m = (c*d/k) * (a/2)^2 * \ln(T_0/T)$$

$$1.9 \quad t_m = 90 * (c*d/k) * a^2$$

$$(Ag) \quad t_m = 0.5 * a^2$$

$$(Cu) \quad t_m = 0.8 * a^2$$

The values mentioned are of the following dimensions:

$$c \text{ (W*s/g*K)} ; \quad d \text{ (g/mm}^3\text{)} ; \quad k \text{ (W*s/mm*s*K)}$$

$$a \text{ (mm)} ; \quad t_m \text{ (ms)}$$

Thus we find

* Eq. 1.9 yields the relation between the length $a=2*x$ *
 * of a wire and the maximum time t_m for a heating process *
 * by current that can be handled as adiabatic process. *

table 2

	a (mm)	1	2	5	10	20	50
Ag	t_m (ms)	.50	2.0	12	50	200	1200
Cu	t_m (ms)	.80	3.2	20	80	300	2000

Eq. 1.9 is valid for wires, small strips or other material too.

* If we have a melting time t_s less than the maximum time t_m *
 * we can assume the heating by current an adiabatic process. *
 * In this case the melting integral will be a constant value. *

$$1.10 \quad \int_{t_0}^{t_s} i^2(t) dt = \text{constant}$$

Hence we can define a virtual melting time t_v as a function of a sine-wave current $i(t)$

$$1.11 \quad t_v = \text{constant}/i^2(t)$$

When the wire is embedded into crystallized sand we cannot expect the heat losses to be zero for great values of melting time.

We assume the heat transfer from the metal surface of the wire to the sand crystal to be faster than from one sand crystal to the next. Hence the thermal conductivity in the sand will not be influenced by the heat transfer from the metal to the sand.

According to Eq. 1.9 we calculate the maximum time t_x for neglectable heat losses from the wire into the sand. A realistic value for the length a in the sand is the mean diameter of the sand crystals, e.g. $a=0.4$ mm. We obtain

$$1.11 \quad t_x = 86 \text{ ms}$$

Hence we may say:

* If a wire embedded in crystallized sand is heated up by a *
 * current pulse $i(t)$ and if the melting time calculated by *
 * means of the melting integral value is less than 80 ms we *
 * can regard the melting time value as a correct value. *

If we have a small strip embedded in crystallized sand the greater surface will allow a greater heat transfer to the sand. The simplest approximation for the calculation of the maximum melting time $t_m(st)$ of a small strip of the width b embedded in sand of crystals of the mean diameter a is obtained by

$$1.12 \quad t_m(st) = t_m * a/b$$

2. Calculation of the melting integral value of wires or strips by means of material constants only.

Due to a defined current in a metallic conductor the temperature rise is derived from a simple model of an adiabatic process. A clever modification of the differential equation for temperature rise creates an equation in which a pure temperature function and a pure time function are connected with an expression of material constants of the conductor only. The combination of the temperature function and the expression of the material constants delivers very good information about the temperature rise of the conductor caused by short current pulses. As a limiting value we find the melting integral value for adiabatic melting.

Berechnen des Schmelzintegralwertes aus Materialkonstanten des Schmelzleiters.

Mit einem einfachen Modell wird die Temperaturerhöhung durch einen Strom in einem Leiter für adiabatische Vorgänge angegeben. Durch sinnvolles Umformen der Differentialgleichung entsteht eine Gleichung, in der eine reine Temperaturfunktion und eine reine Zeitfunktion durch einen Ausdruck mit Materialdaten des Schmelzleiters verbunden sind. Durch Verbinden der Temperaturfunktion mit dem Ausdruck für die Materialdaten ergibt sich eine gute Aussage über die Temperaturerhöhung eines Leiters durch kurze Stromimpulse und als Grenzwert der Schmelzintegralwert für adiabatische Vorgänge.

2.1 Physical background

Adiabatic heating processes are calculated under consideration of the influence of the temperature to material values.

A wire has a constant mass m , a length $x(T)$, a cross section $q(T)$, and the resistance $R(T)$. The wire is heated up by a current depending on the time. In a time dt an amount of heat Q is created in the wire.

$$2.1.1 \quad Q = R(T) \cdot i^2(t) \cdot dt$$

This amount of heat Q creates a deviation dT of the temperature of the wire.

$$2.1.2 \quad Q = c \cdot m \cdot dT = c \cdot d \cdot x \cdot q \cdot dT$$

The combination of Eq. 2.1.1 and Eq. 2.1.2 leads to

$$2.1.3 \quad R(T) \cdot i^2(t) \cdot dt = c \cdot m \cdot dT$$

Hence we obtain the deviation dT caused by the heat of a current pulse.

$$2.1.4 \quad dT = R(T) \cdot i^2(t) \cdot dt / (c(T) \cdot m)$$

2.2 Influence of the temperature to material constants.

The mass m of the wire does not depend on the temperature. When we leave the length x and the cross section q constant then the resistivity R_0 of the wire is a function of the temperature T .

$$2.2.1 \quad R_0 = A_0 \cdot f_1(T)$$

The temperature dependent resistance $R(T)$ can be written as

$$2.2.2 \quad R(T) = R_0 \cdot (x/q) = A_0 \cdot f_1(T) \cdot (x/q)$$

The function of the temperature of the resistivity is expressed by the beginning of a power series.

$$2.2.3 \quad f_1(T) = 1 + A_1 \cdot (T - T_0) + A_2 \cdot (T - T_0)^2$$

$f_1(T)$ is replaced sufficiently correct by the approximation

$$2.2.4 \quad f_1(T) = 1 - A_1 \cdot T_0 + (A_1 - 2 \cdot A_2 \cdot T_0) \cdot T + A_2 \cdot T^2$$

If a wire is heated up by a current the length and the cross section will not remain constant. Both depend on the temperature. The effect of the temperature is given sufficiently correct by the beginning of a power series too.

$$2.2.5 \quad x(T) = x_0 \cdot (1 + A_7 \cdot (T - T_0))$$

$$2.2.6 \quad q(T) = q_0 \cdot (1 + A_7 \cdot (T - T_0))^2$$

Eq. 2.2.5 and Eq. 2.2.6 inserted in Eq. 2.2.2 lead to a formula for the temperature dependent resistance $R(T)$ of the wire.

$$2.2.7 \quad R(T) = A_0 \cdot f_1(T) \cdot x_0 / (q_0 \cdot (1 + A_7 \cdot (T - T_0)))$$

The thermal capacity c depends on the temperature T too.

$$2.2.8 \quad c(T) = A_5 \cdot (1 + A_6 \cdot (T - T_0)) = A_5 \cdot (1 - A_6 \cdot T_0 + A_6 \cdot T)$$

Eq. 2.2.7 and Eq. 2.2.8 inserted in Eq. 2.1.4 lead to a formula for the temperature deviation dT by the heat Q .

$$2.2.9 \quad dT = \frac{A_0 \cdot x_0 \cdot i^2(t) \cdot dt \cdot f_1(T)}{q_0 \cdot (1 + A_7 \cdot (T - T_0)) \cdot A_5 \cdot (1 + A_6 \cdot (T - T_0)) \cdot m}$$

We collect the various temperature dependent expressions.

$$2.2.10 \quad f_2(T) = (1 + A_7 \cdot (T - T_0)) \cdot (1 + A_6 \cdot (T - T_0)) \\ = 1 + A_7 \cdot (T - T_0) + A_6 \cdot (T - T_0) + A_7 \cdot A_6 \cdot (T - T_0)^2$$

A short estimation with the temperature value T considered as the melting temperature T_s shows that we can neglect the last member of the sum in Eq. 2.2.10 .

$$A_7 \cdot A_6 \cdot (T - T_0)^2 = 0.00002 \cdot 0.0003 \cdot 1000000 = 0.006$$

The function $f_2(T)$ can be written simpler.

$$2.2.11 \quad f_2(T) = 1 + A_7 \cdot (T - T_0) + A_6 \cdot (T - T_0) \\ = 1 - (A_7 + A_6) \cdot T_0 + (A_7 + A_6) \cdot T$$

Eq. 2.2.4 and Eq. 2.2.10 give the temperature function $f_3(T)$.

$$2.2.12 \quad f_3(T) = f_1(T) / f_2(T) \\ = \frac{1 - A_1 \cdot T_0 + (A_1 - 2 \cdot A_2 \cdot T_0) \cdot T + A_2 \cdot T^2}{1 - (A_7 + A_6) \cdot T_0 + (A_7 + A_6) \cdot T}$$

We will have the expression $f_3(T)$ compact by the abbreviations

$$2.2.13 \quad W_1 = 1 - A_1 \cdot T_0 \quad W_3 = A_1 - 2 \cdot A_2 \cdot T_0 \\ W_2 = 1 - W_4 \cdot T_0 \quad W_4 = A_7 + A_6$$

and we obtain the temperature function $f_3(T)$

$$2.2.14 \quad f_3(T) = \frac{W_1 + W_3 \cdot T + A_2 \cdot T^2}{W_2 + W_4 \cdot T}$$

$f_3(T)$ is of no dimension.

We insert the function $f_3(T)$ in Eq. 2.2.9 and obtain an expression for the temperature deviation dT .

$$2.2.15 \quad dT = \frac{A_0 \cdot x_0}{q_0 \cdot A_5 \cdot m} * i^2(t) \cdot dt * f_3(T)$$

We replace the mass m which does not depend on the temperature by $A_8 \cdot q_0 \cdot x_0$ and obtain a material constant $C_1(M)$ of the dimension $K \cdot mm^2 / (A^2 \cdot s)$.

$$C_1(M) = A_0 / (A_5 \cdot A_8)$$

Eq. 2.2.15 changes into the equation

$$2.2.16 \quad dT = (C_1(M) / q_0^2) * i^2(t) \cdot dt * f_3(T)$$

2.3 Influence of the time on the temperature deviation

A time dependent current $i(t)$ is considered as a product of a maximum value i_0 and a time dependent function $f(t)$. $i(t)$ may be a single current pulse or a number of several different pulses. The shape of the pulses shall be known by calculation or by measurement. Then it is possible to have an approximation found by the function

$$2.3.1 \quad i(t) = i_0 \cdot f(t)$$

We insert the current $i(t)$ of Eq. 2.3.1 in Eq. 2.2.15 and obtain the temperature deviation dT

$$2.3.2 \quad dT = (C_1(M) / q_0^2) * i_0^2 * f^2(t) * dt * f_3(T)$$

The expression i_0 / q_0 represents the maximum current density D in the wire at normal temperature and does not depend on the time and not on the temperature. The current density D depends on the cross section of the wire. Thus Eq. 2.3.2 yields the following equation for the temperature deviation dT .

$$2.3.3 \quad dT = C_1(M) * D^2 * f^2(t) * dt * f_3(T)$$

$C_1(M) \cdot D^2 = C_2(M)$ depends on material constants only and is of the dimension K/s . We rearrange and obtain the relation

$$2.3.4 \quad dT / f_3(T) = C_2(M) * f^2(t) * dt$$

* The differential equation 2.3.4 is an equation in which a *
 * pure temperature function $f_3(T)$ and a pure time function *
 * $f(t)$ are connected with an expression $C_2(M)$ of material *
 * constants only.

2.4 Calculation of the temperature rise

Formula 2.3.2 enables us to determine the temperature rise of a single wire when a current pulse is going through. The length of the wire defines a maximum pulse length t_m according to Eq. 1.9. The following deduction shall be applied only to such lengths of wires.

We rearrange the variables T and t of Eq. 2.3.2 on different sides of the equal sign.

$$2.4.1 \quad dT/f_3(T) = (Cl(M)/q_0^2) * i^2(t) * dt$$

and we integrate

$$2.4.2 \quad \int_{T_0}^{T_n} \frac{dT}{f_3(T)} = \frac{Cl(M)}{q_0^2} * \int_{t_0}^{t_n} i^2(t) * dt$$

A current pulse flowing in a wire for the time t_n causes the temperature T to rise from a value T_0 up to a value T_n . T_0 shall be equal to or greater than 20 degrees centigrade and T_n shall be less than or equal to the melting temperature T_s . The time function $i(t)$ is known. The integral of the square of the current can be determined e.g. by the Simpson rule with sufficient accuracy. $Cl(M)$ is known too and the product can be calculated.

For practical use the integral of the temperature is determined by means of a programmable calculator.

At first we specify the initial temperature value T_0 at the moment t_0 . Then we calculate the temperature value T_n by varying the value T_n until the value of the integral is very close to the value of the product of the right side of Eq. 2.4.2 .

An example will show some values: material : Ag
 cross section : 1 mm²
 $i^2 * t$ -value : 20 000 A²*s

table 3 :	T_n :	183	471	950	degrees centigrade
	T_0 :	20	200	500	degrees centigrade

2.5 Temperature rise up to the melting temperature

We will determine the amount of energy needed for the heating of a wire beginning at the temperature value T_0 up to the value T_s of the melting temperature. No loss of heat shall be allowed. The melting temperature is known for every sort of metal and the value T_0 is known by the evaluated experiment. The function $f_3(T)$ is found according to chapter 2.2.

Eq. 2.4.2 is integrated from T_0 to T_s . The value of this definite integral is a characteristic constant $K_1(M)$ for each conductor. The value $K_1(M)$ is of the dimension K.

$$2.5.1 \quad K_1(M) = \int_{T_0}^{T_s} (dT/f_3(T))$$

For the deduction of $f_3(T)$ an acceptable simplification has been done due to Cu- and Ag-material. Hence the function $f_3(T)$ in Eq. 2.2.14 is valid only for Cu and Ag. When a different material is used the function $f_3(T)$ must be determined according to the deduction of chapter 2.2. The value of the integral in Eq. 2.5.1 will be determined in a simple way by means of the Simpson rule. We find

$$2.5.2 \quad K_1(\text{Ag}) = 408 \text{ K} \qquad K_1(\text{Cu}) = 441 \text{ K}$$

At the moment t_0 a current $i(t)$ begins to flow in the wire. At the moment t_n the melting temperature T_s is reached. For this period we calculate the integral over the function $f(t)$.

$$2.5.3 \quad F_1(t) = \int_{t_0}^{t_s} f^2(t) * dt$$

$F_1(t)$ is of the dimension s. We remember Eq. 2.3.2 and Eq. 2.4.2. When the temperature reaches the melting point we obtain according to Eq. 2.4.2

$$2.5.5 \quad K_1(M)/C_1(M) = K(M) = (i_0/q_0)^2 * F_1(t)$$

The deduction leads to a known result with the fact that $K(M)$ is calculated. We have

$$2.5.6 \quad K(M) = (i_0/q_0)^2 * \int_{t_0}^{t_s} i^2(t) * dt$$

$K(M)$ is of the dimension $A^2 * s / mm^4$

We apply the result to a wire of the cross section 1 mm^2 and we will have the important statement

- * If we have a short current pulse $i(t)$ and no heat losses *
- * along the wire and the value of the integral of the *
- * square of the current is equal to the value $K(M)$, the wire *
- * will be heated up to the melting point.

If there is no oxidation, this statement is equal to

- * If a short current pulse $i(t)$ results in a value less than *
- * $K(M)$, we will have no permanent deformation of the cross *
- * section of the wire. This means no aging will occur. *

This statement is equal to the following too.

- * If a short current pulse $i(t)$ results in a value greater *
- * than $K(M)$ there may be permanent deformation of the cross *
- * section of the heated wire.

Permanent deformation of the cross section of a heated wire means a change of the value of the cross section of the wire. When a strip is heated up by a current pulse then permanent deformation means either a change in the shape of the cross section with the value remaining constant or a change in both the shape and the value of the cross section. We may neglect the possibility of changing the value and not to change the shape of the cross section.

We can express the above mentioned facts in numerical values.

$$2.5.7 \quad K(\text{Ag}) = 63\,500 \text{ A}^2 * \text{s} / \text{mm}^4$$

$$K(\text{Cu}) = 82\,100 \text{ A}^2 * \text{s} / \text{mm}^4$$

We note that only the $i^2 * t$ -value is important and not the shape of the current pulse.

2.6. The effect of the latent heat

The melting process consists on both the heating of the material up to the melting point and the transition from the solid into the liquid state. The amount of heat needed for the transition is a material constant B_1 .

During the transition solid/liquid the melting temperature T_s remains constant. The resistivity of the solid wire is $R_s = W_9$. The resistivity of the liquid wire is $R_s = A_9$. The transition from the value W_9 to the value A_9 is assumed to be steady and not by a jump. We will describe this by a simple approximation using a linear function $R_s = f(Q)$ of the applied heat Q . The heat Q is thought of as the heat per mass unit, $(W*s/g)$.

We will calculate with a model once more.

At the temperature T_0 a wire shall have the length x_0 , the cross section q_0 and the mass m . The wire is heated up to the melting temperature T_s . The resistance rises up to the value $R(T_s)$. In the time dt a current pulse $i(t)$ is creating a heat dQ per mass unit in the wire at the temperature T_s .

$$2.6.1 \quad dQ = (R(T_s)/m) * i^2(t) * dt$$

At the moment t_0 no latent heat exists. At the moment t_1 the wire has become liquid. The total heat created in the period $t_2 - t_1$ is equal to the value B_1 . We may write the conditions

$$2.6.2 \quad t_1 = 0 \quad Q_1 = 0 \quad R_s = W_9$$

$$2.6.3 \quad t_2 \quad Q_2 = B_1 \quad R_s = A_9$$

Hence we state the following simple relation between the heat Q needed for the transition solid/liquid and the resistivity R_s .

$$2.6.4 \quad R_s = W_9 + (A_9 - W_9) * Q / Q_2 \\ = W_9 * \left(1 + \frac{A_9 - W_9}{W_9} * \frac{Q}{Q_2} \right)$$

We obtain the resistance of the wire in the period $t_2 - t_1$.

$$2.6.5 \quad R(T_s) = R_s * \frac{x(Q)}{q(Q)} = W_9 * \left(1 + \frac{A_9 - W_9}{W_9} * \frac{Q}{Q_2} \right) * \frac{x(Q)}{q(Q)}$$

We will have a linear function between the expression $x(Q)/q(Q)$ and the applied heat Q too.

At the melting point the solid wire has the density B_3 and the liquid wire has the density B_4 . A simple linear approximation for the change in the density during the transition process is found by the formula

$$2.6.6 \quad D(Q) = B_3 + (B_4 - B_3) * Q / Q_2 = B_3 * (1 + (B_4 / B_3 - 1) * Q / Q_2)$$

We shorten $(1 - B_4 / B_3) = W_5$ and obtain the density D depending on the applied heat Q

$$2.6.7 \quad D(Q) = B_3 * (1 - W_5 * Q / Q_2)$$

The mass m does not depend on the heat Q . Hence the change in the density is replaced by the change in the volume. Only the first order approximation will be done. For silver and copper material the value W_5 is less than 0.1. We may write

$$2.6.8 \quad 1 / (1 - W_5 * Q / Q_2) = 1 + W_5 * Q / Q_2$$

Therefore we obtain the volume depending on the applied heat Q .

$$2.6.9 \quad V(Q) = V(T_s) * (1 + W_5 * Q / Q_2)$$

A deviation W_6 of the length equals approximately the third part of the deviation W_5 of the volume, $W_6 = W_5 / 3$. According to chapter 2.2 we obtain

$$2.6.10 \quad \frac{x(Q)}{q(Q)} = \frac{x(T_s)}{q(T_s) * (1 + W_6 * Q / Q_2)}$$

$$= \frac{x_0}{q_0 * (1 + A_7 * (T_s - T_0)) * (1 + W_6 * Q / Q_2)}$$

Eq. 2.6.10 inserted in Eq. 2.6.5 yields the resistance of the wire at the temperature T_s during the transition solid/liquid.

$$2.6.11 \quad R(T_s) = W_9 * \left(1 + \frac{A_9 - W_9}{W_9} \frac{Q}{Q_2} \right) * \frac{x(T_s)}{q(T_s) * (1 + W_6 * Q / Q_2)}$$

We collect the expressions containing Q in Eq. 2.6.11 and establish a function $f_1(Q)$.

$$2.6.12 \quad f_1(Q) = \frac{B_1 + \frac{A_9 - W_9}{W_9} * Q}{B_1 + W_6 * Q}$$

The last equations inserted in Eq. 2.6.1 yield the part dQ of the latent heat created by the current i(t) in the wire at the moment t.

$$2.6.13 \quad dQ = fl(Q) * \frac{W9 \cdot x_0}{m \cdot q_0} * \frac{1}{1+A7*(Ts-To)} * i^2(t) * dt$$

We separate the variables t and Q and integrate. Then we obtain

$$2.6.14 \quad \int_0^{B1} \frac{dQ}{fl(Q)} = \frac{W9}{A8 * q_0^2} * \frac{1}{1+A7*(Ts-To)} * \int_{t1}^{t2} i^2(t) * dt$$

The integral over the heat dQ during the transition solid/liquid is a material constant K(Q) of the dimension W*s/g.

$$2.6.15 \quad K(Q) = \int_0^{B1} \frac{dQ}{fl(Q)}$$

The value of the integral of Eq. 2.6.15 is calculated by means of the Simpson rule. We find

$$K(Q) \quad Ag: 0.770 \text{ W*s/g} \quad Cu: 1.290 \text{ W*s/g}$$

We rearrange Eq. 2.6.14 and obtain according to Eq. 2.5.6

$$2.6.16 \quad (i_0/q_0)^2 * \int_{t1}^{t2} i^2(t) * dt = \frac{A8 * K(Q)}{W9} * (1+A7*(Ts-To)) = Q(M)$$

Q(M) is of the dimension A²*s/mm⁴.

Eq. 2.6.16 gives an important result.

* A wire which is heated up to the melting temperature will *
 * change from the solid into the liquid state if a short *
 * current pulse i(t) with no heat losses along the wire has *
 * a time integral of the square of the current equal to the *
 * value Q(M).

We consider a wire with the cross section 1 mm², insert numerical values in Eq. 2.6.16 and obtain

$$2.6.17 \quad Q(Ag) = 9840 \text{ A}^2 * \text{s} / \text{mm}^4$$

$$Q(Cu) = 12800 \text{ A}^2 * \text{s} / \text{mm}^4$$

2.7 The melting integral value for adiabatic process

We add both the heating up and the transition solid/liquid. This means to add Eq. 2.5.6 and Eq. 2.6.16. We set $t_s=t_l$ and we obtain

$$\left(\frac{i_0}{q_0}\right)^2 * \int_{t_0}^{t_1} f^2(t) * dt + \left(\frac{i_0}{q_0}\right)^2 * \int_{t_1}^{t_2} f^2(t) * dt =$$

$$2.7.1 \quad = \left(\frac{i_0}{q_0}\right)^2 * \int_{t_0}^{t_2} f^2(t) * dt = K(M) + Q(M) = Kq(M)$$

We find the numerical values:

$$2.7.2 \quad Kq(\text{Ag}) = 73340 \text{ A}^2 * \text{s}/\text{mm}^4 \quad Kq(\text{Cu}) = 97900 \text{ A}^2 * \text{s}/\text{mm}^4$$

Then the dynamic forces of the current flowing in the wire cut off the liquid cross section. For the melting integral value the liquid material is not to be vapourised by additional heat.

When the value of the cross section is different from the value 1 mm^2 then Eq. 2.7.1 changes into

$$2.7.3 \quad \int_{t_0}^{t_2} i^2(t) * dt = q_0^2 * Kq(M)$$

The resulting values $Kq(M)$ for Ag and Cu material have been found by many experiments to be correct.

Literature

1. D'Ans Lax: Taschenbuch f. Chemiker u. Physiker, Springer 1967
2. Mende/Simon: Physik, Gleichungen und Tabellen, Leipzig 1976
3. Johann: Elektrische Schmelzsicherungen, Springer 1982
4. Bogenschütz: Technische Unterlagen NH-Sicherungen, TV 112.02
5. Eisler Janos: Elektrische Anlagen, Budapest 1972
6. Conference papers: Liverpool 1976
 - McEwan/Warren: survey of numerical methods for solving time-varying fuse equations
 - McEwan/Wilkins: a decoupled method for predicting time-current characteristics of hrc fuses

APPLICATION OF THE ARC-PINCH-FORCES-INTERACTION THEORY TO THE
CALCULATION OF STRIATION MODULUS OF THE STRIP H.B.C. FUSES

T.Lipski

1. INTRODUCTION

The striation is a term used to determine of the plain wire or plain strip disintegrating kind due to a h.b.c. fuse operation under short-circuit conditions. The origin of name "the striation" / introduced by Nasiłowski [1] / outcomes from the picture of the remainder after uniform cross-section fuse-element disruption, which a typical example is shown in Fig.1. The tubewise fulgurite after short-circuit current interruption does indicate a nonconductive hole stretched between the fuse-link terminals. The hole is surrounded by the sintered quartz-sand grains mixed alternatively: with the fuse-element metal and then with the arc-plasma, according to the Fig.2. In result the photograph obtained after current interruption shows the typical streaks.

In our previous paper [3] the arc-pinch-forces-interaction / APFI / theory has been introduced to explain the number of arising streaks as result of wire disintegration. The paper also suggests the possible physics of the formation striated fulgurities.

It seems, the APFI-theory could also enlight the plain strip striation modulus according to the considerations given below.

2. CONDITIONS OF THE WHOLE STRIP STRIATION

The following Hibner's experimental conditions [4] shall be fulfilled in order to transmit the whole fuse-element strip into the streaks:

-the current-density j_t in kA/mm^2 by the instant of streak disintegration shall respond to the relation

$$j_t \geq \frac{4.6}{\beta} \quad /1/$$

where β - the strip cross-section in mm^2 ;
-the circuit specific energy, given by the ratio of the magnetic energy stored in circuit in the disintegrating instant t_t to the strip volume, shall satisfy the following inequality

$$\epsilon \geq 25 \frac{W}{\text{mm}^3} \quad /2/$$

If one of those conditions is not preserved, a part or several parts of the strip only passes into the streaks.

Usually the second condition is easy to satisfy, for only a fraction of the magnetic energy stored in circuit is sufficient to fit the inequality /2/. This is better described in the paper [3] for a wire striation, but for a strip striation the quantitative conditions are analogous. The more critical is

The author is with Gdańsk Technical University, Institute of High Voltages and Electrical Apparatus, Gdańsk, Poland

the condition defined by the relation /1/. In here rather the large prospective short-circuit currents are necessary, which in rare practical cases have take place, specifically for h.b.c. fuses above say 300A rated current.

3. SUMMARY OF APFI-THEORY

A brief summary of the APFI-theory given in [3] is shown in the Fig.3, but now referring to the strip striation. The essence of that theory is following: the number of pieces arising due to the strip disintegration is dictated by the equilibrium of the forces

$$F_a = F_{px} + F_{py} \quad /3/$$

in which F_a - the arc-force in a disruption directed along the strip-axis, F_{px} - the pinch-force acting perpendicularly to the strip-piece edges, F_{py} - the pinch-force presses also perpendicularly but along the flat surfaces of that piece. All these forces are working in pairs in opposite directions compressing the strip-piece. Obviously, the strip-piece by the instant t_f is completely liquified and is not so regular as it outcomes from the Fig.3. The flat surfaces in reality are wrinkled due to neighbouring sand grains. The slots in which the arcs are acting are not so regularly directed perpendicular to the strip-axis. But for the clearness we consider a regular model agreed with shown in the Fig.3. Indicated in it imagination refers to an instant existing just before the streak formation. Here all strip-pieces and all arcs are still in place of the initial strip.

4. SIMPLIFIED EVALUATION OF THE STREAKS MODULUS

A typical time duration of the transition of a strip into the streaks at normal short-circuit conditions of an a.c. network is of the several decades or hundreds microseconds. It is far shorter than the short-circuit time-constant. Hence one can assume the current magnitude / called in further "the transition current" / constant throughout the whole period of striation. The value of the transition current i_t , which is nearly equal to the cut-off current of a common h.b.c. fuse, is to determine using the following relations [5,6] :
for a.c.

$$i_t \approx 11 \sqrt[3]{S^2 K \cdot I_p} \quad /4/$$

and for d.c.

$$i_t \approx 1,4 \sqrt[3]{\frac{S^2 K \cdot I_u}{T}} \quad /5/$$

in which K - the material Mayer's constant, I_p - the prospective current, I_u - the steady-state short-circuit current, T - the time-constant.

Assuming the constant strip-thickness h and denoting the strip width by a one can easy rearrange above given relations as follows

$$i_t \approx C_1 a^{2/3} I_p^{1/3} \quad \text{for a.c.} \quad /6/$$

$$i_t = C_2 \cdot a^{2/3} \cdot I_u^{1/3} \quad \text{for d.c.} \quad /7/$$

in which C_1 and C_2 are some constants.

The arc-pressure is proportional to the current density square, assuming simplification that the arc cross-section is equal to the strip cross-section

$$p_a = k \cdot j_t^2 \quad /8/$$

where j_t - the transition current density, k - some constant. Remembering that $i_t = j_t S$ from /6/, /7/ and /8/ follows

$$j_t^2 = A \cdot a^{-2/3} \quad /9/$$

and

$$p_a = B \cdot a^{-2/3} \quad /10/$$

Thus the force F_a depends on the width at constant strip's thickness in a very simple form, viz. .

$$F_a = p_a \cdot a = B \cdot a^{1/3} \quad /11/$$

On the other hand the forces F_{px} and F_{py} per piece-length of the strip are defined by the relations derived in Appendix, which are rewritten below replacing i by i_t

$$F_{px} = \frac{\mu_0 i_t^2 \lambda}{4\pi a} \left(\ln \frac{4a^2 + h^2}{a^2 + h^2} + 2 \frac{a}{h} \operatorname{arctg} \frac{h}{2a} - \frac{a}{h} \operatorname{arctg} \frac{h}{a} \right) \quad /12/$$

$$F_{py} = \frac{\mu_0 i_t^2 \lambda}{4\pi h} \left(\ln \frac{4h^2 + a^2}{h^2 + a^2} + 2 \frac{h}{a} \operatorname{arctg} \frac{a}{2h} - \frac{h}{a} \operatorname{arctg} \frac{a}{h} \right) \quad /13/$$

where λ is the strip-piece length, which approximately is equal to the modulus of striation, because the initial length of the two-sided arcs is practically negligible in comparison with the length of the strip-piece itself.

Calculations for the practical range of ratios a/h , given in the chapter 5 in form of the examples, does indicate that the both forces are approximately equal, hence it follows

$$F_{px} + F_{py} \cong 2F_{px} \quad /14/$$

For a thin strip the relation /12/ gets the form

$$F_{px} = \frac{\mu_0 i_t^2 \lambda}{2\pi a} \ln 2 \quad /15/$$

Connecting dependences /6/, /7/ and /15/ easy is to write for both a.c. and d.c.

$$F_{px} = N' a^{1/3} \lambda \quad /16/$$

hence

$$2F_{px} = N a^{1/3} \lambda \quad /17/$$

where N' and N - the constants.

From relations /2/, /11/, /14/ and /17/ yields the following striation modulus

$$\lambda = \frac{M}{N} = \text{const} \quad /18/$$

If the strip thickness is kept constant then the S -changes are proportional to the changes of the strip width a . So arise the following conclusion: the striation modulus of the thin strips is independent from the cross-sectional area.

While the Hibner's experiments [4] made on strips of thickness 0.05-0.2mm and widths 2.5-15mm embedded in quartz sand of granularity 0.3-0.5mm and of standart packing density indicates on the following average modulus

$$\lambda_e = 3,1 \cdot S^{0,3} \quad /19/$$

Hence the exemplary errors outcoming from the relation /18/ in juxtaposition to the /19/ are as follows: for the 2 times greater strip-width the experimental modulus is abt 23% larger than according to APFI-theory, for the 3 times- it is abt 40% larger, but for 5 times,- already abt 63% larger.

Nevertheless the indicated errors, specifically for the practical range of the q/h ratio variations by this same S , are not so large ones taking into considerations the very simple model considered in this chapter.

5. INFLUENCE OF RATIO q/h ON THE STRIATION MODULUS

The formula /19/ does suggest the independence of the modulus on the ratio q/h by this same S . So arise an essential question, why only the cross-section but not the q/h -ratio has the influence on that modulus.

Looking on the possible answers one would suggest as an reason of the mentioned independence a game of the arc pressure relief and the pinch-forces for different q/h ratios.

Referring to the arc-pressure relief logically is that larger the q/h ratio greater the arc-pressure relief. It outcomes from the greater circumferences of the strip at larger ratios q/h by this same strip's cross-sectional area. Greater the strip's circumference larger the resultant cross-sectional area S_i of the interstices between the sand grains surrounded the strip.

Johann's qualitative relation on the pile up pressure of the arc channel existing during the arcing in a h.b.c. fuse [7] does'nt fit the situation in here under discussion, because we have to consider the very initial arcing stage. The plasma outflow into the interstices has been just started only, whereas in Johann's model a part of the arc-plasma is already in the sand of the thickness equalling to the fulgurite thickness. Hence it seems more correct is to assume that the pressure relief degree is invers proportional to the S_i . This assumption accords with the proportionality of the pressure relief to the gas-dynamic time-constant of the considered plasma outflow into the sand. This time-constant by this same strip's cross-section is reciprocal to the S_i , assuming for different q/h ratios this same initial outflow velocity. Because the current i_t for different q/h is also practically exactly this same it is easy to conclude, for the adiabatic heating, that there are the same outflow starting conditions

irrespectively of the area S . In result during this same very short time period, over which the relation /3/ leads to the defined number of streaks, the following proportionality shall be valid

$$p_a \sim \frac{1}{S_i} \sim \frac{1}{c} \quad /20/$$

where c is the strip's circumference. But for thin strips one can write

$$p_a \sim \frac{1}{c} \sim \frac{1}{a} \quad /21/$$

On the other hand the pinch-forces for the thin strips done by the relation /15/ are also reciprocal to the dimensions a . That's why, if for a certain dimension a this relation has been fulfilled, then for any arbitrary a it is also valid. But the obvious condition is that the a/h is rather large one, say several decades. Hence one can conclude that for thin strips the striation modulus should be independent of their cross-sectional area. In turn, if the strip thickness h is not negligible in comparison with its width a , the relations /12/ and /13/ shall be applied. It comes out even here that the pinch-forces again do fit the inverse proportional relation to the dimension a , however with the some approximation. The following examples could demonstrate this approximation.

Example 1. $S = 0.625\text{mm}^2 = \text{const}$ but we have two different strips: 1/ $a \times h = 2.5\text{mm} \times 0.25\text{mm} = 0.625\text{mm}^2$, $a/h = 10$ and 2/ $a \times h = 5\text{mm} \times 0.125\text{mm} = 0.625\text{mm}^2$, $a/h = 40$.

Results of calculations in the case 1/ are: from equation /12/ $F_{px1} = 0.55B_r$ and from equation /13/ $F_{py1} = 0.52B_r$, where $B_r = \frac{\mu_0 I^2}{4\pi}$

Results of calculations in the case 2/ are: $F_{px2} = 0.273B_r$, $F_{py2} = 0.313B_r$.

The circumference ratio $c_1/c_2 = 1.37$. But the ratios $F_{px1}/F_{px2} = 2$ and $F_{py1}/F_{py2} = 1.67$. So the conclusion is that the diminishing of the pinch-forces in the case 2/ in comparison with the case 1/ is approximatively compensated by the force F_a lowering. The latter lowering is proportional to the circumference ratio.

Example 2. Case 1/: $a \times h = 3.75\text{mm} \times 0.2\text{mm} = 0.75\text{mm}^2$, $a/h = 18.8$. Case 2/: $a \times h = 15\text{mm} \times 0.05\text{mm} = 0.75\text{mm}^2$, $a/h = 300$. Results of calculations in case 1/ are: $F_{px1} = 0.367B_r$, $F_{py1} = 0.335B_r$. Results of calculations in case 2/ are: $F_{px2} = 0.0925B_r$, $F_{py2} = 0.105B_r$. Then the ratio $c_1/c_2 = 3.9$. But the ratios $F_{px1}/F_{px2} = 3.98$ and $F_{py1}/F_{py2} = 3.2$. Again the pinch-forces diminishing is nearly compensated by the force F_a lowering.

6. FINAL REMARKS

Despite some differences between the results described by the theoretical relation /18/ and experimental one /19/ it seems that herein given speculations one can recognize as a possible explanation of the magnitude of the modulus of the strip striation occuring under short-circuit current in the h.b.c. fuses. The physics of the formation of the rythmical fulgurite structure shown in the Fig.2 is rather similar to that of the wire striation [3], thus it was'nt described here again.

7. ACKNOWLEDGMENT

Author would like to thank dr.K.Jakubiuk for the derivations given in the Appendix to this paper.

8. REFERENCES

- [1] Nasiłowski J.: Unduloids and striated disintegration of wires. Exploding Wires. N.Y. 1964, vol.3. Plenum Press. Editors Chase W.G., Moore H.K.
- [2] Hibner J.: Gradient resistance method of calculations of the overvoltage crest value generated by the short-circuit current-limiting fuses. / in Polish /. Ph.D.Thesis. Gdańsk Technical University. 1973.
- [3] Lipski T.: On the theory of the striated fuse-wire disintegration. IEEE Trans. vol.PS-10. No4. Dec, 1982. p.339.
- [4] Hibner J.: The number of arcs initiated during striated disintegration of the uniform strip h.b.c. fuse-elements at a.c. short-circuit current interruption. Int.Conf. on " The Electric Fuses and Their Applications". Trondheim. 1984.
- [5] Hibner J.: Calculative method of determination of the cut-off current characteristics of fuses at a.c. / in Polish/. Wiad.Elektr. 1980. No.1, p.7.
- [6] Hibner J.: Determination of the cut-off current characteristics of fuses by calculative method. P.I.D.c. current. Wiad.Elektr. 1978.No.3. / in Polish/
- [7] Johann H.: Interrupting arcs in electric fuses with graded quenching medium./ in German /. Siemens Forsch.- u. Entwickl.- Ber. vol.10.Part 3. 1981. No.3. p.139.



Fig.1 Photograph of fulgurite^t after short-circuit current interruption by a h.b.c. fuse within strip element axh = 5mmx0.1mm. Circuit conditions: $I = 3.8\text{kA}$ /RMS/, $U = 230\text{V}$, 50Hz^p, p.f. = 0.5 [2]

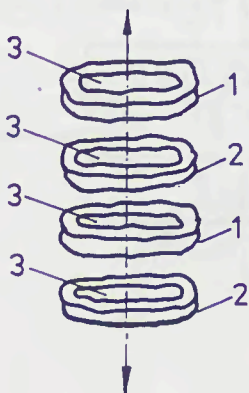


Fig.2 Situation after strip disintegration. Arrows show the original wire axis /1/ parts filled up by the arc plasma mixed with sand, /2/ parts filled up by the molten metal mixed with sand and /3/ nonconductive holes

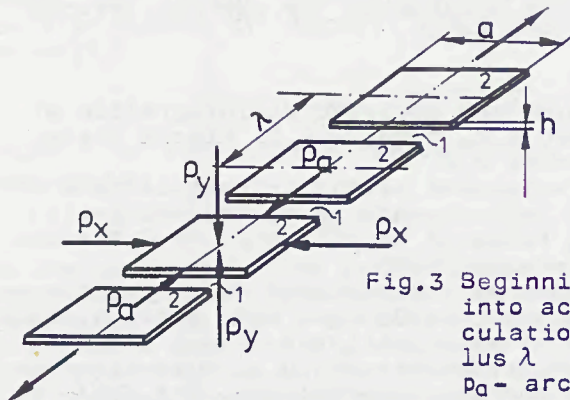


Fig.3 Beginning of the striation taken into account in simplified calculations of the striation modulus λ

p_a - arc-pressure; p_x - pinch-pressure on edges; p_y - pinch-pressure on flats; 1 - slots with arcs; 2 - strip pieces; a, h - dimensions

APPENDIX

We consider pinch-forces acting on the edges F_{px} and the flats F_{py} of a fuse-link strip according to the Fig.1A. The flux density differential in both axis in the point $/ x_0, y_0 /$ can be described as follows

$$dB = \frac{\mu_0 I dx dy}{2\pi ah [(x_0-x)^2 + (y_0-y)^2]^{3/2}}$$

$$dB_x = dB \frac{x_0 - x}{[(x_0-x)^2 + (y_0-y)^2]^{3/2}}$$

$$dB_y = dB \frac{y_0 - y}{[(x_0-x)^2 + (y_0-y)^2]^{3/2}}$$

Assuming in approximation

$$B_x(x_0, y_0) \cong B_x(0, y_0)$$

$$B_y(x_0, y_0) \cong B_y(x_0, 0)$$

one can get the following relations for the flux densities

$$B_x(x_0, y_0) = \int_{-\frac{a}{2}}^{\frac{a}{2}} \int_{-\frac{h}{2}}^{\frac{h}{2}} dB_x = \frac{\mu_0 I}{4\pi ah} \left\{ \left(x_0 + \frac{a}{2}\right) \ln \frac{\left(x_0 + \frac{a}{2}\right)^2 + \left(y_0 + \frac{h}{2}\right)^2}{\left(x_0 + \frac{a}{2}\right)^2 + \left(y_0 - \frac{h}{2}\right)^2} + \right.$$

$$+ \left(x_0 - \frac{a}{2}\right) \ln \frac{\left(x_0 - \frac{a}{2}\right)^2 + \left(y_0 - \frac{h}{2}\right)^2}{\left(x_0 - \frac{a}{2}\right)^2 + \left(y_0 + \frac{h}{2}\right)^2} + (2y_0 + h) \operatorname{arctg} \frac{a\left(y_0 + \frac{h}{2}\right)}{\left(y_0 + \frac{h}{2}\right)^2 + \left(x_0^2 - \frac{a^2}{4}\right)} -$$

$$\left. - (2y_0 - h) \operatorname{arctg} \frac{a\left(y_0 - \frac{h}{2}\right)}{\left(y_0 - \frac{h}{2}\right)^2 + \left(x_0^2 - \frac{a^2}{4}\right)} \right\}$$

$$B_y(x_0, y_0) = \int_{-\frac{a}{2}}^{\frac{a}{2}} \int_{-\frac{h}{2}}^{\frac{h}{2}} dB_y = \frac{\mu_0 I}{4\pi a h} \left\{ \left(y_0 + \frac{h}{2} \right) \ln \frac{(x_0 + \frac{a}{2})^2 + (y_0 + \frac{h}{2})^2}{(x_0 - \frac{a}{2})^2 + (y_0 - \frac{h}{2})^2} + \right. \\ \left. + \left(y_0 - \frac{h}{2} \right) \ln \frac{(x_0 - \frac{a}{2})^2 + (y_0 - \frac{h}{2})^2}{(x_0 + \frac{a}{2})^2 + (y_0 - \frac{h}{2})^2} + (2x_0 + a) \operatorname{arctg} \frac{h(x_0 + \frac{a}{2})}{(x_0 + \frac{a}{2})^2 + (y_0 - \frac{h}{2})^2} - \right. \\ \left. - (2x_0 - a) \operatorname{arctg} \frac{h(x_0 - \frac{a}{2})}{(x_0 - \frac{a}{2})^2 + (y_0 - \frac{h}{2})^2} \right\}$$

It can be demonstrated that the errors by that assumptions is not greater than 10%.

The total average pinch-forces are described by the following dependences

$$F_y = l \int_0^{\frac{h}{2}} B_x dI'$$

$$dI' = \frac{1}{a} dy_0 = \frac{1}{h} dy_0$$

$$F_y = \frac{Il}{h} \int_0^{\frac{h}{2}} B_x(y_0) dy_0 = \frac{\mu_0 I^2 l}{4\pi h} \left[\ln \frac{4h^2 + a^2}{h^2 + a^2} + 2 \frac{h}{a} \operatorname{arctg} \frac{a}{2h} - \frac{h}{a} \operatorname{arctg} \frac{a}{h} \right]$$

$$F_x = l \int_0^{\frac{a}{2}} B_x dI''$$

$$dI'' = \frac{1}{a} dx_0 = \frac{1}{a} dx_0$$

$$F_x = \frac{Il}{a} \int_0^{\frac{a}{2}} B_x dx_0 = \frac{\mu_0 I^2 l}{4\pi a} \left[\ln \frac{4a^2 + h^2}{a^2 + h^2} + 2 \frac{a}{h} \operatorname{arctg} \frac{h}{2a} - \frac{a}{h} \operatorname{arctg} \frac{h}{a} \right]$$

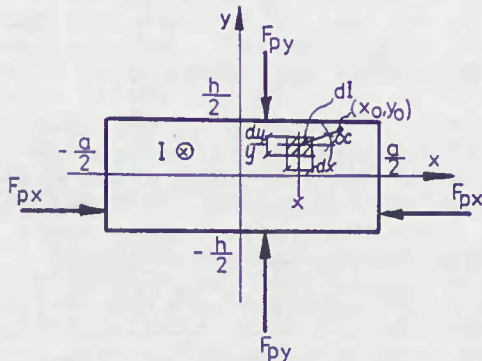


Fig. 1.1

THE NUMBER OF ARCS INITIATED DURING STRIATED DISINTEGRATION OF THE UNIFORM STRIP h.b.c. FUSE-ELEMENTS AT a.c. A SHORT-CIRCUIT CURRENT INTERRUPTION

J. Hibner

PRINCIPAL SYMBOLS

- d - fuse-wire diameter, mm
 h_u - unduloid disintegration modulus of wire-fuse-element, mm
 h_s - striated disintegration modulus of wire fuse-element, mm
 M_f - striated disintegration modulus of strip fuse-element, mm
 i_f - let-through current limited by fuse, A
 j_f - current density in fuse-element, A·mm⁻²
 l - fuse element length, mm
 L - circuit inductance, H
 n - number of arcs appearing at striated disintegration
 S_a - fuse-element cross-section area, mm²
 S_s - area of smallest short-circuit cross-section of fuse element, mm²
 ϵ - magnetic field energy pervolume unit required for copper or silver fuse-element at multi-arc disintegration, W·mm⁻³
 U_p - arc overvoltage peak value on all arcs at striated disintegration, V

1. INTRODUCTION. Since a very long time now-attempts have been made to explain the operation of h.b.c. fuses in the short-circuit conditions. The present state of knowledge does not permit a theoretical explanation of all the h.b.c. fuse-element disintegration phases. Only some of the phenomena of the element deformation and disintegration due to the short-circuit current have been explained by a number of theories [1,2,4,7÷10,12]. It is the result of the still incomplete investigations in the mentioned field. This paper gives some supplementary information in this respect.

2. DISINTEGRATION OF FUSE-ELEMENTS. Studies contributed to the establishment of two basically controversial points of view on the course of the phenomena which accompany the operation of h.b.c. fuses. The first one, according to Mayer [9], known for a number of decades, says: the whole fuse-element charges from its solid state into plasma through a liquid state in the result of extensive temperature rise caused by the Joule's heat. The second one, commenced by Kleen [7],

Mr Hibner is with the Institute of High Voltages and Electrical Apparatus. Gdańsk, Technical University, Poland

does suggest that only some parts of the fuse-element change into plasma whilst the rest of the fuse-elements remains in its solid or liquid state.

2.1. Disintegration of wire fuse-elements. Phenomena relating to the disintegration of wire elements placed in a fine sand have been relatively quite precisely investigated [e.g. 2, 4, 10]: at not very high current densities the cylindrical wire transit into an unduloid shape, during the pre-arc time, and then over the arcing time it is in form of drops detached by the arcs. The average unduloid modulus was found [10,11] to follow from the action of the surface tension forces and the pinch-forces and is determined by the relation:

$$h_u = 5.3d \text{ for } j_{Ag} < 900d^{-0.78} \quad (1)$$

Extensive study by Nasikowski [10,11] has shown that at high short-circuit currents wire elements form no unduloids but disintegrate according to the segment mechanism, the so-called striated mechanism. According to it, the striation modulus is constant and is given by

$$h_s = 0.555 + 2.08d \text{ for } j_{Cu} \geq 4300d^{-0.68} \quad (2)$$

After the current interruption remains a fulgurite i.e. the sintered element metal with sand. In the case of streak disintegration the fulgurite involved has a laminar structure composed of rings streaks of a bright colour - metal rests - and of a dark colour - post - arc rests (see Fig.1).

The possible cause of striation is explained by Nasikowski by mechanical vibration of the wire, to which the fuse element is subjected at the pre-arc time. Theoretical studies of this phenomenon have shown, that at a high-density current flow through the wire, mechanical vibration generated by magnetothermoelastic processes causing lateral cutting stresses may appear in that wire [2].

The initial stage of striation recently has been done by X-rayflash studies by Arai [1] at the current-densities more than 14 kA/mm^2 . The exposition was abt. every $15 \mu\text{s}$. From the Arai's photographs the disintegration shows a segment nature with a determined modulus. In here the wire has in no case any shape that would resemble an unduloid (Fig.1). The very beginning of the wire striation after Arai is caused by the wire thermal buckling. But this buckling was also very clear observed previously and described in [3].

2.2. Disintegration of strip fuse-elements. The plain strip fuse-elements disintegration has been relatively less investigated. But it is known that strip fuse-elements also disintegrate according to the striated mechanism. Now the fulgurites have a similar structure to that from wire fuse-elements. The fulgurite after a strip element has an oval cross section whereas after the wire element a round cross-section (Fig.1).

Before a strip fuse-element undergoes striated disintegration

it also gets waved by a thermal shock. The wave length is considerably bigger than the striation modulus and depends not on the width but on the thickness of the fuse-element. The wave amplitude increases with the current-density increasing [5].

The causes of striated disintegration of strip fuse-elements are still more complicated than those of wire fuse-elements. Because of the limited place the author confined to give the results of study of disintegration modulus without any explanation of the physical causes. The dependence of the striated disintegration modulus on the strip width at constant thickness [6] is only a special case. At present, results will be given with a high degree of generalization for different dimensions of the fuse element.

3. LABORATORY DETERMINATION OF THE DISINTEGRATION MODULUS

3.1. Model fuses. Fuses with a cylindrical 26 mm dia., chamber (Fig.2) were used for the tests. The element active length was 60 mm. The construction makes taking readable X-ray pictures easy.

3.2. Strip fuse-elements. The elements were cut off from a copper band 99.9% Cu. The fuse elements had a length of 60 mm, a width of 2.5; 5; 7.5; 10; 12.5 and 15 mm and a thickness of 0.052; 0.1; 0.144; and 0.184 mm. It gives the cross-sectional areas within the range from 0.13 to 2.76 mm². All the tests were made on elements of the same material as regards its chemical composition, thermal treatment and thickness tolerance. Fuse-elements was selected within similar width of tolerance of $\pm 2\%$.

3.3. Preparation of the fuse-elements. After putting the fuse-elements in their place the fuses were filled with fine quartz sand 99.24% SiO₂ having a granulation of 0.4 to 0.6 mm and a mass density² of the grain material equal to 2.85 g/cm³ or 1.64 g/cm² of the loose sand. In one corner of the cover there was an opening closeable by means of a nut for filling the fuse with sand. The package of the sand was carried out in a shock shaker having a pitch of 20 mm and a cycle of 48 shocks per minute. The shaking process lasted 5 minutes. The fuse shaking method applied in the tests ensured reliable and repeatable filling of them with sand as confirmed by the fact that the increase in weight amounted to abt. 20 to 22% in comparison with the weight before the shaking operation.

3.4. Test circuit. The tests were carried on in a.c. circuit with prospective currents from 3.8 to 37,4 kA at a voltage of 230 V, 50 Hz and $\cos\varphi = 0.2$. Three dry transformers of special construction having a power of 500 kVA and a primary voltage of 15 kV and a secondary voltage of 220 V were applied. In order to avoid any considerable differences in the disintegration current for fuse-elements with the same dimensions the tests were carried out at symmetrical short-circuit current at the first sine half-wave.

Measurement of the let-through (disintegration) current was taken by a loop record with a non-inductive shunt of resistances 1 or 5 m Ω . Measurement of the voltage at fuse-element were taken by a cathodic oscillograph with RC potential divider.

4. TEST RESULTS. All 20 varieties of fuse-elements were subjected to the tests and 10 tests on each type of element were made. The disintegration current density amounted to from 6 to 18 kA/mm², and the disintegration time from 10 to 120 μ s. After each test an X-ray picture was taken of the fuses at a scale of 1:1. Then, the X-ray pictures served for determining the disintegration modulus for the strips (Fig.3). In some cases (at small cross-sectional area of the strips) the structure of the fulgurite involved was highly brittle and there was no possibility of taking it out of the fuse without breaking into pieces.

Similarly as it was the case with wire fuse-elements the fulgurite along the longitudinal axis represented a tube with a characteristic laminar structure having an oval opening, being composed alternately of bright-metalic streaks and dark ones where the arc burned. The distance between the bright and dark streaks was taken as the disintegration modulus. The average modulus was established on the basis of the number of streaks at an element length of a rhythmic, regular, disintegration with a disintegration modulus close to average.

It is to be stressed that a probable number of streaks was assumed for the calculations, and not the true number of them which may appear in the first moment of a sudden disintegration of the element. It is possible that their number may be different at the arc ignition moment than that at the arc quenching instant because of the fact that some of the arcs could get connected and show longer arc breaks in the X-ray pictures. That is why only strip lengths with regular disintegration were taken into consideration.

Tests, during which the disintegration process was limited by shunting the fuse with a switch at the moment when the voltage peak value appeared at it, may be considered as a verification of the above problem to some extent. The disintegration modulus calculated in such case was the same as in the case of a fuse after breaking the current - without shunting.

The modulus as calculated on the basic of the X-ray pictures were subjected to statistical elaboration and the confidence interval for the average value of the modulus at a confidence level of 0.95. Fig.4 shows the range as determined by the confidence regions of the worked-out data collection.

5. DETERMINATION OF THE GENERAL DISINTEGRATION MODULUS DEPENDENCE. Whilst taking readings of the disintegration modulus of various elements it has been found that strips of the same

cross-sectional area in spite of their different widths and thicknesses have the same modulus from the statistical point of view.

This means that it is only the cross-sectional area of the fuse-element that can be taken as a parameter for characterizing the disintegration modulus, and the width and thickness of the strip merely effects the volume of the fulgurite.

The below given dependence (3) has been obtained for the collection of the disintegration modulus mean values in dependence on the cross-section of the strip by the method of least squares:

$$\bar{M}_f = AS^B = 3.07 S^{0.256} \quad (3)$$

The A and B parameters may change within the following limits $A = 2.78$ to 3.19 mm^{-B} and $B = 0.2101$ to 0.3015 in order that the dependence (3) has its course still on the determined range of average values.

In the case of strip fuse-elements of a small width of less than 1 mm the disintegration modulus should be close to the wire elements disintegration modulus according to formula (2) - Fig.4, curve 2. This condition may be fulfilled by the dependence (3) but with a slightly different exponent B, namely:

$$\bar{M}_f = 3.07 S^{0.3} \quad (4)$$

The above formula is one of the permissible deviations from the least squares curve (3), but it is of a more general character.

Whilst investigating the dependence of the modulus on the disintegration current density no logical dependence has been found. It may be stated only that in order to get a regular disintegration with a probable average modulus according to formula (4) it is required that the current density shall satisfy the following inequality:

$$j \geq 4660 S^{-0.29} \quad (5)$$

This condition requires the fuse-element to attain a high temperature in a shorter time than 5 ms.

Further tests show that the magnitude of available energy per element unit volume for rapid and regular disintegration at the whole length of the element shall correspond to the following relation.

$$\epsilon = Li_f^2 : 2Sl \geq 25 Ws.mm^{-3} \quad (6)$$

It should be added that the conditions (5) and (6) must be complied with simultaneously in order that the formula (4) gives good results. If only the condition (5) is fulfilled, the element may not disintegrate into streaks, but undergo common melting as it was found to take place e.g. in a circuit with a voltage of 24 V and $L \approx 0$ [6].

On the other hand fulfillment of the condition (6) only also leads to a different disintegration than the regular striated one. In such case a non-modulus disintegration of the strip may take place (Fig.5).

6. NUMBER OF ARCS APPEARING AT STRIATED DISINTEGRATION.

When the disintegration module is known according to formula (4) it is possible to determine the number of arcs burning at the fuse-element length following from that modulus.

$$n_a = 1 : M_f \quad (7)$$

The number of arcs calculated on the basis of formula (7) may have a deviation of ± 1 depending on the fuse-element length and distribution of the interruptions along strip. The formula (7) may also find application for fuse-element with long narrow strip parts of uniform cross-section area S_s , but only when the following condition is fulfilled:

$$S_s < 0.65 S \quad (8)$$

Condition (8) ensures that it is only the narrow portions of the strip will undergo streak disintegration, as it is shown in the Figure 6.

A comparison of the results based on calculation with those on the measurement of the number of arcs burning at striated disintegration in the carried out tests has proved a conformity of the calculation with a statistical deviation of up to 20 %.

7. CONCLUSIONS

- 1) In the case of fuses with strip elements of an uniform cross-sectional area the calculated on the basis of the formula (7) number of arcs appearing at the element disintegration is comparable with the results of experiment, provided that the conditions (5) and (6) are complied with.
- 2) The disintegration module as well as the number of arcs can be calculated with a good result for strip fuse-elements with constrictions in the strip of a uniform cross-section area. In this case, however, the condition (8) must be also satisfied in addition to conditions (5) and (6).
- 3) Fuse-element strips of a relatively large width of more than 12 mm may disintegrate according to a non-modulus mechanism, if the condition (5) is not satisfied - Fig. 5.
- 4) Taking into account the maximum statistical errors, it may be assumed that the wire disintegration modulus as given by Nasikowski according to formula (2) may also find application for the disintegration of strips. In such case the calculated module will be slightly shorter than that in reality (Fig.4).
- 5) Knowledge of the number of striated disintegration arcs makes calculation possible of the arc ignition voltage at a single streak in the process of over-voltage generation. But

it is necessary to know the peak voltage at the disintegrating strip fuse-element. This voltage one can calculate on the basis of the following formula [6]:

$$U_p = \rho_o \cdot l \sqrt{\frac{i_f}{S_s}} = \rho_o \cdot l \sqrt{j}$$

where: ρ_o - fuse-element disintegration resistivity at peak voltage and let-through current instant, $\rho_{ow} = 0.5 \Omega A^{0.5}$ - for wire element, $\rho_{os} = 0.4 \Omega A^{0.5}$ - for strip element. As proved by the author in his numerous papers the above formula gives good results at conditions (5) and (6) satisfied in comparison with measurements, the maximum statical error being up to $\pm 15\%$.

REFERENCES

- [1] S.Arai, Int.Conf.Electric Fuses and Their Applications, Liverpool, GB, 1976. p.50
- [2] H.Baxter, Electric fuses. London, 1950.
- [3] O.Bethge, Ann.Phys. 1931. p.475.
- [4] I.Faccini L'Elettrotecnica 1967 No.7, p.446.
- [5] J.Hibner, Int.Symp.Switching arc Phenomena Lodz, 1970, p.226.
- [6] J.Hibner, Ph.D.Thesis. Technical Univ. Gdańsk, Poland 1973
- [7] W.Kleen, Ann.Phys. 1931, p.579.
- [8] T.Lipski, IEEE Transactions on Plasma Science Vol.PS-10, No.4, 1982, p.339.
- [9] G.J.Meyer, Zur Theorie der Abschmelzsicherungen. Munchen, 1906.
- [10] J.Nasiłowski, Ph.D.Thesis Electrotechnical Institute, Warszawa, Poland 1965.
- [11] J.Nasiłowski, Int.Conf. Electric Fuses and Their Applications, Liverpool, GB 1976. p.122.
- [12] P.Zimny, Archiwum Elektrotechniki. 1973, No.1, p.169. Poland.

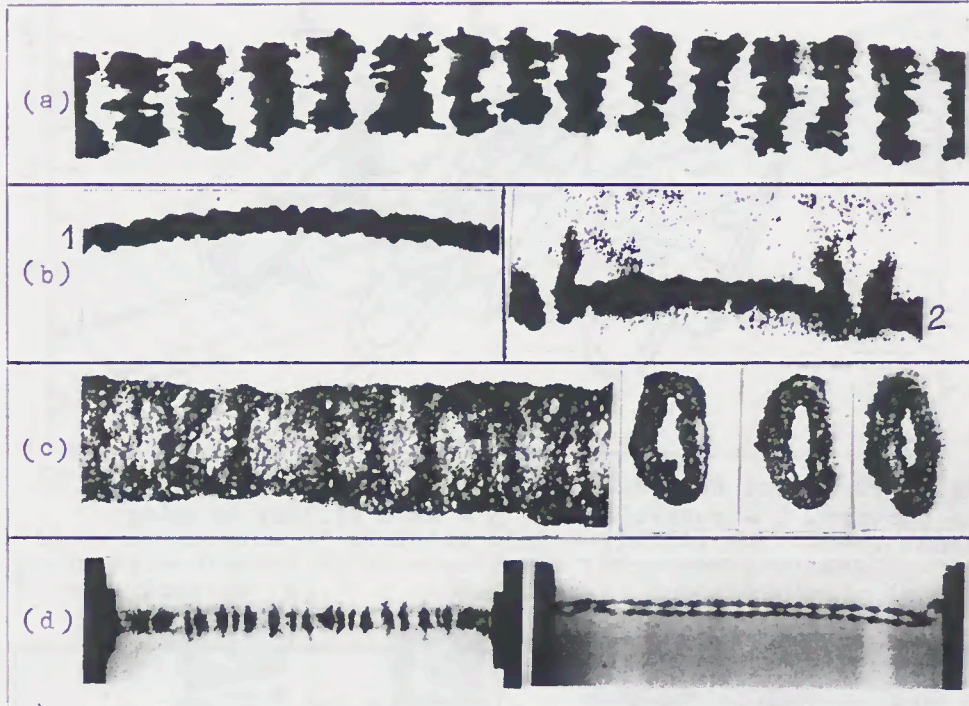


Fig.1. Fulgurities remaining in the h.b.c. fuse after multiple arcing quenching (a) typical X-ray photograph (section) of the disintegration modulus (Ag wire, $d = 0.3 \text{ mm}$, $j_f = 3 \text{ kA mm}^{-2}$ [10]), (b) X-ray flash photographs of deformations and disruption of Ag wire ($d = 0.5 \text{ mm}$, $j_f = 4.14 \text{ kA mm}^{-2}$), 1 - $t_x = 38 \text{ μs}$, 2 - $t_x = 68 \text{ μs}$, t_x - the time from the point 0 on the voltage wave on the oscillograph to the instant the photograph was taken, (c) photograph (section) of the striated (modulus) fulgurite (Cu strip fuse-element with uniform cross-sectional dimension $5 \text{ mm} \times 0.1 \text{ mm}$, $j_f = 8 \text{ kA mm}^{-2}$), (d) X-ray photograph of the disintegration modulus (Cu strip, $5 \text{ mm} \times 0.1 \text{ mm}$, $j_f = 8 \text{ kA mm}^{-2}$).

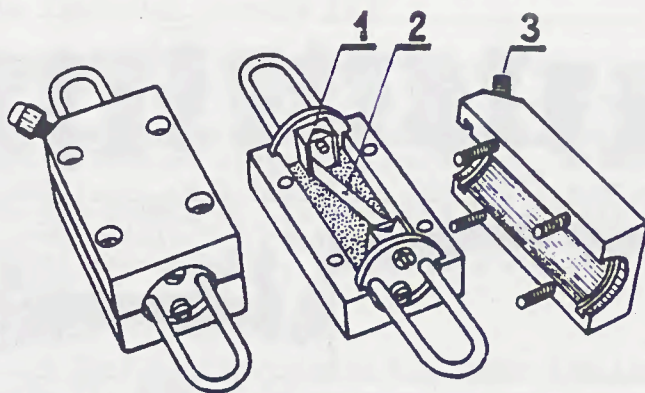


Fig. 2. Fuse-link as used in test.
1 - contact, 2 - fuse-element, 3 - sand filling opening channel.

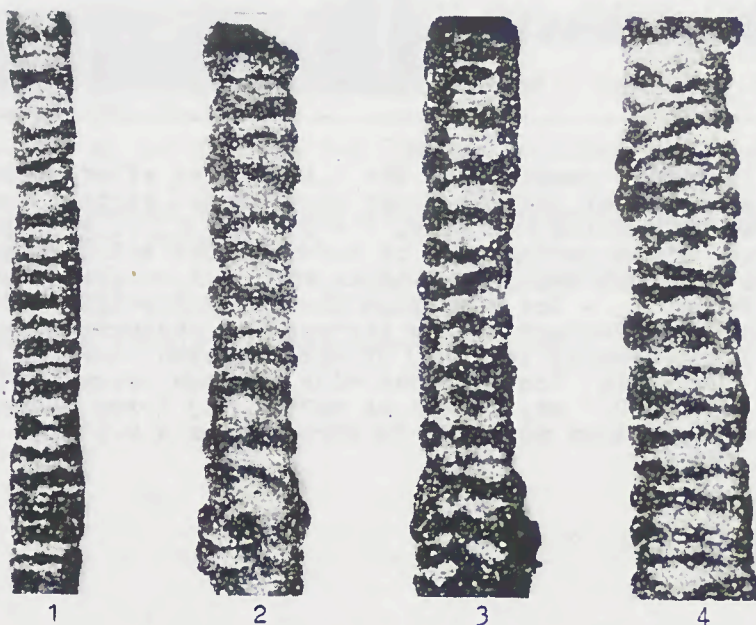


Fig. 3. Fulgurities remaining in the h.b.c. fuse after multiple arcing quenching (Cu strip fuse-element with uniform cross-sectional dimensions: 1 - $2.5 \times 0.18 \text{ mm}^2$, 2 - $5 \times 0.1 \text{ mm}^2$, 3 - $5 \times 0.14 \text{ mm}^2$, 4 - $10 \times 0.1 \text{ mm}^2$).

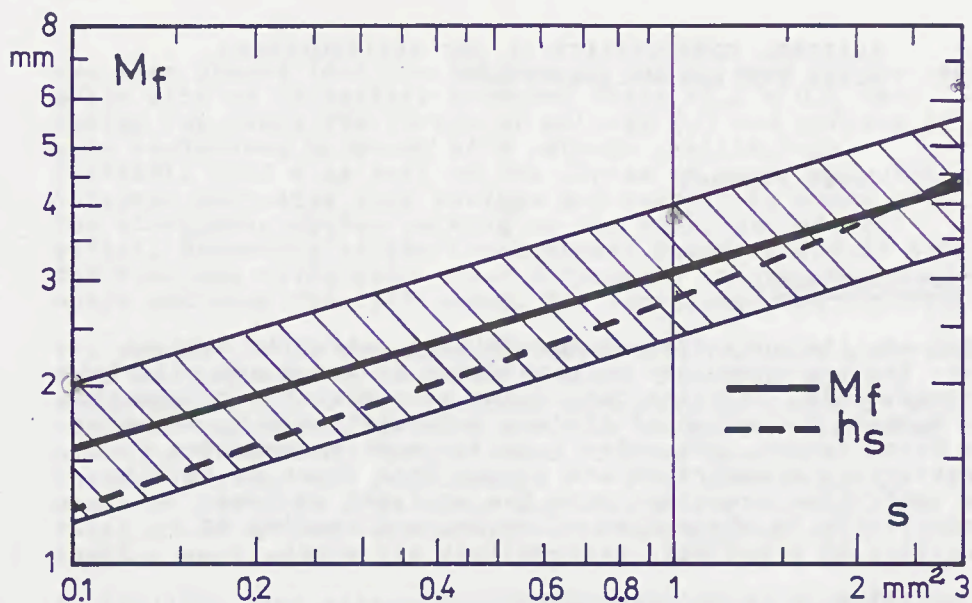


Fig.4. Dependence of striated disintegration modulus M_f of strip fuse-element on short-circuit cross-section area S_s . M_f - on formula (4), h_s - on formula (2).

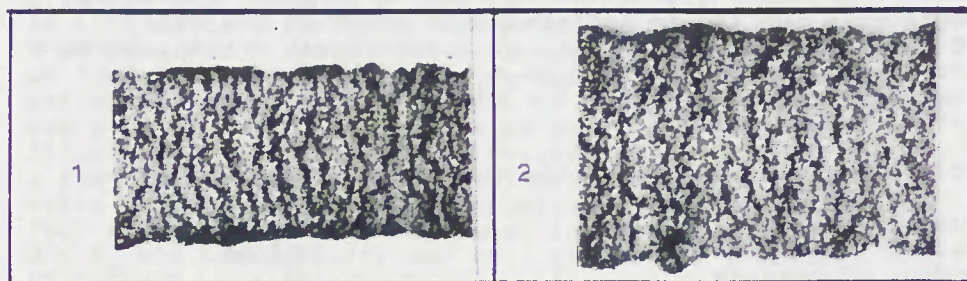


Fig.5. Photograph section of the disintegration fulgurite non-modulus (Cu strip fuse-element with uniform cross-sectional dimension: 1 - 5 = 15 x 0.05 mm², 2 - 5 = 20 x 0.05 mm², $l = 60$ mm). $U = 260$ V, 50 Hz, $j_f = 5$ kA·mm⁻²



Fig.6. X-ray photographs of disintegration of copper strip fuse-element. $U = 260$ V, 50 Hz, $j_f = 7$ kA·mm⁻², $S = 5 \times 0.1$ mm², $S_s = 2.5 \times 0.1$ mm², $l = 60$ mm, $l_s = 15$ mm x 2.

ELECTRIC CONDUCTIVITY OF ARC EXTINGUISHING
MEDIA FOR LOW-VOLTAGE FUSES

Josef Paukert

1. INTRODUCTION

Fuses are the only type of low-voltage switching devices where the arc shape can be considered at least approximately defined. This, in principle, makes also possible to describe the dynamic behaviour of the arc mathematically by means of the Mayr, Cassie, and other equation models presuming a rotationally symmetrical arc shape. This paper deals with the activities resulting from the analysis of fuse conductivity in the period of arcing and leading to a selection of a suitable mathematical arc model.

2. DESCRIPTION OF THE EXPERIMENTS

This study draws from experimental material gathered during a research searching for new kinds of arc extinguishing media for low-voltage fuses and directed to reduce the Joule integral $i^2 dt$. Different kinds of arc extinguishing media were applied in semiconductor fuses of the type PC 100, rated current 100 A, of Czechoslovak origin. Factory produced fuses were tested as a comparative standard for evaluation of the suitability of the corresponding arc extinguishing medium.

PC 100 fuse-elements have the following characteristics:

fuse-element material	Ag
active length	97 mm
number of bridges	7
cross section reduction in a bridge	8 %
fuse-link cavity volume	18.78 cm ³

Breaking tests were carried out in a single-pole circuit at 550 V, 1800 A, $\cos \phi = 0.2$. The breaking current corresponded to the current I_2 , according to the IEC Publication 169-4, at which the arc energy has the highest value. Individual arc extinguishing media were either poured in, or applied straight on the fuse-element which

Switchgear Research Institute, Brno, Czechoslovakia

was then placed into the filling of quartz sand of the same grain size as in factory produced fuses (0.3 - 0.4 mm). During the tests the curves of voltage (u) and current (i) were registered by means of a cathode oscillograph TEKTRONIX 5103 N as well as the curves of power and uidt integral derivated from voltage and current by means of the electronic device working on the principle of Hall effect. According to the Czechoslovak standard ČSN 35 4715 the fuse was being held under a recovery voltage for 5 minutes and when the test ended, its resistance was checked.

The values $\int i^2 dt$ and conductivities $G = i/u$ were determined from oscillograms by means of graphic construction and computation. The u and i values were read by means of BAK recorder together with MEDA analogue analyzer, the total breaking time being divided into 50 time sections. VA characteristics and dependences $G = f(t)$ were drawn by means of the WANG 2200 table computer and a plotter. The total of 28 arc extinguishing media was tested, on 5 samples each.

3. OBTAINED TIME DEPENDENCES OF CONDUCTIVITY $G = f(t)$

The time conductivity curves were evaluated only for perspective arc extinguishing media showing at least the same extinguishing capacities as quartz sand and complying with the requirements of the Czechoslovak standard ČSN 35 4715 as to their behaviour after breaking. There were 7 of them and 3 additional measurements were carried out on factory produced fuses using quartz sand as an arc extinguishing medium. The shape of the dependence $G = f(t)$ was similar at all the evaluated samples and it can be illustrated in an ideal form according to Fig. 1 drawn on a semi-logarithmic paper (the t scale is linear, the G scale is logarithmic). The dependence $G = f(t)$ is divided into 4 or eventually 5 sections. In the first time section $0 - t_1$ the conductivity may fall steeply or gradually (the branches a, b according to Fig. 1) or it may be constant (the branch c) or it may also rise mildly along with the increasing time (the branch d). Further the curve falls monotonously in the sections 2 (the branch between the points A - C in the time interval $t_1 - t_2$) and 3 (the branch f between the points C - E in the time interval $t_2 - t_3$) and in the section 4 (the branch g starting from the point E in the time interval $t_3 - t_4$). Except the branch g all other branches may be approximated with a straight line. In some cases the number of sections increases to 5 by means of shortening the section 2 (the branch e between the points A - B in the time interval $t_1 - t_2$), inserting the branch e' (the section 2' between the points B - D in the time interval $t_2 - t_2'$) and further by continuation of the branch f from the point D. The transitions between the sections 1 and 2 are steep mostly, the transitions between the sections 2 and 3 or 2 and 2',

2' and 3' are steep or gradual with a little bow. The branch f is very short sometimes and it may be approximated with a straight line only with difficulties. In that case the branch g starts already from the point C or D.

The curves of dependences $G = f(t)$ at different samples of the same kind of arc extinguishing medium were showing a great similarity and they testify of both a good reproducibility of the results and of a possibility to use the dependence $G = f(t)$ for diagnostic purposes (see Fig. 2 for quartz sand and Fig. 3 for special ceramics NE 2).

The measured time t_1 , t_2 and t_3 corresponding to transitions in the characteristic $G = f(t)$ and the total breaking time t_b for different kinds of arc extinguishing media are shown in Table 1.

4. EVALUATION OF THE MEASUREMENTS AND A CONCLUSION

During the described experiments the complex time conductivity curves were obtained testifying the complex character of extinguishing process in a low-voltage fuse. It is evident that the extinction cannot be approximated with a simple model, as e. g. the Mayr's. Simple approximation might be possible only in individual time sections in which the conductivity fall is exponential with time. At present time limits of these sections can be determined only empirically from experiments.

The described procedure of evaluating the breaking oscillograms by means of dependences $G = f(t)$ can be considered as a new diagnostic method of breaking process in low-voltage fuses enabling to distinguish the separate time stages of breaking. The classification of the dominant elementary processes in separate time stages still has to be done in the future.

Tab. 1 Time (measured in ms) of transitions in the characteristic $G = f(t)$, t_1 , t_2 , t_3 and the total breaking time t_b for different kinds of arc extinguishing media. Number of samples $n = 5$, except the media NE 1, NE 2 and NE 3 having $n = 3$. Time t_1 is designated according to Fig. 1.

Arc extinguishing medium	Arc extinguishing medium composition and the way of its application	t_1 (ms)	t_2 , t_2'' (ms)	t_3 (ms)	t_h (ms)
NKB 1	borax + PPM /applied	0.480 ± 0.106	1.920 ± 0.211	3.425 ± 0.475	6.60 ± 0.219
PPM	PPM/applied	0.500 ± 0.113	1.690 ± 0.153	3.660 ± 0.339	6.32 ± 0.160
NSV 2	mica + water glass /applied	0.535 ± 0.208	2.07 ± 0.211	4.775 ± 0.325	6.68 ± 0.392
NE 1	special ceramics	0.275 ± 0.054	1.966 ± 0.047		5.80 ± 0.282
NE 2	dtto	0.500 ± 0.071	2.216 ± 0.094	4.175 ± 0.175	5.73 ± 0.188
NE 3	dtto	0.358 ± 0.025	$1.075 \pm 0.075 / 2.050 \pm 0.071$		6.26 ± 0.249
NE 7	dtto	0.510 ± 0.285	$1.062 \pm 0.012 / 1.800 \pm 0.255$	4.725 ± 0.512	6.48 ± 0.160
P 5	SiO ₂ /poured	0.415 ± 0.049	1.37 ± 0.108		6.20 ± 0.282
P 01	dtto	0.430 ± 0.072	$0.8/1.270 \pm 0.246$	4.610 ± 0.224	6.48 ± 0.160
P 7	dtto	0.380 ± 0.058	$0.4/1.180 \pm 0.157$	4.590 ± 0.445	6.46 ± 0.250

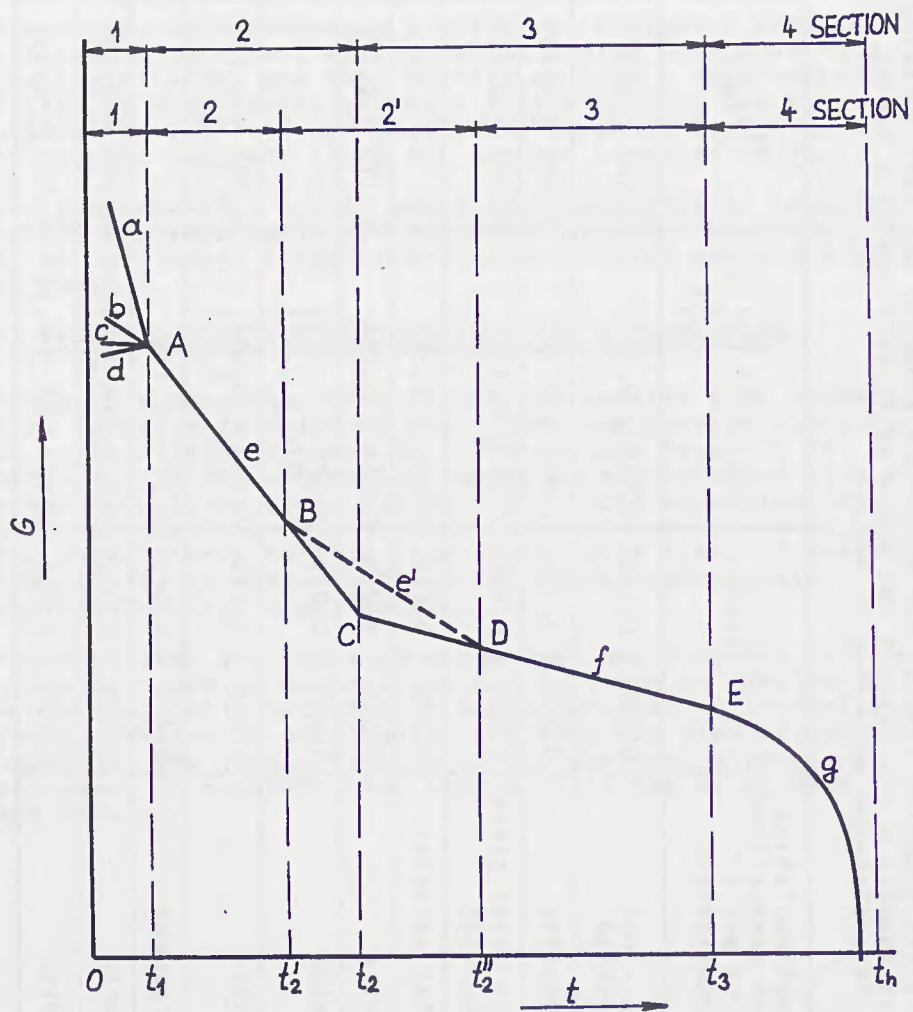


FIG. 1.

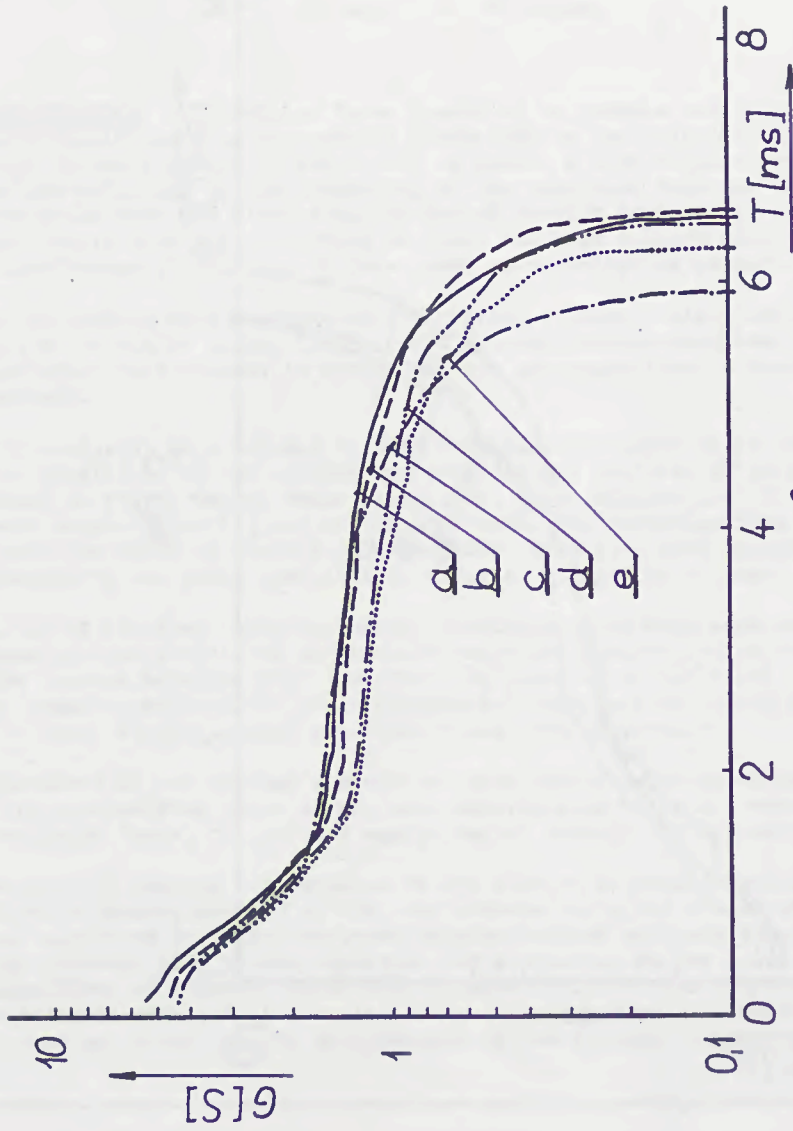


FIG. 2.

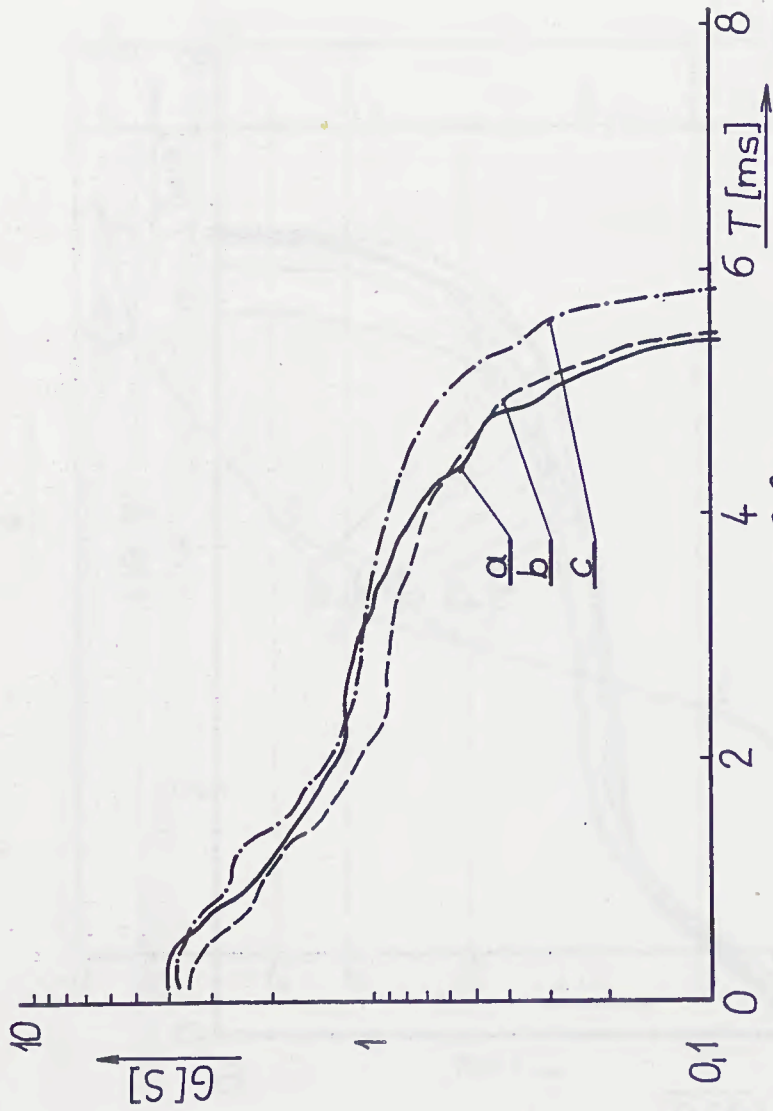


FIG. 3.

RECOVERY OF DIELECTRIC STRENGTH
OF EXPULSION FUSES AFTER ARC CURRENT ZERO

S. Arai & Y. Kawano

INTRODUCTION Expulsion fuses installed in cutouts are quite extensively used for overcurrent protection on the distribution systems at high voltages of 6.6 kV and 3.3 kV in Japan, a high voltage cutout refers to the switching device consisting of the expulsion fuse and the cutout which can open the circuit within normal service conditions. Most of them are mainly used for protection of lines and high voltage distribution transformers of moderate or less power at distribution primary.

In accordance with stepping up the voltage of distribution systems from 3.3 kV to 6.6 kV in the 1960's, high voltage cutouts have been improved for their performances in normal service and operations of breaking fault current.

Particularly, high voltage cutouts have been developed to be used under the conditions of the ambient air considerably polluted by salt or dust as shown in Fig.1. Under these situations, their applications in the field were investigated [1] and at the same time, the investigations for the characteristics of their breaking current abilities were carried out with respect to the power distribution circuits stepped up voltage.

A lot of breaking tests for modern expulsion fuses were made under the same circuit conditions as the modernized power distribution circuits at the current breaking test facility. In parallel to the tests, we intended to study experimentally their fundamental behaviors of breaking current. For these studies, model expulsion fuses were employed.

Behaviors of arc voltage and current were investigated about the fuses with gas-evolving tubes of the same materials as using for modern expulsion fuses, the various magnitudes of current and circuit conditions.

Generally, current interruption of the current switching device such as circuit breaker depends on the race between the speed of recovery of post-arc space and transient recovery voltage between post-arc terminals. It was supposed that it was important for discussion of the breaking current capability of fuses to clear the characteristics of the recovery of dielectric strength of post-arc space. Accordingly, our research was almost put stress on the measurements of the recovery of post-arc space.

S.Arai and Y.Kawano are with Tokyo Denki University,
Tokyo, Japan,

It has been known that the recovery depends on the arc conditions during arc period, tube materials and geometrical dimension of expulsion fuses. Measurement of the recovery of the model expulsion fuses was made by the method applying rectangular voltage to the post-arc space. At the same time, regions of post-arc current flowing, thermal breakdown and dielectric breakdown were investigated with respect to arc energy.

The test circuit which was easily able to control the arc conditions was devised. Using this test circuit, the performances of breaking current of the fuses with respect to various arc conditions were able to be studied relatively easily.

MODEL EXPULSION FUSES Fig.2 shows a model expulsion fuse. The test equipment is mainly composed of a fuse link, a polyvinyl chloride cylinder and a cylindrical insulation container which simulates the cutout. The fuse link is composed of a fuse element, a metal cap, a metal lead and a gas-evolving tube opened at one end. The copper fuse element of 0.5 mm in diameter is pulled down by weight of about 1 kg after fuse link is set. The material used for the gas-evolving tube is kraft paper using electrical insulation in the greater part of tests. The test equipment is mounted on the large closed box which traps gas discharged from the fuse on the operation.

TEST CIRCUIT To investigate the recovery of dielectric strength of the arc space after arc current zero under the controlled conditions of various arc energy and arc starting current, the test circuit was devised so that arc energy and current were easily controlled.

Fig.3 shows schematically the test circuit. The principle of this circuit is that it is possible to transfer from adjustable energy charged in the capacitor to inductive energy. Then, a capacitor bank C_1 is charged to voltage V_1 . Charged energy of the capacitor C_1 is $\frac{1}{2}C_1V_1^2$. Starting the test, a pulse is sent from a trigger pulse generator Trg to a vacuum switch V_s and a delay circuit D_1 . At first, the current discharged from the capacitor bank C_1 flows through a reactor L , a breaker B and the vacuum switch V_s . On the other hand, the pulse sent to the delay circuit D_1 is delayed by the time duration between the discharge starting instant of the capacitor C_1 and the instant of the maximum of discharged current and is sent to the breaker B to open. At the instant of the maximum of the current corresponding to the capacitor voltage of zero, the breaker B is opened, and the current is transmitted to the circuit including the fuse through a high voltage diode D_1 , and a current shunt Sh .

In this process, almost capacitive energy is transferred to inductive energy, so the following relation is given

$$\frac{1}{2} C_1 V_1^2 = \frac{1}{2} L I_m^2 \dots \dots (1)$$

where I_m is the maximum value of the discharging current. The current at arc initiation is a little small compared with the instantaneous current transmitted, since inductive energy is partly exhausted in the fuse and the circuit resistance for the pre-arcing period. The following relation is given

$$E_m = \frac{1}{2} L (I_m^2 - I_c^2) \quad (2)$$

where E_m includes pre-arcing energy of fuse element and circuit loss during the pre-arcing period and I_c is the current at arc initiation. Therefore, inductive energy E_c that is utilized for the arcing period is expressed as follows

$$E_c = \frac{1}{2} L I_c^2 \quad (3)$$

After arc initiation, current decreases almost linearly owing to the effect of high arc voltage. Almost all inductive energy is changed into arc energy. Using elements of constant cross section and length, pre-arcing energy of the fuse element and energy of circuit loss are nearly constant for the pre-arcing period, since they are proportional to the pre-arcing Joule integral of the element. Therefore, arc energy is linearly related with capacitive energy which is easily adjusted by charging voltage of the capacitor C_1 .

MEASUREMENTS The circuit applying voltage to arc terminals is shown in Fig.3. A current zero detector ZD generates a single pulse at a few micro-second before arc current zero. The pulse is delayed in a delay circuit D_2 for setting time T . A gap G is triggered by the pulse from the delay circuit D_2 . The voltage discharged from the capacitor C_2 which is charged to voltage of V_2 is applied to the arc terminals recovered freely after arc current zero through a diode Di_2 , the triggerable gap G and a resistor R .

The recovery of post-arc space between arc terminals is measured by means of following method. On the assumption that for the same fuses and same circuit conditions, arcing phenomena and post-arc space are similar situations, breaking tests are repeated to measure the recovery at the certain instant after arc current zero for the same fuses under the same circuit conditions. The recovery at the some instant is expressed by the maximum impressed voltage over which breakdown of the arc space is brought about.

A digital memory DM7100 was used to measure the impressed voltage and a digital memory DM901 was used to measure breaking current, the appearing voltage between the fuse terminals and the impressed voltage over whole test duration. The data processing system consisted of a data processor SM1330, a microcomputer, a printer and a floppy disk was used for analysis and record of data recorded in the digital memory DM901.

ARC VOLTAGE WAVEFORMES WITH RELATION TO ARC CURRENT AND TUBE DIAMETER

At first, arc starts at element blown out and then burns ultimately between a metal cap and a metal lead in the tube. It is seen from oscillograms that current slightly decreases linearly during the pre-arcing period and more distinctly decreases after arc starting.

Fig.4 shows two types of the arc voltage waveforms observed. In the case of Fig.4 (a), a diameter of the tube is small, arc voltage increases

steeply for some time and then decreases and spike voltage appears just prior to current zero. In the case of Fig.4 (b), a diameter of the tube is large, arc voltage steps up abruptly at the instant of arc initiation and keeps almost constant value fluctuating with small voltage.

If the diameter of the tube is smaller than that of free burning arc column, the wall of the tube intensively heated results in huge evaporating gas from surface of the tube and rapid evolving gas from the tube. Thus the pressure in the tube is built up by huge evaporated gas and arc is intensively blown, so that the arc voltage increases steeply while the condition that arc column fills fully the inside of the tube.

CHARACTERISTICS OF RECOVERY Using the model expulsion fuses, the characteristics of the recovery expressed by relations between the magnitude of the recovery in voltage and a lapse of time after arc current zero were investigated in four parameters of arc energy, arc current at arc initiation, inner diameter and length of tubes.

(1) Effects of arc energy Fig.5 shows the characteristics of the recovery for different arc energies. Arc energies were 2.0 kJ, 1.0 kJ and 0.5 kJ. The tubes of sample fuses were 15 cm in length and 6 mm in diameter. Arc current at arc initiation was 1.0 kA on each test.

In the case of arc energy of 2.0 kJ, attainment of the recovery of 10 kV which is the fastest speed of the recovery in three values of arc energy takes a lapse of 30 μ sec from the instant of arc current zero. It is observed that the speed of the recovery for other arc energy becomes slow in accordance with decreasing arc energy.

Experimental results have shown that mass of the tube lost according to evaporation during arc period increases in proportion to arc energy. Therefore, arc is more strongly blown by the increase of evaporating gas in order to increase of arc energy, so that the speed of the recovery of dielectric strength of arc space becomes higher according to increase of arc energy.

(2) Effects of arc current Fig.6 shows the characteristics of the recovery for arc currents. The arc current which decreases approximately linear is specified by the magnitude of current at arc initiation. In the test, the magnitudes of the arc current at arc initiation were 1.0 kA, 0.7 kA and 0.5 kA. The dimension of sample fuses was same as stated Section (1), and arc energy was about 2.0 kJ on each test.

The speed of the recovery increases in accordance with the arc current at arc initiation. Also, the ratio of arc energy to arcing time, that is, mean arc power increases with the value of the arc current at arc initiation, thus the speed of the recovery increases according to mean arc power.

It is considered that the speed of the recovery becomes higher with increasing the arc current so that the arc space even near current zero is subjected to strong blast action by large quantity of decomposed gas from

the surface of the tube with increase of arc current and mean arc power.

(3) Effects of tube diameter Fig.7 shows characteristics of the recovery with respect to inner diameters of the tubes. Inner diameters were 6 mm, 8 mm, 9 mm and 10 mm respectively. The length of tube was 15 cm and arc energy was about 2.0 kJ and arc current at arc initiation was about 1.0 kA. These constant values of arc energy and arc current at arc initiation on each test were gotten by only charging the capacitor C_1 constant voltage.

It is recognized from Fig.7 that the recoveries of small tube diameters of 6 mm and 8 mm are very fast compared with those of larger tube diameters of 9 mm and 10 mm. The recoveries of smaller tube diameters of 6 mm and 8 mm are very fast in order to strong gas blast so that the inside of the tube is filled fully with arc and is heated intensively and so huge gas is evaporated. Arc diameter of the arc current of 1.0 kA may be smaller than 9 mm [2], so that evaporating mass of the tube wall owing to arc heating is approximately same in the case of exceeding tube diameter of 9 mm. Hence, blowing action of evolving gas of the tube diameter of 9 mm is slightly stronger than that of the tube of 10 mm in diameter.

A change in the cross section of the tube, this fact has been already known, has influence upon the circuit interrupting capacity. With constant rate of gas generation, gas blast action is stronger in small diameter of tube than in large one, therefore the current interruption ability in a small diameter of the tube is superior to a larger one. Corresponding with the phenomena, the speed of the recovery becomes higher in small tubes than that of large ones.

(4) Effects of tube length Fig.8 shows characteristics of the recovery with respect to the lengths of tubes. In this test, the lengths of the tubes were 15 cm, 10 cm, 8 cm and 7 cm respectively. Inner diameter of the tube was 6 mm and arc energy and arc current at arc initiation were same as Section (3).

The remaining length of the metal cap and the metal lead in the tube is 5 cm, so that arc is drawn out after the element blown out and the length between arc terminals ultimately becomes subtracting the remaining length of the metal cap and the metal lead in the tube from whole tube length. It is measured that significant slow speed of recovery occurs for tube length of 7 cm, however, the length of the tube is longer, the speed of the recovery is higher. The recoveries of tube lengths of 10 cm and 15 cm are very fast compared with those of tube lengths of 7 cm and 8 cm.

From the results of severe decreasing arc current according to the high arc voltage of longer tube, it is suggested that the pressure of the inside of the tube is quite high. Owing to the longer gas flowing channel for the longer tube, post-arc space of the longer tube is more intensively blown by high pressure evolving gas than that of the short one, thus the speed of the recovery of the longer tube becomes higher than that of the shorter one.

POST-ARC CURRENT In this test, post-arc current was observed in the region over arc energy of about 0.5 kJ. Fig.9 shows the regions of observed post-arc current. The experiments were undertaken for three cases of arc energy in the gas-evolving tube of inner diameter of 6 mm and length of 15 cm and arc current at arc initiation of 1.0 kA.

No post-arc current flows within the impressed voltage under dotted line as shown in Fig.9.

Post-arc current occurrence is observed between recovery characteristics and the dotted lines. The regions of post-arc current flowing depend on arc energy. The region of post-arc current in arc energy of 0.5 kJ is quite smaller than those of two other conditions of arc energy.

However, instant of impressed voltage elapsing from arc current zero and approaching the dotted lines in every arc conditions, post-arc current diminishes so small that it is difficult to distinguish clearly post-arc current.

It has been known that successful current interruption depends on the magnitude and the speed of recovery of the post-arc space. From above mentioned results, it is considered that states of the post-arc space which depend on arc conditions, the elapsing time after arc current zero and the value of impressed voltage fall into four regions I , II, III and IV , as shown in Fig.10.

No post-arc current is observed in the region I , one reason of the phenomena in this region is that the impressed voltage is not enough to flow post-arc current in the case of a short elapsing time after arc current zero and another is post-arc space recovered enough in a passing long time. The typical waveform of impressed voltage in this region is shown in Fig.11 (a).

Post-arc current is occurred in the region II . The conductance of post-arc space is enough to flow the post-arc current when impressed voltage is applied. However, overcoming the impressed voltage, post-arc space recovers its dielectric strength in this region. Typical waveforms of impressed voltage and post-arc current are shown in Fig.11 (b).

In the region III above region II , thermal failures occur. Fig.11 (c) shows the typical voltage and current waveforms in the thermal failure. As shown in this oscillogram, breakdown occurs at the instant of impressed voltage applied.

In the region IV , dielectric failures are caused. Fig.11 (d) shows the typical voltage and current waveforms in the dielectric failure. Dielectric breakdown occurs at an elapsing time of about 310 μ sec after instant of impressed voltage applied as shown in the oscillogram.

CONCLUSIONS Using model expulsion fuses, fundamental phenomena are observed in respect to behaviors of breaking current of expulsion fuses.

The waveform of arc voltage depends on the relation between the diameter of gas-evolving tube and that of arc column, and arc voltage continues

rising while arc fills fully the inside of the tube.

It is investigated that the recovery characteristics of the model expulsion fuses are obtained under arc conditions and various dimensions of gas-evolving tubes. It is confirmed that the speed of recovery is higher according with increasing arc energy and arc current for the tube of narrower cross section and the longer length in the case of the tube without destruction.

The regions of flowing post-arc current are evident under the influence of the arc condition and the impressed voltage.

REFERENCES [1] Technical research report, " High voltage cutouts in our country. " IEEJ, (II) No.102, 1980.

[2] D.J.Siddons, " Arc diameter in a gas blast. " PROC.IEE, Vol.119, No.9, 1972, pp.1423-1425.

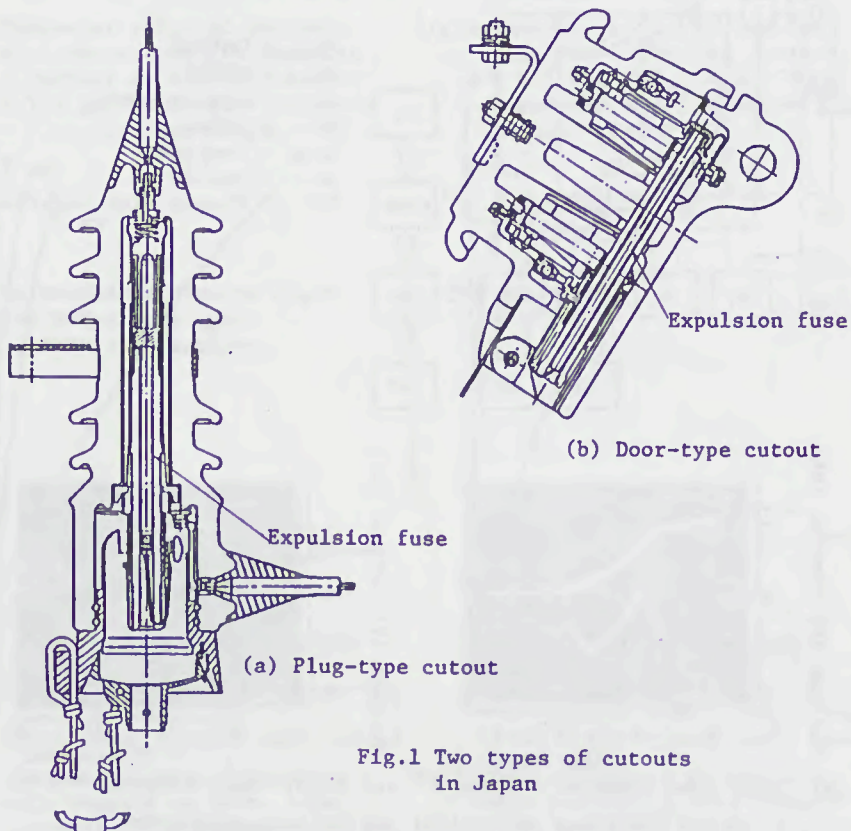


Fig.1 Two types of cutouts in Japan

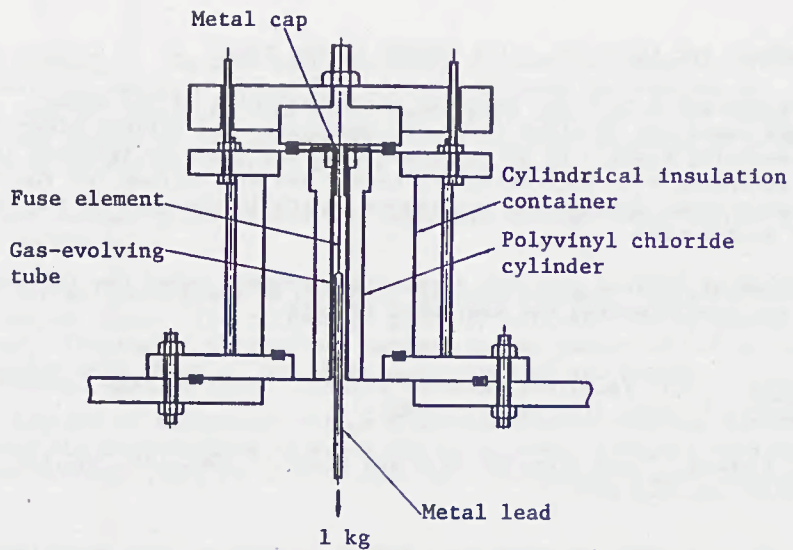


Fig. 2 Test equipment

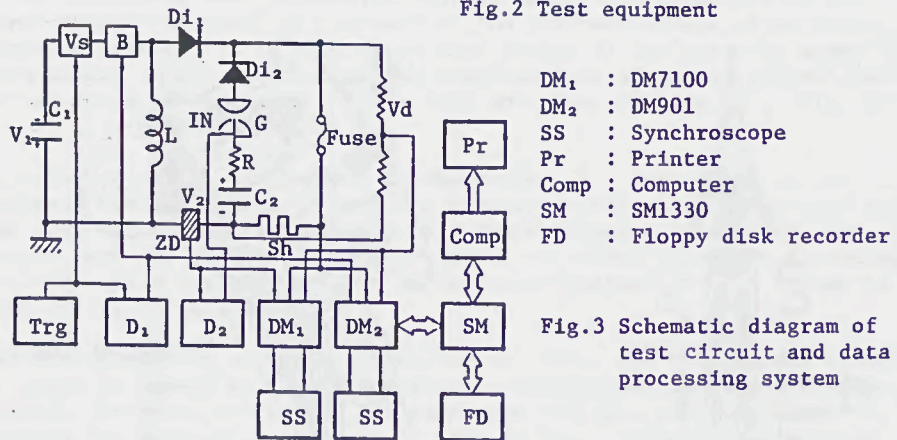


Fig. 3 Schematic diagram of test circuit and data processing system

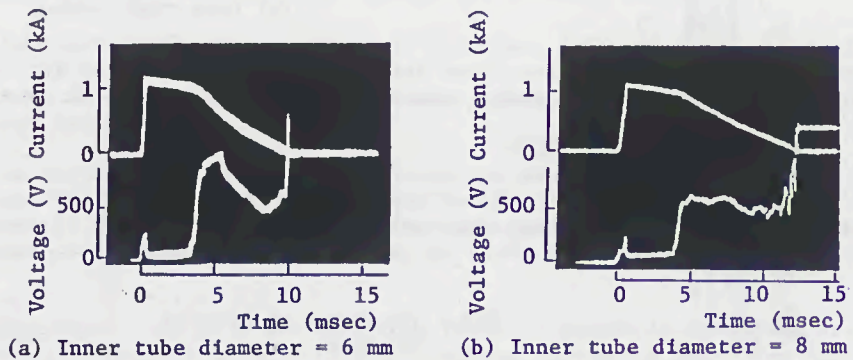


Fig. 4 Two types of typical arc voltage waveforms
 (Tube length = 15 cm, Arc energy = 2.0 kJ
 and Current at arc initiation = 1.0 kA)

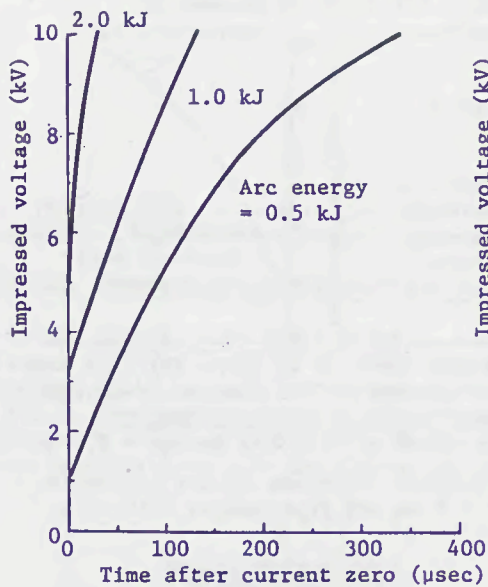


Fig.5 Characteristics of recovery with respect to arc energies (Current at arc initiation = 1.0 kA, Inner tube diameter = 6 mm and tube length = 15 cm)

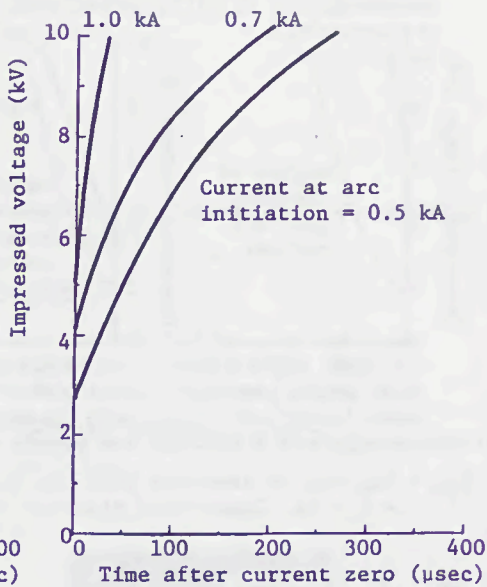


Fig.6 Characteristics of recovery with respect to arc currents (Arc energy = 2.0 kJ, Inner tube diameter = 6 mm and Tube length = 15 cm)

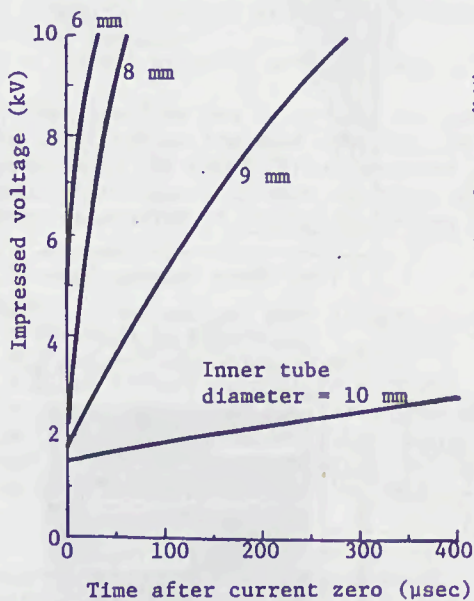


Fig.7 Characteristics of recovery with respect to inner tube diameters (Arc energy = 2.0 kJ, Current at arc initiation = 1.0 kA and Tube length = 15 cm)

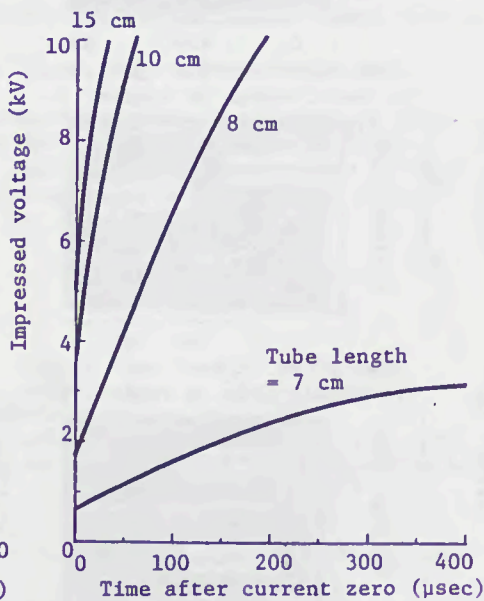


Fig.8 Characteristics of recovery with respect to tube lengths (Arc energy = 2.0 kJ, Current at arc initiation = 1.0 kA and Inner tube diameter = 6 mm)

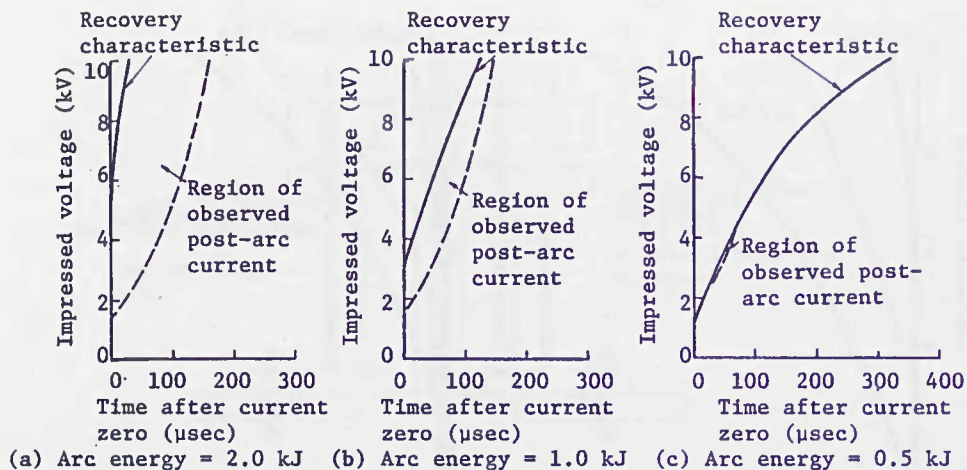


Fig.9 Regions of observed post-arc current (Current at arc initiation = 1.0 kA, Inner tube diameter = 6 mm and Tube length = 15 cm)

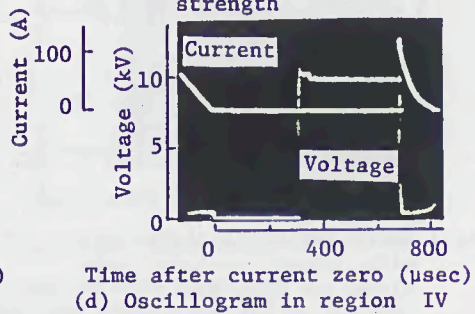
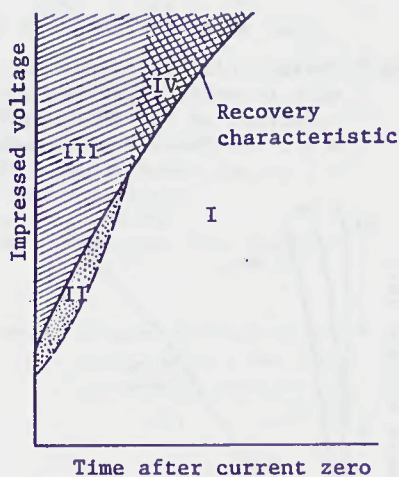
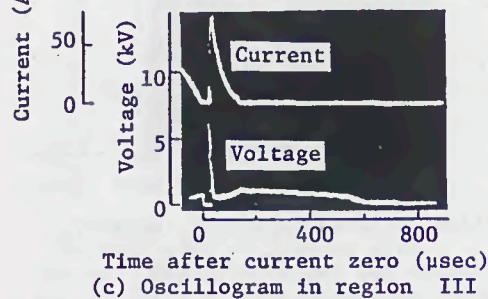
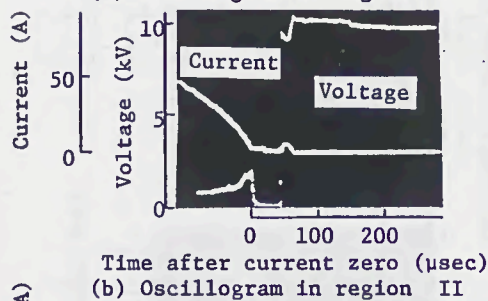
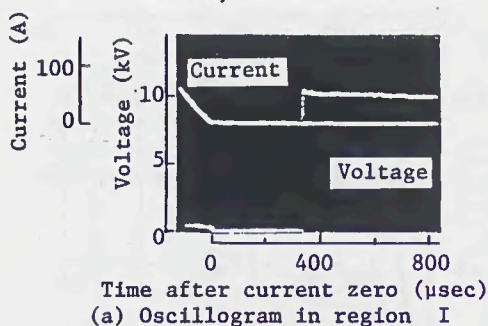


Fig.11 Typical waveforms of current and voltage in four regions

HOW FAR IS AN INSULATED CONDUCTOR PROTECTED BY A FUSE

Y Naot

1. INTRODUCTION The I.E.C. rules regarding the protection of insulated conductors against overcurrent state as follows:

a) 433. Protection against overload current

433.1. Condition of application. Protective devices (in our case, Fuses) shall be provided to break any overload current before such a current could cause a temperature rise detrimental to insulation, etc.

433.2. Coordination between conductors and protecting devices. The operating characteristics of a device (Fuse) protecting a conductor against overload shall satisfy the following conditions:

$$I_B \leq I_n \leq I_z \quad (1)$$

$$I_2 \leq 1.45 I_z \quad (2)$$

where:

I_B = Current for which the circuit is designed (B stands for Betriebsstrom - V.D.E)

I_z = Continuous current carrying capacity of conductor. (z stands for Zulaessiger-strom - V.D.E)

I_n = Nominal current of the protective device. (in our case - rated current of Fuse)

I_2 = Current assuring effective operation of the protective device.

b) When the fuse has to protect the conductor against short circuit only, the I.E.C. rules are more specific and define the maximum permissible duration of the short circuit current until the conductor reaches a limit temperature depending upon the type of insulation. Such time is given, under assumption of adiabatic heating as:

$$t = \left(k \cdot \frac{S}{I} \right)^2 \quad (3)$$

where:

t = duration in seconds

S = Cross sectional area in mm²

I = Short circuit current in A (R.M.S. value)

k = constant equal to 115 for copper conductors

The limit temperature for which k is calculated is 160°C for P.V.C insulation. Other values of k are given for different conductor materials and different types of insulation.

Department of Electrical Engineering
Technion - Israel Institute of Technology
Haifa 32000,
Israel

It has to be pointed out that the assumption of adiabatic heating is nearly accurate only if it is of order of magnitude of a few seconds. For that the short circuit current must be quite strong. In the daily praxis, however, the short circuit current I may be such that will surely cause the Fuse operation, but in a time that may last for minutes instead of a few seconds. In such cases the conductor heating is very far from being adiabatic and Eq. 3 does not hold anymore. Nevertheless, practical engineers prefer to use Eq. 3, instead of embarking in more complicated calculations, because of:

- a) Eq. 3 is simple and immediately applicable.
- b) at first glance it seems that the time t calculated according to Eq. 3 always is on the safe side, because the assumption of adiabatic heating is far more severe than the real heating process in which the conductor loses heat due to its temperature rise.

A more accurate investigation of the heating process and the consequent deterioration of the insulating material, shows that the above mentioned simplified approach and its consequences may be unjustified and in very many cases lead to erroneous conclusions. The aim of this paper is to carry out such investigations and to show its logical consequences.

2. THE HEATING PROCESS Consider Fig. 1, representing an insulated conductor of cross sectional area of $s \text{ mm}^2$.

Let:

- R = the conductor resistance at surrounding temperature. [Ω]
- α^0 = the resistance coefficient related to surrounding temperature. [$1/^\circ\text{C}$]
- h = the equivalent radiation constant, according to installation conditions. [$\text{W}/^\circ\text{C}.\text{m}^2$]
- S = the cooling surface of the conductor. [m^2]
- c = the specific heat of the conductor material. [$\text{W}_s/^\circ\text{C}.\text{kg}$]
- G = the equivalent weight of the insulated conductor reduced to conductor material
- θ = the temperature rise upon the surrounding.

For the sake of concision, in the following, θ shall be referred to as "temperature".

Supposing that a current of I Amp. flows through the conductor, the energy balance for an infinitesimal time dt , is:

$$R_0(1+\alpha\theta)I^2 \cdot dt = hS\theta dt + cG d\theta \quad (4)$$

Eq. 4 can easily be transformed into the following form:

$$\theta'_\infty(1+\alpha\theta)dt = \theta dt + T d\theta \quad (5)$$

where:

$\theta'_\infty = \frac{R_0 I^2}{hS}$ is the temperature to which the conductor would settle after a long time if its resistance would stay constant at the value R_0 , regardless of temperature increase.

$\frac{cG}{hS} = T$ (sec) is the "time constant" of the conductor, having different values for different installation conditions, because of its dependence on h which changes with the varying conditions.

Solving Eq. 5, taking into consideration that at time $t=0$ the conductor temperature may be θ_0 due to previous work, one gets:

$$\theta = \frac{\theta'_\infty}{1-\alpha\theta'_\infty} \left(1 - e^{-\frac{1-\alpha\theta'_\infty}{T} \cdot t} \right) + \theta_0 e^{-\frac{1-\alpha\theta'_\infty}{T} \cdot t} \quad (6)$$

which gives the conductor temperature as a function of time. Eq. 6 points out a very interesting fact. If $1-\alpha\theta'_\infty > 0$ the exponential function decreases with increasing time, and the temperature asymptotically reaches the final value $\theta_\infty = \frac{\theta'_\infty}{1-\alpha\theta'_\infty}$. If $1-\alpha\theta'_\infty < 0$ the exponential is increasing with time, and the temperature steadily increases toward ∞ (Run away effect). See Fig. 2.

Let us suppose, for the moment, that the conductor is protected if the circuit is interrupted before its temperature reaches a maximal permissible value θ_M (160°C for P.V.C). According to Fig. 2, the maximal permissible time t is given by the intersection point of $\theta = f(t)$ with the line $\theta = \theta_M$. Mere observation of Fig. 2, discloses immediately that if $1-\alpha\theta'_\infty > 0$, $t > t_a$, but if $1-\alpha\theta'_\infty < 0$, $t < t_a$. Since t_a is the maximal permissible time by adiabatic heating, one may draw the first important consequence: if the conductor reaches the run away effect range, Eq. 3 gives values of time which are not on the safe side. It is important to observe that run away conditions are easily reached in current praxis. In order to check this point, let us reverse Eq. 6 getting the permissible time t as:

$$t = \frac{T}{1-\alpha\theta'_\infty} \ln \frac{1-(1-\alpha\theta'_\infty) \frac{\theta_0}{\theta'_\infty}}{1-(1-\alpha\theta'_\infty) \frac{\theta_M}{\theta'_\infty}} \quad (7)$$

Let us now compare the values of t calculated using Eq. 7 with those calculated using Eq. 3. The results are given in Table 1 as a function of the relative short circuit current $j = \frac{I}{I_z}$, where I is the actual current and I_z as defined in the introduction. I_z

Table 1 has been calculated for a copper conductor of 50mm², having a continuous current carrying capacity of $I_z=171$ A and a time constant $T=587$ sec. Table 1 clearly shows that any current larger than 5-6 times I_z starts a run away effect. For any current in this range Eq. 3 gives excessive values of t .

3. DETERIORATION OF INSULATION After having investigated the heating process, let us consider the deterioration of insulation caused by the temperature. It is a known fact that insulating materials loose their mechanical and electrical properties as well, with a speed rapidly increasing with the increase of conductor temperature. (Aging effect). In order to evaluate this effect, it is usual to define the Expected Life of the insulation (E.L. in the following) and to express its dependence upon temperature as:

$$E.L. = A.e^{-\beta\theta} \quad (8)$$

where:

A = a constant having the dimension of time (generally years)
 β = a coefficient giving the deterioration speed as a function of temperature. The dimensions of β are $1/^\circ\text{C}$.

Eq. (8) must be rightly understood. The definition of E.L. is "the time after which the insulation of 50% of a large number of new samples held at constant temperature θ still preserve good insulating properties". One may look at this definition with a probabilistic approach, stating that the E.L. is the time span after which the probability of finding the insulation of a new conductor, held at constant temperature θ , in good conditions of insulation still, is 50%. This definition avoids a common misinterpretation of the E.L. concept. The E.L. does not define a time span after which the conductor insulation is surely destroyed. A conductor actually can be used for a time much longer than its E.L. without any fault of insulation, but its reliability is strongly affected because the probability of being in good condition becomes smaller and smaller with increasing time. Basing on Eq. 8 it is possible to evaluate the damage done to the conductor insulation by a short circuit.

Let us assume that a conductor is held at constant temperature equal to the permitted one θ_z . Eq. 8 applied to this case will give an expected life which may be defined as "rated expected life". (R.E.L) If the conductor is at temperature $\theta \neq \theta_z$ its expected life will be $E.L. \neq R.E.L$. Assuming that such situation lasts for a time Δt , the relative loss of expected life will be:

$$\Delta E.L = \frac{\Delta t}{E.L} \quad (9)$$

In order to cause the same relative loss of expected life at temperature θ_z a time $\Delta t'$ will be necessary, which satisfies

$$\frac{\Delta t'}{R.E.L} = \frac{\Delta t}{E.L} \quad (10)$$

$$\Delta t' = \frac{\Delta t R.E.L}{E.L} \quad (11)$$

Putting instead of R.E.L and E.L their expressions as per Eq. (8) one gets:

$$\Delta t' = \Delta t e^{\beta(\theta - \theta_z)} \quad (12)$$

Expressing $\Delta t'$ in percents of the R.E.L one gets:

$$D.F = \frac{\Delta t e^{\beta(\theta - \theta_z)}}{R.E.L} 100\% = \frac{\Delta t e^{\beta\theta}}{A} 100\% \quad (13)$$

Such expression may be considered as deterioration factor D.F. giving how many percents of the R.E.L are lost, due to a temperature θ lasting for a time Δt .

During a short circuit the conductor temperature rises from the initial temperature θ_0 to the maximal one θ_M at the moment of current rupture by the Fuse. After this moment the conductor begins to cool down. The temperature during the heating period is given by Eq. (6). During the cooling period the temperature behaves also according to Eq. (6) where $\theta'_\infty = 0$ and $\theta_0 = \theta_M$. Therefore, for the cooling process:

$$\theta = \theta_M e^{-t/T} \quad (14)$$

Since the insulation deterioration depends on the temperature, regardless of its source, one realizes that there are two deterioration factors:

- a) The prearcing deterioration factor (P.D.F) due to the heating period.
 - b) The "after deterioration factor" (A.D.F) due to the cooling period.
- The total deterioration factor will be:

$$D.F = P.D.F + A.D.F \quad (15)$$

There is no difficulty to calculate both P.D.F and A.D.F. The prearcing time t is given by Eq. (7). The temperature at any time is given by Eqs. (6) and (14) respectively. Thus one gets immediately:

$$P.D.F = \frac{100}{A} \int_0^t e^{\beta \left[\frac{\theta'_\infty}{1-\alpha\theta'_\infty} \left(1 - e^{-\frac{1-\alpha\theta'_\infty}{T} \cdot t} \right) + \theta_0 e^{-\frac{1-\alpha\theta_\infty}{T} t} + \theta_s \right]} dt \% \quad (16)$$

and

$$A.D.F = \frac{100}{A} \int_0^{t_i} e^{\beta(\theta_M e^{-\frac{t}{T}} + \theta_s)} dt \% \quad (17)$$

Both integrals are easily solved by numerical integration. For that a common programmable desk calculator is sufficient.

The integral of Eq. (17) presents a little difficulty in evaluating the integration time t_i . Such difficulty is avoided stopping the integration when the temperature reaches again the value θ_0 . Any prolongation will add to the integral a negligible contribution. θ_s appearing in Eqs. (16) and (17) is the surrounding temperature, which is added to the calculated one because the insulation deterioration is due to the real temperature of the conductor, not by its temperature rise over its surroundings.

The author wishes to point out that the D.F. gives only an indication of the severity of the injury done to the insulation by a short circuit, not an exact calculation, because in real life things are more complicated. A conductor never carries a constant current. There are periods of heavy load, periods of reduced load and periods of no load. Thus the starting temperature is different in any case. Eq. (16) and (17) take into consideration the worst possible situation.

The following Table 2 shows the P.D.F and the A.D.F of various copper conductors, calculated for the worst case in which the starting temperature is 70°C and the maximal permitted temperature is 160°C. In order to ease comparison P.D.F and A.D.F are given in thousandths of percent.

Considering Table 2 one may observe many important facts:

- a) The A.D.F obviously is independent from the relative short circuit current j , but is strongly dependent on the conductor cross section s . For instance by any j , the A.D.F changes from 0.402% for $s=25\text{mm}^2$ to 3.182% for $s=240\text{mm}^2$, being all other conditions equal.
- b) The P.D.F depends on both s and j .
- c) The contribution of the P.D.F to the total deterioration factor becomes more and more heavy when j decreases.
- d) The logical consequence is that from point of view of insulation deterioration the most dangerous overcurrents are those which exceed the conductor rated current by a factor changing from 1 to 3.

In order to emphasize this point Table 3 has been worked out. In this Table the total D.F. has been calculated for a conductor of 240mm^2 for $j=1.6$ to $j=15$. In line 1 are given the results assuming that the conductor is allowed to reach in any case the maximal temperature of 160°C . Line 2 gives the pertinent heating time from 70°C to 160°C . Line 3 gives the maximal temperature reached when the conductor is allowed to heat up until the D.F. reaches the limit of 1%. Line 4 gives the heating time in this case. Table 3 enables more useful observations:

- e) For heavy conductors the maximal temperature limitation criterion may lead to unacceptable heavy D.F. For instance by $j=1.6$ the conductor will loose more than 17% of its rated expected life until it reaches 160°C .
 f) Limiting the maximum permitted D.F., instead of temperature, the maximal temperature will decrease with decreasing j .

Observations e) and f) do not exclude the use of Eq. (3) or a similar one. The necessary change will be that factor k will no longer be constant, but a function of conductor size, its installation conditions and j . Such functions can be given in tabulated form.

Starting from completely different considerations the V.D.E people came to a similar conclusion, recommending that for conductors of cross section exceeding 150mm^2 the limit temperature shall be reduced to 130°C . After these considerations it is possible to answer the question posed in the heading of this paper: How far does a Fuse protect a conductor? Consider first the case that the rated current of Fuse and conductor are equal. $I_n = I_z$. In such case there is no doubt that for $j>3$, the conductor is fully protected because the fuse operating time is much shorter than the permitted heating time in both cases of temperature and D.F. limitation. For $j<3$, the situation is more problematic. A Fuse of size 4, which corresponds to the rated current of a conductor of 240mm^2 shall not interrupt during the test period for $j=1.3$, and shall interrupt within such period for $j=1.6$. The test period in this case is three hours. That means that by $j=1.6$ the Fuse can delay its action up to 10800 seconds still being in accordance with the regulations.

Comparing this time with that given in Table 3, line 4, one realizes that the conductor insulation may be severely deteriorated until the fuse reaction occurs. This behavior is mainly due to the "indifference gap" pertinent to any fuse. There is a specific value of $j=j_s$ which divides the infinite field of j into two zones. The unprotected zone for $j<j_s$ and the protected zone for $j>j_s$. The width of the unprotected zone depends upon the conductor cross section and the fuse rated current as well. Wishing to protect the conductor from $j=1$ to infinity one has to choose a fuse of rated current much smaller than I_z thus wasting expensive active material. Moreover, in specific cases the regulations allow to protect a conductor with a fuse of rated current larger than I_z . In such cases the unprotected zone can be considerably wide, thus enlarging the span of dangerous currents.

3. CONCLUSIONS

- 1) In the author's opinion the criterion of maximum permissible temperature should be replaced by that of maximum permitted D.F.
- 2) The regulations make a distinction between "overload currents" and "short circuit currents", differentiating them with regard to their origin. (Overload if due to excessive load or mechanical faults, short circuit if due to fault of electrical nature). These definitions, and other proposed

ones do not lead to calculatable values, thus leaving the possibility of overlapping or separation between the two ranges. The author suggests to choose j_s as separation point between overload and short circuit currents.

3) Basing on the above mentioned distinction the regulations consider separate protections against overload and short circuit. In many cases the regulations allow to protect a conductor against short circuit only. In such cases it is permitted to protect the conductor by a fuse of $I_n > I_z$. Though such arrangement generally works, it is conceptually not sound. One is able to calculate the maximal short circuit current, but nobody can predict the minimal one, which depends upon the more or less random impedance of the short circuit itself. Especially when $I_n > I_z$ a relatively small impedance can reduce the current into the unprotected zone. By fuse protection there is no completely satisfactory solution of this problem.

4) For the same reason the requirement that the interruption time shall be less than 5 seconds, is illusoric. Any possible short circuit impedance can reduce the current enough to cause a reaction time greater than 5 seconds. On the other hand, a conductor can support the short circuit current for more than 5 seconds without excessive deterioration.

5) Speaking of heavy expensive circuits the ideal protection may be offered by a semiconductor device, rather than by a fuse. Such semiconductor device shall sense both the current and the conductor temperature. It shall include an integrating circuit which starts to calculate the P.D.F when the current exceeds I_z . If the P.D.F reaches a preset limit, the current shall be cut off, until a manual reset. Such device may also include a time element which limits the reaction time to 5 seconds if required.

As a last remark, the author does not suggest any particular value for the maximum permitted D.F. Such a suggestion shall be the result of a team work which would consider both technical and economical considerations as well.

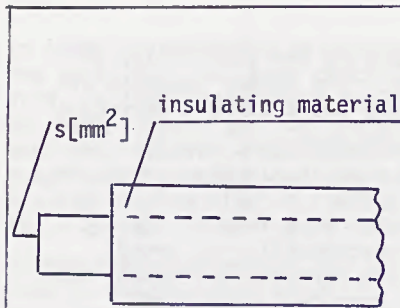


Fig. 1 - Insulated Conductor

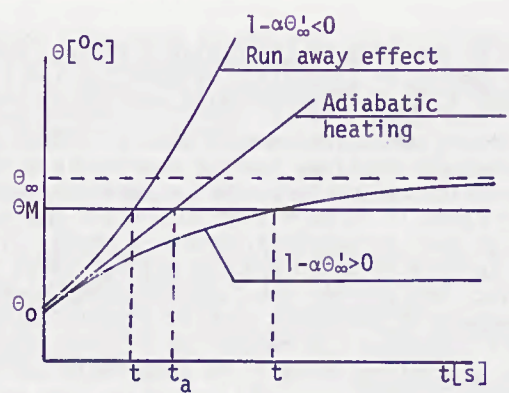


Fig. 2 - $\theta = f(t)$

j	2	3	4	6	8	10	12	14	16	18	20
t(Eq.7)[s]	624	156	77	31.26	17.09	10.79	7.44	5.45	4.16	3.28	2.65
t(Eq.3)[s]	283	126	71	31.41	17.67	11.31	7.85	5.77	4.42	3.49	2.83

Table 1 - t(Eq.7) versus t(Eq.3)

j	3		6		9		12		15	
s	PDF	ADF								
mm ²										
25	104	402	20	402	9	402	6	402	3.5	402
50	203	807	49	807	17	807	11	807	7	807
95	361	1347	66	1347	29	1347	17	1347	11	1347
150	525	2120	104	2120	45	2120	27	2120	17	2120
240	787	3182	156	3182	67	3182	41	3182	26	3182

Table 2 - P.D.F and A.D.F given in % x 10³

Relative short circuit current j	1.6	2	2.5	3	6	9	12	15
1 DF (%) limit temp. 160°C	17.28	6.52	4.72	3.97	3.34	3.25	3.22	3.21
2 Heating time (s) to 160°C	3870	1367	699	436	93	41	23	19.48
3 Max temp. (°C) by DF=1%	141	147	149	149	150	151	151	151
4 Heating time (s) for DF=1%	2650	1148	615	384	84	37	21	13

Table 3 - Comparison between max temp. and max DF

ON THE PROPER COORDINATION OF FUSES
WITH SEMICONDUCTOR DEVICES IN THE HEAVY SHORT-CIRCUIT REGION

J. Czucha

INTRODUCTION The maximum permissible current ratings of diodes and thyristors at short-circuits are characterized by manufacturers in the form of the I^2t parameter which is a non-repetitive survival rating for 10 ms overload. Appropriate correction factors are given for current faults of a shorter duration than 10 ms. This interferes with the until quite recently accepted condition for diodes and thyristors at short-circuits of a shorter duration than 10 ms, in which case $I^2t = \text{const.}$ was recommended to be assumed. After subjecting the I^2t parameter to consideration for a shorter duration than 10 ms it may be easily concluded that the condition I^3t or $I^4t = \text{constant}$ would be more suitable.

The manufacturers of thyristors and diodes also determine the value of the I^2t parameter for fault currents having a sinusoidal wave shape. For $i(t) = I_m \sin \omega t$:

$$I^2t = \int_0^{T/2} [i(t)]^2 dt = \frac{1}{2} I_m^2 \left(\frac{T}{2}\right) \quad (1)$$

In view of the changing character of the I^2t/Th versus time it is possible to determine the power x for the $I^x t$ expression, for which it will be constant for the given type of the thyristor/diode on the basis of the following condition:

$$\left(\sqrt{\frac{2(I^2t)_1}{T_1}} \right)^x \cdot \frac{T_1}{2} = \left(\sqrt{\frac{2(I^2t)_2}{T_2}} \right)^x \cdot \frac{T_2}{2}$$

Mr J. Czucha is with the Institute of High Voltages and Electrical Apparatus, Technical University of Gdańsk, 80-952 Gdańsk, Własna Strzecha 18^a, Poland

thus

$$x = 2 \frac{\log \frac{T_1}{T_2}}{\log \left[\frac{(I^2 t)_2 \cdot T_1}{(I^2 t)_1 \cdot T_2} \right]} \quad (2)$$

For instance, in the case of a certain thyristor its manufacturer gave as follows: $(I^2 t)_1 = 1.45 \times 10^6 \text{ A}^2 \text{ s}$ for $T_1/2 = 10^{-2} \text{ s}$ and $(I^2 t)_2 = 0.45 \times 10^6 \text{ A}^2 \text{ s}$ for $T_2/2 = 10^{-3} \text{ s}$. Thus, on the basis of (2) we have:

$$x = 2 \frac{\log \frac{10^{-2}}{10^{-3}}}{\log \frac{0,45 \cdot 10^6}{1,45 \cdot 10^6} \cdot \frac{10^{-2}}{10^{-3}}} = 4,06$$

Therefore, it may be assumed that the dependence $I^4 t = \text{const}$ is justified for $t < 10^{-2} \text{ s}$.

It is possible to determine $I^4 t$ or $I^3 t$ parameter in the function of the $I^2 t$ parameter found for $\frac{T}{2}$ from the following formulae:

for $n = 3$

$$I^3 t = \int_0^{T/2} i^3 dt = \frac{4}{3\pi} I_m^3 \left(\frac{T}{2} \right) \cong 1,19 (I^2 t)^{3/2} \left(\frac{T}{2} \right)^{-1/2} \quad (3)$$

for $n = 4$

$$I^4 t = \int_0^{T/2} i^4 dt = \frac{3}{8} I^4 \frac{T}{2} = 1,5 (I^2 t)^2 \left(\frac{T}{2} \right)^{-1} \quad (4)$$

As to short circuits with heavy duty prospective conditions the damping resistance (Fig.1a) may be neglected for the accretion phase of the current.

Thus,

$$i_{(SC)}(t) = I_m \sin \omega t \quad (5)$$

when only the symmetrical current (SC) component appears, or

$$i_{(ASC)}(t) = I_m (1 - \cos \omega t) \quad (6)$$

at maximum asymmetry and lack of short-circuit damping (ASC = asymmetrical current).

With regard to the two cases of the short-circuit current wave shape further consideration will be given to calculate true current exposures due to the operation of a fuse as expressed in the third or fourth power.

Extensive studies devoted to fuses designed for the protection of diodes and thyristors have shown that:

- the arc ignition moment is practically equal to the moment at which the limited current appears,
- after arc ignition the current remains at an approximately constant value and practically falls down to zero at the moment of natural commutation of the supply voltage.

The course of the current in such a circuit as shown in Fig.1 and under the above given conditions is shown in Fig.2.

The manufacturer of fuses determines the value of the so-called pre-arcing integral $I^2 t = \int_0^{t_p} i_p^2 dt$. In dependence on the symmetrical component of the amplitude of the prospective short-circuit current usually one determines the so-called virtual pre-arcing time

$$t_{vp}^{(2)} = \frac{\int_0^{t_p} i_p^2 dt}{I_m^2} \quad (7)$$

Within the function of that value the true prearcing time t_p was determined for the currents according to (5) and (6) in the form of diagrams in Fig.3a. As to the pre-arcing time, Fig.3b, the relative value has been determined for the limited current in relation to amplitude of the symmetrical short-circuit current. With the application of the curves in Fig.3c value of the virtual arcing time $t_{va}^{(n)}$ have been described to these values for various values of the power exponent for such current, for which the current exposure at fuse operation is intended to be determined. The virtual arcing time

has been determined under the assumption of the relative value of the arc current:

$$k_{ia} = \frac{i_a}{i_l} \quad (8)$$

as follows:

$$t_{va}^{(n)} = \frac{\int_0^{t_a} i_a^n dt}{I_m^n} \cdot \frac{1}{k_{ia}^n} \quad (9)$$

where:

n - power exponent $n = 2, 3, 4$;

(n) - exponent index for the power for which the calculation has been made.

PROPOSED METHOD FOR THE SELECTION OF SHORT-CIRCUIT PROTECTION FOR DIODES AND THYRISTORS

I. To determine for a given type of diode/thyristor the exponent x for the current power in compliance with formula (2) and to round it off to the closest natural number $n = 2, 3$ or 4 .

II. First to select a fuse for a thyristor/diode e.g. in compliance with the till known criterion

$$I^2 t / Th \gg I^2 t / Fuse Total \quad (10)$$

III. To read in the fuse - catalogue the declared value of the Pre-arcing $I^2 t = \int_0^{t_a} i^2 dt$.

IV. To calculate, from the data relating to the short-circuit the maximum value of short-circuit symmetrical current:

$$I_m = \sqrt{2} I_{(RMS)} (prosp. current) \quad (11)$$

V. To calculate, according to formula (7), the virtual pre-arcing time $t_{vp}^{(2)}$ for the fuse.

VI. To take from the diagrams in Fig.3a for the calculated $t_{vp}^{(2)}$ time according to item (V) the real pre-arcing time t_p

for the symmetrical current $t_{p(SC)}^{(2)}$ and the asymmetrical current $t_{p(ASC)}^{(2)}$.

VII. For the t_p as read off in (VI) take the value of the relative limited current $\frac{i_1}{I_m}(SC)$ and $\frac{i_1}{I_m}(ASC)$ from Fig.3b.

VIII. Take the virtual arcing time for $n = 2$: $t_{va(SC)}^{(2)}$ and $t_{va(ASC)}^{(2)}$ from Fig.3c for the values $\frac{i_1}{I_m}$ read according to item (VII).

IX. On the basis of the catalogue data for the fuses, calculate the value:

$$\text{Arcing } I^2 t = \int_0^{t_a} i_a^2 dt = \text{Total } I^2 t - \text{Pre-arcing } I^2 t \quad (12)$$

X. Calculate, for the smaller of the $t_{va}^{(2)}$ values calculated according to (VIII), and the Arcing $I^2 t$ value according to (IX), the relative arc current value by transforming the equation (9):

$$k_{ia} = \frac{i_a}{i_l} = \sqrt{\frac{\text{Arcing } I^2 t}{t_{va}^{(2)} I_m^2}} \quad (13)$$

XI. According to exponent n from (I), and to $\frac{i_1}{I_m}$ from (VII), read from Fig.3c the value of $t_{va(SC)}^{(n)}$ and $t_{va(ASC)}^{(n)}$

XII. Calculate the value of the arc integral according to criterion $I^n t = \text{const.}$ from the dependence:

$$\text{Arcing } I^n t = \int_{t_p}^{t_a} i_a^n dt = (k_{ia} I_m)^n t_{va}^{(n)} \quad (14)$$

for the bigger of the $t_{va}^{(n)}$ values read off according to (XI).

XIII. For the calculated, according to (V), virtual pre-arcing time t_{vp} for the $I^2 t = \text{constant}$ criterion, carry out recalculation for the exponent n as assumed according to (I) in compliance with the curves given in Fig.3d.

XIV. Calculate for the $t_{vp}^{(n)}$ as calculated according to (XIII) the value:

$$\text{Pre - Arcing } I^n t = \int_0^{t_p} i_p^n dt = I_m^n t_{vp}^{(n)} \quad (15)$$

XV. Calculate the fuse total integral on the basis of the dependence:

$$\text{Total } I^n t = \text{Pre-Arc. } I^n t \text{ (acc. to XIV)} + \text{Arc. } I^n t \text{ (acc. to XII)} \quad (16)$$

XVI. Recalculate the catalogue value of $I^2 t$ for the thyristor/diode for the n exponent as determined according to (I) in compliance with Fig.4 or according to the dependence (3) or (4).

XVII. Check, if the condition (17) has been complied with:

$$I^n t / I_{Th} \text{ (acc. to XVI)} \stackrel{if}{>} \text{Total } I^n t / I_F \text{ (acc. to XV)} \quad (17)$$

If so, it is safe to assume, that the selected fuse protects the diode/thyristor against the short-circuit current. If the above given condition is not complied with, however, it is necessary either to select a diode/thyristor of a higher warranted value of its $I^2 t$, or a fuse having a smaller total integral, and above all of a lower prearcing integral. In such case the checking cycle according to the above described algorithm is to be repeated.

CONCLUSIONS There is no doubt that the $I^2 t$ parameter is not a constant value for semiconductors in the region of short-circuit current. In addition, it is determined that such wave-shape of short-circuit currents never appears in 50 (60) Hz networks. From the catalogue data for the diode/thyristors it follows that the $I^3 t = \int i_T^3 dt$, or $I^4 t = \int i_T^4 dt = \text{const. value}$ is more true. This makes recalculation necessary of the fuse short-circuits parameters. Suitable dependences and diagrams are given in this paper. The proposed method is more universal than the thus far applied one. It stresses the effect of the short-circuit current value which is more significant than its duration.

In the example given in the appendix it was demonstrated, that a fuse that had been selected in compliance with the classical method does not fulfil the requirements for correct protection according to the proposed method.

APPENDIX. EXAMPLE FOR THE SELECTION OF SHORT-CIRCUIT PROTECTION FOR A THYRISTOR BY A FUSE

Classical method for short-circuit current protection.

Thyristor data: $I_{T(AV)} = 65 \text{ A}$, $I_{T(RMS)} = 100 \text{ A}$

$$(I^2t)_1 = 5.5 \times 10^3 \text{ A}^2\text{s}, \quad T_1/2 = 10^{-2} \text{ s}$$

$$(I^2t)_2 = 4.1 \times 10^3 \text{ A}^2\text{s}, \quad T_2/2 = 3 \times 10^{-3} \text{ s}$$

Fuse data: $I_{F(RMS)} = 100 \text{ A}$

Pre-arcing $I^2t = 10^3 \text{ A}^2\text{s}$, Total $I^2t = 4.6 \times 10^3 \text{ A}^2\text{s}$

The "classical" condition for short-circuit protection the thyristor by the fuse with the above given data is complied with:

$$I^2t/Th = 5.5 \times 10^3 \text{ A}^2\text{s} > I^2t/F_{total} = 4.6 \times 10^3 \text{ A}^2\text{s}$$

Proposed method for short-circuit current protection.

I. From the thyristor catalogue data, (acc. to 2), we have:

$$x = 2 \times \frac{\log \frac{10^{-2}}{3 \times 10^{-3}}}{\log \frac{4.1 \times 10^3}{5.5 \times 10^3} \times \frac{10^{-2}}{3 \times 10^{-3}}} = 2.65$$

Assumed: $n = 3$.

II, III. The following has been assumed in compliance with the previous example: $I_{F(RMS)} = 100 \text{ A}$, Pre-Arcing $I^2t = 10^3 \text{ A}^2\text{s}$; Total $I^2t = 4.6 \times 10^3 \text{ A}^2\text{s}$.

IV. The following has been obtained from the short-circuit data: $I_m = \sqrt{2} \times I_{(RMS)} \text{ (prosp. current)} = \sqrt{2} \times 70 \times 10^3 = 10^5 \text{ A}$.

$$\text{V. } t_{vp}^{(2)} = \frac{\text{Pre-Arcing } I^2t}{I_m^2} = \frac{10^3}{(10^5)^2} = 10^{-7} \text{ s.}$$

VI. For $t_{vp}^{(2)}$ (acc. to V) = 10^{-7} s Fig. 3a $t_p(SC) = 0.13 \times 10^{-3} \text{ s}$;
 $t_p(ASC) = 0.77 \times 10^{-3} \text{ s}$.

VII. For $t_p(SC)$ (acc. to VI) $\xrightarrow{\text{Fig. 3b}}$ $\frac{i_1}{I_m} (SC) = 5 \times 10^{-2}$;
 $\frac{i_1}{I_m} (ASC) = 3 \times 10^{-2}$.

VIII. For $\frac{i_1}{I_m}$ (acc. to VII) $\xrightarrow{\text{Fig. 3c}}$ $t_{va}^{(2)}(SC) = 2 \times 10^{-5}$ s ;

IX. Acc. to (12):
 Arcing $I^2t = \text{Tot. } I^2t - \text{Pre-Arc. } I^2t = 4.6 \times 10^3 - 10^3 = 3.6 \times 10^3 \text{ A}^2\text{s}$

X. Acc. to (13):
 $k_{ia} = \frac{i_a}{i_1} = \frac{\text{Arcing } I^2t}{t_{va}^{(2)} \times I_m^2} = \frac{3.6 \times 10^3}{1.8 \times 10^{-5} \times (10^5)^2} \cong 0.14$

XI. For n (acc. to I) = 3, $\frac{i_1}{I_m}$ (acc. to VII) $\xrightarrow{\text{Fig. 3c}}$
 $t_{va}^{(3)}(SC) = 7 \times 10^{-7}$ s ; $t_{va}^{(3)}(ASC) = 3 \times 10^{-7}$ s .

XII. For k_{ia} (acc. to X), I_m (acc. to IV), $t_{va}^{(3)}(\text{max})$ (acc. to XI) we calculate:

Arcing $I^3t = k_{ia} \times I_m^3 \times t_{va}^{(3)}(\text{max}) = 0.14 \times (10^5)^3 \times 7 \times 10^{-7} = 1.9 \times 10^6 \text{ A}^3\text{s}$

XIII. For $t_{vp}^{(2)}$ (acc. to V), and n (acc. to I) $\xrightarrow{\text{Fig. 3d}}$
 $t_{vp}^{(3)}(SC) = 7 \times 10^{-9}$ s ; $t_{vp}^{(3)}(ASC) = 4.8 \times 10^{-9}$ s .

XIV. For $t_{vp}^{(3)}(\text{max})$ (acc. to XIII); I_m (acc. to V) and n (acc. to I) we calculate:

Pre-Arcing $I^3t = t_{vp}^{(3)}(\text{max}) \times I_m^3 = 7 \times 10^{-9} \times (10^5)^3 = 7 \times 10^6 \text{ A}^3\text{s}$

XV. For Pre-Arcing I^3t (acc. to XIV) and Arcing I^3t (acc. to XII) we calculate:

Total $I^3t = \text{Pre-Arcing } I^3t + \text{Arcing } I^3t = 7 \times 10^6 + 1.9 \times 10^6 = 8.9 \times 10^6 \text{ A}^3\text{s}$.

XVI. For n (acc. to I), and the value of the thyristor I^2t (acc. to I) $\xrightarrow{\text{Fig. 4}}$ $I^3t/Th = 5 \times 10^6 \text{ A}^3\text{s}$

XVII. The condition (17) has not been complied with:
 I^3t/Th (acc. to XVI) = $5 \times 10^6 \text{ A}^3\text{s}$ $\overset{\text{NO!}}{>} \text{Total } I^3t_{\text{Fuse}}$ (acc. to XV) = $8.9 \times 10^6 \text{ A}^3\text{s}$

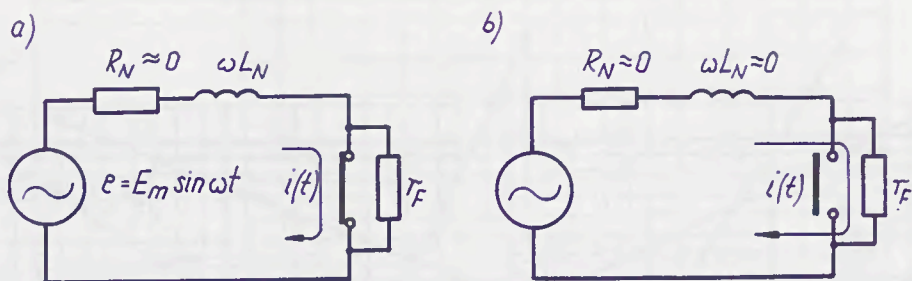


Fig. 1. Substitute diagram for a short-circuit with a fuse operating: a) in the prearcing time, b) during the arc burning time.

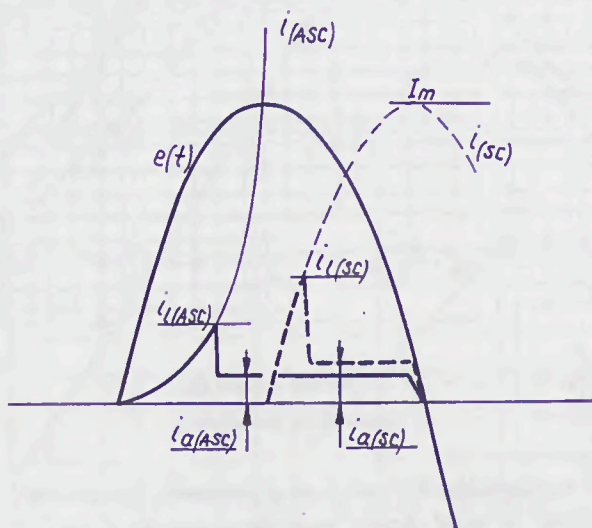


Fig. 2. Short-circuit current limited by a fuse:
 $i(SC)$ - symmetrical current, $i(ASC)$ - asymmetrical current.

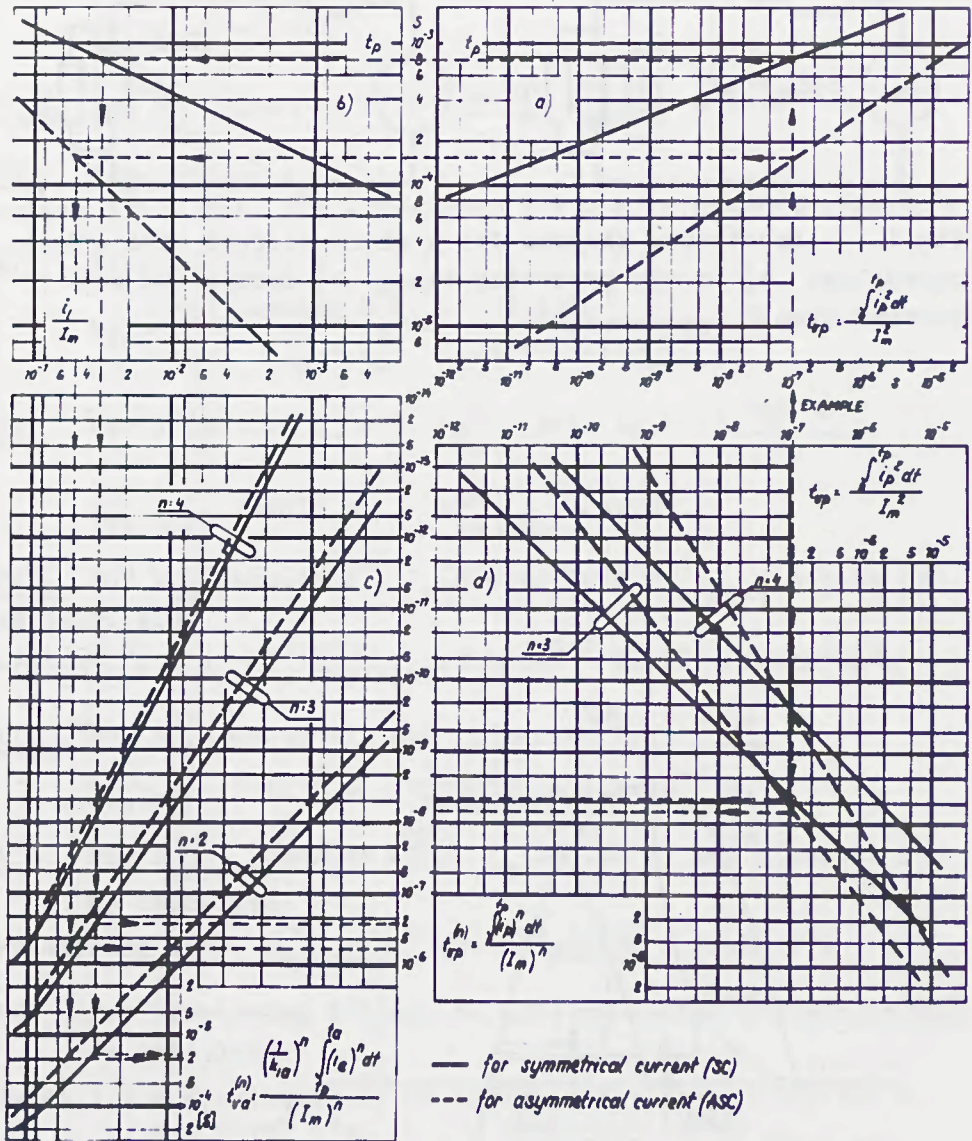


Fig.3. Diagrams for recalculating the values of characteristic parameters of a fuse operating at short-circuits under the assumption of the $I^n t = \int i^n dt$

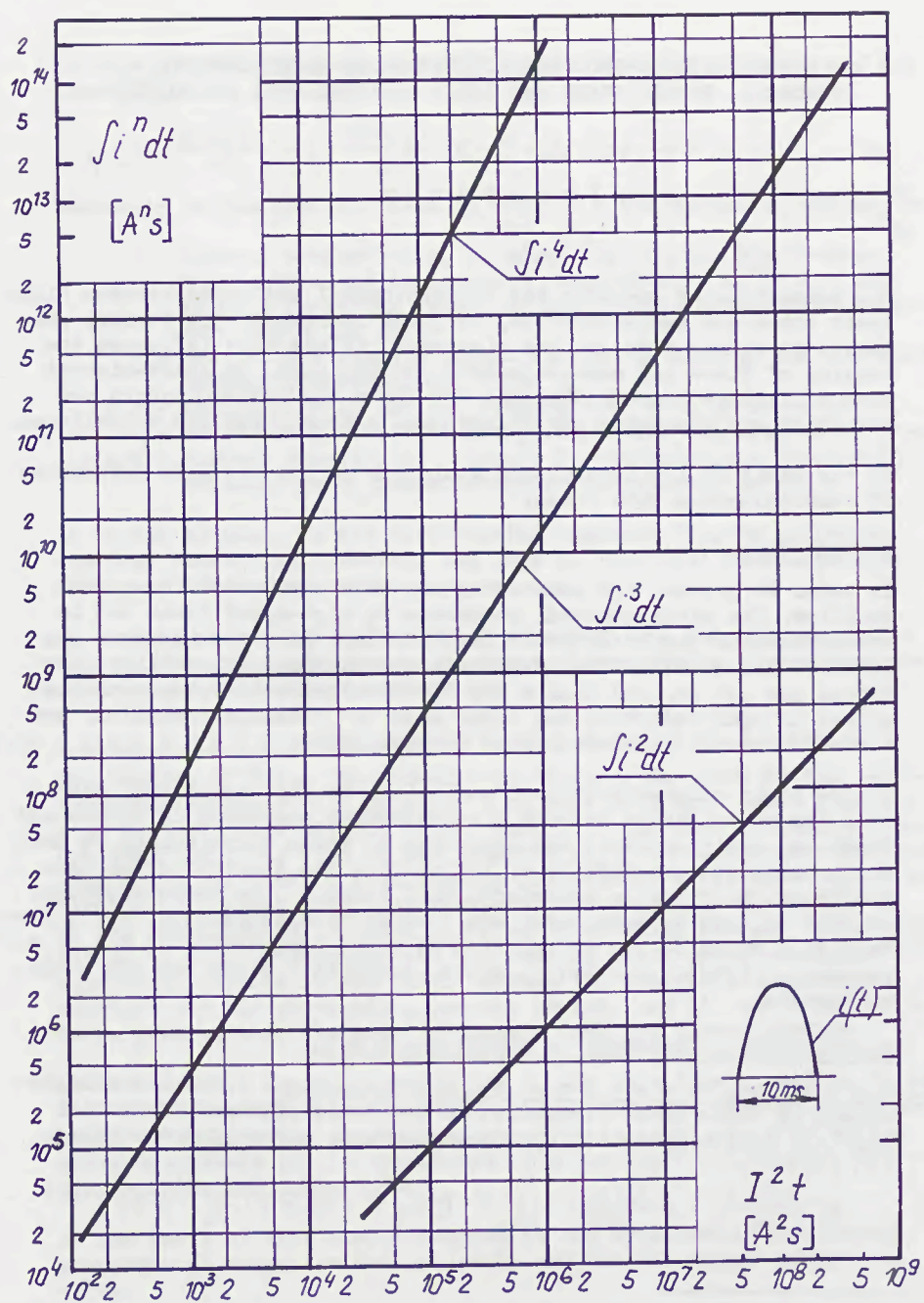


Fig.4. Dependence of the $\int (I_m \sin \omega t)^n dt$ versus the value of the $\int i^2 dt$ for $T/2 = 10^{-2}$ s.

CONSIDERATIONS UPON THE ANALOGY AMONG ELECTROTHERMAL
PHENOMENA WITHIN FUSES AND THEIR SEMICONDUCTOR PROTECTION

I o n B a r b u

The present paper presents the electrothermal analogies between high-speed fuses and semiconductors, in joint operation. The thermal phenomena in rating mode and the electrical values that influence the heating of fuses and semiconductors are analyzed. In short-circuit mode equivalent thermal diagrams for fuses and semiconductors are presented and analogies and differences between them are established.

On the basis of the established analogies we present safe procedures of semiconductors with fuses.

1. INTRODUCTION

In order to protect the semiconductors with electrical fuses with fusibles, the electrothermal phenomena in high-speed fuses and in semiconductors should obey the same physical laws and the same qualitative and quantitative mathematical relations. In reality the things are not so, and that's why the electrothermal phenomena that appear in semiconductors and fuses must be thoroughly studied, and their functional parameters must be correlated.

On the basis of electrothermal analogies, we must establish exactly the correlations between electrothermal phenomena in high-speed fuses and semiconductors and depending on these correlations we must study first the possibility of influencing the electrothermal parameters of the fuses in accordance with those of the semiconductors; we must do this because fuses are cheaper than semiconductors. A further step would be the correlation of these parameters for all in operating conditions: steady - state, overload - state and short-circuit state.

2. ELECTROTHERMAL PHENOMENA IN STEADY-STATE MODE

2.1. General heating equations. The thermal phenomena in fuses could be studied on the basis of the differential heating equation, in its most general form, given by the relation [1]; [2] :

$$\rho c \frac{\partial T(x,t)}{\partial t} = \lambda \frac{\partial^2 T(x,t)}{\partial x^2} - \left[\frac{l_x K - \rho_{00} \int^2(x,t)}{A_x} \right] \sigma(x,t) + \rho_a \int^2(x,t) \quad (1)$$

Dr. Eng. Ion Barbu - Head of Laboratory with The Institute of Scientific Research and Technological Engineering for the Electrotechnical Industry - Bucharest - Romania

In case of semiconductors the differential heating equation has the form [3]:

$$\gamma c \frac{\partial \theta(x,t)}{\partial t} - \lambda \frac{\partial^2 \theta(x,t)}{\partial x^2} = p(x,t) = U_0 j(x,t) + r j^2(x,t) \quad (2)$$

where: γ - is the specific mass in $\frac{g}{cm^3}$; c - the specific heat in $\frac{Ws}{Cg}$

λ - thermal conductivity, in $W/cm^2 \text{ } ^\circ C$; $\tau(x,t)$, $\theta(x,t)$ - over-temperature and temperature respectively, in $^\circ C$; l_x - the fusible perimeter length or the fusible's isthmus perimeter length, in cm;

A_x - area of the fusible cross-section or area of the fusible's isthmus cross-section, in cm^2 .

ρ_a - resistivity at ambient temperature, at $0^\circ C$, in Ωcm ;

α_{ρ_0} - resistivity variation coefficient with temperature in $\frac{1}{^\circ C}$;

$J(x,t)$ - current density, in A/cm^2 ; U_0 - semiconductor threshold voltage, in V; r - semiconductor resistance, in Ω .

As it can be seen, in the differential equation (2), we neglected the heat convection transfer, and this is justified by the little length of the semiconductor.

If we compare the two differential equations (1) and (2), we notice that in fuses and semiconductors nonstationary thermal phenomena are governed by different equations.

2.2. Electrothermal phenomena in fuses.

The heating of fuses in steady-state mode, is given by the differential equation (1), in which - in case of a very exact analysis - we must consider all the terms. That's to say that we should also consider the first form of the equation (1). The explanation of this fact would be, that in steady-state conditions, at alternating or intermittent current, the temperature varies evidently with time. As it was demonstrated in paper [4], at alternating current, overtemperature is also alternating and the heating alternating component amplitude, depends on the ratio between the fusible thermal time constant and the alternating current period, and it can be at limit, twice greater than the overtemperature from the direct current.

It is difficult to analyze equation (1) in this paper, neither do we have the necessary space for such an analysis, and that's why we are going to analyze the current square value depending on time and the space coordinate (x) in accordance with the fuses utilization diagram and the isthmuses form.

At the basis of this simplification is the hypothesis that thermal phenomena in fuses are determined by the current square effective value.

In Fig. 1 different forms of current depending on time are presented and in Fig. 2 different forms of fuses' isthmuses.

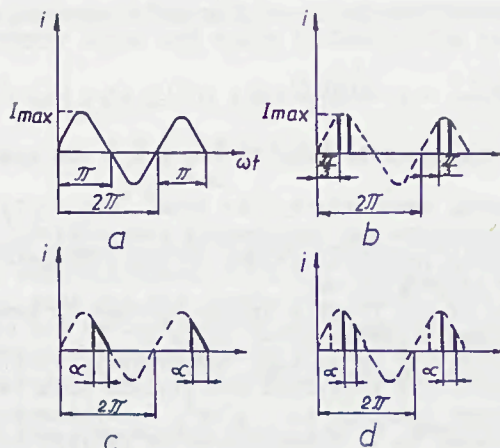


Fig.1 Forms of current depending on time

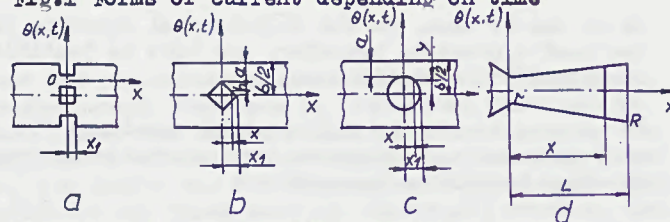


Fig.2 Forms of fusibles' isthmuses

Taking into account those mentioned above, the effective value of the electric current density for the fusibles' isthmuses (which must be introduced into equation (1)) is given by the expression:

$$J(x, t) = \frac{I_{max}}{A(x)} \sqrt{\frac{1}{2\pi} \int_{\alpha_c}^{\alpha_b} f^2(\omega t) d(\omega t)} = \frac{I_{max}}{A(x)} K \quad (3)$$

where: $f(\omega t)$ - current variation in time; T - alternating current period, in s; $A(x)$ - fusible's section area, in cm^2 ; α_c, α_b - angle of conduction and the thyristor blocking respectively.

Generally, $f(\omega t)$ has a sinusoidal form for resistive loads.

Considering relation (3) and Fig.1 and Fig.2, in Table 1, the current density values $J(x, t)$ depending on the electric current maximal value (I_{max}) for different angles of conduction of the electric current and different isthmus forms, are given.

Fusible heating can be calculated by means of the thermal effects superimposing method, which had been described in paper [1].

Current density effective value $J(x, t)$

Table 1

Form of isthmuses Form Figure 2 of current Figure 1		Figure 2a	Figure 2b	Figure 2c	Figure 2d
Figure 1a	$\frac{KI_{max}}{A(x)}$	$\frac{0,707 I_{max}}{gb}$	$\frac{0,707 I_{max}}{2g \left[a + \frac{x}{x_1} \left(\frac{b}{2} - a \right) \right]}$	$\frac{0,707 I_{max}}{2g(r+a-\sqrt{r^2-x^2})}$	$\frac{0,707 I_{max}}{\pi \left(r + \frac{R-r}{b} x \right)^2}$
Figure 1b	$\frac{KI_{max}}{A(x)}$	$\frac{0,39 I_{max}}{gb}$	$\frac{0,39 I_{max}}{2g \left[a + \frac{x}{x_1} \left(\frac{b}{2} - a \right) \right]}$	$\frac{0,39 I_{max}}{2g(r+a-\sqrt{r^2-x^2})}$	$\frac{0,39 I_{max}}{\pi \left(r + \frac{R-r}{b} x \right)^2}$
Figure 1c	$\frac{KI_{max}}{A(x)}$	$I_{max} \sqrt{\frac{\pi}{2\pi} + \frac{1}{8\pi}} \sin 2(\pi - \alpha)$ gb	$I_{max} \sqrt{\frac{\pi}{2\pi} + \frac{1}{8\pi}} \sin 2(\pi - \alpha)$ $2g \left[a + \frac{x}{x_1} \left(\frac{b}{2} - a \right) \right]$	$I_{max} \sqrt{\frac{\pi}{2\pi} + \frac{1}{8\pi}} \sin 2(\pi - \alpha)$ $2g(r+a-\sqrt{r^2-x^2})$	$I_{max} \sqrt{\frac{\pi}{2\pi} + \frac{1}{8\pi}} \sin 2(\pi - \alpha)$ $\pi \left(r + \frac{R-r}{b} x \right)^2$
Figure 1d	$\frac{KI_{max}}{A(x)}$	*	$\frac{*}{2g \left[a + \frac{x}{x_1} \left(\frac{b}{2} - a \right) \right]}$	$\frac{*}{2g(r+a-\sqrt{r^2-a^2})}$	$\frac{*}{\pi \left(r + \frac{R-r}{b} x \right)^2}$

$$* I_{max} \sqrt{\frac{\pi}{2\pi} - \frac{\sqrt{3}}{16\pi} - \frac{1}{8\pi}} \sin 2 \left(\frac{\pi}{6} + \alpha \right)$$

2.3. Electrothermal phenomena in semiconductors.

The analogies and differences between semiconductors and fuses are, roughly speaking, the following: in general, the fuses have long fusibles as compared with the semiconductors which are short; in semiconductors the electric current density to the space coordinates, at high frequencies is not constant; heating variation in semiconductor is important in the radial direction, too; l and A are constant in a semiconductor etc. The most important difference between semiconductors and fuses lies in the fact that whereas in fuses the thermal phenomena are determined by the alternating current effective value, in semiconductors the thermal phenomena - especially in steady - state mode - are determined by the alternating current effective and, especially, mean values. Considering the threshold voltage in the semiconductor, and accepting the hypothesis that $U=f(I)$ characteristic is a straight-line, the dissipated power in a semiconductor is given by relation (5)

$$p(t) = U_0 i(t) + r i^2(t) \quad (4)$$

from which we obtain the mean power in a period of time, under the form:

$$P = \frac{1}{T} \int_0^T p(t) dt = \frac{1}{T} \int_0^T U_0 i(t) dt + \frac{r}{T} \int_0^T i^2 dt = U_0 I_{med} + r I_{ef}^2 \quad (5)$$

Since the effective current determines the heating in steady-state mode for fuses, and the mean current in semiconductors (at a rate of 80 %), we consider necessary to show that there is a great diffe-

rence between the effective and mean currents from the same branch of a rectifier circuit, thus, in a branch of a three-phase diagram with double alternance, for a commutation of 60 electric degrees, $I_{ef} = 1.73 I_{mean}$, and this ratio increases very much for little angles of commutation [1] .

3. EQUIVALENT THERMAL DIAGRAMS

On the basis of electrothermal analogies, equivalent thermal diagram with limited parameters (for semiconductors) were elaborated, diagrams that had been presented in literature [5] , [6] . In the present paper we shall also delimitate, on the same principles, an equivalent thermal diagram for fuses.

3.1. Semiconductor equivalent thermal diagram. In Fig. 3 equivalent thermal diagrams for diodes (fig.3.a) and for thyristors (fig.3.b) are presented:

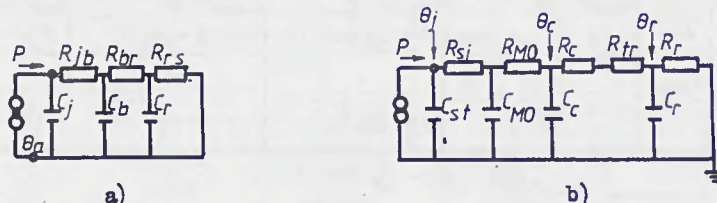


Fig. 3 Semiconductor equivalent thermal diagrams

Thermal resistance is given by relation 6 :

$$R_t = \frac{\Delta\theta}{P} = \frac{1}{\lambda} \int \frac{dl}{A} \quad \left[\frac{^{\circ}C}{W} \right] \quad (6)$$

Thermal capacity is given by relation:

$$C_t = \frac{\int P dt}{\Delta\theta} = cM \quad \left[\frac{Ws}{^{\circ}C} \right] \quad (7)$$

Thermal time constant results from relation:

$$\tau_t = R_t \cdot C_t \quad [s] \quad (8)$$

The thermal diagrams from Fig. 3 can be solved by means of analogy with an electrical circuit. The values in Fig. 3 have the following significance; p - power developed in semiconductor; C_j, C_b and C_r - junction, basis and radiator thermal capacities, in $Ws/^{\circ}C$; R_{jb}, R_{br}, R_{rs} - thermal resistances between junction - basis, basis-radiator and radiator - environment, in $^{\circ}C/W$. The parameters for the thyristor thermal equivalent diagram are established in the same way.

3.2. Fuse equivalent thermal diagram. The simplest equivalent thermal diagram of a tube fuse, can be elaborated, considering the constructive type of the respective fuse. Thus, in Fig. 4 a tube fuse with a simple fusible, is presented

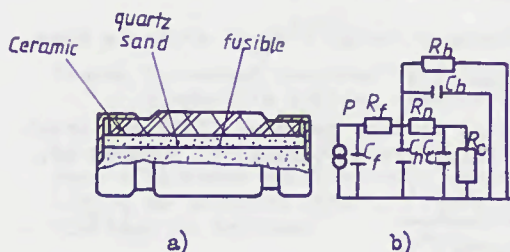


Fig. 4 Fuses with fusibles

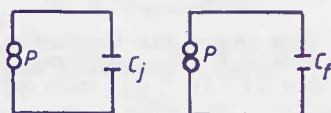


Fig. 5 Equivalent thermal diagrams in short - circuit mode

In Fig. 4.b the thermal equivalent diagram of such a fuse is presented. R and C represent the thermal resistances and the thermal capacities respectively of: fusible (R_f, C_f), quartz sand (R_n, C_n), ceramic body (R_o, C_o) and junction pole (R_p, C_p).

4. ELECTROTHERMAL PHENOMENA IN SHORT-CIRCUIT MODE

4.1. Semiconductor safe procedures. The condition of semiconductor protection with fuses against short-circuit is satisfied if between (I^2t) admitted by the semiconductor and total (I^2t) of the fuse is observed the relation:

$$(I^2t)_{\text{semiconductor}} < \text{total } (I^2t)_{\text{fuse}} \quad (9)$$

When connecting in parallel identical semiconductors with individual protection fuses of the same type, it is also necessary to observe the condition of selectivity. That means that in case of semiconductor malfunction, the fuse on the respective branch melts and breaks the short-circuit current before the fuses on the complementary branch melt too. This condition is satisfied if the pre-arch (I^2t) of n fuses from the complementary branch is greater than the total (I^2t) of the defect fuse.

The pre-arch (I^2t) value, produced by the $\frac{c}{n} i$ current in any of the n fuses on the complementary branch is:

$$(I^2t)_{\text{prearch}} = \int_0^{t_p} \left(\frac{c}{n} i\right)^2 dt = \frac{c^2}{n^2} \int_0^{t_p} i^2 dt \quad (10)$$

where: c is a fuse loading factor.

Total (I^2t) value of a fuse on the defect branch is:

$$\text{total } (I^2t)_{\text{of fuse}} = \int_0^{\infty} i^2 dt \quad (11)$$

The pre-arch (I^2t) value of the n fuses on the complementary branch is given by the relation:

$$\text{total pre-arch}(I^2t) = \text{pre-arch } n^2(I^2t)_{\text{of the } n \text{ fuse}} \quad (12)$$

So, the selectivity condition is satisfied if :

$$\begin{aligned} \text{Total pre-arch } (I^2t) \text{ of the } n \text{ fuses} &> \text{total } (I^2t) \text{ of a single fuse} \\ \Rightarrow \text{pre-arch } n^2(I^2t) &> \text{total } (I^2t) \end{aligned}$$

From where the connecting relation between pre-arch (I^2t) and total (I^2t) of a fuse that assures a selective protection is inferred by:

$$n^2 > \frac{\text{total}(I^2t)}{\text{pre-arch}(I^2t)} \quad (13)$$

Considering relation (13), the ratio between total (I^2t) and pre-arch (I^2t) of a fuse with selective protection, used with 2 thyristors connected in parallel, must be less than 4; for 3 fuses in parallel it must be less than 9 and for 4 fuses in parallel it must be less than 16.

We underline the fact that the ratio presented in relation (13) is less than 4, and that it is difficult to be obtained in case of high-speed fuses. The fuses produced by firms such as Siemens, LK-NES or Soviet firms etc. have this ratio between 5 and 11. From what we know, only the Romanian high-speed fuses and those produced by Ferraz have this ratio less than 3. It results that two thyristors functioning in parallel can be selectively protected only with these fuses.

- 4.2. Individual protection analyzed on the basis of equivalent thermal diagrams. For very short periods, while the short-circuit lasts and when the heat transfer can be neglected, the equivalent thermal diagram from Fig. 3 and Fig. 4 can be simplified as in Fig. 5. Considering the analogies mentioned above, the following relation between overtemperature and energies developed in fuses and semiconductors, are obtained:

In semiconductor we obtain:

$$\tau_j = \frac{1}{C_j} \int p dt \quad (14)$$

and in fuse:

$$\tau_f = \frac{1}{C_f} \int p dt \quad (15)$$

At short-circuit, we can consider that the whole energy developed in a semiconductor is stored by the capacity C_j , and then, considering the expression (4) we obtain the relation:

$$E_s = \int_0^t p dt = U_0 \int_0^t i dt + r \int_0^t i^2 dt = C_j \tau_j \quad (16)$$

By analogy, the energy developed in the fuses' fusibles is obtained in:

$$E_f = \int_0^{t_p} p dt = r_f \int_0^{t_p} i^2 dt = C_f (\theta_f - \theta_a) \quad (17)$$

where: E_f - energy necessary for fusible melting; t_p - pre-arch time;
 θ_f - fusible melting temperature; θ_a - ambient temperature

In case of semiconductors - for very short periods - which is the case of intense short-circuit currents - the term $U_0 \int i dt$ is very little as compared with $r \int i^2 dt$ and in these conditions relations (16) can be written:

$$I^2 t = \int_0^t i^2 dt = \frac{C_j}{r_j} \tau_j \quad (18)$$

So, total ($I^2 t$) produced by the short-circuit, in a period t is directly proportional with the junction thermal capacity and invers proportional with its resistance.

In the same way, the highest the junction temperature is the highest ($I^2 t$) is. Generally this temperature is not higher than 140°C.

In case of fuses, from relation (17) we obtain:

$$(I^2 t)_{prearch} = \int_0^{t_p} i^2 dt = \frac{C_f}{r_f} (\theta_f - \theta_a) \quad (19)$$

Comparing relations 18 and 19, we notice that thermal effects in semiconductors and fuses, at short-circuit, are relatively analogous if we take into consideration total ($I^2 t$) for semiconductors, and pre-arch ($I^2 t$) for fuses. But as we have already demonstrated, pre-arch ($I^2 t$) in fuses represents only a little part from the total ($I^2 t$). The most serious drawback is the fact that in case of fuses there is no well determined relation between pre-arch ($I^2 t$) and total ($I^2 t$).

Consequently, in case of fuses, pre-arch ($I^2 t$) and total ($I^2 t$) vary depending on many factors. Out of these factors we could mention: type of fusible; electric circuit parameters; moment of apparition of the electric arch; power - supply voltage evolution during the electric arch etc.

However, we determine in case of fuses a maximum arch ($I^2 t$) for the same voltage value. But since the arch ($I^2 t$) is for some types of fuses about 9 times greater than the pre-arch value, we can't use relation (19) with the same exactity as relation (18).

There is another big difference between the behaviour of fuses and semiconductors in case of short-circuit. These differences are even more obvious, if we analyze comparative by the parameters presented in Tabel 2 for fuses and semiconductors and the physical constants of materials used for fuses and semiconductors, presented in Table 3.

Some fuses and semiconductors parameters

Table 2

Parameter	The isthmuses of the fusible	Semiconductor	
		The junction of the diode	The junction of the thiristor
Generated specific power $\left[\frac{W}{cm^3}\right]$	360	10	10
Steady state temperature $[^{\circ}C]$	300 ÷ 400	190	150
Thermal resistance $\left[\frac{^{\circ}C}{W}\right]$	10	0.13 ÷ 3	1
Thermal capacity $[^{\circ}C]$	203	—	735

Table 3

Physical constants of materials used for fuses and semiconductors

Constants of materials	Specific heat capacity $20^{\circ}C$ $\left[\frac{J}{g^{\circ}C}\right] \cdot 10^{-3}$	Thermal conductivity $\lambda \left[\frac{W}{cm^{\circ}C}\right] 10^{-2}$	Diffusivity $a = \frac{\lambda}{c} \cdot 10^{-6}$ $\left[\frac{m^2}{s}\right]$
SILVER	230	418	171
ALUMINIUM	920	204	81
TIN	235	64	37.8
COPPER	393	380	108
MOLYBDENUM	270	145	53
SILICON	735	84	49
WOLFRAM	141	130	61

5. CONCLUSIONS

The above analysis demonstrated certain analogies and differences between the electrothermal phenomena in fuses and semiconductors.

The analogies consist in the fact that both the fuses and semiconductors under go the electric current heating.

In steady-state mode, the difference lies in the fact that in base of fuses only the effective current is the cause of heating where as in case of semiconductors, the heating is determined by both the current effective value and - especially - by the current mean value R_t and C_t parameters and the volumetric power differ very much from fuses to semiconductors the thermal time constant of fusibles'isthmuses are very close as values to the semiconductor junction time constant.

At short-circuit, (I^2t) produced by the short-circuit current deter-

mines the heating of the semiconductor, but in case of fuses, the pre-arc (I^2t) leads to the melting of the fuse, and the total (I^2t) assures the semiconductor protection.

In case of fuses, pre-arc (I^2t) and total (I^2t) differ very much. The physical constants of materials used in fuses (Ag) and of materials used for semiconductor junction (Mb, Si etc.) differ very much too.

Despite the differences between the thermoelectrical parameters of fuses and semiconductors, we can choose a corresponding safe procedure and correlation between them.

BIBLIOGRAPHY

- [1] Barbu, I. : Siguranțe electrice de joasă tensiune. Editura tehnică, București, 1983, 333 p.
- [2] Barbu, I. : Contribuții privind unele fenomene electrotermice din siguranțele cu fuzibile și modelarea lor. Teza de doctorat, Timișoara 1971 (Biblioteca I.P. Traian Vuia).
- [3] Lupăș, O. : Principii de dimensionare a dispozitivelor semiconductoare de putere. Teză de doctorat, I.P. București, 1973, Biblioteca I.P. București.
- [4] Barbu, I. : Untersuchung des Zusammenhanges zwischen termischen und elektromagnetischen Erscheinungen. Lucrările ICPE nr. 20, 1968, pag. 49-55.
- [5] Korb, F. : Die thermische Auslegung von fremdgekühlten Halbleitern bei netzgeführten Stromrichtern ETZA, 92 (1971) nr. 2 pag. 100-107.
- [6] Zeissig, F. : Messung des transienten Hämewiderstände undzeitkonstanten von Thyristoren, Elektrik 1968, nr. 3 pag. 101-104.
- [7] Panaite, V. : Procese termice în aparatele de comutație. Teză de doctorat I.P. București, 1975, Biblioteca I.P. București.
- [8] Barbu, I. : On phenomena, in the electric arc of fuses and their influence upon the pre-arc and arc I^2t values. Fourth International Symposium on Switching arc Phenomena, 22-24 September, 1981, Lodz, Poland.

RESEARCH ON POWER-FUSE CO-ORDINATED WITH VACUUM CONTACTOR

Wang Jimei

INTRODUCTION

In recent years so many industrial departments in China commenced to adopt the vacuum contactor as main switch in high voltage arc furnace, controlling and starting switch in high voltage motor and high voltage switch for frequently operated equipments. It has the features of small volume, light weight and fitness to frequent operation. However, the vacuum contactors in China are still in lack of back-up fuse co-ordinated with them. In this case, once the heavy overload or short-circuit fault occurs, not only the vacuum contactor itself will be damaged, but also the interruption of power supply will happen. For this reason, the vacuum contactor co-ordinated with power-fuse to undertake heavy overload and protect from short-circuit fault is necessary.

The performance of high voltage H.R.C. fuse has much improved, such as the raise of rated current, enhancement of interrupting capacity and use of high stress glass-fibre cartridge.

DESIGN OF FUSE CONSTRUCTION

The fuse should be so designed that it possesses high ability to withstand multi-time low overload impulse current many times, e.g., it can withstand the heating cycle more frequently than that of ordinary distribution power fuse. Hence, if a fuse of general construction is used, the fuse element around the sand may have a displacement due to heat expansion and cold shrinkage, so it causes the fuse element itself to undertake more stress. Thus, there is a possibility to crack the fuse element. For this purpose, we selected the fuse element with larger section area and adopted self-support construction without support-structure in designing fuse construction. But, there is expansion ribbon in both ends and middle part of the fuse element.

To meet the requirements of back-up fuse performance (e.g., delaying the operating time of current-time characteristics of fuse-element under multi-time low overload and fast operation under short-circuit fault), the geometric form of element was specially designed, which is different from ordinary distribution power fuse.

Professor Wang Jimei is a Head of Electrical Apparatus Section at Xi'an Jiaotong University, a consultant of Xi'an Fusegear Factory, a member of State Council Academic Degree Committee, a member of National Science Committee of China and a councilor of Chinese Society of Electrical Engineering in China.

To satisfy the ability of interrupting capacity under large rated current, a cartridge made of glass-fibre cemented with inorganic glue was used. The wall of cartridge is thinner and lighter than that of porcelain one, so it eliminates any dangerousness of crack of cartridge.

In order to proceed our research work smoothly, we performed beforehand a series of theoretical calculation for the main performance of fuse as follows:

(1) Calculation for steady-state temperature-rise

The average value of steady-state temperature rise of fuse element was estimated with the formula recommended by K. K. Namintokoff et al. [1].

$$T = (k^2 + T_0) / (1 - k^2 B) = ((I^2 R / aS) + T_0) / (1 - (I^2 R / aS) B) \quad (1)$$

where

I—current passing through fuse element, A;

R—resistance of fuse element, ohm;

a—coefficient of heat dissipation, w/cm².°C;

S—dissipated area of fuse element, cm²;

T₀—ambient temperature, °C;

B—resistance-temperature coefficient of fuse element, °C⁻¹.

when I=300 A, R=0.00095 ohm, a=25x10⁻⁴ w/cm².°C, S=350 cm², T=20°C and B=4x10⁻³ °C⁻¹, we have

$$\begin{aligned} T &= (300^2 \times 0.00095 / 25 \times 10^{-4} \times 350 + 20) / \\ &\quad / (1 - (300^2 \times 0.00095 / 25 \times 10^{-4} \times 350) (4 \times 10^{-3})) \\ &= (98 + 20) / (1 - 0.392) = 165 \text{ } ^\circ\text{C}. \end{aligned}$$

The average temperature rise of cartridge surface can be calculated through the following formula:

$$T_1 = I^2 R / a_1 S_1 \quad (2)$$

where a₁—coefficient of heat dissipation on fuse cartridge surface, w/cm².°C;

S₁—surface area of fuse cartridge, cm².

when a₁=10x10⁻⁴ w/cm².°C, S₁=1470 cm², then

$$T_1 = 300^2 \times 0.00095 / 10^{-3} \times 1470 = 58 \text{ } ^\circ\text{C}.$$

(2) Estimation of rated interrupting capacity

In accordance with IEC Standard, after testing the rated interrupting capacity, the interrupting ability of H.R.C. fuse under maximum arc energy should be also examined. The value of this tested current should be selected in satisfying the following formula, when φ_i=0~20°,

$$I_{\text{fusing}} = (0.6 \sim 0.75) I_m \quad (3)$$

where I_m—the peak value of prospective current to be determined.

For obtaining this peak value, it is necessary to use a certain quantity of sample fuse for test. Before the test, a calculation of maximum arc energy was made on the newly designed fuse. It showed that the result of calculation was close to that of maximum arc energy test. The calculation is recommended as follows.

When the fuse is inserted in a source supply, the general expression is

$$U_m \sin(\omega t + \phi_i) = L \frac{di}{dt} + (R + R_0(1 + BT))i \quad (4)$$

where L —circuit inductance, henry;

R —circuit resistance, ohm;

B —resistance temperature coefficient of fuse element, $^{\circ}\text{C}^{-1}$;

T —temperature rise of fuse element, $^{\circ}\text{C}$;

ϕ_i —phase angle at closing instant, electrical degree.

If the resistance of fuse element is negligible, the equation (4) can be written as follows

$$U_m \sin(\omega t + \phi_i) = L \frac{di}{dt} + Ri \quad (5)$$

Solving equation (5), we get

$$i = I_m (e^{-t/\tau} \sin \omega t_0 + \sin(\omega t - \omega t_0)) \quad (6)$$

where $\tau = L/R$, $\omega t_0 = \phi - \phi_i$, $\cos^2 \phi = 1/(1 + \omega^2 \tau^2)$ and $I_m = U_m \cos \phi / R$. From equation (6), the square of current density integrates to time, then we have,

$$\begin{aligned} \int_0^{t_{\text{fusing}}} \left(\frac{i}{S}\right)^2 dt &= \int_0^{t_{\text{fusing}}} \sigma^2 dt = \\ &= \int_0^{t_{\text{fusing}}} \left(\frac{I_m}{S}\right)^2 (\exp(-t/\tau) \sin \omega t_0 + \sin(\omega t - \omega t_0))^2 dt \end{aligned} \quad (7)$$

In according to equation (7), if ϕ_i and ϕ are given and the material of fuse element be known, (for instance, silver as fuse element it is

$$C = \int_0^{t_{\text{fusing}}} \left(\frac{i}{S}\right)^2 dt = 8 \times 10^4 \text{ A}^2 \text{s}^2 / \text{mm}^4$$

a relationship between the density of prospective current and fusing time can be obtained. Then we take equation (6) to calculate the density of fusing current. Figure 1. shows the results of this calculation, when $\cos \phi = 0.2$, $\phi_i = 0^{\circ}$ and 45° in which a series of given values of prospective current density are taken. Correspondently, with the similar proceduces we got the curves by the calculation of fusing current density.

Meanwhile, the slop-curves of $\mathcal{J} = f(\mathcal{J}_m)$, $\mathcal{J} = f(0.75\mathcal{J}_m)$ and $\mathcal{J} = f(0.6\mathcal{J}_m)$ plotted by the prospective current density and its correspondent current density were taken. We may obtain the range of prospective current density of maximum arc energy from the slop curves $0.75\mathcal{J}_m$ and $0.6\mathcal{J}_m$ intersected at $\phi_i = 0^{\circ}$ and 45° curves respectively.

When $\phi_i = 0^{\circ}$, the range of maximum arc energy from Figure 1. is $1.15 \times 10^4 \text{ A/mm}^2 < \mathcal{J} < 1.5 \times 10^4 \text{ A/mm}^2$, when $\phi_i = 45^{\circ}$, it is $1.2 \times 10^4 \text{ A/mm}^2 < \mathcal{J} < 1.6 \times 10^4 \text{ A/mm}^2$. When the rated current are 150A and 300A, total cross-section areas of fuse-notch will be

$$S_{150} = 3 \times 0.2 \times 0.4 \times 5 = 1.2 \text{ mm}^2 \text{ and } S_{300} = 6 \times 0.2 \times 0.4 \times 5 = 2.4 \text{ mm}^2$$

respectively.

Therefore, the possible ranges of prospective current of Max. arc energy are $I_{150} = (1.15 \sim 1.6) \times 10 \times 1.2 = 13.8 \sim 19.2 \text{ Ka}$ and $I_{300} = (1.15 \sim 1.6) \times 10 \times 2.4 = 27.6 \sim 38.4 \text{ Ka}$ respectively.

(3) Calculation of cut-off characteristics

For estimation of the cut-off current values at different condition of short-circuit current, we used the formula reported in reference [2] for calculation. There are two cases for calculation i.g. symmetrical short-circuit and unsymmetrical short-circuit currents.

One of the calculated results is shown in table I. for prospective short-circuit current values 20Ka, 24Ka, 30Ka, 36Ka, 40Ka and 48Ka.

(4) Starting characteristics

For selection of reasonable rated current fuse to co-ordinated a motor under different starting conditions, the selection charts were plotted between starting current, number of starts per hour, run up time and fuse current rating on the basis of the thermal characteristic of fuse.

One of them is shown in Figure 2.

TESTS AND ANALYSIS OF RESULT

In order to testify the performance of fuse in conformity with the design data required, the type test was carried out on fuse samples. IEC Standard was adapted as the conditions of type test criteria. The test items and specific contents of test are as follows.

(1) Temperature-rise test

The temperature-rise test is to check the temperature-rise of fuse under normal working condition. It should not exceed permissible value. As stipulated in IEC Standard, the maximum permissible temperature of the fuse knife-terminal should not exceed 65 °C.

For testing, we set up 6 pieces of sample fuse in vertical parallel position on the frame, to which the rated currents were flowed. These currents were supplied by low-voltage transformers. The temperature was measured with thermocouple at the knife-terminals of fuse. The section areas of connected bus-bar were 25x3 mm and 40x4 mm for 150A and 300A respectively. Ambient temperature was 15 °C under the test. The highest temperature rise of 300A sample fuses was 58 °C, while 150A sample fuses was 48 °C. There is much room for temperature rise of sample fuses.

(2) Interrupting capacity test

The interrupting capacity tests consist of rated interrupting current test, approaching to maximum arc energy interrupting current test and minimum interrupting current test.

These tests were performed in Xi'an High-voltage Apparatus Institute in China. The transient recovery voltage of sample fuse after interrupting was measured by cathode-ray oscillograph.

(a) Rated interrupting current test According to the design requirements, rated interrupting current was defined for 30Ka. The actual prospective current under test was 29.5Ka (r.m.s.), $\cos\phi < 0.15$, testing voltage was 6.3Kv, amplitude coefficient of recovery voltage $K_1 = 1.6$, inherent oscillating

frequency $f_0=3.48$ KHz. After testing, the instant interrupting current measured was 31Ka (peak), operating time was 7 ms and overvoltage recorded by the mechanical scanning cathode-ray oscillograph was 1.2 times of rated voltage, one of recorded wave form is shown in Figure 3.

(b) Approaching to maximum arc energy interrupting current test This test was proceeded after the rated interrupting current test and through analysis of the magnitude of cut-off value from the waveform of rated interrupting current test to estimate the prospective current of maximum arc energy. As requested in the stipulation of IEC Standard, if the test of rated interrupting current is carried out at 150 times or more, the estimated prospective current I_2 of maximum arc energy should be calculated from the following equation

$$I_2=i_1\sqrt{i_1/I_1} \quad (8)$$

where i_1 —instant value of prearcing current of the prospective current I_2 .

The prospective current I_2 under actual testing was 27.5Ka (r.m.s.), $\cos\phi < 0.15$. Testing voltage 6.3~6.6 Kv, amplitude coefficient of recovery voltage and inherent oscillating frequency adjusted to $K=1.3$ and $f_0=7.6$ KHz respectively. After testing, the instant value of interrupting current was 28.3Ka (peak) which was obtained from the recorded curve. Operating time was 6.2 ms, and no overvoltage appeared from the recorded curve. The results are shown in Figure 4.

From both the recorded curves of rated interrupting current test and maximum arc energy interrupting current test, we think the fuse interrupting test met with success. The body of fuse cartridge was dissected, then we examined the surface of fulgurite structure. All of the burned structure appeared quite homogeneous.

(c) Minimum interrupting multiple current test. For the back-up fuse, the minimum interrupting multiple current test must be performed in according to IEC Standard. The value required is 8 times of the rated current, e.g. $150 \times 8 = 1200A$ and $300 \times 8 = 2400A$. This test was also successfully passed.

(3) Time-current characteristics test
Time-current characteristics are shown in Figure 5. These curves were plotted on the basis of actual tests.

CONCLUSION

In the power fuse co-ordinated with vacuum contactor, a self-support fuse body is adopted in construction. The cartridge which is made of temperature resistant and high strength glass-fibre cemented with inorganic can meet the ability of interrupting capacity under large rated current. The construction of this type will be the main trend in high voltage H.R.C. development.

Through the rated interrupting current test and the maximum arc energy interrupting current test of the power fuse, it showed that the theoretical analysis was in conformity with the actual results of the tests. After the examination of fulgurite surface of sample fuse, it appeared that the inter-

rupting action was rather easy, and was much room for operation.

TABLE I Cut-of current peak value at symmetrical short-circuit current with rated current 150A

Prospective Short-circuit Current Value (Ka)	Fusing Time (ms)	Angle Refer to Fusing Time (degree)	Value of sine	Peak Value of Cut-off Current (Ka)
20	1.56	28.1	0.47	9.4
24	1.47	26.4	0.44	10.7
30	1.37	24.6	0.41	12.3
36	1.29	23.2	0.39	14.1
40	1.23	22.1	0.38	15.4
48	1.16	20.9	0.37	17.8

REFERENCES

- (1) K.K. Mamintoff et al. , "Fuse" , Power publishing house, USSR. , 1979.
- (2) Wang Jimei , "Low-voltage Fuse" , Machine-building industrial publishing house , China. , 1979.
- (3) E. Jack , "High Rupturing Capacity Fuses" , E. & F.N. SPON LTD , London , England. , 1975.
- (4) J. Feenan , "Trend in the desugn of high-voltage high-rupturing-capacity fuses" , Proc.IEE , Vol.118 , No.1 , 1971.
- (5) IEC Standard , 282-1 , 1974.

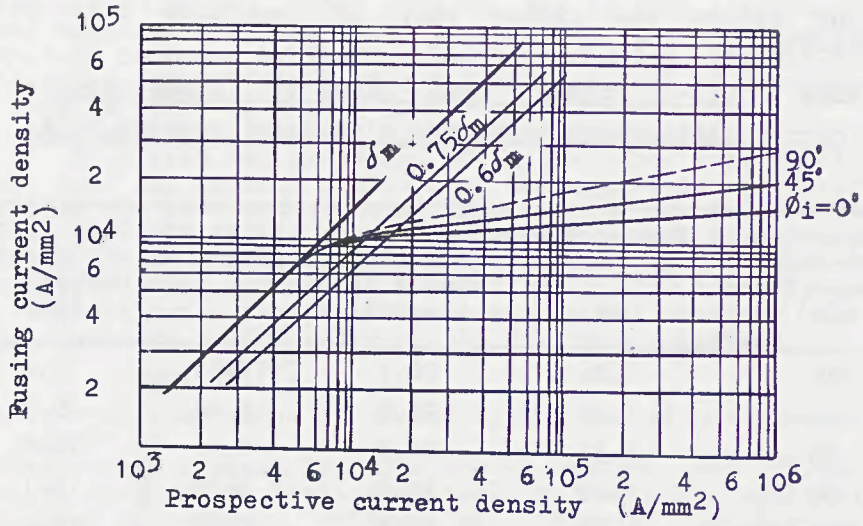


FIG. 1. Curves for determination of current density under maximum arc energy.

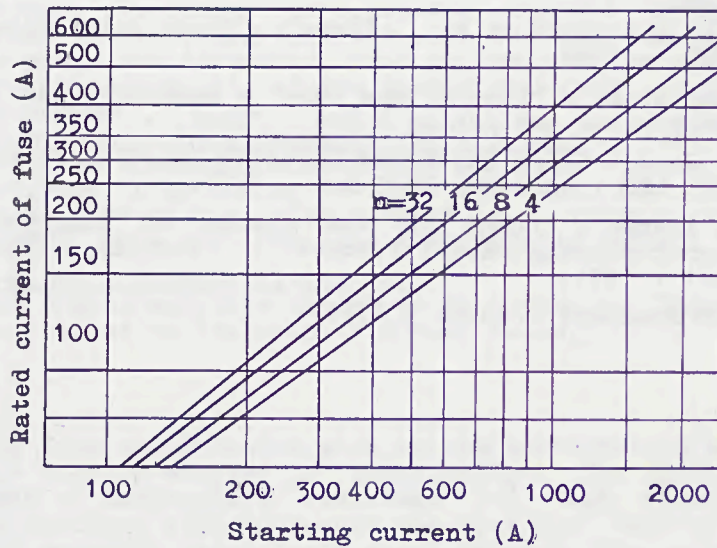


FIG. 2. Fuse selection chart for motor with run up times not exceeding 6 seconds.

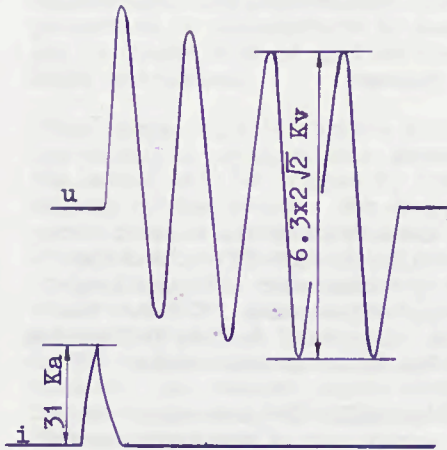


FIG. 3. Wave forms from rated interrupting current test.

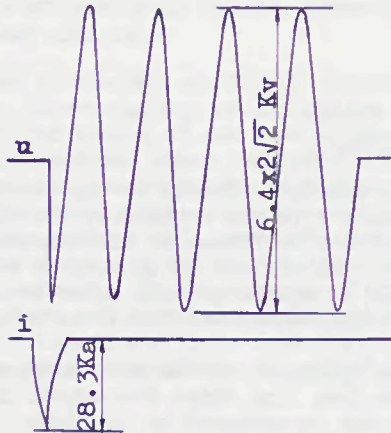


FIG. 4. Wave forms from interrupting current test under maximum arc energy.

X
Wrong.

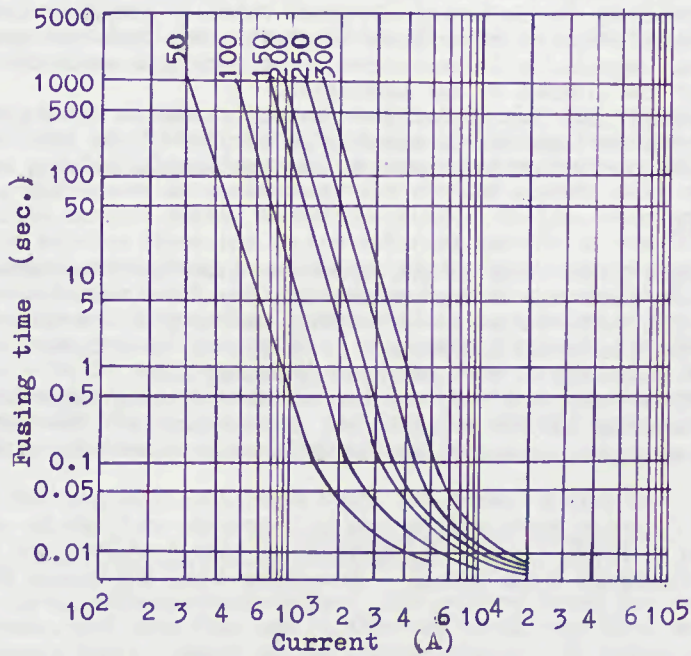


FIG. 5. Time/current characteristics

THE STRIKER SYSTEM IN THE FUSE SWITCH COMBINATION

A. Ofte and W. Rondeel

ABSTRACT

While the requirements to high-voltage fuse-links of the current limiting type are covered by the IEC Publication IEC 282-1, and the load-break switches (or disconnectors) by Publication 265, the fuse switch combination is covered by a special Publication IEC 420. The latter is at the present under revision. Important factors influencing the requirements which will have to be specified in Publication 420 are

- the operation of the striker system, specially in those cases where the fuse link trips the switch in a current region where the current is not interrupted by the fuse.
- The maximum permissible arcing time in the fuse link without explosion or expulsion of gases which may initiate a flash-over in the three-phase system.

A systematic study into these two aspects are reported in this paper. The main conclusion being that normally the maximum permissible arcing times will be in excess of the minimum time necessary to have the fault current cleared by the in series connected switch. A malfunctioning of the combination could be experienced due to extreme fuse-link body temperatures, especially in enclosures, - or immediate explosion of fuse-link at the instant of arc initiation.

With the present IEC recommendations a better guarantee for a proper functioning of the combination can only be secured if the fuse link is tested in the current range between I_3 and the minimum melting current.

INTRODUCTION

By combining a load-break switch, which can interrupt load currents and low fault currents, with a current-limiting fuse, which can interrupt high fault currents and normally having problems with the lower currents, an ideal combination is obtained. In addition to the special IEC publications for load-break switches and switch-disconnectors, IEC 265, and for current-limiting fuses IEC 282-1 a special document for the combination, IEC 420 exists. The latter has not been unanimously accepted, and is still under discussion within the IEC.

A. Ofte and W. Rondeel are with
A/S Norsk Elektrisk Brown Boveri Switchboard and Switchgear Group.

The combination of load-break switches, or switchdisconnectors, and current-limiting high-voltage fuses, are commonly used for the protection of transformers in distribution networks. The combination may of course also be applied for the protection of motors, capacitor banks and cables.

Often (especially in markets dominated by the BS and DIN/VDE Standards) the switch is equipped with automatic fuse-tripping, which implies that the switch will be tripped by the striker system of the fuse upon melting of the latter. The cooperation between these two devices is perfect in that respect that the fuse will interrupt the high fault currents (which the switch is unable to interrupt), while the switch (being tripped by the fuse-link striker system) will interrupt the low fault currents. Most current-limiting fuses are not able to interrupt currents below 2-4 times their rated current. In the diagram of figure 1, the mentioned cooperation between fuse and switch is explained in a diagram. The current region where the transition from interruption by the switch to the interruption by the fuse takes place, is called the "take-over-current".

High voltage fuses are tested according to IEC 282, and in figure 2 are indicated the current zones for the three test duties 1, 2 and 3. The lower limit for safe operation, verified by Test Duty 3, is the so-called minimum-breaking-current.

Below the minimum-breaking current, the safe operation of fuse-switch combination is dependent on the tripping of the switch by the fuse-link striker system. The proper functioning of the striker is then important. Figure 3a shows one possible mechanical construction of a spring operated striker system, while 3b shows the electrical connections.

The resistance of the individual silver fuse elements varies from about 0,8 to 0,005 ohms, while the resistance of the striker element is between 9 and 30 ohms, dependent on the rated current and voltage. Due to this difference in resistance, the striker element will carry only a negligible current during normal operation. In the overcurrent region, when the melting times are in the order of seconds or minutes, each of the parallel fuse elements will melt one by one. At the moment when the last element melts, the current path will be commutated to the striker element. When the current path is commutated to the striker element, the striker release wire will melt first, as the cross section of this wire is smaller than that of the striker element. Hereby it is guaranteed that the release wire will melt before the current path is interrupted. The release wire releases the charged spring, and the striker pin activates the switch mechanism.

Except for the very small arcs which are formed during the initial melting of the fuse elements, no real arcing takes place in the fuse before the striker system is activated.

Below the minimum-breaking-current, the melting times for the fuse may be extreme, and both fuse and striker may reach very high temperatures. This causes heavy demands on the striker system. At temperatures around 250°C, which are possible in fuses with pure silver elements, a

spring operated striker system may change its characteristics. Low-loss fuses with so-called M-effect (melting point reducing alloy) are advantageous in this connection.

In the fuse-switch combination with trip release initiated by the fuse-link striker, the following points are critical:

1. The minimum arcing time the fuse link can withstand without explosion or expulsion of any ionized gases, has to be longer than the maximum trip-open time plus interruption time of the in series connected switch.
2. Even after extremely long melting times, at low fault currents below the minimum-breaking current, when the fuse-link has become very hot, the striker system has to function properly.
3. The circuit must be able to supply the striker system with sufficient power, voltage/current to melt the release wire.
4. The take-over-current, i.e. the current for which the minimum possible trip-open time of the switch is equal to the arcing time in the fuse-link, must be below the maximum interruption performance of the switch.

The last point is illustrated in figure 4, which shows the arcing time as a function of the fault current in the Test Duty 3 test circuit. Below the minimum-breaking-current the arcing time is infinite.

Normally a fuse-switch combination is arranged in such a way that if one (or more) of the 3 fuses in a three-phase system fuses, the switch is tripped in all three phases. If the switch is tripped by one of the fuses, due to the intrinsic variation in the melting time of the fuses, or because the fault currents in the three phases are unequal, the switch contacts may open when current is still flowing in the two remaining phases. With two phases in series, the switch will have to interrupt the fault current. (We assume that the fault current is in excess of the minimum-breaking-current, and the first fuse to melt interrupted the current). This aspect, together with the problem of the take-over-current, determines the requirement to be met for the interruption performance of the switch. This investigation is concentrated on the fuse-link striker system, with reference to the critical points already mentioned.

MEASUREMENTS ON DIFFERENT BACK-UP TYPE HIGH-VOLTAGE FUSE-LINKS.

Measurements of temperature distribution, permissible arcing times and electrical and mechanical characteristics on four different types of commercially available fuse-links, all rated 12kV and 40 Ampere, have been carried out. The purpose of these measurements has been to obtain a better knowledge regarding the critical points which have been mentioned.

TEMPERATURE MEASUREMENTS.

In a commercially available fuse-base according to DIN 43625 the

temperatures were measured in 5 different locations on the fuses. All fuses were brought to the fusing temperature with melting times in excess of 1 hour. In most cases the melting time was between 65 and 120 minutes, and the melting current (chosen according to data supplied by the manufacturers) between 65 and 90A. The current, which had been chosen to give melting times of approximately 60 minutes, was kept constant during the melting period for the fuses rated 40A. The location of the 5 thermocouples are shown in figure 5, together with a schematic presentation of the results. In figure 5 the maximum temperatures recorded for the four fuse-types are given for the three most interesting locations, i.e.:

- On the porcelain fuse body.
- On the electrical contacts spot between fuse-base and fuse-link.
- On the cable connection to the fuse base.

The cable connection arrangements are also shown in the figure.

As can be seen from the diagram, maximum temperatures of more than 400°C, have been measured for fuses type "C" and "D". These fuses are without the melting point reducing M-spot, - where the melting point of the small amount of applied tin on the silver fuse-element determines the melting point. From the diagram also can be concluded that the temperature of the mechanical part of the striker system will have to sustain maximum temperatures of around 200°C for a longer period of time, depending on the melting current. For striker systems based on spring actuation in fuse-links without melting point reducing action, special material qualities will have to be applied.

ARCING TIME MEASUREMENTS.

At the moment when real arcing commences in a fuse-link, the striker system will be activated. Most load-break-switches need approximately 50 ms to open the contacts, and on the average another 10-15 ms to interrupt the current. Some manufacturers of switches even delay the switch opening in order "to give the fuse more time to clear the circuit". It is then of some interest to investigate whether a fuse-link can sustain arcing below the minimum-breaking-current for a period of 50 to 100 ms without explosion or expulsion of ionized gases.

In a Test Duty 3 circuit according to IEC 282-1, with a power factor 0,4-0,6, the four fuse-links (type A, B, C and D) were tested below I_3 . Figure 6 shows the test circuit, with a specially developed automatic switch-over system for disconnecting the low-voltage-circuit and connecting high-voltage at the moment of arc initiation in the fuse-link. Systematic comparison between I_3 values obtained in this test circuit, and other laboratories where change-over to h.v. has been made just before arc initiation, never have revealed any difference between these two test methods. This comparison has been made for fuses with and without M-effect.

The arcing time from arc initiation to explosion or expulsion of ionized gas, was measured by using the signal from the charge-over-switch tripping device to start the time counting, and an

impuls from a photodetector (registering the light from the fuse explosion) to stop counting. Time delays in this measuring system was calibrated and corrections were made.

The results from these measurements are given in table 1. In the table the "arcing time to failure" is the measured arcing time to explosion or expulsion of ionized gas. The observed minimum-breaking current I_3 " given in table 1, is not necessarily equal to the I_3 given by the manufacturer. The I_3 in table 1 is estimated from our own measurements during this investigation. Only test results at current levels which led to failure is given in the table.

The following conclusions can be made from the data given in the table:

- The spread in tolerable arcing time is substantial.
- The safety margin in a fuse-switch combination where the switch has a mechanical opening time of approximately 50 ms is acceptable.
- For one of the tested types of fuses, the fuse-link exploded before the switch would have had any possibility to interrupt the circuit. This was never observed for any other fuse-link.

Reignitions, leading to failures, but also in some cases effectively interrupted, were observed for a number of fuses. It may be concluded that retaining the full recovery voltage for at least 60 seconds after first interruption during Test Duty 3 is of great importance. (All four fuse-link bodies were made of porcelain).

Figure 7 shows some of the oscillograms recorded during the tests. The upper oscillogram shows the normal arc voltage behaviour - with the characteristic voltage build-up after switching over from low to high voltage. The "dead-time" is very short, and arcing before change-over is negligible.

The abnormal behaviour of the fuse-links that exploded immediately after change-over, is shown in the lower oscillogram. In this case there is no voltage build-up, the arc voltage is the arc voltage of a free burning arc from the very first moment.

A possible reason for the abnormal behaviour could be sought in the fuse-body porcelain quality, combined with thermo-mechanical stresses caused by the elevated temperatures obtained during the long melting time of approximately 1/2 hour.

MECHANICAL AND ELECTRICAL CHARACTERISTICS OF STRIKERS.

During the test carried out on a substantial number of different fuse-links, none of the strikers failed to operate. Both from cold conditions and after the heat treatment caused by at melting time in excess of 1 hour, all strikers fulfilled the IEC requirements for the energy/force characteristics, IEC 282-1 Am. No. 3 Table XII medium type.

Electrically the striker systems, one of which had an explosive drive, were tested in a low-voltage circuit with a supply voltage of 210 Volt. All strikers functioned properly, with a melting time of 100-150 ms. As no real arcing can be sustained at this low voltage, the conclusion can be drawn that in a normal H.V. circuit, the delay time of the striker (i.e. from the moment of arcing until striker movement) is negligible.

DISCUSSION AND CONCLUSIONS.

Fuse-switch combinations where fuse-tripping have been relied upon in connection with the interruption of currents below the fuse-link minimum-breaking current, have been in practical use for many years without too many failures being recorded. It is therefore not surprising that this limited investigation did not reveal any major shortcomings. Nevertheless, a few negative observations should be noted:

- surface temperatures measured at a fuse-links subjected to small fault currents and long melting times were in excess of 400°C. In compact switchgear where the fuse-link may be surrounded by organic insulation material (as epoxy resin) these temperatures could be harmful.
- one brand of fuse-link examined exploded immediately after arc initiation, leaving the switch no time to clear the circuit. This was only experienced for melting times longer than approximately 30 minutes.
- most manufacturers seems to be rather "optimistic" when the minimum-breaking-current of a fuse-link is given in the data sheet.
- fuse-link failure below the minimum-breaking-current appeared both as an explosion where the porcelain body ruptured, and as a burn-through where the arc penetrated the contact ferrules. In an open 3 phase system the ultimate result would be the same in both cases: a flash-over between phases, and a full short-circuit.

On the positive side must be concluded:

- the permissible arcing time of a fuse link below the minimum-breaking-current is far beyond the time needed to trip the switch, i.e. the switch will have interrupted the circuit before any ionized gases are expelled.
- the tested striker systems all fulfilled the IEC requirements, even after being subjected to melting times (and high temperatures) longer than 60 minutes.

During these tests it was observed that reignitions, of which some led to complete fuse failure, occurred after time intervals up to 30 seconds. Holding the recovery voltage for at least 1 minute therefore seems to be of outmost importance. The most important conclusion to be drawn from this investigation is that if full guarantee for a proper functioning of a fuse-switch combination is wanted with the present IEC recommendations, the actual combination of fuse-link and switch will have to be tested in the low-current region. As a minimum requirement the fuse-link should be tested in the current range between the minimum-breaking-current and the minimum-melting-current.

TYPE	Rated current	Rated voltage	Observed min.br.c.	Test current	Melting time	Arcing to failure	REMARKS
	I_N	U_N	I_3''	I_t	t_s	t_a	
fuse-link	A	kV	A	A	min.	mS	Observation
A	40	12	85	84	18	670	
	"	"	"	75	-	710	
	"	"	"	"	-	830	
B	40	12	120	100	25	28200	Interrupted, reignited and exploded.
	"	"	"	85	-	810	
C	40	12	100	84	27	220	
	"	"	"	"	26	1250	
	"	"	"	"	27	145	
D	40	12	120	84	21	0	Fuse exploded at arc initiation.
	"	"	"	"	39	0	
	"	"	"	"	32	530	

TABLE I

Total arcing time to failure below the minimum breaking current for the fuse-links type A, B, C and D.

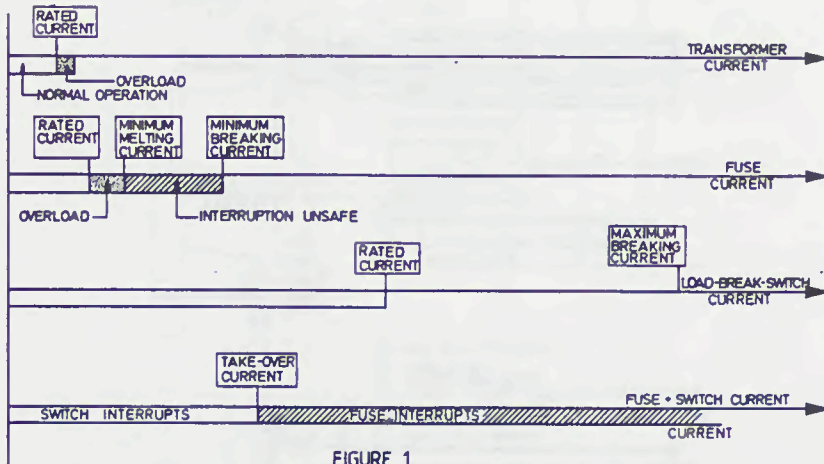


FIGURE 1
Coordination between load-break-switch and fuse

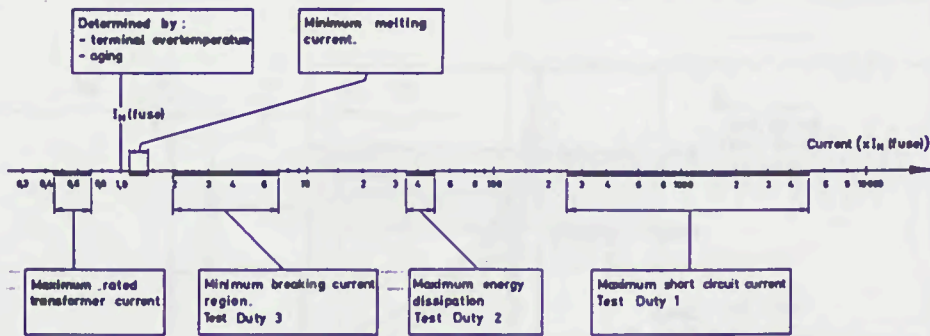


Figure 2
H.V. fuse link rated current
with reference to normal load
and test currents according
to IEC 282-1

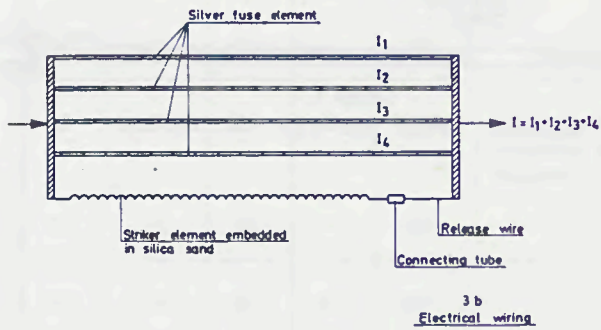
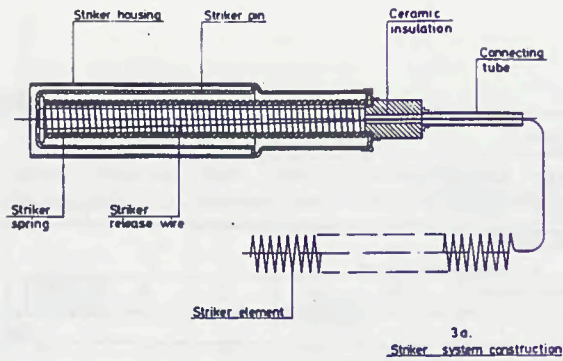


Figure 3
Striker system

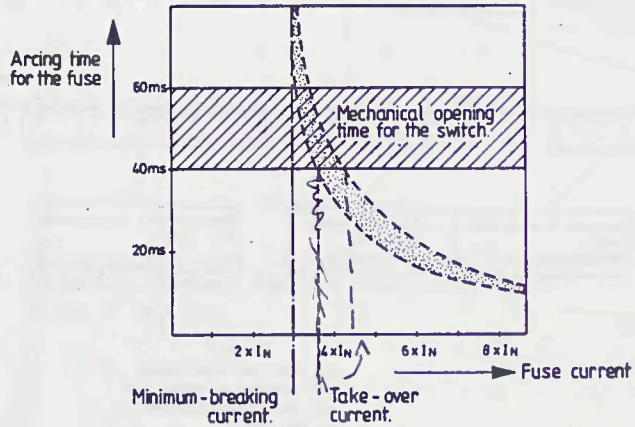


Figure 4

The arcing time in the fuse compared with the mechanical opening time of the switch

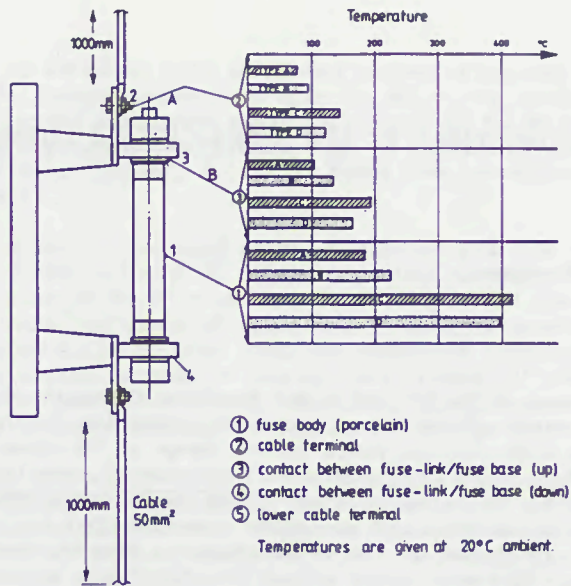


Figure 5
 Temperature distribution at the moment of fuse melting.

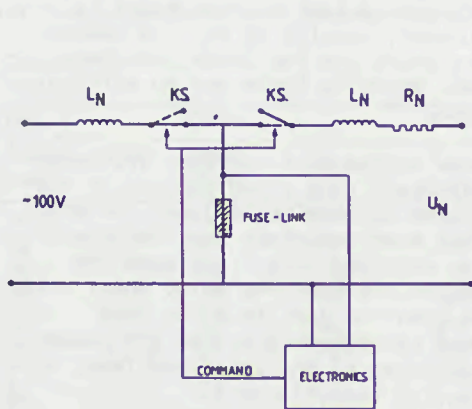


Figure 6
 Special test circuit for
 Test Duty 3 acc. to IEC 282-1

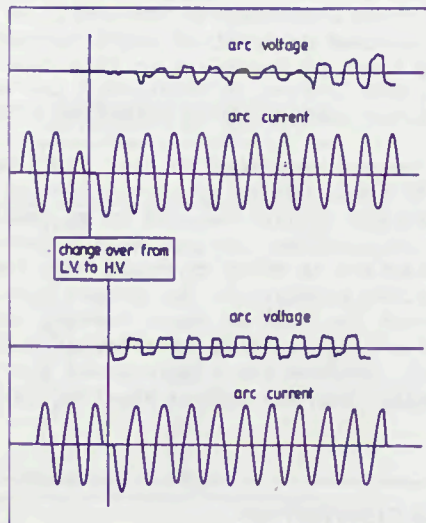


Figure 7
 Arc voltage during the first arcing period.
 The upper diagram shows the normal behaviour,
 the lower when fuse explosion takes place immediately
 after arc initiation.

OPERATING TIMES AT LOW SHORT-CIRCUIT CURRENTS

Sven Lindgren

ABSTRACT According to IEC 269-1 the breaking capacity of fuses is verified in the range of small over-currents, near the fusing current, and for relative high over-currents in the range of 50 times the rated current of the fuse and higher. In practice, however, short circuit currents may appear in the range of 15-20 times the rated current of the fuse. Tests have shown that the operating times in that region can be much longer than what is stated in the manufacturer's time/current characteristic for the fuse. This may become a problem when fuses are used for short-circuit protection of motor starters and the starters (contactors) are damaged because of the longer exposure to short-circuit currents.

COORDINATION WITH CONTACTORS According to IEC standard 158-1 for contactors the manufacturer shall state the maximum prospective short-circuit current and the type and characteristics of the short-circuit protective device, for instance a fuse, to be used in order to achieve a given type of protection. Two tests shall be made to verify the ability of the contactor to withstand short-circuit currents.

The first coordination test shall be made with a test current equal to the maximum prospective short-circuit current, usually 50 kA. The operating times of fuses are in this case very short and the Joule integrals, I^2t , are limited to relatively low values. Normally there are no difficulties for contactors to withstand this test.

The second coordination test is to be made with a test current, I_T , equal to 30 times the rated current of the contactor. (The rated current of the contactor is here assumed to be equal to the maximum operational current for utilization category AC-3.) One of the most important applications of contactors is motor control. Here thermal overload relays are used for overload protection. For proper coordination the overload relay shall trip and not the fuse at heavy starts, locked rotor or jam. Thus the fuse characteristics must be selected such that the current, I_C , at the cross-point, between the time/current characteristics of the relay and fuse, is greater than the actual starting current, I_{st} (see figure 1).

ASEA DISTRIBUTION
Subdivision ASEA CONTROL
Development Office
S-721 83 VÄSTERÅS SWEDEN

As an example a 22 kW motor with the rated current 43 A has a starting current of 300 A. A recommended fuse size is 100 A and contactor size 50 A. The test current mentioned above corresponding to 30 times the rated current of the contactor is then 1500 A. Related to the 100 A fuse consequently the test current, I_T , is 15 times the rated current of the fuse (see figure 1).

When coordinating motor, overload relay, contactor and fuse as described above, the second test current 30 times the rated current of the contactor, will be in the range of 15-20 times the rated current of the fuse. In this range the operating times of fuses are in general relative long. But the current is also still so high that the contactor contacts may separate and give rise to arcing because of the current forces. If the operating times of the fuses then are too long there is a risk of heavy contact burning, flash-over between phases or to earth and damage to the contactor.

SHORT-CIRCUITS IN INDUSTRIAL PLANTS Industrial plants are generally equipped with high power transformers and assemblies of switchgear and controlgear are often located near the transformer. Thus short-circuits inside or close to the controlgear result in high short-circuit currents and the problem with fault currents in the range of 15-20 times the rated current of the fuse do not arise in this case. However there is a trend to concentrate the assemblies of switchgear and controlgear to one place even if the plant is extended over a large area. The cables from the controlgear to the motors are for that reason often very long and the short-circuit current in case of a fault on the cable at the motor side or on the motor terminals, may be relatively small (see figure 2). The probability of a fault occurring in this case is greater than for a fault inside or near the assembly. Table 1 shows the calculated short-circuit current for different motor sizes in relation to the rated current of the fuse. The calculated maximum cable length is based on a voltage drop of 15 % at the motor terminals during start.

Table 1

Motor	Cable		Fuse	Short-circuit current	
Rated power [kW]	Area [mm ²]	L_{max} [m]	I_n [A]	I_{sc} [kA]	I_{sc}/I_n
18,5	10	99	80	0,88	11
22	10	77	100	1,1	11
30	16	59	125	1,9	15
37	25	105	160	1,7	11
45	35	103	200	2,1	11
55	35	83	200	3,0	15
75	70	121	250	4,5	18
90	95	112	315	5,8	19
110	120	99	355	7,1	20
132	150	132	400	8,3	21
160	185	102	500	11,4	23

L_{max} = cable length that gives 15 % voltage drop on the motor terminals during start
 I_n = rated current of the fuse
 I_{sc} = short-circuit current with a cable of length L_{max} to the fault.

The coordination of contactor and fuse according to IEC 158-1 is verified by the conventional test current, I_r , which for motor application lies in the critical range of 15-20 times the rated current of the fuse. Table 1 confirm that current of that magnitude also may appear in practice.

OPERATING TIMES Tests on fuses with currents in the range of 15-20 times the rated current of the fuses have shown that the operating times can be much longer than what is stated in the manufacturer's time/current characteristic for the fuses. In figure 3 the result of four tests on gL(gI)-fuses of different manufacturers is shown. The first fuse to clear in each test has an operating time that is about 2-6 times the nominell stated operating time. The second fuse to clear in each test usually has a pronounced longer operating time mainly due to the fact that the current is decreased to 87 % of the 3-phase short-circuit current when the first fuse has interrupted one phase.

CONCLUSION The operating time of a fuse at low short-circuit currents in the range of 15-20 times the rated current of the fuse, is a critical parameter for design of contactors and for dimensioning of controlgear and cables in motor circuits. Tests have shown that the operating times in that region can be much longer than what is stated in the time/current characteristic of the fuse, a fact which is videly unknown inspite of it's great significanse. The reduction of operating times at low short-circuit currents should be made a target for future research on fuses.

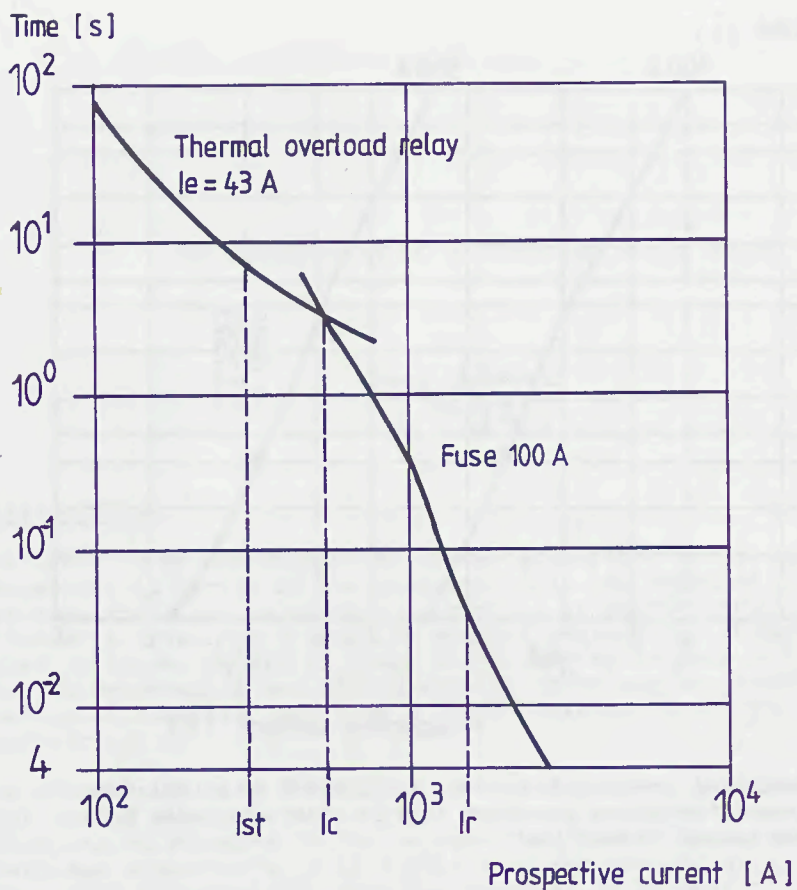


Figure 1 Time/current characteristic coordinating thermal overload relay and fuse

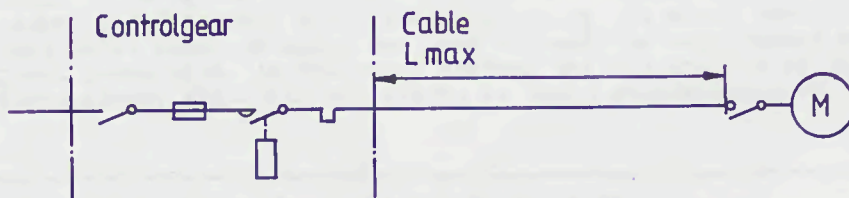


Figure 2 Coordination of controlgear and cable. L_{max} is the cable length that gives 15% voltage drop on the motor terminals during start.

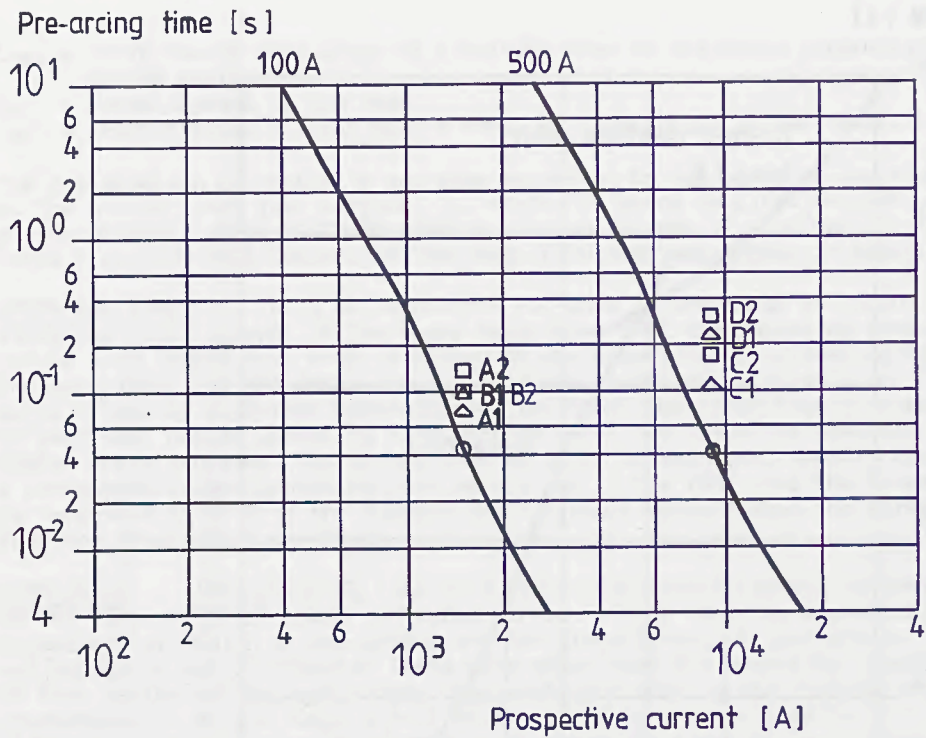


Figure 3 Operating times in four test, A,B,C and D on gL(gI)-fuses. Index 1 refers to the first fuse to clear and index 2 to the second in each test.

THE DEVELOPMENT OF ELECTRIC FUSES IN CHINA

Chang Gyan-Son

INTRODUCTION

Electric fuses are used as a typical protective device which are connected in series in the circuits. When the carrying current exceeds the rated value due to overload or short-circuit, the fuse-link will break the circuit to achieve protection. Although the fuse is blown, damage of other electrical equipments in the circuit due to overheating and strong dynamic force can be avoided. So the action of fuselink just like a local "weakness link" for fault protection.

In comparison with mechanical circuit breakers, the fuse is without moving mechanism and contact parts in construction. Thus the fuse may be belonged to the category of "static apparatus" or "contactless apparatus". It is simple construction and quick action. There are two essential parts or "organs" in automatic circuit breakers. One is for sensing and responding the fault current and the other is executive "organ" for breaking the fault current. The former function is accomplished by relays or released devices, the later function by contacts and arcing quenching elements. As to fuse, the two "organs" are combined in one body--fuselink. This may be an important reason to make the fuse simplified in construction and quick in action.

The fuselinks are suitable both for overload and short-circuit protection. It is rather difficult to chose the proper material for the fuselink to satisfy both requirements. In the early time low melting point metal or alloy was used to meet the requirement of overload protection. As the fault current was not too big to be safely cleared. Following the growth of fault current in power sys-

Director CES (Chinese Electrotechnical Society)

tem, it is necessary to use high melting point metal and adopt narrow-neck form for the fuselink to obtain the current-limiting effect. Considering the requirement of overload protection, low melting point metal to yield a "metallurgical effect". The design of modern L.V. fuses is still following the "weak-chain" idea, i.e. applying variable section of the fuse neck for the high melting point fuse so that quick breaking is effected. In the case of quick-acting fuses for the protection of semiconductor devices, higher ratio of section variation for the fuselink is adopted.

The main advantages of modern cartridge fuses are high rupturing capacity, stable time/current characteristic and low cost. Of course, there are several disadvantages, namely the monotony of protective characteristic and poor discrimination. The fuses in the three poles can not open in all, in the case of single-phase short-circuiting, resulting single-phase operation of induction motor. However, these shortcomings of fuses do not exist in mechanical circuit breakers. Thus it is a problem to be solved to overcome these shortcomings in the development of modern fuses.

From the application point of view, it is necessary to develop 'a' type fuses for backup protection and 'g' type fuses for motor protection, so that better protection is assured and it would be more economical. At the same time, the development of combined switchgears, such as the incorporation of fuses with mechanical circuit breakers to form high current-limiting gears or the incorporation of fuses with knife switches to form compact switchgears is also needed. In such combined switchgears, interlock devices are provided to prevent single-phase running of induction motors.

From the design point of view, it is necessary to improve the construction of fuses. For instance, to reduce temperature of the fuse-body, to reduce the heat loss of the fuselink and its accessories, to lower I^2t and to prevent deterioration of the fuselink to ensure stable time/current characteristics should be considered. It is also necessary to improve the rupturing capacity, discrimination ability and reliability. In recent years, the development of self-recovery fuses basing on a new design idea has been quite successful which have high rupturing capacity and can recover their property after clearing the faults without replacing any part.

FUSE PRODUCTION IN CHINA

Fuses are widely used in L.V. power circuits in China. And many manufacturers are producing various types of fuses to meet the requirements of different users. Some typical type L.V. fuses are introduced as follows:

TABLE 1

No	Type	Rating Voltage V	Rating current A	Rating breaking capacity KA
1	RTO	AC 380	100,200,400,600,1000	50
		DC 440		25
2	RT10	AC 440	20,30,60,100	50
3	RT11	AC 440	100,200,300,400	50
4	RM7	AC 380	15,60,100,200,400,600	2-20
		DC 440		
5	RM10	AC 500	15,60,100,200,350,600	1.2-20
		DC 440	1000	
6	RLS	AC 500	15,20,25,30,40,50	80
		AC 250	50,100,200,350,500	50
7	RSO	AC 500	50,100,200,350,500	40
		AC 750	350	30
8	RS3	AC 500	50,100,200,300	25-50
		AC 750	200,300	50
9	RZ1-100	AC 380	100	100
10	HR3	AC 500	100,200,400,600	50

Note: No 1-3 powder filled cartridge fuse
 No 4-5 cartridge fuse
 No 6 screw type fuse
 No 7-8 quick-acting fuse or fuse for protecting semiconductor
 No 9 self-mending fuse or self-recovery fuse
 No 10 fuse switch

FUTURE WORK AND PROSPECT

The design of new type fuses and improvement of fuse characteristics should be based on a large amount of research work. The following problems have been considered in our research work.

1. The application of fuses There is close relationship between fuse production and application. The fuse must satisfy the protection requirements of networks or other objects, on the other hand,

the networks or other protective systems will push the fuse research to a new level. The research work includes the coordination of characteristics between protective devices and fuses, and combination of fuse with mcbs or contactors to form hybrid apparatus etc.

2. Reduce of silver consumption in fuses How to save silver which has limited resources should be studied in fuse manufacturing. As mentioned above L.V. fuses of type RT10, RT11, RSO and RS3 all use silver for fusebody. We are applying aluminum instead of silver in cartridge fuselink. The surface galvanized copper and copper-silver composed plate are also considered.

3. Selection of quartz sand for filling powder The purity of quartz, as well as its shape and size influence the breaking capacity and time/current characteristics of fuselink. China is rich in natural quartz sand resources. We have found several kinds of quartz which are as good as import products.

4. Renew of design and construction The improvements of fuse performances include the increase of voltage rating. Our manufacturers have produced fuselinks suitable for 660 V and 1140 V used in mine systems. The aluminum cartridge fuses are also produced. The quick-acting fuses on higher voltage and larger scale rating current for protection of semiconductor and protection of rotating machines are considered. The new type of fuse-switch and the domestic enclosed fuses in miniature are ready to produce.

5. Research work on basic theory and design method The heating and other prearcing phenomena, arcing period phenomena, aging and deterioration phenomena, mathematical and physical modelling and optimum CAD are interesting to study.

To conclude, I should emphasize that the fuses have keep unchallenged for over 100 years. Recent development shows that they will still play an important part in protective devices. Although other current limiting devices are said to approach the performance of cartridge fuses, recent developments show that fuses are expected to keep them to the fore. There should be a good prospect in the development of better fuses.

REFERENCE

- 1 Wang Jui-Mea Low Voltage Electrical Fuses The mechnary industry press, China, 1979
- 2 Chang Gyan-Son Some Problems Analysis in Electric fuses
Low Voltage Apparatus (in Chinese) Vol 36, No 2, 1975
- 3 P.G.Newbery Low voltage fuses are here to stay
Electrical Review Vol 208, No 24, 1981

NEW LINE IN THE H.B.C. FUSES DEVELOPMENT

B.Krasuski, T.Lipski, E.Szymański, W.Związek

1. INTRODUCTION

The vast majority of nowadays fuses are the h.b.c. and gas-expulsion fuses. H.B.C. fuses are the short-circuit current-limiting devices. From the short-circuit current-limiting ability point of view a typical h.b.c. fuse-element shall fulfil two requirements: first is to keep its cross-section as small as possible in order to have the smallest pre-arcing time and the second one, - to create an as high as possible arc-voltage using quite reasonable fuse-link length. That's why in comparison with the gas-expulsion fuses, which are not current-limiting ones, the h.b.c. fuses do indicate several times larger watt-losses. This is the price paid for the current-limiting ability.

For instance, a 15kV h.b.c. fuse has the element-length of order 100cm, whereas a 15kV gas-expulsion one, - few cm only. So the h.b.c. fuses are very much electrical energy consuming devices. Some general purpose h.b.c. fuses of 10kV rated voltage and 100A rated current for example indicate abt 200W rated power-losses. Or a h.b.c. fuse for protection of diodes and thyristors of 1000V a.c. rated voltage and 100A rated current shows abt 20W, but of 500A rated current, - abt 100W. This is a waste energy, which specifically in the case of large power semiconductor invertors shall be artificially removed.

Another drawback of such fuses is their relatively large fuse-element cross-sectional area which by given rated current is dictated by the heat transfer ability into the fuse-terminals and, especially for high voltage fuses, into direction of the sand. In result the h.b.c. fuses in prior art do demonstrate comparatively great pre-arcing and in cosequence ^{total} great I^2t . It makes difficult the economic solution of the proper protection for instance of the power semiconductor equipment.

Besides, the substantial power-losses yield the hot running fuse-links. In consequence the thermal stresses of fuse-element are very likely, resulting in the eventual damage of that element. This is a factor that also deteriorates the operating characteristics of the fuse and renders it unfit for further use.

Obviously, there are manufactured several h.b.c. fuses in which is visible an effort to diminish of the mentioned drawbacks. But the general principle of operation remains still this same, which does limit the further improvement.

One of the possible way of the drastic avoiding of those inco-

The authors are with Gdańsk Technical University, Institute of High Voltages and Electrical Apparatus, Gdańsk, Poland

nviniences are h.b.c. fuses based on the new principle described further.

2. PRINCIPLE OF NEW H.B.C. FUSES

In all existing h.b.c. fuses the fuse-element does play two roles: it fits the current-carrying ability for long period and it assures the correct interruption of the overload currents. While according to the new idea these roles are divided between the two independent fuse-elements. Hence the name of new fuses is the two-path h.b.c. fuses^{1/}. In here a fuse comprises (Fig.1) : the basic fuse-element manufactured of a good conducting metal, placed in an open casing or in a casing within good dielectric gas, or in vacuum or dielectric liquid, and the arcing fuse-element placed in a casing filled up within quartz-sand or another arc-quenching means. Both mentioned fuse-elements are connected in parallel to terminal contacts. The length of basic fuse-element is many times smaller than the length of arcing fuse-element. It could be in the range of 0.5 to 10mm, whereas the length of arcing fuse-link has to be selected to the correct current breaking ability at fuse rated voltage.

Due to entire heat conduction to the contact terminals the cross-sectional area of so short basic fuse-element largely depends upon its length. For instance, the minimum fusing current (MFC) density of a silver element of the 2mm length is 3.5 times greater than that of the 7mm length [1]. That's why a long silver fuse-element of the same MFC indicates a larger cross-section than that of the short fuse-link. An example, loaned also from reference [1], gives MFC of 44.5A for 0.2mm dia. Ag wire of 5mm length, while a long wire of this same MFC should have appr. 0.475mm dia.

A fuse agreed with the new idea does operate as follows: under normal working conditions practically the entire current is flowing along the basic fuse-element, meanwhile the arcing fuse-element is practically free of the current. The latter then in steady state conditions practically does reach the temperature rise of the terminal contacts only. That's why the casings 5 and 6 (Fig.1) can be manufactured even from a cheap insulating material say of the heat-resistance class A.

But at an overcurrent in relatively short time the basic fuse-element does interrupt without the arc-ignition, because the current in this instant is turning-over into the arcing fuse-element surrounded by an arc-quenching medium such as the quartz-sand. After a defined time the latter also does operate, but in this case, say in the constrictions of arcing fuse-element, if any, the arcs do ignite and then they are finally extinguished as soon as current interruption has take place.

Generally, to obtain the correct operation two fundamental conditions should be fulfilled:

- i the current turn-over from the basic fuse-element into the arcing fuse-element must be free of the arc-ignition in

^{1/}Polish patent application P.245953, 27.01.84

- that basic element,
 ii the recovery strength of the gap which arise in the basic fuse-element as result of turn-over process shall be sufficient to withstand of the recovery voltage.

The first condition one can consider generally using the following relations (Fig.2)

$$L_B \frac{di_B}{dt} + R_B i_B = L_A \frac{di_A}{dt} + R_A i_A \quad (1)$$

$$i_B + i_A = i_t \quad (2)$$

In here the turn-over current i_t over the turn-over period t_t is practically constant because the time constant L/R in comparison with the time t_t is very large one. A short-circuit current due to the rapid adiabatic heating yields the instant increasing of the basic fuse-element resistance. Hence the current i_B is forced to decaying, but the inductivity L_B does oppose to that. On the other hand, the forced increasing of the current i_A in the arcing-element has been delayed due to the inductivity L_A . The magnitude of the fuse terminal voltage u_t , which appears in very turn-over instant, shall be lower than a defined value. Otherwise an electric arc does ignite in place of the disrupted basic fuse-element. Such a case would be disastrous for described arrangement. To avoid this the ratios R_A/R_B and L_B/L_A shall be kept in certain limits. Some particular data of those ratios are given in the next chapter.

The second condition one could stress as follows: neither the maximum arc-voltage nor arc-extinction voltage generated by fuse-element shall exceed the recovery strength of the gap arising in the place of the basic fuse-element.

To satisfy above given conditions, generally speaking, the cross-sectional area of arcing fuse-element shall be rather large one.

From the general point of view, this "new idea" is well known from the switchgear technology. Already very old circuit-breakers have got the basic- and arcing-contacts. Again, the short-circuit current-limiting devices such as I_s-limiters manufactured already several decades by Calor Emag (GFR) or e.g. ULTRUP-Fuse made by Fuji (Japan) are only some examples of application of this same idea. But the consistent difference is that the suggested h.b.c. fuse is a parallel combination of two fuse-elements. On the contrary, I_s-limiters of ULTRUP-Fuse and others instead of a basic fuse-element have the basic contact driven by an explosive detonator or by use of the electrodynamic Thomson principle or have basic current carrying path of a large cross-sectional area interrupted also by an explosive means. To that they shall have a special control system in order to fire on of the detonator in an appropriate instant.

Already ab.20 years ago we have endeavoured to create a h.b.c. fuse agreed with the described principle, but we didn't succeed due to failures during the short-circuit interruption. Recently we did new approach and overcame them. The technical data of a representative of the improved h.b.c. fuses for

protection of semiconductor devices will be demonstrated below.

3. AN EXAMPLE OF NEW H.B.C. FUSES

An example of new fuses for diodes and thyristors is of the following rated data (Fig.3) : rated current, $- I_n = 315A$; rated voltage, $- 500V$; rated power-losses, $- 30W$; rated breaking capacity, $- 110kA$ at $500V$, p.f. = 0.15 (Fig.4) ; ability of interrupting of the small overcurrent, $-$ not lower than $3I_n$ (Fig.5) ; clearing I^2t , $-$ abt $120000 A^2s$; upper terminal temperature rise, $- 62^\circ C$; casing temperature rise, $- 62^\circ C$; very steep time-current characteristic.

Some internal data of that fuse are: the ratio $R_B/R_A = 1:15$ ($0.16m\Omega : 2.4m\Omega$) ; again the ratio $L_A/L_B = 1$ and shall be as small as possible; the ratio of the fuse element cross-sections $S_A/S_B =$ abt 6 . It exists a close relationship between the required cross-sectional area and the inductivity of the arcing fuse-element. The greater inductivity needs the larger cross-sectional area in order to reach the correct turning-over.

4. CONCLUSIONS

Thereinbefore described two-path fuses do create a new possible line in the h.b.c. fuses development. This line does characterize by the following advantages:

- Drastical diminishing of the rated power-losses. Given example indicates abt 2 times smaller losses than that of a comparable present days h.b.c. fuses destined for diodes and thyristors.
- Substantial lowering of the temperature rises at the rated current. As result the fuse insulating body could be manufactured from an insulating material even of the heat resistance class A.
- Sharp diminishing of the silver consumption, from which is made the very short basic fuse-element only. The cold running arcing fuse-element makes possible to manufacture it from any kind of metal.
- Because the very short basic fuse-element, the time-current characteristic is rather a very steep one. It predestinate them to use as the protective means for semiconductor devices.

Logically, there are also several drawbacks of new fuses:

- The small insulating gap arising in the basic fuse-element during the turn-over period can have too small recovery withstand, needed to keep the recovery voltage. One could improve that withstand placing this element e.g. in vacuum, or in a good insulating gas, or liquid.
- Above given drawback may take place specifically at smaller overcurrents.
- In order to get an exact length of the basic fuse-elements during the mass manufacturing rather a precise manufacturing process has to be applied.

5. REFERENCE

- [1] Vermij L., Short fuse elements enclosed in a small slit, 'Switching Arc Phenomena' Int. Symp. Łódź, Poland, 1970, p.247

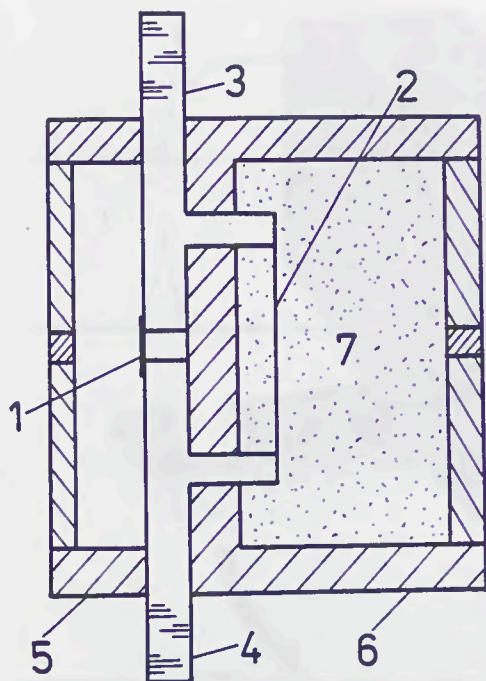


Fig. 1
Partial cross-sectional view of a fuse-link assembly acc. to the new idea
1-basic fuse-element; 2-arcing fuse-element; 3,4-contact terminals; 5-casing of basic fuse-element; 6-casing of arcing fuse-element; 7-arc-quenching medium /e.g. quartz-sand/

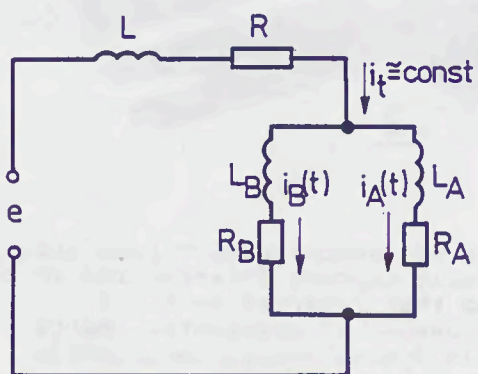


Fig. 2
A scheme of the current turn-over indices; B-basic fuse-element; A-arcing fuse-element

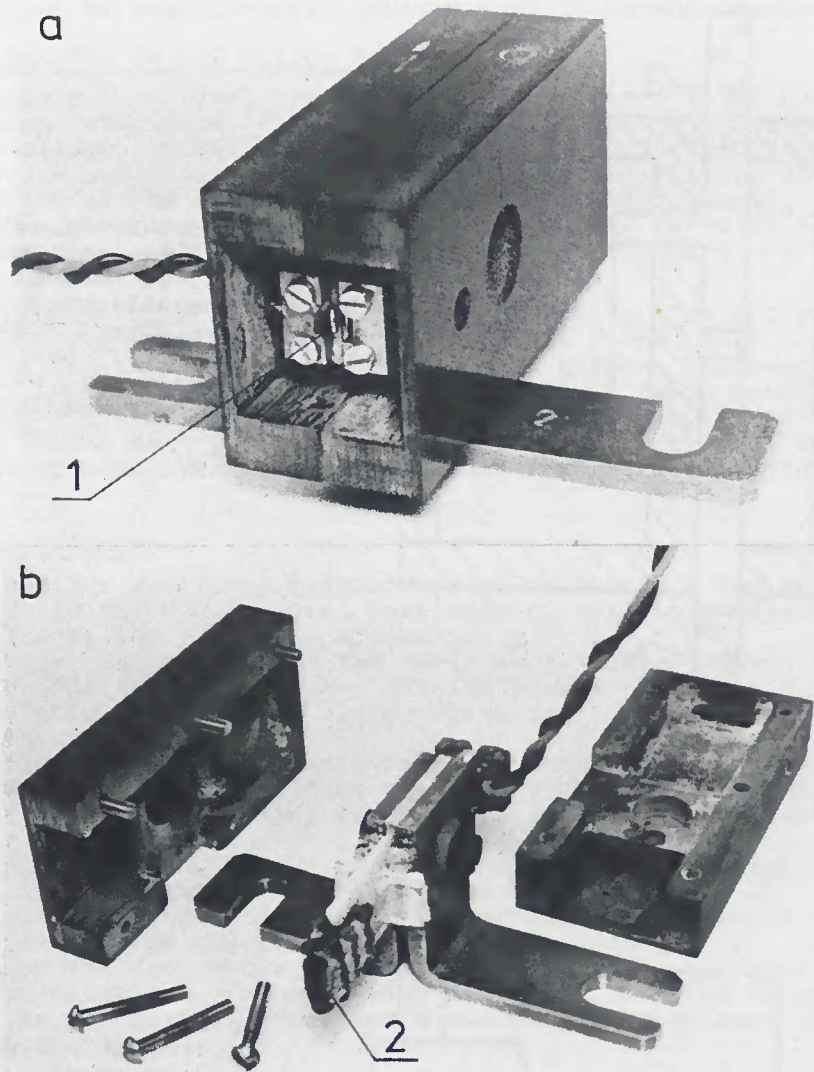


Fig.3 Photographs of a new semiconductor fuse 315A, 500V after short-circuit current interruption in conditions similar to that recorded in Fig.3 a-general view, b-view of substantial parts 1-disrupted basic fuse-element, 2-fulgurite after arcing fuse-element

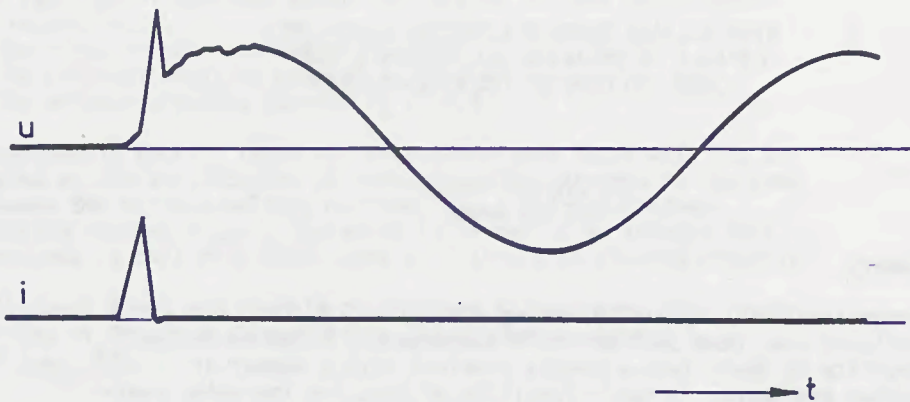


Fig.4 A loop record of the interrupting of 110kA, 550V, 50Hz, p.f. ≤ 0.15 by a new semiconductor fuse of 315A, 500V

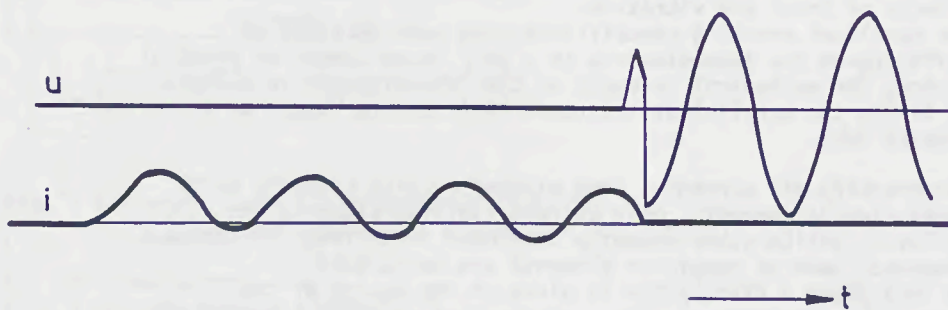


Fig.5 A loop record of the interrupting of abt 1kA, 550V, 50Hz, p.f. ≤ 0.15 by a new semiconductor fuse of 315A, 500V

HIGH VOLTAGE CURRENT LIMITING FUSE-LINKS
CAPABLE OF BREAKING ALL CURRENTS THAT
CAUSE MELTING OF THE FUSE-ELEMENT

D. van der Scheer
H.F.J. Reith

Summary.

Conventional H.V. current limiting fuse-links, as they are available now, have some marked disadvantages. First it is the fragility of their fuse-elements provided with a number of notches and second is their inability of breaking low value over-currents.

Holec has recently developed a range of current-limiting fuse-links, branded "Fullran" which don't possess those disadvantages. "Fullran" fuse-links are able to break all currents which cause melting of the fuse-elements, whilst the construction is such that the fuse-elements are extremely resistant against the effects of shock and vibration.

The excellent breaking capabilities have been obtained by splitting-up the fuse-elements in a very large number of parallel strips. The mechanical strenght of the fuse-elements is assured by fixing the parallel strips, over their entire lenght on a support tube.

For breaking all currents, from minimum melting currents up to short-circuit currents, only current limiting elements are employed. Unlike other recently developed fuse-links, no series elements, such as expulsion elements are being used.

In this paper a discription is given of the design of the fuse-links, the test circuits and the test results. A number of those tests are not specified in IEC 282-1, such as e.g. breaking of minimum melting currents and verification of resistance against shock and vibration.

INTRODUCTION

IEC Publication 282-1 - High Voltage current-limiting fuses, distinguishes two categories, known as "Back-Up" fuses and "General-Purpose" fuses.

For some time now a third category is being marketed known, however unofficially, as "Full-Range" fuses.

A Full-Range fuse could be described as "A current-limiting fuse capable of breaking, under specified conditions of use and behaviour, all currents from the rated breaking current down to the current that causes melting of the fuse-element".

Although this is not a formally accepted phrasing, it might cover the concept "Full-Range".

IEC Publ. 282-1 mentions three Test duties for the verification of respectively:

- . The rated breaking current I_1 (T.d.1)
- . The critical breaking current I_2 (T.d.2)
- . The minimum breaking current I_3 (T.d.3)

Consequently Back-Up fuses and General-Purpose fuses will not be tested on the verification of operation with currents in the zone between the minimum melting current (I_{mmc}) and the minimum breaking current (I_{mbc}). Therefore it is not to be assumed that overloads in this particular zone will always be cleared properly.

Full-Range fuses are capable of breaking all currents that cause melting of the fuse-element hence also currents between I_{mmc} and I_{mbc} . Fig. 1.

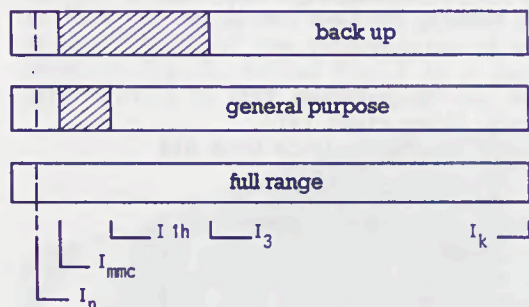


Fig. 1 -  zone where breaking of fault-currents is not guaranteed.

- I_n = rated current
- I_{mmc} = minimum melting current
- I_{1h} = 1 hour melting current
- I_k = rated breaking current
(FULLRAN = 40 kA)
- I_3 = minimum breaking current

THE CONSTRUCTION OF FULLRAN FUSE-LINKS

Fig. 2 shows an exploded view of the fuse-link. The silver strips (4), provided with notches are attached to a tube made of quartz glass (2). This tube supports the strips over their entire length. By doing so it is possible to apply a large number of parallel strips. In the centre the strips are provided with a low melting point metal and at the ends connected to common sleeves (6).

The connection between the common sleeves and the silverplated brass endcaps (10) is made by toroidal, helically wound, springs made of silverplated beryllium bronze (7). This multiple contact arrangement with high contact pressure, results in a connection with low contact resistance. These contact springs also centre and support the tube radially in the porcelain outer-tube (1).

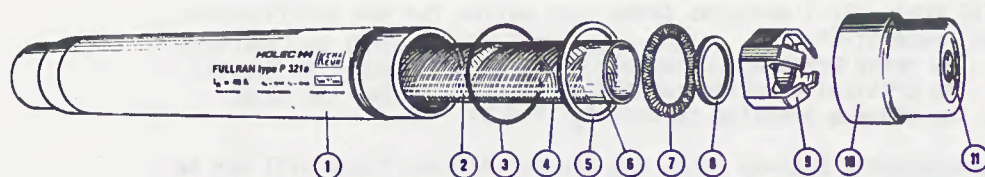


Fig. 2 - Exploded view of a FULLRAN H.V. fuse-link.

Flexible plastic spacers (9) and rubber buffer rings (8) provide for correct axial positioning of the supporting tube, along with protection against the effects of shock or vibration. Rubber washers (5) between porcelain barrel and endcaps together with silicon rubber bands (3) in the hemming grooves enable an air-tight construction.

After filling the fuse-link with fine quartz-granules, the filling hole is sealed with a gas-tight blind rivet (11). Dimensions of 12kV FULLRAN fuse-links are in accordance with DIN 43.625.

For the current-rating 6,3A - 40A the diameter of the porcelain outer-tube is 54 mm. The fuse-element of this series consists of 15 parallel strips of similar design except for their thickness and resistance, which vary per current-rating (6,3A - 8A - 10A - 12,5A - 16A - 20A - 25A - 31,5A and 40A). For the series 40A - 80A the diameter of the porcelain outer-tube is 76 mm, accommodating a fuse-element with 35 strips in parallel. The fuse-element is now composed of 2 parallel supporting tubes with 20 and 15 strips respectively. Like the series 6,3 - 40A the basic pattern of the fuse-elements of this series (40A-50A-63A and 80A) is also identical except for their thickness and resistance.

PRINCIPLES OF OPERATION

In FULLRAN fuse-links the breaking of fault currents after fusing of the elements proceeds in one of two fundamentally different ways.

In the zone of high fault currents ($>10.I_n - 20.I_n$), the currents are carried by parallel conductors formed by silver strips and/or arcs. The respective arcs continue to exist side by side because they are in the so-called positive part of the arc-characteristic.

In the zone of low fault currents ($<10.I_n - 20.I_n$) there always is only one conductor, strip and/or arc, carrying the current after fusion of the melting-element. Parallel arcs cannot continue to exist because they are in the negative part of the arc characteristic.

When a fuse-link is being charged with a high fault current, this current is split up in as many parallel arcs as there are parallel strips. As a result the arc-energy, developed during arcing-time, is efficiently spread over the arc-quenching media.

The arcs are exposed to optimum cooling, which leads to a relatively high arc-voltage gradient. In FULLRAN fuse-links of the 12 kV series, having 520 mm long melting strips, an arc-voltage gradient of 50 to 60V per mm has been obtained.

After a fuse-element melts as a result of a low fault current, there is always only one strip or arc that will carry the current. For each individual strip this means, however, a relatively high fault current. FULLRAN fuse-links are designed such, that after melting at their low melting-point spot, strips also melt on their notches and consequently multiple arcing occurs. This again means that all currents are broken "the current limiting way".

Fig. 3 shows a fulgurite of a FULLRAN fuse-link $I_n = 40A$ after breaking a short circuit current of 40kA r.m.s. at 10.4 kV, being the test voltage of a 12 kV system. An oscillogram of the interruption of a low fault-current is shown in fig. 4, whilst fig. 5 is a photograph of the fulgurite appertaining to this oscillogram.



Fig. 3 - Fulgurite of a 40A fuse-link after breaking 40 kA in a 12 kV system.

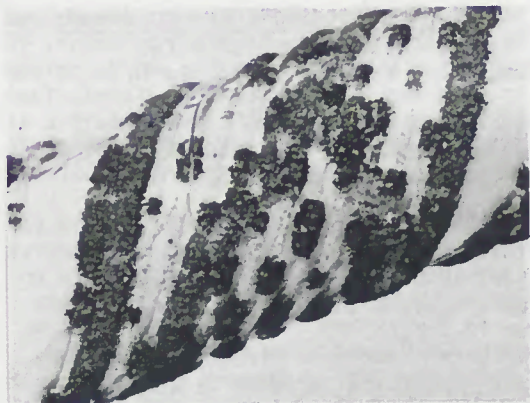
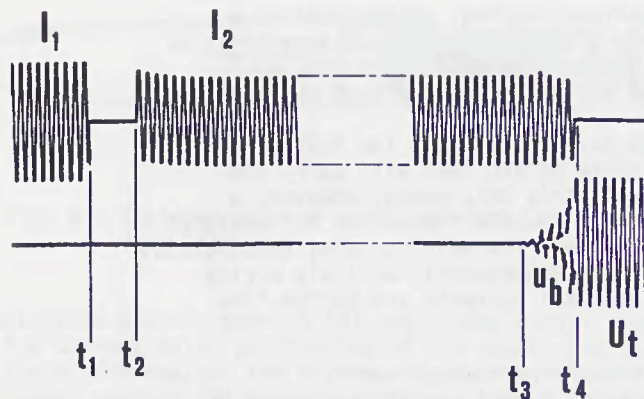


Fig. 5 - Fulgurite appertaining to oscillogram of fig. 4.



t_2-t_1 = change-over time ($< 0,2$ s)
 t_3-t_0 = melting time (1 hr.)
 t_4-t_3 = arcing time (120 ms)
 I_1 = 1 hr. current ($I_1 = 68A$)
 I_2 = test current ($I_2 = 50A$)
 U_b = arc voltage
 U_t = recovery voltage ($U_t = 12$ kV)

Fig. 4 - Oscillogram showing the breaking of 50A at 12 kV by a FULLRAN fuse-link 40A.

TYPE TESTING, CERTIFICATION AND SUPPLEMENTARY TESTS.

For H.V. Current-Limiting fuse-links IEC Publ. 282-1 is the best accepted recommendation for various National Standards. FULLRAN fuse-links are tested and certified by KEMA in accordance with IEC Publ. 281-1 as being "General-Purpose" fuses. Supplementary tests have been made to prove their "full-range" qualities. Separate tests have shown that fuses of the 12 kV series can be used in 3,6 kV and 7,2 kV systems without undue voltage-surges.

Testing of low fault currents Testing the behaviour of H.V. fuses at low fault currents can usually not be fully performed in a H.V. circuit.

Long melting times of minutes or even hours would cause insurmountable problems of heat dissipation in the circuits of the testing laboratories. Therefore those tests are made in a dual circuit.

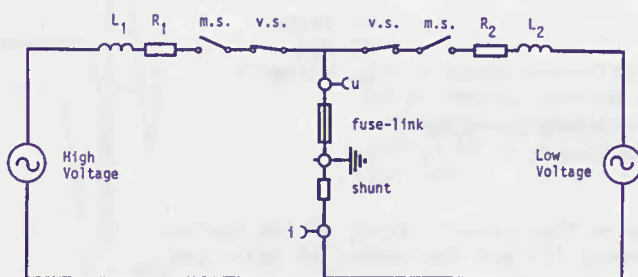
The fuses are preheated in a L.V. circuit until melting of the fuse-element starts. Just before final melting occurs, the fuse is connected to the H.V. circuit after less than 200 milliseconds change-over time. This test is in accordance with the conditions described in IEC Publ. 282-1, clause 13.2.2.1.

Final melting of the fuse-element occurs in the H.V. circuit so the verification of breaking of (very) low fault currents is done eventually in a "direct" circuit.

In case tests are to be made at currents higher than or equal to the 1 hour melting-current, the value of the test-currents in both the L.V. circuit and the H.V. circuit are identical. FULLRAN fuses have also been tested at currents lower than the 1 hour melting-current. During these tests the L.V. circuit is set at the 1 hour current and the H.V. circuit at the desired value, which shall be less than the 1 hour current.

In this way tests have been made in the KEMA-laboratories at $1.25.I_n$ in free air and at I_n in an insulation enclosed Holec Magnefix unit.

The diagram of the test-circuit for low fault currents is shown in fig. 6.



Circuit components.

- L_1 and R_1 = control inductance and resistor in H.V. circuit
- L_2 and R_2 = Do. in L.V. circuit
- m.s. = make switch
- v.s. = breaker
- u = voltage measurement
- i = current measurement

Fig. 6 - Test circuit for low faultcurrents.

Resistance against transformer inrush currents The amplitude of inrush currents of offload transformers is depending on the design of the transformer itself, the firing angle and the fault-level of the supply system.

If a transformer at the H.V. side is protected by fuses, then those fuses have to withstand all inrush currents of that particular transformer.

The effects of inrush currents on FULLRAN fuses have been extensively investigated in a 10 kV supply system.

The aim of these tests was to determine

- . the highest fuse rating at which inrush currents can cause melting of the fuse element, and
- . whether the fuses will adequately break inrush currents.

Fig. 7 shows a diagram of the test-circuit.

The tests have been made at a 500 kVA-substation transformer 10/0,4 kV.

The fault-level of the supply system amounts to 280 MVA. The maximum recorded inrush current was 450A or 15.5 times the rated current of the transformer. The tests were conducted in a three phase system. Except where melting had already occurred, each current rating was tested 10 times. The firing angle was random.

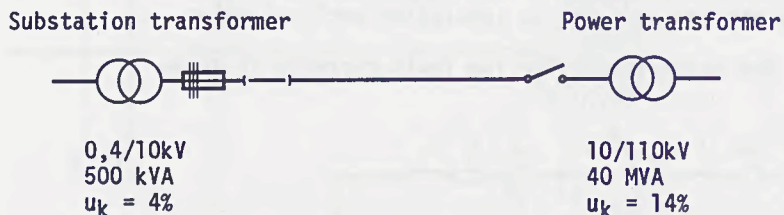


Fig. 7 - Test circuit for inrush currents of off-load transformers.

Table 1 gives information on the current rating of the various fuse-links, the peak currents (\hat{i}) and the number of tests per current-rating (n).

The fuses $I_n = 40A$ and $I_n = 31,5$ did not melt and neither mechanical nor thermal ageing of either the silver strips or the low melting point spot could be observed.

I_n (A)	Type no.	\hat{i} (A)	n
40	P321a	55 - 440	10
31,5	P321a	20 - 450	10
25	P321a	130 - 390	6
20	P321a	160 - 390	2

Table 1.

One fuse $I_n = 25A$ melted during the first test and another one during the sixth test. One fuse $I_n = 20A$ melted during the second test.

In all three cases the fuse exposed to the highest peak current melted and the fuse has cleared the current properly.

The two remaining fuses were unaffected, and there was no detectable ageing.

Fig. 8 is the oscillogram of the melting and breaking of an inrush current by a fuse $I_n = 25A$.

A photograph of the fuse-element after breaking this inrush current is shown in fig. 9. It can clearly be seen that melting of the strips took place at the notches, whilst the tin spots are still intact.

The conclusion for this particular test is that, as far as inrush currents are concerned, this 500 kVA transformer ($I_n = 28,8A$) can be protected by a FULLRAN fuse $I_n = 31,5A$.

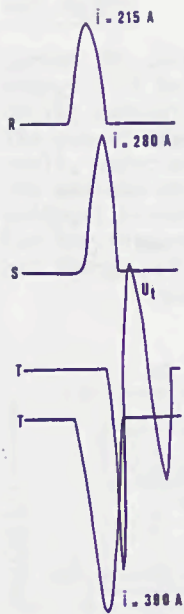


Fig. 8 - Oscillogram recording the breaking of an inrush current of a substation transformer 500 kVA - 10/0,4 kV by a FULLRAN fuse-link $I_n = 25A$.



Fig. 9 - Detail of the fuse element after breaking the inrush current. Clearly to be seen is that melting occurs at the notches; the tin-spots are still intact.

VERIFICATION OF RESISTANCE AGAINST SHOCKS AND VIBRATION

IEC Publ. 282-1 does not contain recommendations for the verification of shock and vibration resistance of H.V. fuses.

FULLRAN fuse-links have been tested in own laboratories to check whether they are shock and vibration resistant.

The fuses have successfully passed following tests:

Vibration tests The tests have been made in a vibrating frame with variable frequency and amplitude control.

- . According to Veritas specifications: Vibrating at a resonance frequency or 25 Hz and an amplitude of 2 mm for 1 hour.
- . According to Lloyds specifications: Three dimensional vibrating. In the zone 1 Hz-13,2Hz at an amplitude of 1 mm. In the zone 13,2 - 100 Hz with an acceleration of 0,7 g, vibrating time 2 hours at a resonant frequency or 13,2 Hz.

Shock test This test is meant as a transport simulation test. Three fuse-links in their original packing have been tested on the vibrating frame.

Vibration in vertical direction at an amplitude of 12 mm and resonance frequency for 15 minutes.

Drop test This test is a free fall test according to IEC 68-2-32, test Ed. It contains a vertical free fall of unpacked fuse-links on a 20 mm steelplate.

Fullran fuse-links withstand this fall from a height of 500 mm without fracture of the fuse-element.

Operation test This contains withdrawing and inserting 3 fuse-links in a Magnefix-unit. Inside this unit the fuses were continuously charged with their rated current. In total 500 operation tests have been made at a rate of 25 times per day.

ARC ENERGY

During the current-breaking process in a fuse a certain arc energy will be generated. This arc energy is the integral of arcing current, arcing voltage and arcing time.

The amount of arc energy generated in FULLRAN fuses is relatively small, especially when breaking low fault currents.

The maximum arc energy will be generated during breaking of critical currents.

For the fuse ratings of 25A, 40A and 80A measured values of arc energy are given in the graphs of fig. 10.

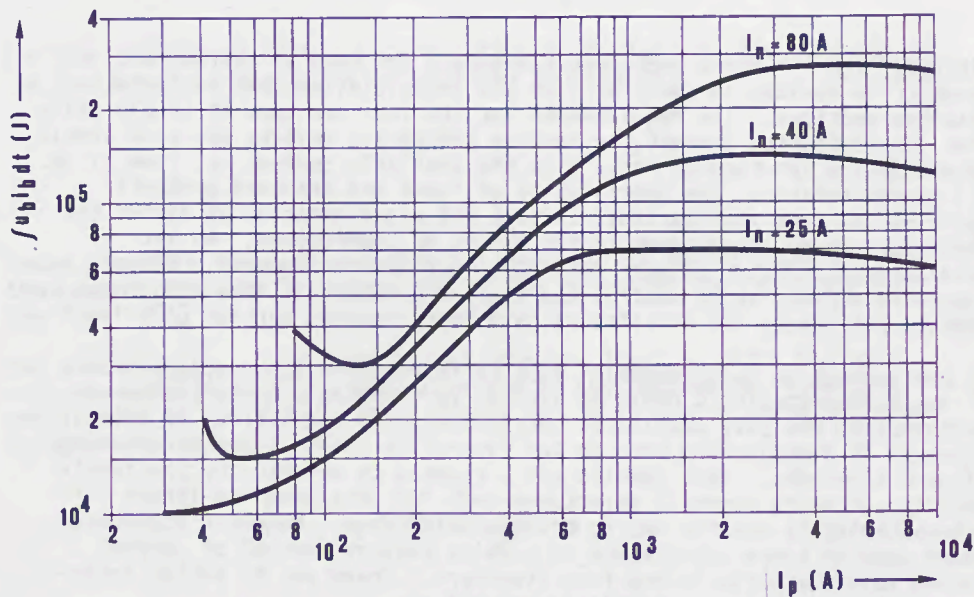


Fig. 10 - The arc energy as function of the prospective current. Values shown are the maximum values.

PROGRAMMABLE FUSES

R. L. Boggavarapu

INTRODUCTION Fuses and circuit breakers are used as overcurrent protective devices in power utility and industrial systems to isolate faulted sections. The requirements for the fuse are that it should allow for discrimination amongst the various protective devices and also should minimize the let-through I^2t . With the available current vs. time (i vs. t) characteristics, the coordination of fuses and breakers presents problems in some applications, in that the discrimination at either the high-current or low-current region has to be compromised. An i - t characteristic which is more desirable is shown in Figure 1. Use of magnetic structures to control the flow of currents in fuse structures to obtain non-linear characteristics have been proposed earlier [1].

A new concept of "programmable" fuse to represent a fuse package whose i vs. t characteristic could be altered by changing a circuit element external to the fuse package is introduced. The feasibility of this concept is demonstrated both in the laboratory and in experiments using Type K fuselinks. Test results are presented to demonstrate the feasibility of using magnetic structures both for obtaining non-linear characteristics and for making programmable fuses. Magnetic structures were used in these experiments to provide passive control of current along multiple paths in the fuse structure. There was no active interaction between the magnetic field and the arc.

NON-LINEAR FUSE The principle of this fuse, called Augmented fuse by Aubrey, was described by him in the article referred to earlier [1]. Figure 2 shows schematically the arrangement of the fuse. A toroidal current transformer with a primary winding of N_p turns is connected to its secondary winding of N_s turns. Two fuselinks with their room temperature resistances of R_1 and R_2 are connected to the finish terminals of primary (F_p) and secondary (F_s); the other ends of these fuselinks are connected together to form terminal 2. The fuse package with its terminals (1) and (2) is to be connected in series as an over-current protective device. The total current, i_T , entering terminal 1 has to be leaving terminal 2. Transformer action controls the current division among the two fuses until a level of fault current is reached

Dr. R. L. Boggavarapu is with the Research and Development Center, Westinghouse Electric Corporation, Pittsburgh, PA 15235 USA

that saturates the magnetic core. Neglecting the magnetizing current, the secondary and primary currents are related by equation (1):

$$i_2 \approx -\frac{N_p}{N_s} i_T \quad (1)$$

The actual direction of current flow in fuselink R_2 is opposite to that shown in Figure 2. The current in fuselink R_1 is given by equation (2):

$$i_1 = i_T - i_2 \approx \left(1 + \frac{N_p}{N_s}\right) i_T \quad (2)$$

For the transformer having a turns ratio of $(N_p/N_s) = 1$, the currents in the two fuselinks are given by equations (3) and (4):

$$\begin{aligned} i_2 &\approx -i_T \\ i_1 &\approx 2i_T \end{aligned} \quad (3)$$

These equations indicate that the two currents are out of phase and that the current division is independent of the values of the resistances of the fuselinks.

For a fault current, i_T , much higher than the level at which the core saturates, the current divides according to the inverse ratio of the resistances of the fuses. The currents i_1 and i_2 are in phase and given by equations (5) and (6):

$$i_1 = \frac{R_2}{(R_1 + R_2)} i_T \quad (5)$$

$$i_2 = \frac{R_1}{(R_1 + R_2)} i_T \quad (6)$$

By proper design of the transformer and choice of cross-sectional areas and resistances for the fuses, a package could be built such that both fuses melt at approximately the same time to isolate the faulted section.

The core size is determined by two factors: the current level at which the "non-linearity" (or change) in fuse characteristic is desired and the total resistance in the secondary loop. The current i_2 in the secondary loop is determined from equation (1). The transformer has to be designed so that a voltage necessary to sustain this current is induced in its secondary winding. Hence this voltage, V_{sec} , is given by equation (7) and the core size is determined by equation (8):

$$V_{sec} = i_2 (R_1 + R_2) \quad (7)$$

$$V_{sec} = 4.44 B_m A_c f N_s * 10^{-8} \quad (8)$$

where B_m is flux density in gauss, A_c is cross-sectional area of the core in sq. cms, f is the frequency and NS is the number of turns in the secondary.

The operation in a real fuse package is as follows. For a given fault current, the initial resistances of the fuses may not be large enough to cause saturation of the core. As the resistances of the fuses increase due to the heating effect, the core reaches saturation and the current division changes. The waveshapes also change progressively as a function of time. For much higher fault currents, the current waveshapes will be distorted even initially depending on the relative magnitudes of the fault current and the designed current level at which the core saturates. Also, in a real fuse package the initial resistances (R_1 and R_2) of the two fuses need not be the same, and the selection depends on the desired characteristics of the fuse package and the design of the transformer. The determining factor would be to make both the fuses rupture at approximately the same time.

PROGRAMMABLE FUSE In the laboratory investigation of the concept of non-linear fuse using resistors in place of the fuses, it was observed that magnetizing current could cause distortion of the currents in the two paths and also cause errors. The total current i_T is unaffected. Since the r.m.s. values of currents in the two paths represent the effectiveness of melting when fuses are used, ways of reducing these errors were investigated. The principles used in zero-flux transformer [2] for improving the accuracy of current transformer seemed to be applicable here. The circuit shown in Figure 3 is one of the several circuits investigated in the laboratory using resistors. R_1 and R_2 represent the fuses; the winding connections on the transformer marked CT1 are essentially the same as before. The variable resistor R_3 is inserted in series in the branch containing fuse FI (R_1). The primary winding of an auxiliary current transformer marked CT2 is connected in series with the primary of the main current transformer (CT1). The secondary winding of CT2 is connected across R_3 . By varying the resistance R_3 , the current division between fuses R_1 and R_2 and the current level at which the core of CT1 reaches saturation could be altered. Thus the $i-t$ characteristics of the fuse package could be altered. The waveshapes and magnitude of the current change with different values of R_3 and for a real system with fuses the $i-t$ is important in causing melting. In the laboratory experiments a change in r.m.s. current in different paths of about 19% to 39% was achieved by changing R_3 alone without altering R_1 and R_2 . A voltage is introduced into the loop formed by R_1 and R_2 and by varying the resistance value of R_3 and changing the polarity of this voltage by changing connections, a large number of fuse characteristics could be achieved. Since these results are obtained with the same fuse elements and with only a change in the value of a circuit element external to the fuse package, this is termed a "Programmable" fuse.

EXPERIMENTS WITH FUSELINKS The results of laboratory experiments on both of the above concepts were very encouraging. Changes in r.m.s. values of current of up to 40% were achieved. The size of the core required was calculated from the nominal resistance of the fuselinks of different voltage and current rating and from the required "transition current". This was found to be not too large and did not vary widely for

different fuses. A series of tests using Type K fuselinks were conducted at the A.C. Laboratory of Westinghouse, in East Pittsburgh. The test set-up is shown schematically in Figure 4. A 100 V A.C. supply with variable resistor packs, R_c , is used to obtain a unity power factor circuit. The power factor is not specified in standards for determining the melting characteristics. A brass block is used to mount the two fuselinks, with the buttonheads held in place by two brass nuts. The pigtailed hang free in air. The current transformer of the fuse package is mounted on a horizontal board and connections are made through terminal blocks mounted on the same board. Through-type current transformers were used to record the waveforms of the total current, i_T , and the two branch currents, i_1 and i_2 . The resistance values of the fuselinks and the information on the cores is given in the appendix.

TEST RESULTS: NON-LINEAR FUSE Test results for one series of tests in which both the primary and secondary of the current transformer have 20 turns and in which 6 amp fuselinks are used in both current paths are reported here. Before conducting these experiments the melting characteristic for this non-linear fuse was "calculated" based on very simple approximations. In a very simplistic approach the current division was assumed to be controlled by the transformer action up to 60 amps and by the resistances alone for currents higher than 60 amps. Based on these assumptions the melting times for the two fuses of four different currents was read from the curves and the maximum melting time is plotted. Oscillographic traces for two real tests are shown in Figures 5 and 6. The currents are distorted due to the magnetizing current component and the phase relationship between i_1 and i_2 is accurately shown. The ratio of current transformer used to indicate total current, i_T , was changed and its polarity is not consistently shown. The peak value of the voltage induced in the search coil on the CT is seen to increase with time. This is attributed to the increase in the resistance of the fuselinks. The time for the total current to go to zero is used to plot the melting characteristic shown in Figure 7. Because of the low voltage of the power supply, the arcing time is assumed negligible. The resulting characteristic in Figure 7 shows a smooth transition from the 6 amp fuse in the low current region to the 12 amp fuse characteristic in the high current region. This measured characteristic agreed very well with the one calculated from the simplistic assumption described earlier. However, the transition was much smoother than was calculated.

TEST RESULTS: PROGRAMMABLE FUSE These tests were conducted with two current transformers. Both transformers have primary and secondary windings of ten turns each. Two 25 amp fuselinks were used. The resistance of the external resistor R_3 should not change due to the momentary large currents. Available current shunts with resistances of 0.5 m Ω and 2.0 m Ω were used and no effort was made to optimize or design for any specific desired characteristics. As before, the melting time characteristics were constructed from the oscillographic traces. The results are shown in Figure 8. The effect of changing the external resistance was clearly evident; this was the only change in the two series of tests.

DISCUSSION The preceding sections described the principles involved in the use of magnetic circuits to obtain non-linear characteristics for fuses, the laboratory work and the tests conducted to determine the

melting characteristics of fuselinks. The purpose of this very short program was to explore as many new concepts as possible, rather than to continue with feasibility studies. As such, there was not enough time to investigate completely every phenomenon that was observed. Several series of tests were conducted on the non-linear fuse with different turn ratios of current transformer and with combinations of fuselinks having different rating. At low currents the i - t characteristics of the fuse package should approach those of the lower rated fuse. Sometimes this was not observed. The discrepancy was attributed to the heat loss from the fuselinks to the brass block. In the high current region, beyond the core saturation level, the i - t characteristics of the fuse package should be equivalent to those of a fuse having a rating equal to the sum of the ratings of the two fuses. This has generally been observed. In a few cases the melting characteristic of the fuse package did not follow the slope representing that of the fuselinks and a "speed-up" was observed. The cause of the speed-up and the effect of different magnetic materials and current transformer design and optimization on the characteristics of the fuse packages was not fully investigated.

The errors due to magnetizing current and the distortions introduced in the current waveform due to magnetic nonlinearities could be estimated. The currents i_1 and i_2 for a transformer turn ratio of 1 are given by equations (9) and (10) than equations (3) and (4):

$$|i_2| = i_T - \delta \quad (9)$$

$$i_1 = 2 i_T - \delta \quad (10)$$

$$\frac{i_1}{|i_2|} = 2 + \frac{\delta}{i_T} \quad (11)$$

The ratio of currents, given by equation (11), approaches 2 for large values of currents. The fuse elements could be so chosen that the fuse element carrying the current i_1 will melt first. Other choices could be made depending on the desired characteristics. However, when one of the fuses melts first, the circuit conditions change and the transformer in effect becomes an inductor. The magnitude of the inductance depends on which fuse melts first. If the fuse in branch 2 melts first, the inductance will be due to the primary winding alone. However, if the fuse in branch 1 melts first, the inductance introduced in the circuit would be that due to the primary and secondary turns in series. In the test circuits, this additional inductance could have caused distortions in waveforms. No attempts at making correction due to this factor were made. In real systems the additional impedance may not be large compared to the total system impedance; the design should aim for minimizing such effects.

Several circuits for programmable fuses have been investigated in the laboratory. Only one circuit was used in tests with fuselinks in the available time. Sensitivity aspects could be explored more fully.

The size of the core required is quite small. No attempts at optimization of the core or transformer construction were made. The core loss under steady state conditions is negligible. Depending on the application the fuse can be built with current transformer as an integral part or as a separate component.

CONCLUSION The novel concept of "programmable" fuse, where a change in external element is used to alter the current vs. time characteristic of the fuse package is introduced and investigated. This concept is successfully demonstrated in tests with fuselinks. The use of magnetic structures to control the current flow along multiple paths of fuse package coupled with the use of external circuit elements to alter its characteristics might provide greater flexibility in system design. Solutions based on these principles could be developed for other problems in the application of overcurrent protective devices.

ACKNOWLEDGMENTS The author extends his thanks to Westinghouse Electric Corporation for supporting this work and for permitting publication of the results. He is very grateful to D. D. Blewitt for his help and valuable discussions and to Mrs. I. M. Hesselbart for typing the manuscript.

REFERENCES

- (1) D. R. Aubrey, "Coordination of fuses and circuit breakers during lightning storms", IEE Conference on Lightning and the Distribution Systems, Publication No. 108, 1973.
- (2) A. Hobson, "The zero-flux current transformer", A.I.E.E. Trans., August 1953, pp. 608-615.

APPENDIX Transformer and fuselink information for the experiments.

A. Non-Linear Fuse

Core: Material: 0.004" thick hypersil
 Strip Width: 1.0"
 Cross-Sectional Area: 0.438 sq. in.
 Number of Turns in Primary and Secondary: 20

Fuselinks: Rating: 6 A each
 Resistance: 13.45 m Ω (each)

B. Programmable Fuse

Cores: CT1
 Material: 0.012" thick hypersil
 Strip Width: 2.0"
 Cross-Sectional Area: 1.0 sq. in.
 Number of Turns in Primary and Secondary: 10

CT2
 Core is same as for non-linear fuse
 Number of Turns in Primary and Secondary: 10

Fuselinks: Rating: 25 A each
 Resistance: 3.2 m Ω

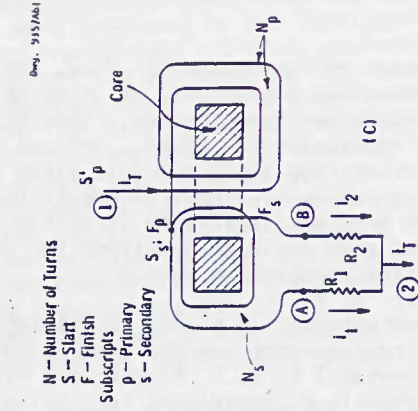


Fig. 2 - Non linear fuse

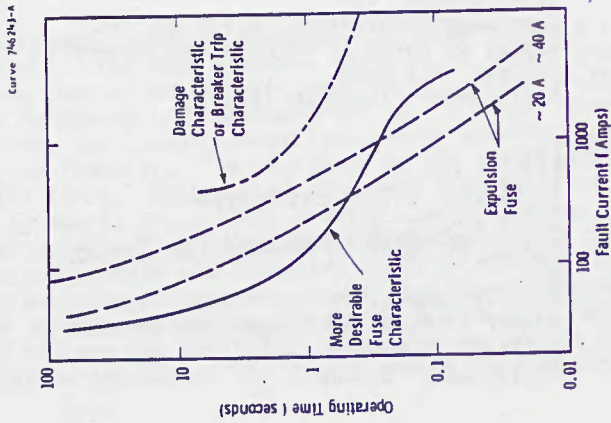


Fig. 1 - General characteristics of fuses and breakers (not to scale)

Doc. 9357A62

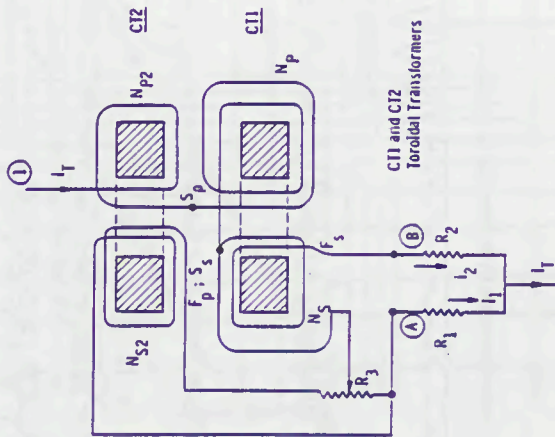


Fig. 3 -- Schematic of programmable fuse

Doc. 9357A63

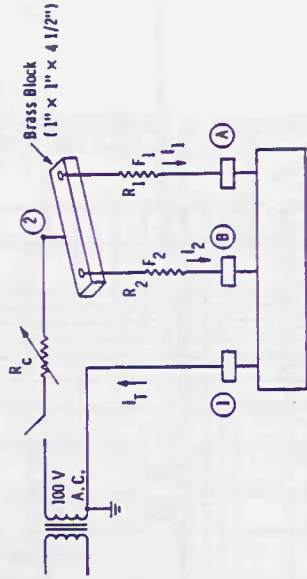


Fig. 4 -- Schematic of set up for test on fuses

FIGURE 6 TEST RESULTS FOR NON-LINEAR FUSE

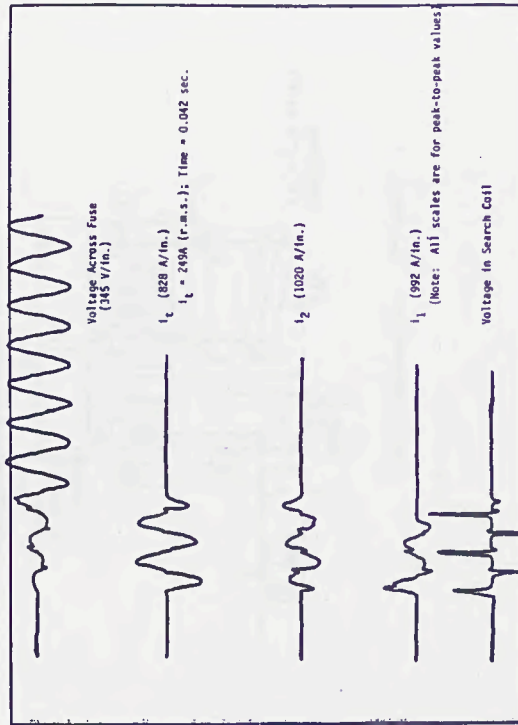


FIGURE 5 TEST RESULTS FOR NON-LINEAR FUSE

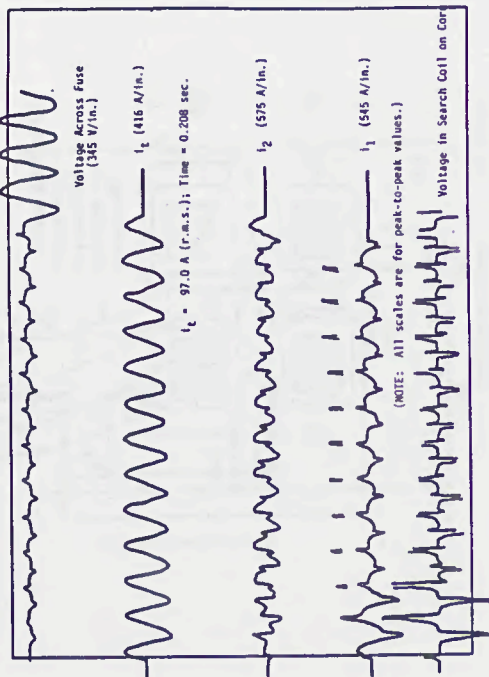


FIGURE 7 MELTING CHARACTERISTIC OF NON-LINEAR FUSE WITH TWO 6 AMP FUSELINKS

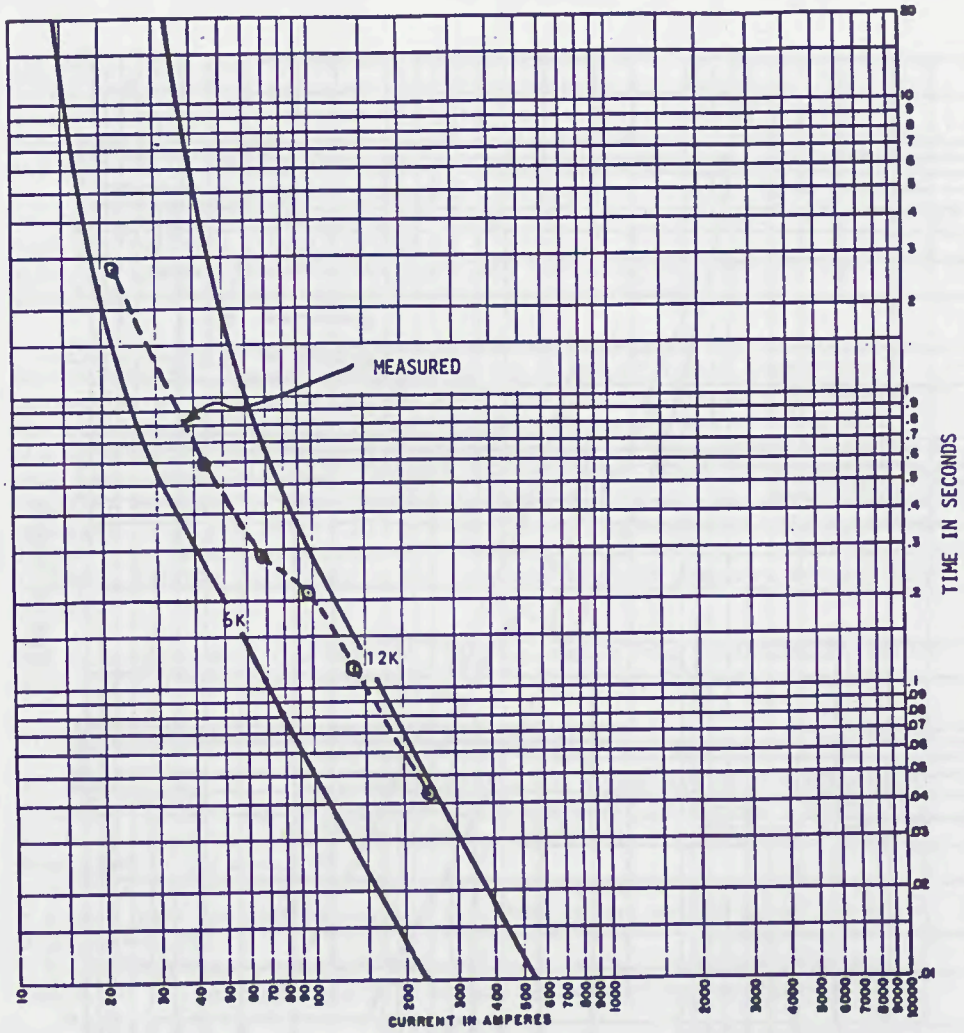
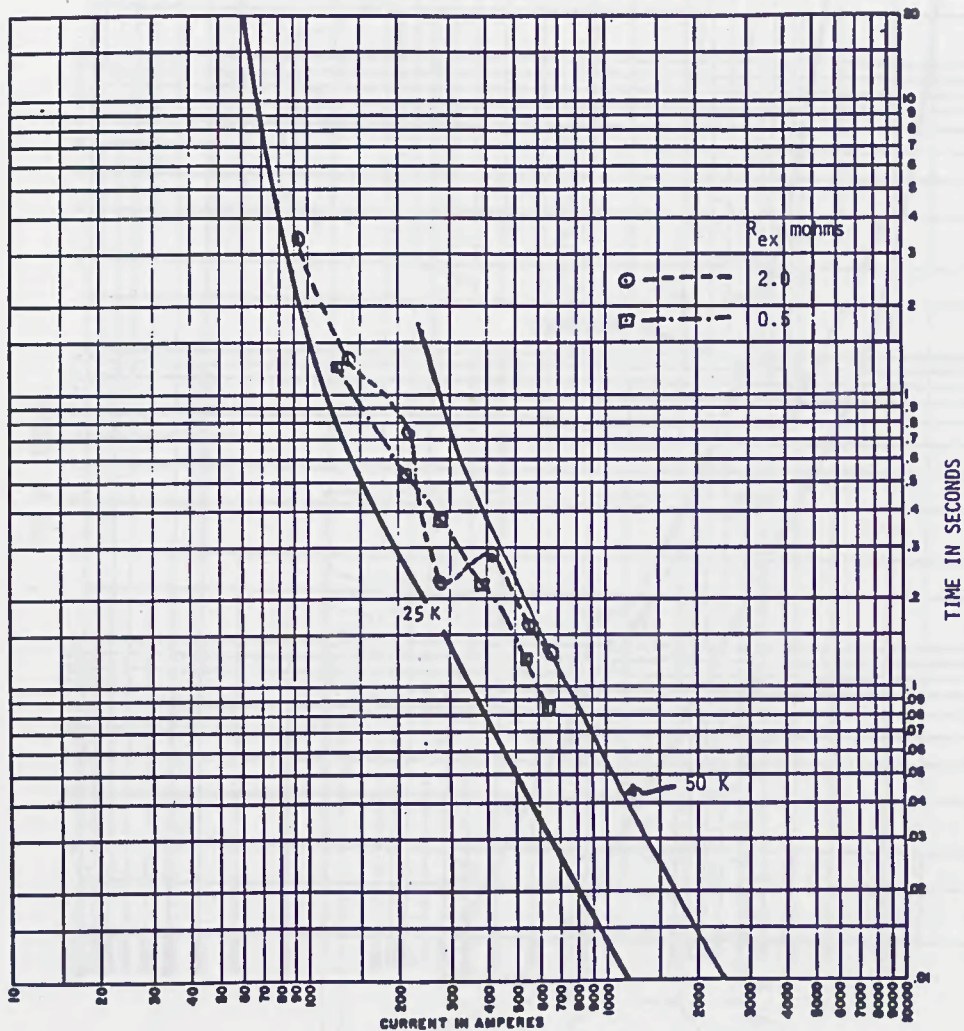


FIGURE 8 MELTING CHARACTERISTICS OF PROGRAMMABLE FUSE WITH TWO 25 AMP FUSES



A FUSE USED AS AN ARC QUENCHING CHAMBER
GENERATES A NEW CONCEPT OF POWER CIRCUITS PROTECTION

C. MULERTT

ABSTRACT : The description and the application of a new current limiting device using a fuse as an arc quenching chamber are described. This new device consists of a current carrying bypass switch and of a parallel fuse. The role of the bypass switch is to provide a large current rating and the fuse's role is to handle the arc ignition and extinction. Therefore the fuse replaces the arc quenching chamber of traditional circuit breakers, and has generated a new range of current limiting devices faster than any existing circuit breaker. This new device represents an important technological breakthrough in protection of electric and electronic power circuits.

1. INTRODUCTION : The need for a new ultra high speed current limiting device appeared several years ago in the field of static converters protection as well as in the field of distribution systems. An example is the protection of medium voltage variable frequency drive using many SCR's in series and parallel. Another example is the protection of equipment where available short circuit currents have grown and surpassed the breaking capacity of the existing protective devices. For these protection problems it is not realistic or even impossible to design multi-parallel fuses in order to carry large continuous current and still provide current limiting and I²t protections, and moreover circuit breakers are not fast enough.

For such problems a new current limiting device (the PYROBREAKER) offers economic and operating advantages for both AC and DC protection.

2. DEFINITION AND DESCRIPTION OF THE PYROBREAKER :

2.1. Definition : the PYROBREAKER is one component of a system (the PYRISTOR SYSTEM). In this system the pyrobreaker is the part which actually opens the circuit at a very fast speed. The PYRISTOR SYSTEM is described in paragraph 3.

A pyrobreaker consists of two parts (see figure 1) :

- a very fast opening percussion operated bypass switch using pyrotechnique material,
- a limiting fuse connected in parallel across the bypass switch.

These two are integral parts of a unit and cannot be separated.

C. MULERTT
L. FERRAZ & Co.
28, rue St Philippe
69003 LYON/FRANCE

2.2. Roles of the bypass switch and the fuse :

- The role of the bypass switch is to provide a low power loss path through which the required continuous current load current flows. The bypass switch is not designed to open the circuit by itself (no provision for arc extinction incorporated in the bypass switch).
- The fuse's role is to handle the arc and absorb the whole interrupting energy. The fuse's role is also to provide a prearcing duration long enough to let the bypass switch build an insulating distance that prevents any arcing inside the switch.

2.3. Description (see figure 2)

- motor (1) : this motor contains the explosive charge and a detonator. The detonator is activated by an electrical discharge supplied by the other components of the PYRISTOR SYSTEM described in paragraph 3.
- piston (2) : this is a part of the motor and is forced out violently by the explosion inside the motor.
- solid copper bar (3) : this bar carries the current and has very low power losses. It is a solid monoblock machined from a single copper bar which means that unlike traditional systems, current does not have to flow through any soldered joints or contacts held together under pressure.
- reception chamber (4) : when the piston strikes the center of the bar, a copper rod is sheared and propelled and lodges in the conically shaped reception chamber.
- copper connections (5)
- body (6)
- fuse (7) : this is a high-breaking capacity ultra fast-blowing fuse whose design is based upon the quality and advanced techniques of semiconductor protection fuses.

3. DESCRIPTION OF THE PYRISTOR SYSTEM : Figure 3 shows the four main components and the basic interconnections required in the PYRISTOR circuit protection system. These components are :

- pyrobreaker : this is the part which actually opens the circuit to be protected. It is triggered by an electrical discharge.
- controller : it supplies the electrical discharge to the pyrobreaker and it monitors and processes a signal coming from a sensor.
- transformer : it is a pulse transformer designed to isolate the controller from the pyrobreaker.
- sensor : this is a measuring device which continuously monitors a circuit parameter.

4. PYROBREAKER OPERATION : the parameter to be monitored (temperature, current, di/dt , etc...) is detected by the sensor. The controller continuously monitors and processes the measured signal. As soon as the signal reaches a preselected "fault value", the controller supplies the electrical discharge which triggers the pyrobreaker. Figures 4, 5, 6 and 7 show the main stages in the operation of the pyrobreaker. The main stages are :

4.1. Explosion inside the motor and shearing (figure 4) : the explosion occurs 5 microseconds after the start of the electrical discharge supplied by the controller. At this moment the piston begins moving out from the motor to strike the copper bar. A copper rod (8) is sheared from the copper bar.

Figures 5, 6 and 7 show how the copper rod (8) moves away and lodges

inside the reception chamber (4).

Note : the time from the beginning of the explosion to the end of shearing is only 100 microseconds (approximately).

4.2. End of piston stroke and fuse prearcing (figure 5) : the piston travels only 5 mm. Its role is to shear the copper (8) and to propel it. At the moment the thrust ends, the copper rod is moving towards the reception chamber at a speed of 45 m/second. At this time the current is no longer flowing through the bypass switch but through the fuse. At the end of the fuse's prearcing process current limit I_c has been established.

4.3. Arcing period (figure 6) : the copper rod has already travelled a distance "d" at the moment the arc appears in the fuse. The distance "d" is interconnected to the prearcing time since it must be reached to prevent the development of arcing inside the bypass switch.

4.4. End of arcing period, circuit completely open (figure 7) : the arc has developed in the fuse which alone ensures its extinction. At this moment the current has dropped to zero and the pyrobreaker remains open. It can be seen that the sheared copper rod (8) has reached and is lodged inside the reception chamber.

5. DETAILED DESCRIPTION OF CURRENT LIMITING FUNCTION : figure 8 shows how the current is interrupted in 5 stages. These stages are :

5.1. TS : time period required to reach the triggering current $I_{D \max}$, measurement tolerance included. $I_{D \max}$ is a maximum value considering I_D as a minimum and $1.1 I_D$ a maximum including tolerance.

5.2. TF : time period required by the controller - approximately 50 microseconds.

5.3. TR : mechanical response time of the pyrobreaker. That includes the mechanical inertia of the motor and the time required to shear the copper bar. This is about 100 us.

5.4. TP : fuse prearcing duration. This is a few hundreds microseconds.

5.5. TA : fuse arcing duration. This is 5 milliseconds or less.

We can therefore write the following equation :

$$I_C = I_D + (TF + TR + TP) di/dt$$

Where di/dt represents the fault current rate of rise.

6. IMPORTANCE OF THE FUSE : the fuse must be designed to provide
 - a sufficient prearcing time to allow the copper rod to establish enough insulating air gap and prevent arcing in the bypass switch,
 - a sufficient chamber length and volume to allow the absorption of the whole interrupting energy.

6.1. The prearcing duration : immediately after the end of the shearing operation inside the bypass switch, the current is diverted to the fuse. At this moment the current value is (see figure 8) :

$$I_R = 1.1 I_D + (TF + TR) di/dt$$

It can be seen from figure 9 that :

$$IC - IR = TP \cdot di/dt$$

This means that the prearcing I^2t (adiabatic since TP is only a few hundreds microseconds) must have a minimum value K :

$$K = TP \cdot \frac{IC^2 + IR^2 + IR \cdot IC}{3}$$

$$\text{Then } TP = \frac{3K}{IC^2 + IR^2 + IR \cdot IC}$$

The fuse has been determined from ID, di/dt and the working voltage so that TP has the predetermined value.

It is then important to see that :

- if during operation the fault to be interrupted is as expected, the fuse prearcing time will be TP,
- if the current ID is lower, or if the maximum fault di/dt is lower than expected, time TP will therefore increase. This means that the isolating distance in the bypass switch has increased with respect to that expected and that therefore no danger exists.
- conversely, if ID or di/dt are higher than expected, time TP will decrease and the pyrobreaker will operate incorrectly.

6.2. Interrupting energy absorption : since the arc is totally handled by the fuse, the corresponding energy W_a must be fully absorbed inside the fuse chamber. The W_a value and the working voltage are taken into account to determine the fuse dimensions.

It is well known that :

$$W_a = \frac{1}{2}LIC^2 + \int_{TA} e(t) \cdot i(t) \cdot dt - \int_{TA} R \cdot i^2(t) \cdot dt$$

where : L : inductance of the circuit

R : resistance

e(t) : source voltage versus time

i(t) : current versus time

IC : peak let through current of the pyrobreaker as shown in

figure 7

TA : arc duration

It is common to get W_a values around or above 10^6 joules.

7. SOME CHARACTERISTICS OF THE PYROBREAKERS : the pyrobreakers are available for various voltages and current ratings. There are 6 models as shown in table 1. The ultra high speed of the devices is demonstrated by the duration ΔT between the triggering signal appearance and the moment when the current is limited.

Therefore $\Delta T = TF + TR + TP$ (see figure 7)

ΔT varies with the working voltage. Table 1 gives, for each model, the ΔT value corresponding to the rated voltage and the minimum value of ΔT with the corresponding working voltage value. For lower working voltages the ΔT value remains equal to that minimum (see table 1 on the next page).

- Breaking capacity : the breaking capacity is function of the following :

. Nature of voltage : AC or DC

. Under AC conditions : . F frequency

. U voltage

. ID triggering current, or the current value in the circuit when the triggering parameter value is reached.

. Under DC conditions : time constant (= L/R)

ID triggering current, or the current value in the

circuit when the triggering parameter value is reached.

For example the breaking capacity of the 7200 V 4000 A model is :

- 220 KA at 50 hertz or 180 KA at 60 hertz with $I_D = 18000$ A and $U = 7200$ V
- 100 KA at 50 hertz or 80 KA at 60 hertz with $I_D = 27000$ A and $U = 7200$ V

TABLE 1

VOLTAGE RATING AC or DC (KV)	CURRENT RATING (KA)	ΔT (microseconds)	WATTS LOSS AT RATED CURRENT (W)
2,5	2,6	260 μ s at 1,2 KV 400 μ s at 2,5 KV	120
2,5	4,5	300 μ s at 1,2 KV 440 μ s at 2,5 KV	220
2,5	8 in AC 10 in DC	330 μ s at 1,2 KV 560 μ s at 2,5 KV	320
7,2	4	480 μ s at 2,5 KV 1050 μ s at 7,2 KV	230
11	4	900 μ s at 6 KV 1500 μ s at 11 KV	230
20	3	530 μ s at 4,6 KV 1400 μ s at 20 KV	320

8. OSCILLOGRAM : figure 10 gives an oscillogram with test conditions and results.

9. APPLICATIONS AND ADVANTAGES OFFERED BY THE PYROBREAKERS : the pyro-breaker is ideal for the protection of both low and medium voltage equipments designed for high continuous applications and requiring fast action in the event of faults. The pyrobreaker offers technical and financial advantages.

9.1. Applications : the pyrobreaker is well adapted for the protection of power static converters and the protection of distribution systems. For example, it already protects the following :

- Rectifiers on AC and DC sides, such as :
1400 VAC rectifiers used to supply large current pulses to electromagnet.
1000 VDC trimmer rectifiers
- Cyclo converters, on AC or DC sides (see figure 11)
- Variable frequency drives on input and output (see figure 12) such as :
. 1500 V 3500 A drive
. 10000 V 2000 A drive
. 15500 V 1500 A drive
- DC motor protections
- Distribution panels fed by 2 sources coupled in parallel (see figure 12) at 11 KV

- Distribution circuit of plants : in order to upgrade the breaking capacity of existing circuit breakers.
etc...

9.2. Technical and financial advantages : the following advantages are offered by the pyrobreaker.

- adjustable triggering value (or another type of signal)
- peak current limited to very low values
- very low let through I_{2t}
- low watts loss
- breaking capacity as high as several hundreds kiloamperes
- the equipment size and components size can be reduced to handle the low stress associated with the I_{2t} and peak current limited by the pyrobreaker
- costly replacement of old circuit breakers is avoided by using a pyrobreaker
- costly current limiting reactors can be replaced by a pyrobreaker
- watts loss of current limiting reactors are drastically reduced by a pyrobreaker mounted in parallel across them
- for a new equipment that requires a current limiting reactor in order to delay the shut down, the pyrobreaker in parallel also allows the diminution of the reactor dimensions and cost.

10. CONCLUSION : the pyrobreaker is an economical solution for the protection of high power equipment in commercial and industrial electrical power generation and distribution systems. It is sometimes the unique solution for the protection of semi-conductors in medium voltage systems.

References :

- N.J. KING, H.E. GALLAGHER, W. KNAUER : "145 KV current limiting device-design, construction and factory test". IEEE-PES Summer meeting in Vancouver - July 1979.
- Arthur FREUND "Overcurrent protection". Mc Graw Hill Inc. New York.
- D.S. CAVERLY and R.H. PATEL : "Air core reactors : Important considerations for their specification and application". CANADIAN PULP AND PAPER ASSOCIATION meeting in February 1984.
- G.D. HOLDER, J.R. ALEXANDER and D.K. DIMOND : "Electrical fault levels in paper mills. Nature source and reduction". CANADIAN PULP AND PAPER ASSOCIATION meeting in February 1984.
- P. BARKAN "The current-diverting FCL. A practical solution to fault current limiting". IEEE-PES Summer meeting in Vancouver, July 1979.
- P. ROSEN "Arcing phenomena in HRC fuses under varying test conditions". Int. conf. on electric fuses and their applications, Liverpool Polytechnic 1976.
- M.R. BARRAULT "Pressure in enclosed fuses". Int. Conf. on electric fuses and their applications, Liverpool Polytechnic 1976.
- S. GNANALINGAN and R. WILKINS "Digital simulations of fuse breaking tests". IEE PROC Vol. 127, Pt.C. N°6 November 1980.

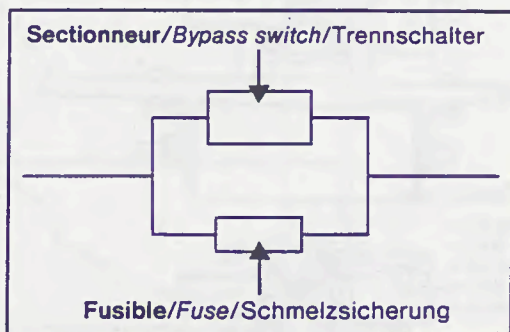


Fig. 1

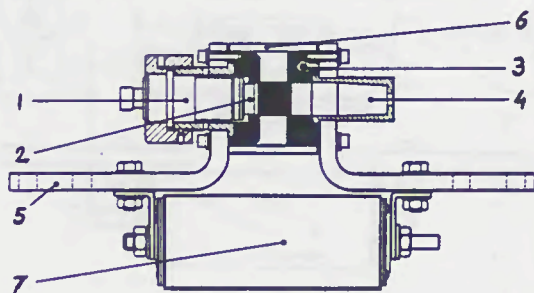


Fig. 2

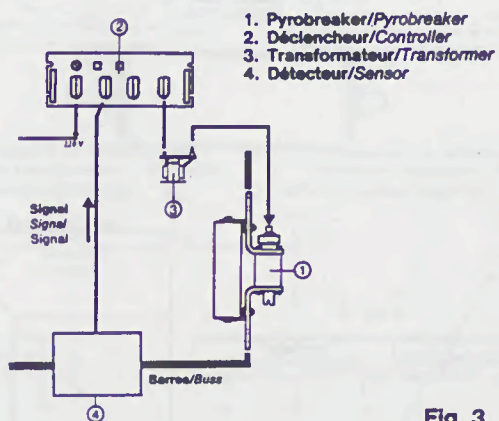


Fig. 3

Fig. 4

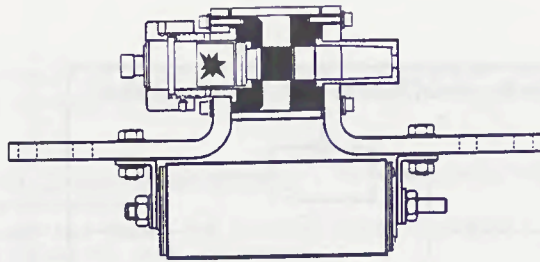


Fig. 5

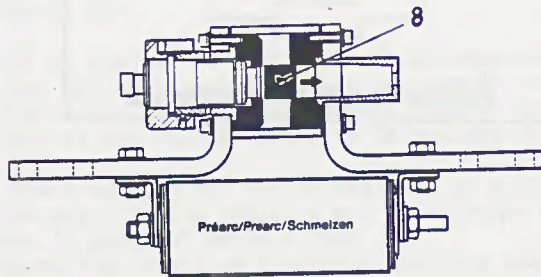


Fig. 6

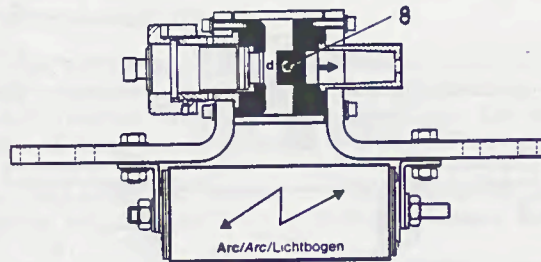


Fig. 7

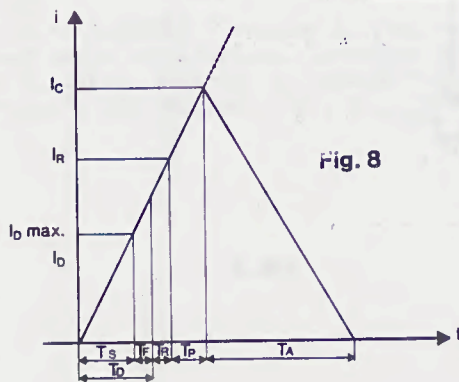
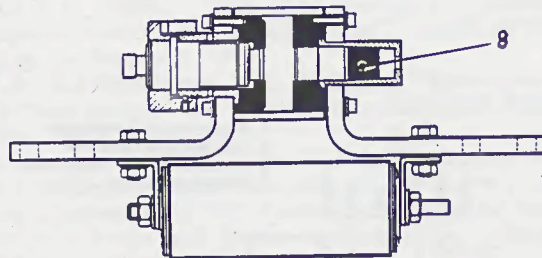


Fig. 8

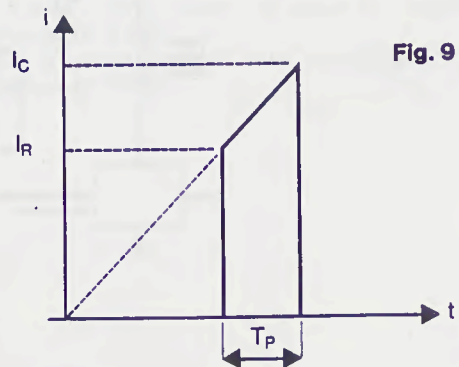


Fig. 9

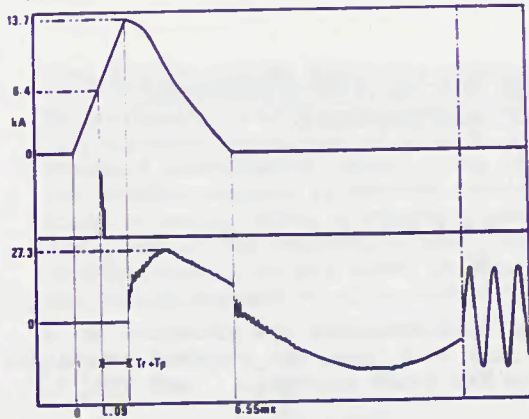


Fig. 10

Test conditions

- U = 13 500 V (voltage)
- I_p = 14.5 kA (prospective fault current)
- θ = 55 degrees (closing angle)
- \cos = 0.06 (power factor)
- I_D = 6 400 A (triggering current)

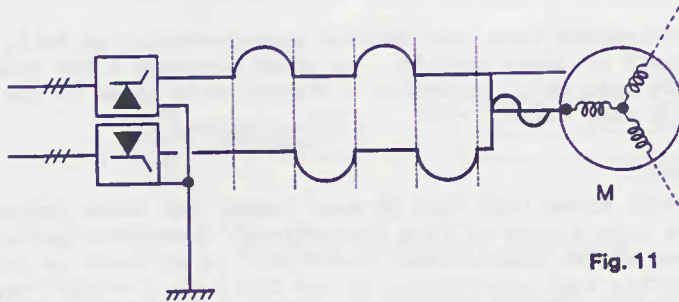


Fig. 11

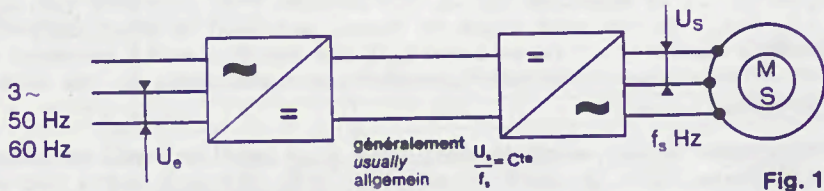


Fig. 12

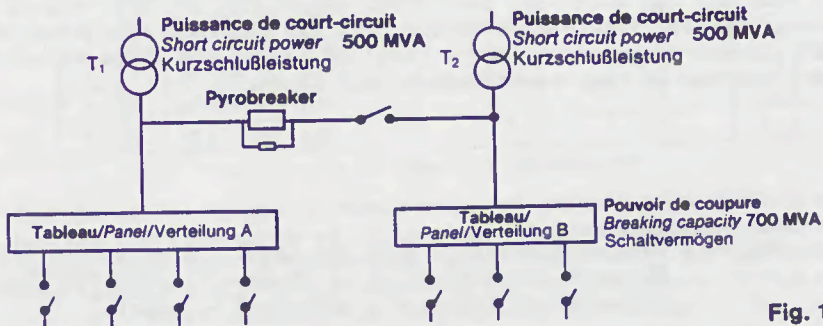


Fig. 13

NOTES ON HEATING OF FUSES WITH ORDINARY SUBSTITUTION
ELEMENTS AND STANDARD UNITS

I o n B a r b u

The theoretic and experimental considerations are presented as a consequence of tests made on real unit fuses and standard substitute unit fuses, recommended by the IEC draft project [1] and VDE [2] .

Out of the brief analytical thermal computations it results that the overtemperatures of the tested standard fuses are higher than the overtemperatures of the steady - state substitute units.

These conclusions have been checked experimentally as well. On the basis of these results, the paper suggests a new standard substitute unit which generates a thermal mode close to the one developed by real fuses.

1. INTRODUCTION

It is a well known fact that in many cases, the tests imposed by standards have a more or less conventional character. Anyhow, the conditions of the conventional tests must be as close as possible to the operating real conditions. In the field of electric fuses, the conventional tests are generally referred to the determination of breaking capacity and to overtemperatures. As regards the breaking capacity, it is measured to all the imposed test currents ($I_1; I_2; I_3; I_4; I_5$ etc.) in the cold state of fuses, although in operation, the greatest majority of fuses interrupt the short-circuit currents after having worked for a certain time with currents close to the rated current.

The present paper, we shall deal only with heating tests on industrial fuses (type gI and type aM etc.) with standard units and real substitution units.

The analysis was made both analytical and on the basis of experimental results, thus demonstrating that the standard substitution unit element proposed by IEC [1] and VDE [2] is not close enough to the behaviour of real substitution unit fuses.

Dr. Eng. Ion Barbu - Head of Laboratory with The Institute of Scientific Research and Technological Engineering for the Electrotechnical Industry - Bucharest - Romania.

2. NORM SPECIFICATIONS REGARDING STANDARD UNITS

In conformity with the suggestion made by IEC 32 B (Secretariat) 91 [1] the overtemperature of support terminals is measured by means of standard substitution units, also, with respect to VDE 0636 [2], the overtemperature at support terminals of fuses type NH is determined by using, also, a standard substitution unit, whose dimensions are given by the respective norm. The structures of these standard substitution units are shown in Fig. 1, and their dimensions are given by the respective norms and partially by Table 1.

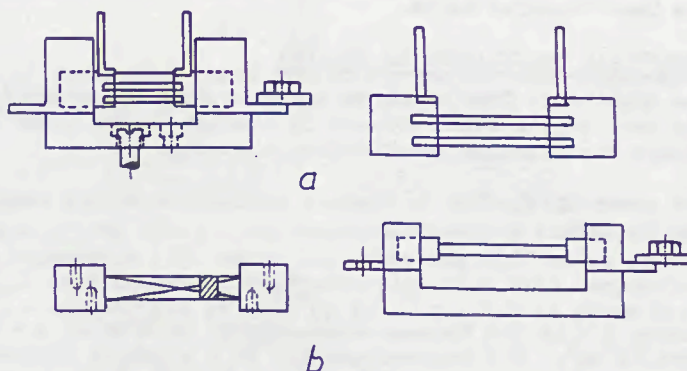


Fig. 1 Standard substitute unit fuses

The conductors of the standard unit which simulate the fusible are made of CuNi 56/44, in conformity with VDE [2] and of CuMn 12 Ni, in conformity with IEC [1] whose resistivity, practically does not vary with temperature.

Table 1
Dimensions of standard substitute unit fuses

Size	b* (mm)		P (W)	R (mΩ)	Proposes CEI		Proposes CE.Roman	
	CEL	CER			CU Mn 12 NI - Bars			
					Number (mm)	Diameter (mm)	Number (mm)	Diameter (mm)
00	30.5 ⁻⁰ ₋₃	45 ^{±15}	12	0.47	1	7	1	7.3
0	46 ⁻⁰ ₋₂	62 ^{±15}	25	0.97	1	6	1	6
1	46 ⁻⁰ ₋₆	62 ^{±25}	32	0.51	1	8	1	8.2
2	46 ⁻⁰ ₋₄	62 ^{±25}	45	0.281	2	8	2	7.9
3	46 ⁻⁰ ₋₆	62 ^{±25}	60	0.151	3	9	3	8.8
4	54 ⁻⁰ ₋₆	62 ^{±25}	90	0.09	3	12	3	11.3
4a	54 ⁻⁰ ₋₆	84 ^{±3}	100	0.07	4	12	4	11.6

See Fig. 2 p 20 from 32B (secretariat) 91

The powers dissipated by these standard substitution units are selected for the fuse class of the highest admissible powers for substitution units with corresponding rated currents. As it can be seen in Fig. 1.a. and Fig. 1.b, the conductor or the conductors of the standard unit which simulate the fuse element are placed in the open, unlike the real fuse elements which are located in an extinction

place (quartz sand) which constitutes a heat transfer medium as well. Between the standard substitution element and the real fusible of electric fuses, there are qualitative differences, as for example: differences between the cross section and the lateral surface of fuses and standard conductor; different heat transfer at the ends of fuses and standard conductors etc. These differences lead-though the dissipated power might be the same- to a different heat transfer, both by thermal conduction and thermal convection and to different overtemperatures. In order to make prominent, at least qualitatively, these discrepancies, we present a brief analytical calculation of the heat transfer below.

3. ANALYTICAL CALCULATION OF HEATING

The hypothesis from which we start is that the power developed within the real substitution element is similar to the power developed within the standard substitution element.

The power dissipated by thermal conduction within conductors of fuses is given by the relation:

$$P_{\lambda} = \lambda \frac{\partial \theta}{\partial x} A \quad (1)$$

where: λ - is the thermal conductivity in $W/cm^{\circ}C$; A - cross section area in cm^2 ; θ - temperature in $^{\circ}C$; x - length of conductor in cm. Therefore, the values which differ sensibly in real steady-state unit as compared to standard substitution units are λ and A .

The power dissipated by thermal convection is given by the relation:

$$dP_c = K (\theta - \theta_a) S \quad (2)$$

Where: K - overall coefficient of heat transfer, in $W/cm^2^{\circ}C$; S - lateral surface heat transfer area of conductors, in cm^2 .

As it can be noted, in relation (2) too, K and S are different for standard substitution units as compared to real substitution units. Consequently, P_{λ} and P_c being different for the real substitution unit and for the standard substitution unit, it results that the overtemperatures will be different.

In order to throw light on the qualitative differences between the standard element and the real substitution unit, we note down a brief thermal calculation.

Thus, from Fig.1, it results the power developed within the standard unit is constant, practically independent of the temperature, due to the fact that the coefficient of variation of resistivity with temperature of CUMN 12 Ni is about $10^{-5} 1/^{\circ}C$, and of CuNi 56/44 is of the same order, consequently an overtemperature of the conductor of $400^{\circ}C$ leads to an increase in resistivity with 4% and implicitly of the dissipated power. At the same temperature ($400^{\circ}C$) the resistivity of copper increases with 170% and the dissipated power implicitly. Another qualitative difference is connected to the analytical expression of the overtemperature variation with the length of the fuse element.

Thus, in the case of the standard substitution unit, the overtemperature of the standard element is given by [3] :

$$\tau(x) = \frac{\rho_a A J^2}{Kl} \left[1 - \frac{gch a' x}{ash a' x_1 + gch a x_1} \right] \quad (3)$$

where: K - heat transfer coefficient, in $W/cm^2 \text{ } ^\circ C$; ρ_a - resistivity at ambient temperature in $\Omega \text{ cm}$; l - length of conductor perimeter, in cm ; $g = \frac{\lambda}{A}$; π - represents the heat transfer coefficient at the end of the fuse element, given in $W/cm^2 \text{ } ^\circ C$.

The value of "a" is given by the relation:

$$a' = \sqrt{\frac{Kl}{\lambda A}} \quad (4)$$

In the case of fuses with which resistivity varies with temperature the overtemperature is given by the relation [3] :

$$\tau(x) = \frac{\rho_a A J^2}{Kl - \infty_0 \rho_0 A J^2} \left[1 - \frac{gch a x}{ash a x_1 + gch a x_1} \right] \quad (5)$$

where the data of the above - written relation have the significance of those in expression (3), with the following difference or additions: ∞_0 - coefficient of resistance variation with temperature, in $1/^\circ C$; ρ_0 - resistivity at zero $^\circ C$, in $\Omega \text{ cm}$; "a" is given by:

$$a = \sqrt{\frac{Kl}{\lambda A} - \frac{\rho_0}{\lambda} \infty_0 J^2} \quad (6)$$

In case the temperature at the distance x_1 is known, there can be used formulae, where the heat transfer coefficients are not required. This formula has the following expression for the standard element [3] :

$$\tau(x) = \tau_1 \frac{ch a' x}{ch a' x_1} + \frac{\rho_a A J^2}{Kl} \left[1 - \frac{ch a' x}{ch a' x_1} \right] \quad (7)$$

and in the case of a real substitution unit, heating is given by the expression [3] :

$$\tau(x) = \tau_1 \frac{ch a x}{ch a x_1} + \frac{\rho_a A J^2}{Kl - \infty_0 \rho_0 A J^2} \left[1 - \frac{ch a x}{ch a x_1} \right] \quad (8)$$

Taking into consideration the relation (1) and the expressions of overtemperatures in (3); (5); (7) and (8) the powers conveyed by thermal conductance have the following forms. For the standard unit they are obtained out of the relation:

$$P_{\lambda_e} = -2\lambda A a' \tau_1 t h a' x_1 + \frac{2\lambda a' \rho_a I^2 t h a' x_1}{Kl} \quad (9)$$

$$P_{\lambda_e} = \frac{2\lambda a' \rho_a I^2}{Kl} \frac{gsh a' x_1}{ash a' x_1 + gch a' x_1} \quad (10)$$

and for the real substitution unit, they are given by :

$$P_{\lambda r} = -2\lambda A a \tau_1 t h a x_1 + \frac{2\lambda a \rho_a I^2}{K(1-\alpha_o \rho_o A J^2)} t h a x_1 \quad (11)$$

$$P_{\lambda r} = \frac{2\lambda a \rho_a I^2}{K(1-\alpha_o \rho_o A J^2)} \cdot \frac{g s h a x_1}{a s h a x_1 + g c h a x_1} \quad (12)$$

The powers developed in continuous mode within the substitution unit, the contacts of the test support being included, and taking into consideration the variation of the conductor's resistivity and of the electrical contacts with temperature, are given by [4] [5]:

$$P(\theta) = R_f I^2 + 2R_c I^2 = R_{af} \left[1 + \alpha(\theta - \theta_a) \right] I^2 + 2R_{pc} \left[1 + \frac{2}{3}(\theta - \theta_a) \right] I^2 \quad (13)$$

where: R_f - is the fuse resistance in Ω ; R_c - resistance of support contacts in Ω ; I - current in A; R_{pc} - resistance of contacts at the ambient temperature.

We admit that the power conveyed by fuses by means of thermal conduction P_{λ} is equal to the power conveyed by convection, P_c , which is practically real for low voltage fuses, thus it results that $P_c = P_{\lambda}$. Also, we suppose that P has the same value for the standard unit and for the real element.

By a real substitution unit we understand the substitution element which has fuses or conductors and which are tested within ceramic hoses filled with quartz sand.

The power conveyed by convection by the standard substitution unit, taking into consideration (2), is given by the relation:

$$P_{ce} = K_e l \pi n d (\theta - \theta_a) \quad (14)$$

where: l - standard conductor's length, in cm;

d - diameter of standard conductors, in cm;

n - number of standard conductors in parallel

The output of the real substitution unit at the external ceramic hose in a rectangular shape with sides e_1 and e_2 is given by the relations:

$$P_{cr} = 2K_r l (l_1 + l_2) (\theta - \theta_a) \quad (15)$$

The report between the overall output of the real unit P_{tr} and the overall power conveyed by the standard substitution unit P_{ts} , is:

$$\frac{P_{tr}}{P_{te}} = \frac{P_{cr} + P_{\lambda}}{P_{ce} + P_{\lambda}} = \frac{2P_{cr}}{P_{ce} + P_{\lambda}} = \frac{2}{1 + \frac{P_{ce}}{P_{cr}}} = \frac{4(l_1 + l_2)}{\pi n d + 2(l_1 + l_2)} \quad (16)$$

In relation (16) is was considered $K_e \approx K_r$, an acceptable fact, because the heat transfer is made in both cases by convection. Also, it was

supposed highly approximately, that the temperature θ of the ceramics is equal to the temperature of the standard conductor.

The real calculation value of the relation between P_{tr}/P_{te} for fuses of 630 A, size 3, with the dimensions given by IEC [1], is equal to 1.56, taking into consideration the following values of the data in the relation (16): $a_1=76$ mm; $a_2=75$ mm; $n=3$; $d=9$ mm.

Taking into account the dimensions of the standard unit in VDE 0636 [2], the following expression of the relation P_{tr}/P_{te} is obtained:

$$\frac{P_{tr}}{P_{te}} = \frac{4c}{a+b+2c} \quad (17)$$

Having the concrete values for a, b and c from VDE 0636 [2], for size [3], the report P_{tr}/P_{te} becomes equal to 1.51.

4. CALCULATION AND EXPERIMENTAL RESULTS

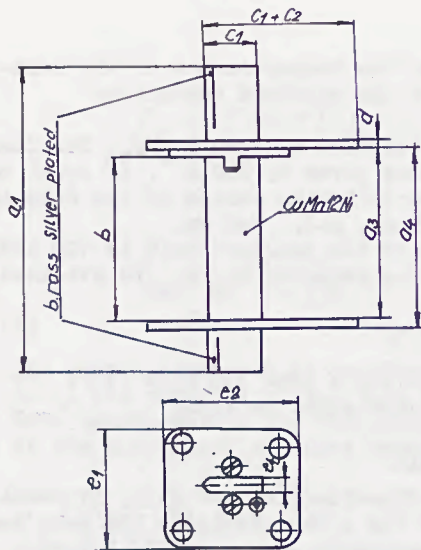
Out of the calculations made with formulae (16) and (17), it results that the real substitution unit of 630 A can dissipate 56% more heat than the standard unit with the dimensions given in IEC [1] and respectively 51 % more than the standard substitution unit with the VDE 0636 [2] dimensions.

The dissipated power depends on the contact system, as can be seen in relation (13). Two types of supports with the same real substitution element have been experimented at ICPE-Bucharest. With the first type, the dissipated power was of 60 W and the overtemperature at terminals of 55.4°C, and with the second type (of less pressure on the contact), the dissipated power of the same substitution unit was of 73.7 W while the overtemperature at terminals was 64.9°C. This test shows that the support, due to the different contact resistance R_{pc} , can influence the fuse heating, owing to the increase of resistivity with temperature.

The increase of resistivity leads to the implicit rise of dissipated power with the real substitution unit, the first data in relation (13). Since the thermal calculations developed above are approximate there have been experimented standard unit proposed by IEC [1] and VDE [2], and the standard unit we wish to propose and which is shown in Fig. 2.

The fundamental dimensions, the number and the sizes of the standard conductors for size 00; 0; 1; 2; 3 and 4 are shown in Table 1. The standard substitution units in Fig. 2 are mounted within the ordinary ceramics, taking the shape of the real substitution units, as in Fig. 3.

Thus, out of Fig. 3, it results that the suggested standard substitution unit has at its basis the standard substitution unit of IEC [1] supplemented with ceramic within which quartz sand is introduced. In this way, two important requirements are met; firstly, the heating of the standard conductor and secondly, the heat transfer is made in similar conditions to those of steady - state fuses.



Dimensions (mm)	a ₁	a ₃	a ₄	a
Size 1	135	60	65	58.5

c ₁	c ₂	e ₁	e ₂	e ₄
22	28	47	46	6.1

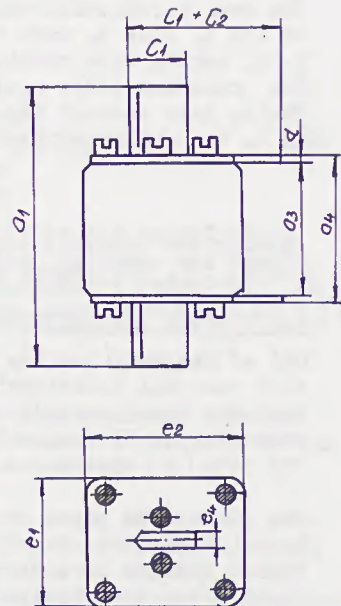


Fig. 2 Standard substitute unit fuses proposed by C.E. Román

Fig. 3 Standard substitute unit fuses mounted within the ceramic

The experimental results of tests performed on both the standard substitution unit in conformity with IEC and on the one that we proposed, have demonstrated the validity of the approximate analytical calculations presented above.

The calculation and experimental data for the real substitution unit, applied to the above written formulas are the following:

- for the standard substitution unit: $I=250$ A; $l=4.2$ cm; $\lambda=0.21$ W/cm²°C; $\rho_a=0.435 \times 10^{-4}$ Ω cm; $K=0.005$ W/cm²°C; $\tau=2$ W/cm²°C; $A=0.54$ cm²; $\tau=82$ C; $J=463$ A/cm²;

- for the real substitution unit; $I=250$ A; $l=5.32$ cm; $\lambda=3.93$ W/cm²°C; $\rho_a=0.018 \times 10^{-4}$ Ω cm; $\rho_o=0.017 \times 10^{-4}$ Ω m; $K=0.009$ W/cm²°C; $\tau=12$ W/cm²°C; $A=0.04$ cm²; $\tau=69$ C; $J=6250$ A/cm².

Thus, at a dissipated power of 32 W of the first group standard unit (see Fig. 3), built in a strap of CuMn 12 N1, the experimental results are those shown in Table 2.

From Table 2 we could note that the highest overtemperatures are obtained when the IEC proposed standard unit is used, and the lowest when our standard unit is used.

Table 2

Experimental results

Kind of dummy fuse-link Over temperature	Dummy fuselink in air see fig. 2	Dummy fuse-link in ceramic corp without any quartz sand	Dummy fuse link in ceramic corp filled with quartz sand see fig 3	Real fuse link
0	1	2	3	4
Over temperature measured at E point [°C]	74	71	65	63
Over temperature measured at S point [°C]	85	84	82	69
Maximum over temperature of the conductor of the ceramic corp [°C]	136	40	47	51
Power transfered by convection [W]	14	15	18	20
Power transfered by thermal conduction [W]	18	17	14	12
Total disipated power [W]	32	32	32	32

It is obvious that the standard unit we propose simulates the best the thermal phenomena which take place within real fuses. The experimental differences presented above would have been higher, in case a IEC [1] standard substitution unit had been employed, a unit which is made of a round conductor with a diameter of ϕ 8 mm, whose lateral surface (of heat transfer by convection) is of 11.56 cm^2 compared to 23.4 cm^2 of the standard substitution element on which the present tests have been made, or 24.85 cm^2 of the VDE [2] standard substitution unit.

Another phenomenon which influences the change of heat transfer conditions with real fuses as compared to standard units, is the heat transfer by thermal conduction at the fuse ends or at the standard element ends. Thus, Table 3 shows the values of λ for real fuses of the Romanian type of fuses NH and for the standard units in conformity with IEC [1] and VDE [2].

As it can be seen, the respective value is almost double with the real fuses, as compared to standard units. Though these values are a lot different, $P\lambda$ being influenced by the variation of temperature with distance ($\frac{\partial \theta}{\partial x}$), it is possible that this derivation

to balance the discrepancies among λ A. In case the work group is interested in this, The Romanian Electrotechnical Committee may continue the researches and supply additional information.

Table 3

The values of λ A for real fuses and for the standard units

Size	00	0	1	2	3
Parameters					
Romanian fuse links. $\lambda_f \cdot A_f (W/m/^\circ C) \times 10^{-6}$	990	1540	2358	6539	9808
Dummy fuse link see IEC [1] $\lambda_{ce} \cdot A_{ce} (W/m/^\circ C) \times 10^{-6}$	808	594	1056	2111	4008
Dummy fuse links see VDE [2] $\lambda_{ce} \cdot A_{ce} (W/m/^\circ C) \times 10^{-6}$	462	735	1449	2772	5145
$\frac{\partial \theta}{\partial x} [^\circ C/cm]$	Will be calculated with the relations (3) and (5) see appendix 1				

5. CONCLUSIONS

Taking into consideration the thermal calculations presented above and the experimental results obtained from the tests on standard units proposed by IEC [1] and the Romanian Electrotechnical Committee, we can notice the following:

- 5.1. The heat dissipation with standard units proposed with a view to determining the heating of supports is dissimilar as compared to the heat dissipation with real fuses. As a consequence of this understanding, the heating is different too, resulting higher overtemperatures (with about $10^\circ C$) with fuses tested with standard units proposed by IEC [1].
- 5.2. If the heating tests are to be more reproducible, it is necessary for the standard units to have a constant dissipated power, independent of their heating. This can be achieved with two standard units, made of conductors whose resistivity does not vary with temperature ($\alpha_0 \approx 0$). It is the case of the conductors proposed by IEC [1].
- 5.3. If we require the thermal phenomena with real fuses, to be found to a large extent within tests on standard units, they should be made of conductors with strap shape as well as the fuse elements, and the respective bands to be constructed out of materials whose resistivity does not vary with temperature.

These fuses should be introduced within ceramic hoses, or hoses in other materials (similar to those used in real operation), and the respective hoses should be filled with extinguishing substances of the electric arc.

- 5.4. Since the variant presented by 4.3. is difficult to be practically, we consider that the Romanian proposition shown in Fig. 2 Appendix 1

satisfies the requirements and the compromises needed for these tests.

As it can be seen, it satisfies the need to have a constant dissipated power and to obtain a heat transfer close to that of real steady - state fuses.

- 5.5. In our opinion, the ideal standard unit could be made without a quartz-filled ceramic hose, but establishing an equivalence among the convection heat transfer surfaces and the thermal conduction of real substitution units and standard units. The standard units, we think, should be made of a number of bands in CuMn 12 Ni (for example), whose surface S should be as close as possible to the surface S of ceramic bodies and very similar to the two types of units.

6. BIBLIOGRAPHY

- [1] x x x : Drift - First supplement to IEC-Publication 269-2; low-voltage fuses. Part 2; Supplementary requirements for fuses for use by authorized persons. 32 B(Secretariat)91 July 1983
- [2] x x x : VDE Bestimmung für Niederspannungssicherungen bis 1000 V Wechselspannung und bis 3000 V. Gleichspannung VDE 0636 Teil 1 August 1976.
- [3] Barbu, I.: Siguranțe electrice de joasă tensiune, Editura tehnică București, 1983
- [4] Holm, R.: Electric Contacts Theory and Application. Berlin Heidelberg New York Springer Verlag, 1967
- [5] Suciu, I.: Bazele calculului solicitărilor termice ale aparatelor electrice. Editura tehnică, București 1981.

TEST PROCEDURES AND ARCING PHENOMENA IN H.V. FUSE LINKS
NEAR THE MINIMUM BREAKING CURRENT

Aslak Ofte and W. Rondeel

ABSTRACT

Most high voltage fuse links have an uncertain zone of interruption, from the largest melting current (just above rated current I_N) to I_3 , at about 2 - 4 times I_N .

However, the minimum breaking current I_3 has come closer to I_N , and the melting time has increased to several minutes. For the fuse links belonging to the classes General Purpose or Full Range, the melting times are more than one hour.

We have been testing fuses at I_3 in a "synthetic" test circuit (melting current by low voltage) according to IEC 282-1 clause 13.2.2.1, but with melting currents different from the arcing current. The results showed that the different melting currents have very little influence on the min. breaking current I_3 . The value of I_3 is mainly dependent on the H.V.-current, anyway if the melting current is so small that the fuse link melts by the M-spot.

Some physical properties at the interruption process near min. breaking current are presented in the paper. The sand quality is very important, and can give large variations in attainable min. breaking current.

INTRODUCTION

The problem for high-voltage current limiting fuses to interrupt small overcurrents has initiated much attention and research work in the past, and is still a phenomenon of further study.

Most construction principles for fuses affect the breaking performance, and smaller changes in the design can result in large variations in obtained minimum breaking current I_3 .

Central design-parameters, as far as I_3 is concerned, are: fuse-element-material, fuse-element "design", use of M-spot, sand-quality and sand-grain size.

A. Ofte and W. Rondeel are with
A/S Norsk Elektrisk & Brown Boveri, Switchboard and Switchgear Group

A continuous increase in the fuse-quality has taken place, and the minimum breaking current has come closer to the rated current I_N of the fuse. Fuses of the class "General purpose" with I_3 resulting in a melting time more than one hour, and "full-range"-fuses with I_3 lower than the smallest current that can melt the fuse have been designed. Low I_3 means long melting times t_m of the fuses and time-consuming and expensive testing at this current.^m

Acc. to IEC 282-1 clause 13.2, there are two alternative test methods for Test Duty 3:

- a Testing at the specified voltage for the full test period.
- b Melting of the fuse by low-voltage and switching to high voltage for the conclusion of the test.

Alt. b is the only possible method for testing modern H.V.-fuses with melting times of several minutes at I_3 . If a new test method at I_3 reducing the melting time without changing the breaking performance of the fuse can be found, this would be of interest for development and certification of fuses. This article will indicate such a method. However, only "conventional" back-up fuses of different design have been investigated.

ARCING PHENOMENA

The arcing process in c-1. fuses near I_3 is fundamentally different from the process at short circuit current. Arcing time is longer, arcing performance is less distinct and the fuse is not current limiting.

For fuses with M-spot the melting process starts in one of these spots. Then the other M-spots melts until the current density in the remaining intact fuse-element(s) is so high that melting occurs in the constrictions (fig. 1).

The arcing time starts from this moment with burn-back of fuse element and increase of arc-voltage. Acc. to investigations at NIH (Tech.university of Norway) (1), P. Rosen (2) and our own laboratory (3) the arcing current is carried by one single parallel fuse element in turn during the arcing periode. See also fig. 2.

The current will repeatedly commutate to the element with lowest insulation level until eventually the last element obtains the withstand voltage equal to the system voltage and interrupts the current. If the current is below I_3 , the insulation level will not reach the system voltage, and this results in explosion (4).

At currents higher than I_3 the arcing time will be a function of I_3 (fig. 3), with increasing arcing time for decreasing current.

The silica-sand must have the ability to sustain high voltage withstand very quickly at current zero. The voltage increase and also heat transfer ability are important parameters in the arcing process. Different sand qualities have been tested, and smaller amounts of

"pollution" (< 2%) e.g. Fe_2O_3 or mica has a damaging effect. The grain size is of particular significance for the value of I_3 . Identical sands, except for the grain size, have been tested (3) with the following result:

$I_3 = 1,2 \times I_n$ with average grain \emptyset at 0,70 mm

$I_3 = 1,6 \times I_n$ with average grain \emptyset at 0,20 mm

This is confirmed by R. Oliver et.al (9) who mentions large grain-size favourable for interruption of small overcurrent.

I_3 is heavily influenced by the design of the fuse element and especially the constrictions. The length, smallest cross section and number of constrictions all affect on I_3 . Number of fuse elements also affect I_3 .

It is difficult to find a general formula for the I_3 taking care of all the factors influencing it. However, the fundamental notion is to create several arcs in series very fast to increase voltage (5). If these multiple arcing can be controlled to particular points on the fuse elements, the value of I_3 can be reduced even more.

Special designs have been developed to control the multiple arcing. H.W. Mickuleny (6) uses an auxiliary element ("arc electrodes") for each fuse element to start the arcing process (fig. 4).

Control of the arcing process for low currents by thermally insulating parts on the elements is also used (fig. 5) (7) (8).

TEST PROCEDURES

According to IEC 282-1 clause 13.2.2.1 Test Duty 3 (I_3), the fuse can be tested in a low-voltage test circuit (with correct current value) for the major portion of the test period and then switched to a high-voltage test circuit for the conclusion of the test. The switching time must be less than 0,2 sec.

The switching device (fig. 6) used for the tests referred to in this paper operates when the voltage across the fuse exceed approx. 50 V. Two mechanical interlocked vacuum switches interrupt the low-voltage circuit and closes the high-voltage within 20 ms (see fig. 2)

The influence of the melting current I_m (melting time t_m) on the arcing process for currents near I_3 is tested for four types 12kV 40A fuses of four different makes. Two of the fuses have M-spots, the other two have not, and all fuses are of the type back-up of a "conventional" design. Melting current varies within the interval 1 - 3 times minimum breaking current.

Some differences in arcing time (t_a) occur, but no obvious trend in t_a with respect to I_m and t_m can be drawn, especially if the l.v. melting current is less than about $2 \times I_a$.

DISCUSSION

All tests show that the value of I_3 is very constant for the particular design, and not much dependent upon the melting time.

The arcing process is completed long before the voltage increase seems to reach the actual voltage of the circuit (fig. 2). Interruption completes at current-zero, and the very good voltage recovery of the silica-sand enables successful interruptions.

Two different fulgurites at I_3 are observed for the fine and coarse sand respectively. The fulgurite of the fine sand is made of molten sand grains at the inner part of it, and is very compact. Coarse sand has porous fulgurite with crushed sand-grains. The fulgurite is also larger with coarse sand. This observation indicates two different physical processes.

The arcing time in table 1 is used as an indication of the low current clearing ability (fig. 3). Influence of the melting current for the I_3 interruption is because of this indicated by the arcing time. The test material is limited and a 100 % reliable conclusion of the influence of the melting current can not be drawn. Still, the test results indicates that the melting current (and melting time) has very little influence on the breaking performance, and the value of I_3 .

With reduced melting time (and increased current), the total heating of the fuse is reduced, but the fuse-elements and the sand close to them reaches the same temperature as for smaller melting current. The arcing time is short compared with the thermal time constant of the sand. Therefore, the temperature of the fuse at reduced melting time is similar to the temperature at "correct" melting time, as far as arcing condition is concerned.

If the melting time is essentially shorter than correct melting time, another commencement of the melting processes may occur. E.g. melting in a constriction instead of M-spot, or melting in several constrictions simultaneously. As the melting is the basis of the arcing, this must be avoided. For the fuses mentioned in tab. 1, the melting process is different for melting times shorter than a few seconds. This explains the successful result of fuse type C with melting time $t_m = 3,7$ sec. and $I_a = 84$ A.

The test circuit used in the tests is not exactly acc. to IEC 282-1 recommendations. Acc. to this standard the high-voltage has to be switched in for the conclusion of the test, before the melting of the last of the parallel fuse-elements. The test circuit used in the tests registres the melting of the last element and then switches to high voltage (in less than 20 ms). This is to ensure safety and identical switching for all tests, and has no influence on the arcing and I_3 value. See also (4).

CONCLUSION

Design parameters as silica-sand, fuse-elements and use of M-spot has significant influence on the value of I_3 . Special additional requirements to ensure multiple arcing at low currents also influence I_3 .

Acc. to international standards fuses can be tested for T.D.3 with melting at low voltage and switching to high voltage with the same current value I_3 . Variation in melting current seems to have little influence on the value of I_3 and arcing performance as long as the melting current ensures that the arc initiation is the same as with the I_3 as low voltage melting current.

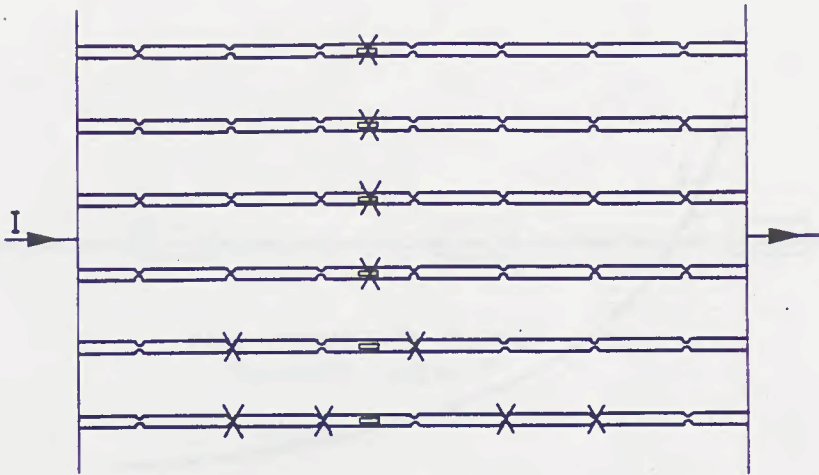
REFERENCES

1. Eriksen, Lars S e: Str mfordeling mellom parallelle smelteledere i en str mbegrensende h yspentsikring ved bryting av sm  str mmer. M.sc. thesis. Electrotechn. department, Norwegian University of Technology 1981.
1. Rosen, P.: Arcing phenomena in HRC fuses under varying test conditions.
3. Ofte, A.: Kartlegging av forhold som p virker minste brytestr m for en h yspenningsikring. M.sc. thesis. Electrotechn. department, Norwegian University of Technology 1981.
4. Ofte, A. and Rondeel, W.: The striker system in the fuse switch combination. Int. conf. on Electric Fuses and their Application. June 1984.
5. Rosen, P.: The low overcurrent breaking performance of high-voltage current-limiting fuses. Frouth international symposium on Switching arc phenomena. Lodz 81.
6. Mikulency, H.W.: Current-limiting Fuse with Full-Range Clearing Ability. IEEE Trans. on Power App. and Syst. Vol. PAS-84 No. 12 s 1107-1116. Dec. 1965.
7. Zlupko et al: Current limiting fuse with improved means for interrupting low overcurrents. US-pat. no. 4, 358,747, Nov. 9, 1982.
8. Kozacka: Ribbon-type fusible element for high-voltage fuses and fuse including the element. US-pat: 3, 743,994, July 3, 1973.
9. Oliver, R., Lakshminarasimha, C.S., Barrault, M.R.: The influence of Filler on the Properties of Arcs in Cartridge Fuselinks. Third International Symposium on Switching arc phenomenon. Lodz 77.

TYPE	Rated current	Rated voltage	Melting current	Melting time		Arcing current	Arcing time	Remarks
	I_N	U_N	I_m	t_m		I_a	t_a	
Fuselink	A	kV	A	min.	s.	A	ms	Observation
A	40	12	84	17	08	84	240	
	"	"	"	17	05	"	75	
	"	"	145		27	"	55	
	"	"	"		24	"	70	
	"	"	"		20	"	55	
	"	"	"		25	"	55	
	"	"	252		0,52	"	28	
	"	"	100	6	30	100	30	
B	40	12	120	8	49	120	60	
	"	"	145	1	12	"	110	
	"	"	"		43	"	100	
	"	"	252		0,4	"	200	
C	40	12	84	26	35	84	∞	Exploded after 220ms —— " —— 1250ms —— " —— 145ms
	"	"	"	26	00	"	∞	
	"	"	145		13	"	∞	
	"	"	252		3,7	"	105	
	"	"	102	13	30	102	40	
	"	"	145	2	54	"	70	
D	40	12	120	5	36	120	30	Reignited after 7,2 s and exploded.
	"	"	145		44	"	75	

Arcing time for different melting times
Fuselinks type A, B, C and D.

Table 1



Melting process for M-spot fuses

Figure 1

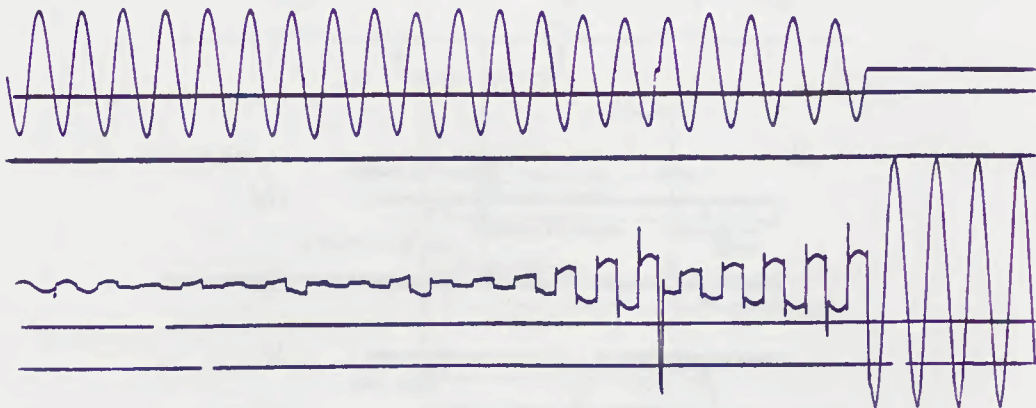
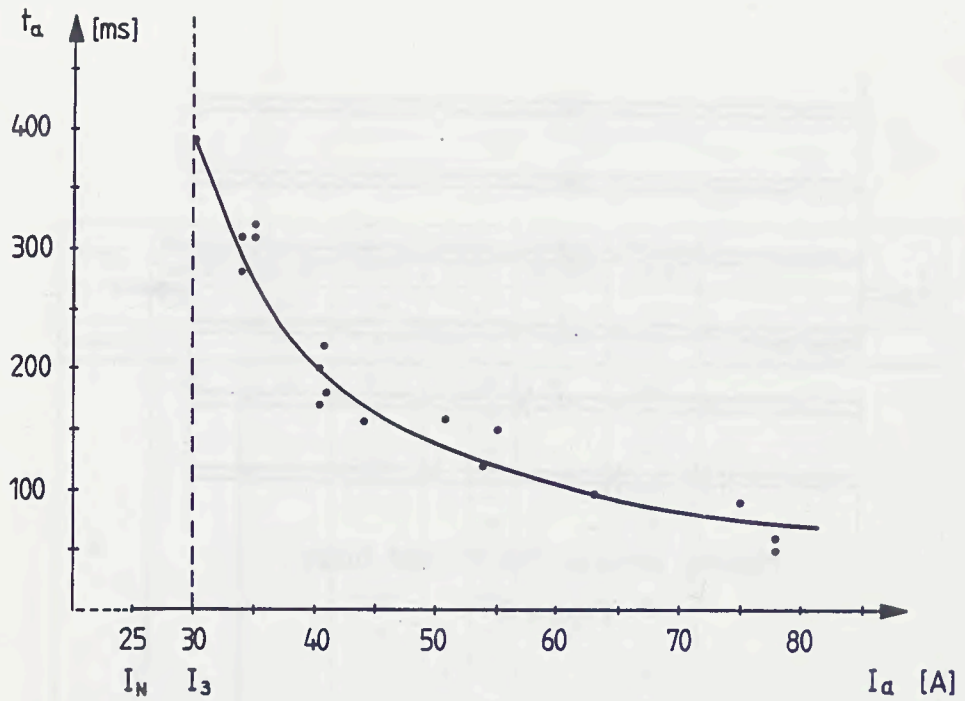
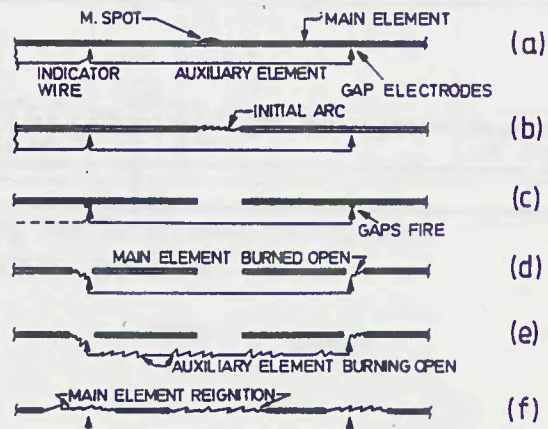


Figure 2



Example from developing tests of 17,5kV 25A fuse.

Figure 3



Sequence of operations for fuses with arc electrodes, low current interruption.

Figure 4



Fuse element with thermal
insulating beads.

Figure 5

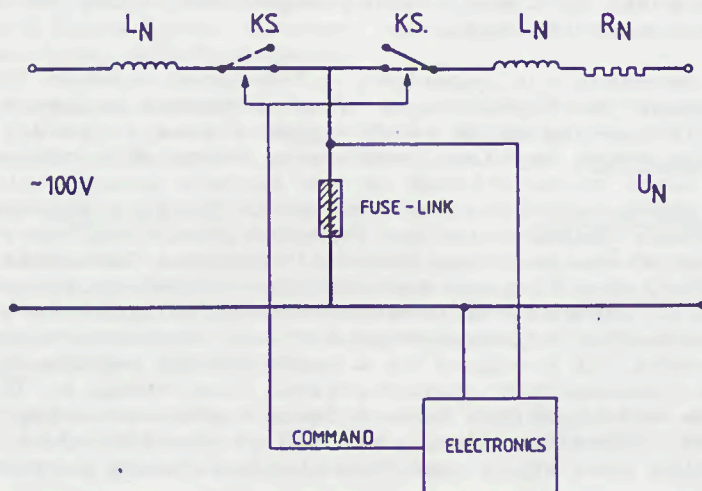


Figure 6

Special test circuit for
Test Duty 3 acc. to IEC 282-1

HARMONISATION OF IEC & UL REQUIREMENTS FOR LOW
VOLTAGE FUSES - IS IT POSSIBLE?

J. Feenan.

The recent revision of IEC.269 Part 1 contains internationally standardised time-current gates and pre-arcing I^2t limits for general purpose fuses type gG, and also requirements for fuses for motor circuits. This marks a significant advance in International standardisation and there will inevitably have to be a period of time to enable the various National fuse systems, examples of which are given in IEC.269 Parts 2a and 3a, to align with these new requirements. There is however no indication that such requirements are acceptable to U.S.A. and it is well known that the typical requirements for low voltage fuses contained in the Underwriters Laboratory Specification UL.198 differ considerably from those contained in the revised IEC.269 Part 1. There are a number of reasons for these differences, many of which stem from the requirements of the American National Electrical Code, which at present is not harmonised with the IEC Installation Rules. Nevertheless with the increasing involvement of U.S.A. in many of the low voltage product Committees, e.g. circuit breakers, contactors, switches, etc, it seems inevitable that the problem posed by the differing requirements has to be met, and some agreement reached.

This Paper compares the important differences between IEC and UL requirements for low voltage fuses, comments on the reasons why these differences exist, and suggests some lines of investigation which may lead towards an acceptable compromise.

Historical Background The fundamental difference between the IEC and UL fuse characteristics seems to stem from the requirements of the American National Electric Code which specifies that over-current devices must operate within a stated time at 135% of their rated current in order to ensure overload protection of associated cables. Fuses with such low fusing currents, if produced in a conventional manner, have a much faster time-current characteristic than those to IEC requirements and therefore have inferior motor starting capabilities. This inevitably has led to the introduction of the time-delay fuse which combines the low fusing current

TECHNICAL DIRECTOR,
GEC INSTALLATION EQUIPMENT LTD
FUSEGEAR DIVISION

required with an improved withstand capability in the region of 10 seconds. The very popular range of fuses manufactured to what is known as the 'Code' dimensions at present dominate the North American market. These dimensions, rating for rating, are considerably larger than those to the British or DIN dimensions given in IEC.269 Part 2 (FIG.1). The breaking capacity of such fuses vary according to UL classifications but the highest value is 200kA r.m.s. symmetrical at 600 volts a.c. The cut-off and I^2t limits for such fuses have varied in the past but the existing limits which are recognised as an acceptable maximum are referred to as K5 values, in other words a time-delay fuse complying with the requirements of UL.198D and classified as K5 must have total I^2t values and cut-off values not exceeding those given in Table 1.

In the early 1960's another set of dimensions was introduced into UL Specification 198C covering a range of non-time-delay fuses known as Class J whose outline dimensions are similar to the British and DIN low voltage fuse systems. (FIG.2). The main purpose of these fuses, in addition to the introduction of compact dimensions, was to introduce much lower values of cut-off and I^2t than the K5 values. The 'J' fuses have not proved to be very popular, presumably because their very fast characteristic makes them unsuitable for the protection of motor circuits. A recent modification to UL.198C provides for a time-delay type 'J' fuse whilst still requiring the same I^2t limits as the non-time-delay type but to date such fuses have not appeared in any quantity.

There is another set of cut-off and I^2t values for a class known as K1, which is intermediate between the 'J' and K5 values and these cover standard characteristics in the Code dimensions i.e. non-time-delay.

Table 1 compares the K5 and 'J' I^2t values with those of IEC.269 Part 1. One of the problems of comparison is the fact that IEC.269 Part 1 specifies limits of pre-arcing I^2t at 10 milliseconds whereas the UL Specification specifies limits of total I^2t at either 100kA or 200kA. A study of the time-current characteristics of popular American fuses, together with an assessment of designs of elements used in such fuses, indicates that the pre-arcing I^2t of the type K5 and 'J' fuses at 10 milliseconds are as shown in FIG.2. This figure also shows the limits of pre-arcing I^2t at 10 milliseconds specified in IEC.269-1.

It is evident from FIG.2 that whereas the K5 limits are of a similar order to those in IEC.269-1, the values for the 'J' type fuses are considerably lower.

Overload Protection IEC Committee TC20 has spent a considerable amount of time and effort in determining the overload withstand capability of P.V.C. insulated cables in collaboration with IEC Committee TC64. The Rule, which is now contained in IEC.364 'Electrical Installation of Buildings' states that a P.V.C. insulated cable is protected if the associated overcurrent device operates at $1.45I_z$, within a

specified time. (I_z = current rating of cable). This is based upon the assumption that on overload the total temperature which the conductor must not exceed is 120°C for a specified time. The rated current of the IEC cable is based on a maximum conductor temperature of 70°C . Therefore to provide the necessary protection to the IEC requirements, the fusing current (I_f) of the fuse must not exceed $1.45I_z$. This value takes into account the possibility of repetitive overloads in the life of the installation.

The N.E.C. requirements for cable protection are fairly comprehensive and stipulate different current ratings for conductors with different insulating coverings. Table 310-12 of the National Electrical Code gives data for P.V.C. insulated cables having a total temperature limit of 60°C . This limit is reflected in the overload requirements of UL198. Table 2 compares the time-current characteristic requirements of UL.198D with IEC.269-1.

Overload protection of cables rated for a 60°C limit in the N.E.C. Rules is the nearest installation condition to that which exists in the IEC Rules and has been used for the following comparison:-

There are two restrictions imposed by N.E.C.

- (1) The Code only recognises a 60°C temperature limit for P.V.C. insulated cables.
- (2) The protective device must operate at not more than $1.35I_z$.

There is, however, one alleviation. In the Code, Exemption 1 of Article 240-5 states that if the fuse rating does not coincide with the cable rating in a particular situation, then a fuse of the next higher current rating can be used. This infers that that factor of $1.35I_z$ can be exceeded in certain circumstances.

Figure 3 compares the IEC and N.E.C. current ratings for various sizes of P.V.C. insulated cable, together with the IEC ratings adjusted to the N.E.C. requirements of 60°C total temperature, and it shows the significant difference in the basis of rating and the overload protection requirements required between N.E.C. and I.E.C. for P.V.C. insulated cables.

Short Circuit Protection. If short circuit protection of cables is considered, then regardless of what limits are imposed for overload protection, it is reasonable to assume that the formula given in IEC.364 is equally applicable to both IEC and N.E.C. rated cables and Figure 2 compares the I^2t withstand limits of P.V.C. insulated cables with the pre-arcing I^2t values for both IEC and UL fuses. Also superimposed on this Figure are typical I^2t withstand levels of popular contactors and switches of European design.

Determination of breaking capacity. Another comparison which must be made is the method of determining the breaking capacity of fuses. In IEC.269 Part 1 for General Purpose Fuses, there are five test duties ranging from the prospective current equating to the breaking capacity of the fuse, down to $1.25I_f$. (See Table 1). The breaking capacity tests in UL.198D consist of six test duties from the breaking capacity rating of the fuse down to twice rated current (which equates to $1.5I_f$) so it is reasonable to state that the range of test currents are similar, but one noticeable difference is the fact that the power factor required for the test at twice rated current ($1.5I_f$) in UL.198D is 0.8 or less which can permit a considerably easier test duty than that specified in IEC.269 Part 1 for a similar test current (I_5) where the power factor is 0.35.

Another noticeable difference is that UL.198D does not specify any breaking capacity tests for minor ratings in a body size and does not recognise the Rules for a homogeneous series which is a significant deviation from IEC.269-1.

Fuse-switch combinations. IEC.269 Part 1 recognises fuses specifically designed for motor circuit protection (type gM and aM) and many European fuse switch arrangements permit the use of such fuses to fully utilise the capability of the switch and the fact that in such instances the fuse only provides back-up protection. For example, a fuse-switch combination of 100 amps rating can utilise a motor circuit fuse capable of withstanding the starting current of a motor whose full load current is 100 amps without the need for such a fuse to have an I_f as low as 145A ($1.45I_N$). The N.E.C. does not permit such an arrangement except in certain restricted circumstances and this is a further difficulty in trying to align UL and IEC fuse requirements.

Discussion. It is obvious from the foregoing that the difference between UL and IEC practice with regard to fuse design and application is considerable but as stated earlier in this Paper, the discussions which are now taking place in many of the Committees dealing with associated low voltage equipment, indicate that some effort must be made to find a compromise.

The areas of compromise fall into three categories, breaking capacity, overload protection and short circuit protection.

Breaking Capacity. As the two requirements are similar, apart from the issues of the test power factor for the 200% test and the absence of tests on minor ratings in UL.198D, it seems reasonable for UL to accept the IEC Rules particularly the reduction of the power factor to 0.35 in the test at $1.5I_f$ because this reflects the power factor of a stalled motor and as the time delay fuses are specifically designed for motor circuits, it is logical that this alignment is made. It is also significant that in the recent amendment to 198C it is required, for type 'J' fuses, that all of the ratings in each body size must be tested at 100kA to establish the value of total I^2t let-through.

Overload Protection. The obvious solution to this problem would be if N.E.C. recognised the IEC requirements for the overload protection of P.V.C. insulated cables but this is a major change which may not be possible to achieve. Nevertheless, the fact that the National Electrical Code permits a fuse of the next size up to the cable rating in certain instances, shows that there is some flexibility permitted. A simple step would be to agree that fuses to IEC.269 Part 1 could be applied to the existing N.E.C. Rules provided the current rating of the fuse did not exceed 90% of the current rating of the cable in the N.E.C. Tables. This ratio takes account of the fact that the IEC fuse rating must comply not only with an I_f value not exceeding $1.6I_n$ but must also comply with the conventional cable overload test given in IEC.269 Part 1.

Short Circuit Protection A study of Figure 2 shows that the K5 values, which are in popular use in U.S.A. compare very favourably with those of the IEC values for pre-arcing I^2t at 10 milliseconds but the 'J' values are substantially lower. Figure 2 also shows that the IEC and K5 values give adequate short-circuit protection to P.V.C. insulated cables and also appear to give adequate protection to associated equipment such as contactors and switches.

This is probably the area which requires the greatest investigation. The low values specified for the type 'J' fuses would suggest that the associated devices which this type of fuse must protect in U.S.A. are much more sensitive to short circuit let-through than their European counterparts. This is not borne out by experience and there must be some other explanation which is not obvious from an examination of the basic equipment.

If the K5 limits have given satisfactory protection over many years, then one must query the basis for the type 'J' fuse limits particularly when such fuses (except those which claim compliance with the recently introduced time-delay requirements in UL.198C) have a much inferior performance when used for motor circuit protection. It is in all probability this fact which has stifled the use of the 'J' range fuse in U.S.A. up to the present time when it has the obvious advantage of compact dimensions. It is significant that in the draft Canadian Standard for Low Voltage Fuses, there is a proposition to include requirements for time-delay type 'J' fuses, but at the present time, the cut-off and I^2t limits for such fuses are not finalised. It is also of significance that type 'J' dimensioned fuses with cut-off and I^2t values greater than the UL limits for type 'J' have been used in Canada for at least 25 years for the protection of equipment manufactured in U.S.A., without any service problems whatsoever. It is obvious from the foregoing that the basis for these low I^2t values for the type 'K' fuse must be critically reviewed.

Standard time-current gates A comparison of the time-current characteristics of popular American fuses show that although all characteristics would readily fall within the IEC limits of $1.25I_f$ and $1.6I_f$, problems occur at the other gates. If the $K5^{nf}$ values are considered, it would appear that there is a distinct possibility that they could fall within the IEC limits for pre-arcing I^2t at 10 milliseconds and this also suggests the possibility for a non-time-delay fuse to comply with the IEC gates at 0.1 seconds and also the 10 second minimum and 5 second maximum gates. A problem would undoubtedly arise when considering the time delay characteristic which, whilst meeting the 10 millisecond pre-arcing I^2t limits and possibly the 0.1 second minimum and maximum gates, would not comply with the 5 second maximum-10 second minimum gates for general purpose fuses. There is however a distinct possibility that the time-delay fuse could be classified in a similar manner to a gM fuse by relating its short-time time current characteristic, (less than 30 seconds) to a fuse of a higher standard current rating. (See FIG.4.). More accurate information on the time-current characteristics of the popular types of American fuses would be necessary in order to verify this proposal as a possibility.

Conclusion The main objective of this Paper is to outline the difference which exist at present between UL and IEC with regard to Low Voltage Fuse Specifications, and to give some of the reasons for this situation. The proposals for a possible compromise are given primarily to initiate discussion on this subject because sooner or later this problem must be faced if we are to have truly International Rules for low voltage fuses and this particular forum seems an ideal starting point.

TABLE 1.

COMPARISON OF BREAKING CAPACITY REQUIREMENTS.

IEC.269-1		UL198D		
TEST AT 110% RATED VOLTAGE I ₁ : 3 tests at 0.1-0.2 PF I ₂ : 3 tests at 0.1-0.2 PF I ₃ (3.2I _f): 1 test at 0.3-0.5 PF I ₄ (2.0I _f): 1 test at 0.3-0.5 PF I ₅ (1.25I _f): 1 test at 0.3-0.5 PF Pre-Arcing I ² t at 0.01 seconds		TEST AT RATED VOLTAGE I ₁ : 1 test at max 0.2 PF I ₂ : 1 test at max 0.2 PF 50kA : 1 test at max 0.2 PF 25kA : 1 test at max 0.2 PF 10kA : 1 test at max 0.5 PF 2I _n : 1 test at max 0.8 PF Total operating I ² t specified for I ₁ (100kA or 200kA RMS Symm).		
Fuse Rating	P.A. I ² t kA ² secs.	Fuse Rating	Total I ² t Class K5 kA ² secs	Total I ² t Class J KA ² secs
32A	5	30A	50	7
63A	27	60A	200	30
100A	86	100A	500	80
200A	400	200A	1600	300
400A	2250	400A	5000	1100
630A	7500	600A	10000	2500
Minor Ratings in Body Size : which for a homogeneous series I ₁ : 3 tests		Minor Ratings in Body Size No tests required in UL198D		

TABLE 2.

COMPARISON OF OVERLOAD CHARACTERISTIC REQUIREMENTS

IEC.269-1	UL198D AND C. CLASS K AND J FUSES														
$I_{N.F} \geq 1.25I_N$	$I_{N.F} \geq 1.1I_N$														
$I_F \leq 1.6I_N$	$I_F \leq 1.35I_N$														
I (10 SECS) : Withstand for 10 seconds specified currents from 2.3 to $3.6I_N$ (Refer NOTE 1)	I (10 SECS): TIME DELAY ONLY - withstand $5I_N$ for 10 secs														
I (5 SECS): Operate in 5 seconds with specified currents from 4.7 to $8.1I_N$ (Refer NOTE 2)	Operate at $2I_N$ in specified time <table border="1" data-bbox="729 962 1074 1212"> <thead> <tr> <th>Fuse Rating</th> <th>Time</th> </tr> </thead> <tbody> <tr> <td>30A</td> <td>2 Minutes</td> </tr> <tr> <td>60A</td> <td>4 "</td> </tr> <tr> <td>100A</td> <td>6 "</td> </tr> <tr> <td>200A</td> <td>8 "</td> </tr> <tr> <td>400A</td> <td>10 "</td> </tr> <tr> <td>600A</td> <td>12 "</td> </tr> </tbody> </table>	Fuse Rating	Time	30A	2 Minutes	60A	4 "	100A	6 "	200A	8 "	400A	10 "	600A	12 "
Fuse Rating	Time														
30A	2 Minutes														
60A	4 "														
100A	6 "														
200A	8 "														
400A	10 "														
600A	12 "														

NOTE 1 : IEC 10 second Current Limits (minimum)

Fuse Rating	Min I (10 Secs)
32A	75 amps
63A	160 "
100A	290 "
200A	610 "
400A	1420 "
630A	2200 "

NOTE 2 : IEC 5 second Current Limits (maximum)

Fuse Rating	Max I (5 secs)
32A	150 amps
63A	320 "
100A	580 "
400A	2840 "
630A	5100 "

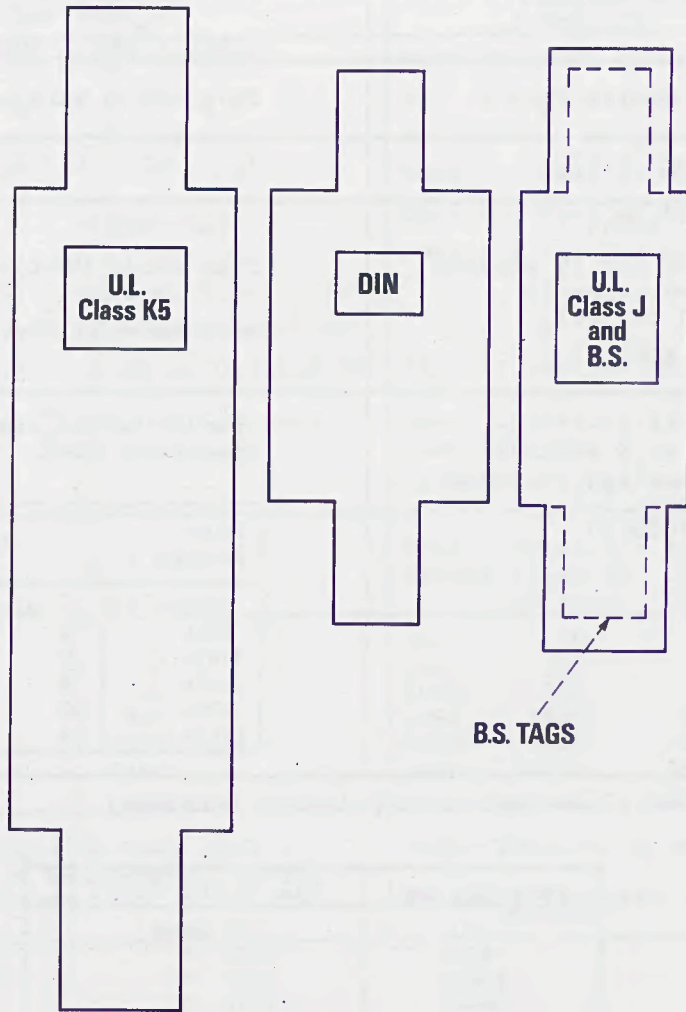
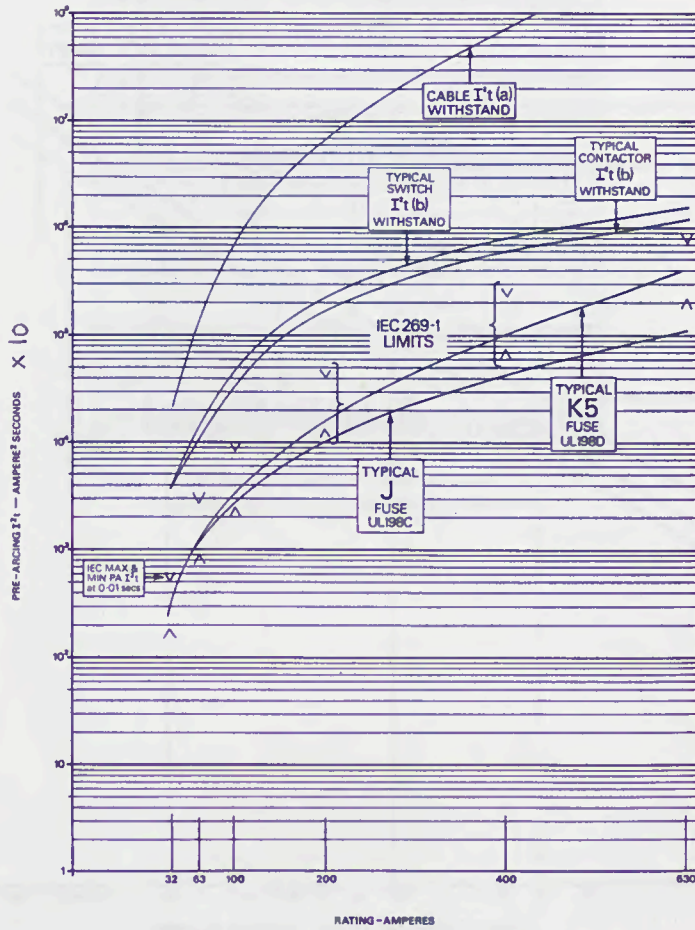


FIG.1 COMPARISON OF DIMENSIONS OF 200A FUSES

FIG.2: Comparison of I^2t withstand values of (a) PVC Insulated Cables
 (b) Typical Switches and Contactors with prearcing
 I^2t of Fuses to IEC 269-1 and UL198D



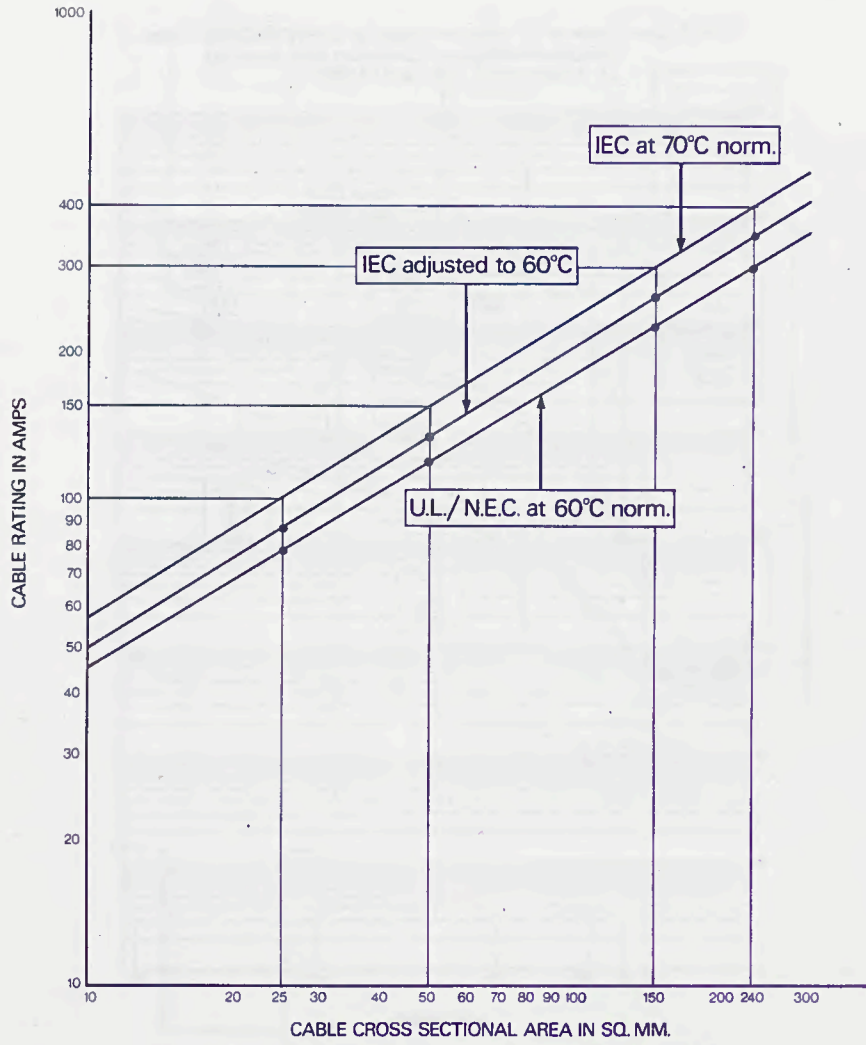


FIG.3: Comparison of IEC & NEC Current Ratings for PVC. Insulated Cables

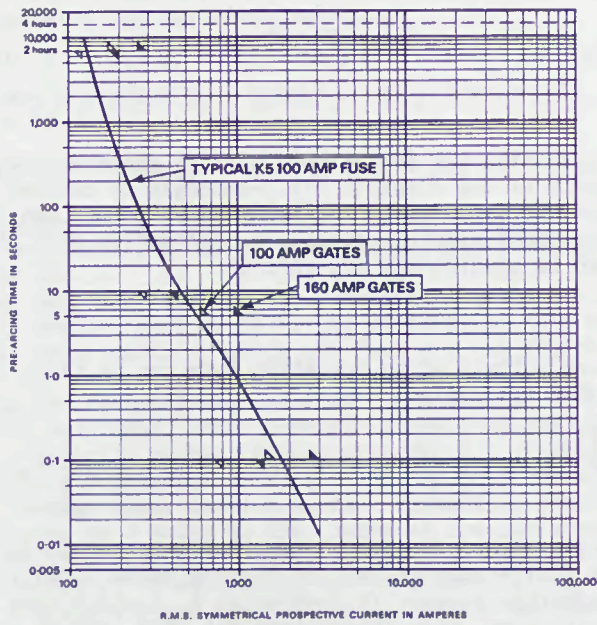


Fig. 4 COMPARISON OF TYPICAL K5 100 AMP CHARACTERISTIC WITH IEC289 GATES FOR 100 AMP AND 160 AMP FUSES

THE ARCING VOLTAGE IN HIGH VOLTAGE FUSES

J.E. Daalder

Abstract.

Prime parameters governing the arc voltage of fuse elements are investigated. The dependency of the electric field-strength on current is analysed and checked by experiment. The arc channel growth was observed from fulgurite structures. These results, in combination with data on burn-back were used to predict the arc voltage.

INTRODUCTION.

In principle the arc voltage of an operating fuse can be calculated by (neglecting electrode effects):

$$U_{\text{arc}} = \int_0^{\ell} E \, dx = \int_0^{\ell} \frac{\rho I}{A} \, dx. \quad \text{Here } \ell \text{ is the arc length,}$$

ρ the specific resistance of the arc plasma, A the arc cross-section, and E and I the column field-strength and the current respectively. The solution of this equation however is complex as ℓ , ρ and A vary with current, position and time. Also the current may vary from kA to zero in a few msec.

In this report we describe some theoretical and experimental results on these main parameters which control the arc voltage. Arc lengthening by burn-back and arc expansion by volume increase due to melting of silica have been investigated together with the dependency of the field-strength of the arc plasma on current. These results were combined and used to calculate the arc voltage for specific conditions.

THE ARC MODEL.

Wheeler [1] and Gnanalingam [2] developed one-dimensional and stationary models of fully ionized arcs. They calculated the field-strength E starting from a simple energy balance where Joule heating is solely balanced by thermal conduction. In a one dimensional approximation (see fig. 1; $D \ll b$) the power balance can then be written as:

$$\frac{d}{dy} \left(\lambda \frac{dT}{dy} \right) = -GE^2, \quad \text{where } \lambda \text{ is the thermal conductivity,} \quad (1)$$

J.E. Daalder is with the Department of Electrical Engineering, Eindhoven University of Technology, P.O. Box 513, 5600 MB Eindhoven, Netherlands.

G the electrical conductivity and T the temperature. Spitzer's [3] relations for electrical and thermal conductivity of an ionized plasma are used, together with the boundary conditions:

($x=0$; $\frac{dT}{dx}=0$; $x=\pm 0,5 D$; $T=0$). The power balance can be solved semi-numerically and analogous to a method used by Wheeler [1]. The result is [2, 4]:

$$E = 3,4 \cdot 10^{-2} [Z \ln \Lambda]^{0,4} I^{0,4} b^{-0,4} D^{-1} [V m^{-1}] \quad (2)$$

Z is the ion charge and Λ the Coulomb cut-off. Dependant upon the plasma temperature and density Z may range between 1 and 4 whereas $\ln \Lambda$ may vary between 5 and 10.

Eq. (2) shows that provided the arc dimensions remain the same the field-strength E is proportional to $I^{0,4}$. The validity of this result was investigated by experiment, in which the fuse arc was short-circuited [4].

Copper strips (cross-section $5 \times 0,2 \text{ mm}^2$) are mounted in a cartridge which is filled with pure sand. After compacting the sand the cartridge is placed in a critically damped LRC-circuit (fig. 2). Initially current is flowing through a breaker in parallel with the fuse element. Near current maximum the breaker opens and the current commutates into the fuse element. The arc initiates at a notch in the centre of the strip and arcing occurs during some milliseconds at a nearly constant current (variation less than 5%). Current is again commutated by firing a parallel thyristor and the decrease of arc current and arc voltage is registered simultaneously by a computer system. The time the current needs for commutation is varied by the series inductance L_c . Its value is chosen such that the commutation time (t_{com} in fig. 2) is significantly longer than the arc time constant which may range from several microseconds up to tens of microseconds [5]. Too long commutation times are prohibited by the demand that the arc channel dimensions shall not change during current decay. (The assumption is made that the lumen dimensions are identical with the arc channel dimensions, at least for not too low currents).

Fig. 3 shows an oscillogram of fuse current and arc voltage in the commutation phase. The voltage-current characteristic obtained is plotted on a logarithmic scale. The curve is very similar to the quasi-static characteristic measured by Maecker [6] for wall-stabilized arcs. For low currents the arc voltage is independant of current [7]. In case of $I > 200 \text{ A}$ the characteristic closely follows a relation $U_{arc} \sim I^{0,4}$ as predicted by eq. 2. In a series of 15 experiments the current prior to commutation was varied in the range 800 - 2200 A, and the value of β in $V \sim I^\beta$ was determined. An average value of $\beta = 0,41$ was found [4] which agrees well with the theoretical result. It was proven that β did not depend on the commutation time provided its value was not less than approx. 60 μsec . For lower values deviations from the static characteristic were observed.

THE ARC CHANNEL EXPANSION.

Due to the transfer of arc energy to the surrounding sand melting and evaporation of silica will occur. By the melting process an increase in space occurs as the molten quartz will occupy only a part of the original sand volume. Due to the arc pressure the molten silica will (partly) be pressed into the voids of the solid sand leading to a further increase of

the lumen area. Expansion of the arc is thus possible and will lead to a decrease of the arc voltage.

Using a one-dimensional approach the increase of the thickness D (fig. 1) was calculated on the basis of an energy balance [4]. Under the assumption that the arc energy is transferred exclusively in the $+y$ direction and is used for the heating and melting of silica it was found that (for a constant current):

$$D = \sqrt{(D_0')^2 + B t} \quad (3)$$

Here D_0' is the initial thickness of the arc channel at the onset of arcing and B a parameter whose value depends on the current and the properties of the silica and the arc discharge. (B has the dimension of the diffusion coefficient). The parabolic dependency of the thickness on time was investigated by experiment.

Copper strips ($5 \times 0,1 \text{ mm}^2$; $5 \times 0,2 \text{ mm}^2$) were arced at constant current in the range of 300-2600 A. Arcing was initiated at a notch in the centre of the strip. Each fulgurite was cut at several places and from each cross-section the lumen dimensions were measured by microscope. The width D (fig. 1) showed a small increase (less than 20%) in comparison with the increase in thickness (up to ten times) and justified therefore a one-dimensional approach.

In order to check eq. 3 D^2 was plotted as a function of the distance x from the fulgurite ends (see fig. 4). Because the burn-back rate V_f in each experiment is known the x -axis can be transformed into a time axis by $t = xV_f^{-1}$. The underlying supposition of this transformation is that the local channel growth at a specific cross-section is entirely decided by the energy flow in that cross-section (no axial dependency). Probe experiments showed that this supposition is justified [4]. As a result the variation D with position is transformed to a *local* variation of D with time. 17 Fulgurites were investigated in this manner. Although the data points showed a certain scatter and deviations occurred for longer arcing times a fair linear relation between D^2 and t was found for all currents investigated. On the average no differences were found between the channel growth on cathode- or anode side. The value of B in eq. 3 could be established and proved to be:

$$B = 1,23 \cdot 10^{-8} I^{1,4} (\text{m}^2 \text{sec}^{-1}) \quad (4)$$

It was not possible to establish the initial value D_0' by experiment. Generally it will have an average value larger than the width of the fuse element due to the voids present between the sand grains and the fuse element [4].

THE BURN-BACK RATE.

Erosion of the fuse element by the arc footpoints leads to an increase in arc length and a rise in the arc voltage. Generally the rate of arc length increase is a factor ten higher than the rate of increase of the arc cross-section. As a consequence (cf eq. 2) the increase of the arc voltage by burn-back is significantly higher than the decrease of the arc voltage by channel expansion.

Experimental and theoretical results on the burn-back rate of silver and copper elements have been reported elsewhere [8]. We have found that in

case of moderately high current densities and not too long arcing times the burn-back rate V_f is given by $V_f = cJ$ (msec^{-1}) (5)

Here J is the current density in the fuse element and c is a material constant which has a value of $1,06 \cdot 10^{-9}$ (m^3C^{-1}) for copper elements and $1,03 \cdot 10^{-9}$ ($\text{m}^3 \cdot \text{s}^{-1}$) for silver. For high current densities and for long arcing times preheating of the fuse element occurs and this increases the burn-back rate value [8].

In recent experiments silver elements were deposited on quartz glass as a carrier and enclosed in compacted sand. The burn-back rate was measured for different values of the thickness of the element. For a value larger than $50 \mu\text{m}$ results were the same as found for elements entirely enclosed in sand. However for a thickness of $15 \mu\text{m}$ the burn-back rate decreased by a factor two i.e. the value was $c = 0,5 \cdot 10^{-9}$ (m^3C^{-1}). Analysis showed that the decrease of the burn-back rate was not due to the presence of the quartz carrier but most likely is caused by a restricted energy transfer from the anode/cathode fall regions to the very thin fuse element. It seems therefore that eq. 5 is only valid provided its thickness is larger than $50 \mu\text{m}$; for lower values the constant c depends on the size of the element.

THE ARC VOLTAGE.

Combination of the data on arc plasma, arc channel expansion and arc elongation gives the possibility to calculate the arc voltage. A series of experiments were done [4] in which the arc voltage of Cu fuse elements ($5 \times 0,1 \text{ mm}^2$; $5 \times 0,2 \text{ mm}^2$) were registered as a function of time. The elements had a single notch. Current was kept constant during arcing. During the entire observation time burn-back of the element occurred. The current density in the experiment was varied between $0,7 \cdot 10^9 - 3,8 \cdot 10^9 \text{ Am}^{-2}$.

Using the equations mentioned in this report one can calculate the arc voltage as a function of time in case of constant current. The result is:

$$U_{th} = 0.068 [Z \ln \Lambda]^{0,4} I^{0,4} D_0' V_f b^{-0,4} B^{-1} [\sqrt{1 + B(D_0')^2 t} - 1]$$

In order to compare theoretical and experimental values we used the function $R = U_{th} \cdot U_{exp}^{-1}$. A value of $Z \ln \Lambda = 3,56$ was taken as derived from the work of Chikata *et al* [9].

Fig. 5 shows some results. For current densities less than $2 \cdot 10^9 \text{ Am}^{-2}$ the results are quite satisfactory as they lay close to an average value R . For higher current densities deviations occur. Analysis showed that they are mainly due to preheating of the fuse element which leads to higher burn-back rates. If this effect, which was not included in the calculations, is taken into account, the agreement will be improved.

The average value of R for 17 measurements was $R = 0,62$ (instead of 1). This difference is probably due to a too low value of $Z \ln \Lambda$. In case of $Z \ln \Lambda = 11,5$ an optimum agreement is found. This value is also more in accordance with Maecker's experiments on wall stabilized arcs. Another unsure parameter is the initial thickness of the arc D_0' . The value was estimated [4] from the space available between the sand grains and may have been taken too low.

CONCLUSIONS.

We have found expressions for the burn-back rate of fuse elements, the arc expansion in the fulgurite and the dependency of the electric field strength on current. Combination of these effects make it possible to calculate the arc voltage.

REFERENCES.

- [1] Wheeler, C.B. (1970), J.Phys.D. Appl.Phys.; 3, 1374-130.
- [2] Gnanalingam, S. (1979). Thesis, Liverpool Polytechnic, Liverpool U.K.
- [3] Spitzer, L. (1956). Physics of fully ionized gases, Interscience Publishers, N.Y.
- [4] Daalder, J.E.; Schreurs, E.F.(1983). Arcing Phenomena in High voltage Fuses. EUT Report 83-E-137, Eindhoven University of Technology, Netherlands.
- [5] Frind, G. (1956). Trans. Power App. Syst. PAS-84, 1125-1131.
- [6] Maecker, H. (1960). Z.f. Physik, 158, 392-404.
- [7] Edels, H.; Fenlon, F.H. (1965); Brit. J.Appl.Phys., 16, 219-230.
- [8] Daalder, J.E.; Hartings, R.M. (1981). 4 Symp. Switching Arc Phenomena, Prt II, 158-164. Lodz, Poland.
- [9] Chikata, T.; Ueda, Y.; Murai, Y.; Miyamota, T. (1976). Int.Conf. on Electric Fuses and their applications, Liverpool, U.K., 114-121.

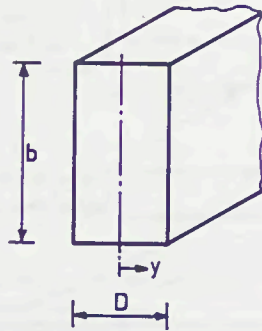


Fig. 1 Dimensions of the rectangular arc.

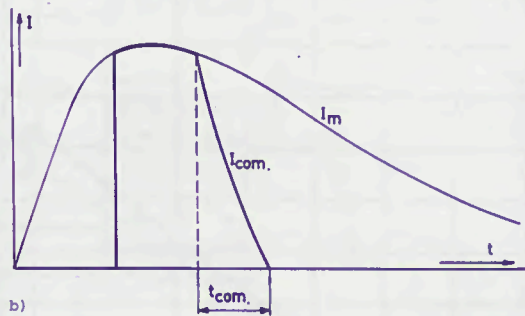
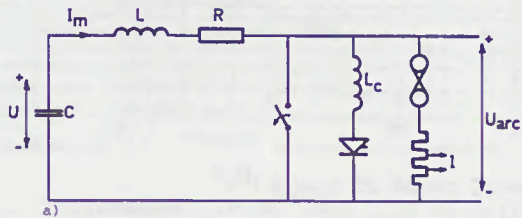


Fig. 2 a) Experimental circuit $R = 4,4 \text{ } \Omega$; $L = 45 \text{ mH}$,
 $C = 6,8 \text{ nF}$; $U = 0 - 15 \text{ kV}$; $L_c = 10 - 200 \text{ } \mu\text{H}$.
 b) Current flow: I_m through the main circuit
 I_{com} through the fuse.

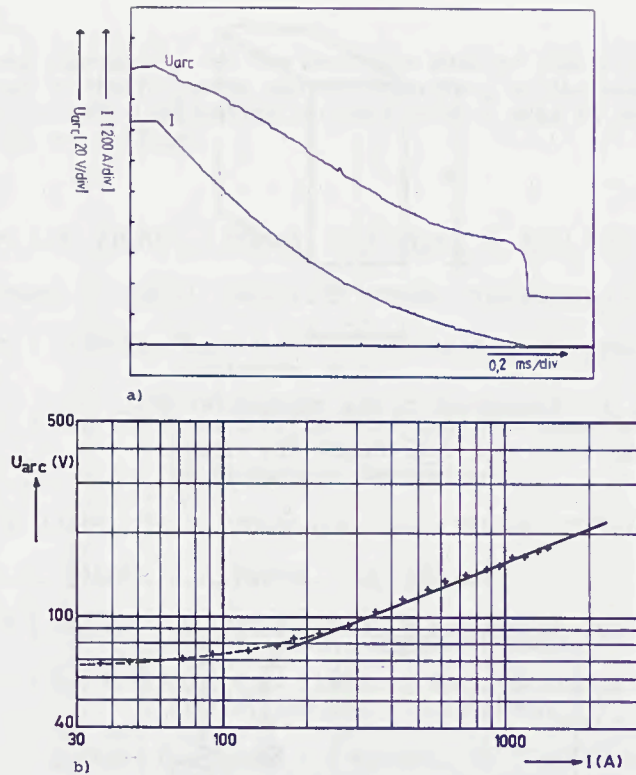


Fig. 3 Experimental proof of $U_{arc} \sim I^{0.4}$
 a) variation of U_{arc} and I during commutation
 b) $U_{arc} - I$ characteristic derived from a).

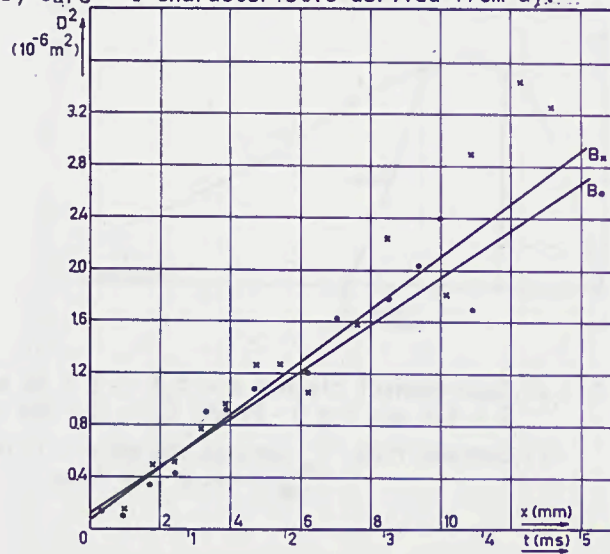


Fig. 4 Increase in channel thickness for copper $5 \times 0.2 \text{ mm}^2$
 $I = 2420 \text{ A}$ (.) anode side; (x) cathode side.

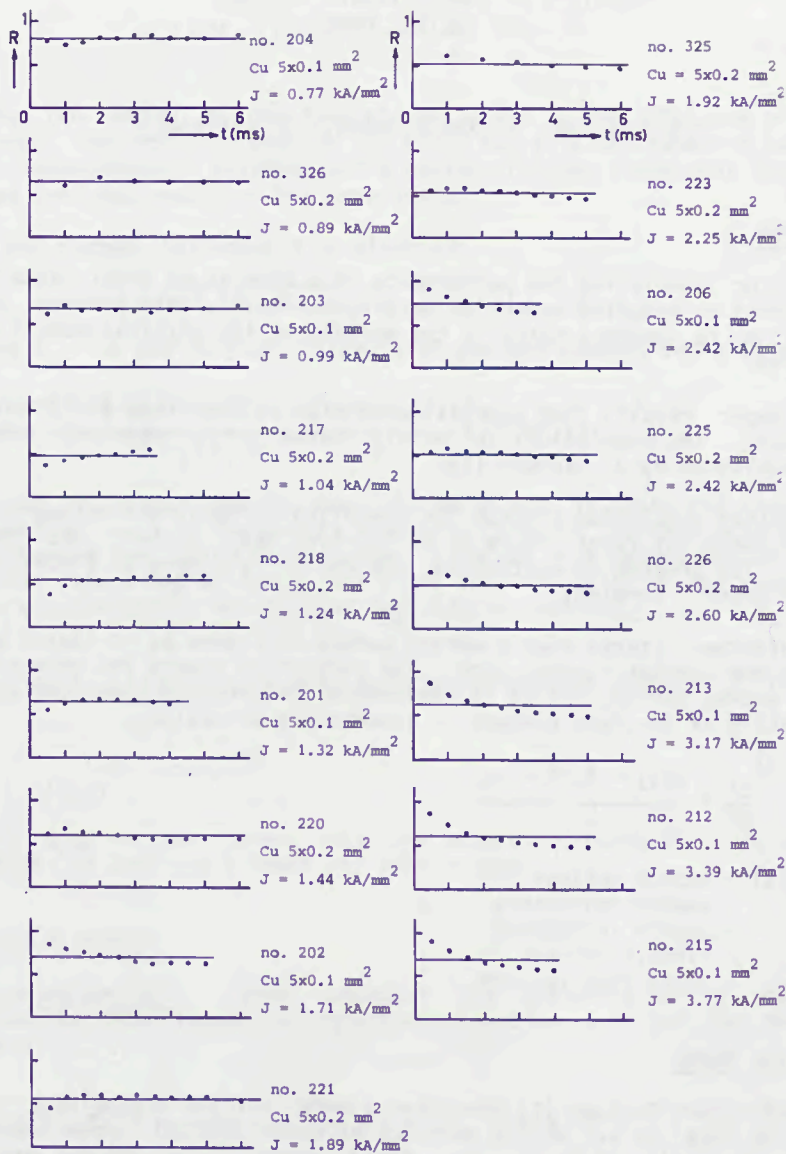


Fig. 5 Comparison of measured and calculated values of the arc voltages in different trials.

$$R = U_{th} \cdot U_{exp}^{-1}$$

SIMULATION OF SHORT CIRCUIT TESTING
OF HIGH VOLTAGE FUSES

P.O. Leistad, H. Kongsjorden, J. Kulsetås.

INTRODUCTION

A method for simulating the performance of a fuse is of great value to fuse designers by reducing expensive development tests. At present the main problem to achieve this, is the quality of the physical models of fuse behavior.

In this paper results from simulation of high voltage fuse performance are discussed. The simulation is mainly based on a physical model recently published by J. Daalder [1].

An interactive simulation program for computing current, arc voltage and arc energy input for fuses tested in an IEC-type test circuit has been developed. The program is written in FORTRAN 77 and runs on a minicomputer with graphic terminal.

The computations starts when a making switch S, figure 1, is closed and stops when the current reaches zero. The simulation covers the prearcing and the arcing period, and it is applicable for currents where the prearcing heating of the fuse element is essentially adiabatic.

$$\frac{di}{dt} = \frac{u(t) - R \cdot i - u_F}{L} \quad (1.1)$$

where: $u(t)$ - source voltage
 R - source resistance
 L - source inductance
 i - circuit current
 u_F - total fuse voltage

PHYSICAL ARC MODEL

In a recent report Daalder [1] describes a model for the arc voltage in a high voltage fuse. An arc with a rectangular cross section is considered. Based on Wheeler's [2] theory the field strength in the arc can be written:

P.O. Leistad and H.Kongsjorden are with The University of Trondheim, Norwegian Institute of Technology, Department of Electrical Engineering, Trondheim, Norway
 J.Kulsetås is with The Norwegian Research Institute of Electricity supply, Trondheim, Norway

$$E = 0.034 \cdot (Z \ln \Lambda)^{0.4} \frac{i^{0.4}}{b^{0.4} \cdot D} \quad (2.1)$$

b is the width of the fuse element and D is the thickness of the arc channel. According to Wheeler [2] $Z \ln \Lambda$ has a value between 5 and 10 for most experimental plasmas, while Daalder [1] has found that $Z \ln \Lambda = 11.5$ gives the best result in his experiments.

The arc channel thickness D is given by:

$$D = \sqrt{(D_0')^2 + B \cdot t} \quad (2.2)$$

where D_0' is the initial thickness of the arc channel and B is given by:

$$B = \frac{0.034 \cdot [Z \ln \Lambda]^{0.4} \cdot \gamma \cdot (1 - \rho_s / \rho_l)}{b^{1.4} \cdot H} \cdot i^{1.4} \text{ [m}^2/\text{s]} \quad (2.3)$$

ρ_s and ρ_l is the specific mass of quartz sand in solid and liquid state respectively. H is the energy necessary to raise the temperature in the sand beyond the fusion temperature. A factor γ is introduced to describe to what extent the molten silica flows into the voids of the sand. It has been experimentally established that H/γ is constant.

The single side burn back rate for a given current density, j , is:

$$v = \frac{j \cdot U_{\text{con}}}{H} \quad (2.4)$$

where U_{con} is the power loss per ampere arc-current. H is the total enthalpy of the fuse element per unit volume.

NUMERICAL MODEL

Prearcing period. When computing the prearcing current the voltage across the fuse element is neglected. Equation (1.1) can then easily be solved:

$$i(t) = \frac{u(t)}{|Z|} (\sin(\omega t + \omega t_1 - \varphi) - \sin(\omega t_1 - \varphi) \cdot e^{-t/\tau}) \quad (3.1)$$

where: $\varphi = \arctan \frac{\omega L}{R}$

$$\tau = L/R$$

$$Z^2 = R^2 + (\omega L)^2$$

t_1 = time corresponding to making angle

ω - angular frequency

It is assumed that the parallel fuse elements share the circuit current equally, and that all the notches disintegrates simultaneously. The

moment of arc initiation is found by solving the equation for the melting integral.

Arcing period. After arc initiation equation (1.1) cannot be solved analytically. A second order Runge-Kutta method is used to solve the equation. The current is then given by:

$$i_{n+1} = i_n + (K1 + K2)/2 \quad (3.2)$$

where K1 and K2 are the Runge-Kutta parameters.

The total fuse voltage, u_F , is computed in a separate program unit.

The burn-back rate is given by equation (2.4), and the length of a single arc can then be found:

$$l_{n+1} = l_n + v \cdot \Delta t \cdot 2 \quad (3.3)$$

The channel thickness, $D_{x,n+1}$, in position x , figure 2, is given by:

$$D_{x,n+1}^2 = D_{x,n}^2 + B \cdot \Delta t \quad (3.4)$$

$D_{x,n+1}$ must be computed for all positions x along the channel. Figure 2 shows the asymmetric part of the arc channel in the way it is represented in the simulation.

u_F is given by equation (3.5) when l_{n+1} and $D_{x,n+1}$ is known:

$$u_F = m \cdot \sum_{x=1}^k 0.034 \cdot [Zln\Delta]^{0.4} \frac{(i_n/p)^{0.4}}{D_{x,n+1}} \cdot \Delta x \cdot 2 + m \cdot 15 \quad (3.5)$$

where: $2k = l_{n+1}/\Delta x$ is an integer, p is the number of parallel conductors in the fuse, m is the number of notches.

The last term in equation (3.5), representing the electrode voltage fall, is reduced to 2-15 when the burn back is completed.

COMPUTER PROGRAM

The program is interactive and it is easy for the user to make changes in the input data. The following data can be specified by the user:

- Physical data of the fuse element
- Quartz average grain size
- Physical data for quartz sand
- Model parameters ($Zln\Delta$, H/γ)
- Prospective current

- $\cos\phi$ for the test circuit
- Making angle
- Time step (Δt)

The parameters R and L in the test circuit will automatically be calculated when prospective current and $\cos\phi$ has been specified.

Current and arc voltage is presented as curves on a graphic monitor. Curves from the last simulation is stored on a file, so that results from different simulations can be compared. The program also computes the total energy input into the fuse, maximum arc voltage, prearcing time and arcing time.

RESULTS

Data for 12 kV/40 A -and 36 kV/40 A -fuses have been used as input in the program for computation of current and arc voltage. The computed curves are compared with oscillograms from I1 and I2 certification tests for these fuses. The oscillograms, which are fed into the computer with relatively rough resolution, are referred to as "test curves".

Figure 3 and 4 show computed currents and arc voltages compared with the test curves using the values for D_0' and B purposed by Daalder [1]. The source voltage is included in fig. 4 a). There is a considerable discrepancy between the two sets of curves. It is evident that the simulation model gives too high values for initial arc voltage, and too low values for the maximum arc voltage. The discrepancies in arc voltage leads to a profound difference between simulated and measured currents.

The weaker points of the simulation model are supposed to be the estimates of B and D_0' , as these parameters are based on empirical results and, to some extent, relatively rough physical models. For these reasons the effects of varying B and D_0' are studied (fig. 5 and 6).

The quartz grain size, and thus D_0' , effects the initial arc channel thickness. An increase in B has the desirable effect of reducing the initial arc voltage, but a large B leads to a slower arc voltage raise and a reduced maximum voltage. The latter effects tends to increase the difference between the simulation model and the real fuses.

The discrepancies between the calculated curves and the test curves can be greatly reduced by altering the values of B and D_0' as compared to those purposed by Daalder [1]. Figure 7 and 8 show results from simulation with adjusted values. It should be pointed out that these values of B and D_0' improves the results both for I1 and I2 test simulation.

There is no strong evidence, neither theoretical, nor experimental that the parameters D_0' and B really are constants during the entire arcing period.

An improved conformity between calculated and measured currents and voltages could be obtained by making D_0' and B slightly time dependant functions.

It seems likely that D_0' is larger during the disintegration of the notches than it is during the burn-back period. The expansion rate of the channel possibly decreases as the channel grows. This would imply that B are gradually reduced during the arcing period.

These changes in the simulation model would cause a lower initial arc voltage, a steeper voltage curve in the arcing period before the maximum value is reached, and a reduced rate of voltage decrease in the last part of the arcing period.

CONCLUSIONS

A simulation model describing the behaviour of high voltage fuses during the breaking period based on presently available physical models of arcs in quartz sand has been made.

There is a reasonable conformity between the experimental and the calculated curves when the parameters for the initial arc channel thickness and the arc channel expansion rate are adjusted. The experience with the model is, at present, not sufficiently extensive to evaluate the usefulness of the simulation model for fuse designers.

The simulation results indicate that the proposed constants in the expression for the arc channel expansion rate and initial thickness may be dependant on time.

REFERENCES

- [1] Daalder, J.E.; Schreurs, E.F.(1983). Arcing Phenomena in High Voltage Fuses. EUT report 83-E-137, Eindhoven University of Technology.
- [2] Wheeler, C.B. (1970), J.Phys.D. Appl.Phys.; 3, 1374-1380, Part. 1.
- [3] Gnanalingham, S. and Wilkins, R. (1980), IEE Proc.,127,434-440.

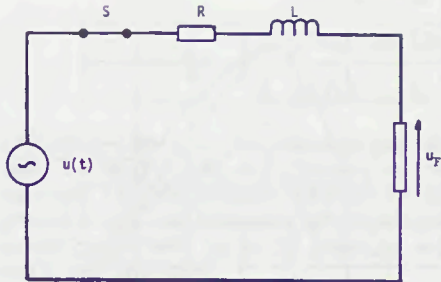


Fig. 1. Test circuit

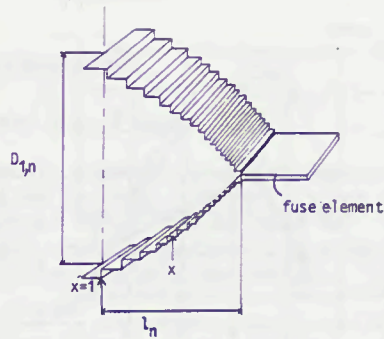


Fig. 2. "Numeric" arc channel.

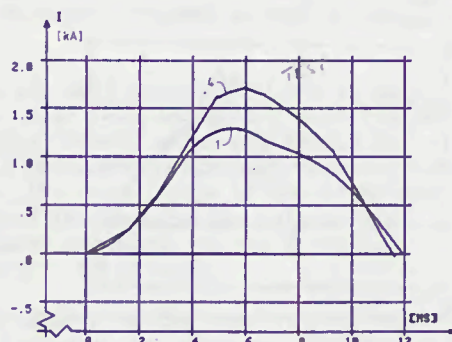
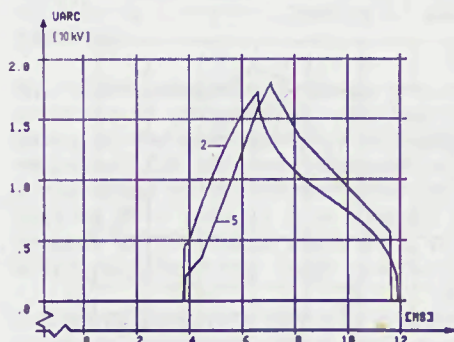


Fig. 3. 12 kV/40 A. I2-test. $B=3,25 \cdot 10^{-8} \cdot i^{1,4} \text{ m}^2/\text{s}$, $D_0^1=0,14 \text{ mm}$
 a) Arc voltage. (2) Computed curve, (5) Test curve
 b) Current. (1) Computed curve, (4) Test curve.

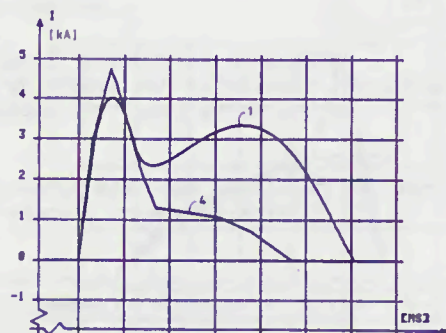
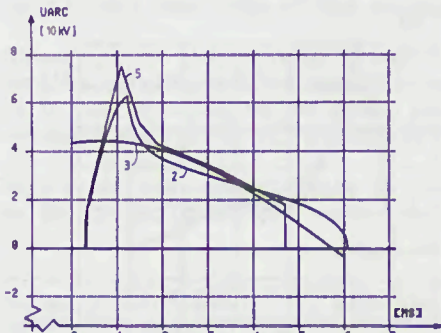


Fig. 4. 36 kV/40 A. I1-test. $B=3,25 \cdot 10^{-8} \cdot i^{1,4} \text{ m}^2/\text{s}$, $D_0^1=0,14 \text{ mm}$
 a) Arc voltage. (2) Computed curve, (5) Test curve, (3) Source voltage
 b) Current. (1) Computed curve, (4) Test curve

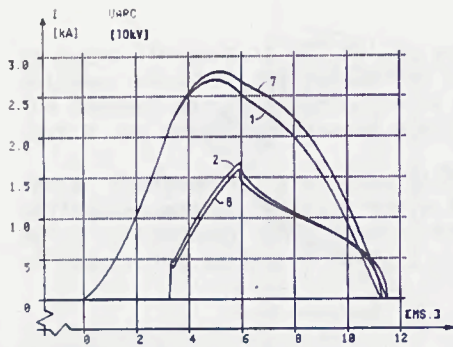


Fig. 5. Influence of D_0' .
12 kV/63 A. I2-test.
(1,2) $D_0' = 0,14$ mm, (7,8) $D_0' = 0,22$ mm

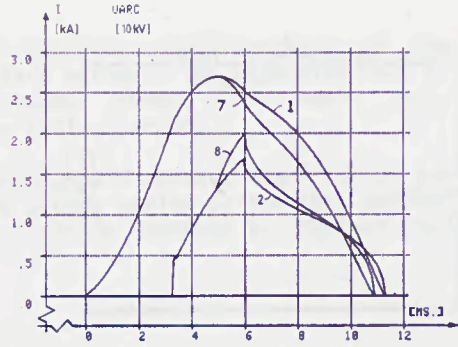
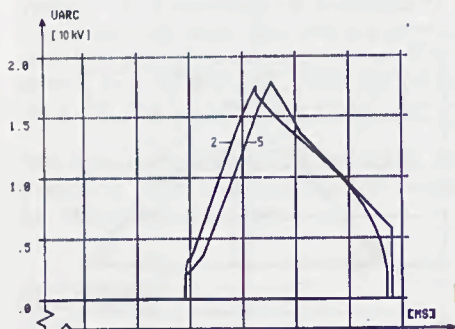
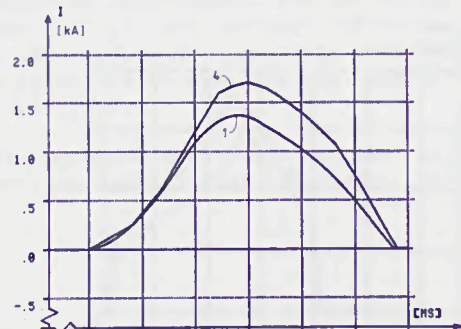


Fig. 6. Influence of B . 12 kV/63 A.
I2-test. (1,2) $B = 3,25 \cdot 10^{-8} \cdot i^{1,4} \text{ m}^2/\text{s}$.
(7,8) $B = 1,62 \cdot 10^{-8} \cdot i^{1,4} \text{ m}^2/\text{s}$.

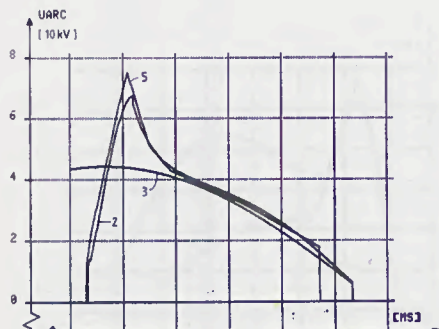


a)

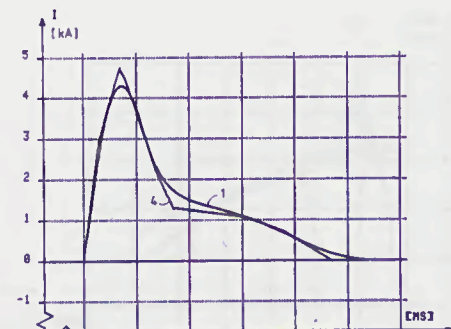


b)

Fig. 7. 12 kV/40 A. I2-test. $B = 1,62 \cdot 10^{-8} \cdot i^{1,4} \text{ m}^2/\text{s}$, $D_0' = 0,22$ mm
a) Arc voltage. (2) Computed curve, (5) Test curve
b) Current. (1) Computed curve, (4) Test curve



a)



b)

Fig. 8. 36 kV/40 A. I1-test. $B = 1,62 \cdot 10^{-8} \cdot i^{1,4} \text{ m}^2/\text{s}$, $D_0' = 0,22$ mm
a) Arc voltage. (2) Computed curve, (5) Test curve, (3) Source voltage
b) Current. (1) Computed curve, (4) Test curve

A SUITE OF INTERACTIVE PROGRAMS
FOR
FUSE DESIGN AND DEVELOPMENT

R. Wilkins, S. Wade and J.S. Floyd

INTRODUCTION The design and development of power fuses requires considerable time and expense to be spent on testing. There is scope for savings in development effort if mathematical models can be used to predict the performance of proposed designs, and the possibility exists of using computers to help produce more effective products or optimise existing designs.

Compared with the equipment which it normally protects, the HRC fuse is a physically small item, yet extremely large generating plant with complex control and measuring facilities, is needed to prove the fuse's capability. When considering the cost of manufacturing all the necessary test samples, (and usually a number of alternative designs are included), together with the very high charges involved in the use of high-power testing plant, the ability to carry out meaningful tests 'on paper' becomes a very useful advantage.

Whilst computer-aided design procedures are well established now in many branches of engineering, application to power fuse design has been limited, owing to the complexity of the mathematical models which are needed to represent the various important physical phenomena which govern the performance of such fuses. For example, the calculation of the transient heating of a typical fuse element requires the computation by numerical methods of the temperature at a vast number of points on the element, which requires very large and fast computers to be used.

There has been considerable research world-wide on the modelling of the physical processes, which include heat transfer, arc physics, circuit modelling and the choice of the numerical methods most appropriate for obtaining solutions. Although many research workers have developed computer programs for the purpose of validating mathematical models, these programs have not been of general usefulness, often requiring to be run in an inconvenient batch-processed mode, and requiring an inordinate amount of time to be spent preparing data by the user, who needs specialised knowledge of the programs themselves.

However, with the increasing availability of interactive computing facilities with massive memory sizes, high speeds and relatively low costs, it is now feasible to implement CAD programs for fuses which are of reasonable accuracy at reasonable cost.

This paper describes a suite of programs which has been developed for use by design engineers and researchers and reports upon some initial

Dr. R. Wilkins and Dr. S. Wade are with Liverpool Polytechnic, Byrom Street, Liverpool, U.K.

Mr. J.S. Floyd is with GEC Installation Equipment Ltd, East Lancashire Road, Liverpool, U.K.

experience of using the programs. A key requirement was that programs were user-friendly, so the user need have no detailed knowledge of the algorithms used to obtain solutions and that data input and output should be as simple as possible.

In designing the suite of programs attention has been paid to the facility of examining the effects of changing one or more design or test parameters, and in this respect it offers great assistance to the designer who previously, may have had to evaluate the 'remains' of a test sample before deciding upon the next step.

Computer simulations can never replace testing altogether, but the availability of these simulations should permit a reduction in the amount of testing done, by preliminary screening of designs using the engineer's judgement and the computed results as a guide. A second important application is that of simulating non-standard situations, which in some cases are almost impossible to reproduce in the test laboratory, for example the response of a fuse in one phase of a power converter subjected to a particular type of transient fault.

OVERVIEW OF SUITE Fig. 1 shows the arrangement of the suite of programs, in block diagram form. The type of fuse which can be accepted by the program is illustrated in Fig. 2. This fuse has a number of silver or copper elements in parallel within a sand-filled body. The element profile can be specified to be one of a number of standard shapes, or with some of the programs, a generalised profile specified by the user can be accommodated.

Data describing the fuse design is input via the data management program and then this is stored permanently in a named datafile. Simulated tests may then be carried out using one of the 'applications' programs, which at present are (i) temperature rise; (ii) time-current characteristic and (iii) short-circuit. The applications programs are designed so that the user 'tests' the fuse required, according to the IEC requirement appropriate for the fuse type (low voltage, semiconductor type, or high-voltage). Alternatively, if the user requires, non-standard test conditions can be specified and entered.

All the applications programs access the same bank of datafiles, which have a standard format. Thus, addition of new programs to the suite, or replacement of existing programs by more accurate versions, is simplified. The programs are written in FORTRAN and mounted on a DEC-20 mainframe computer.

DATA MANAGEMENT PROGRAM Datafiles describing fuse construction are created by the very important data management program.

The following data is input using a VDU terminal:-

Fusename
 Type (low-voltage, semiconductor, high-voltage)
 Nominal Current
 Body material and dimensions
 Number of bodies
 Filler type

Dimensions of end-cap and tags
 Fuse element material
 Number of elements and PCD
 Element profile (3 standard profiles plus 1 generalised)
 M-spot type (if any)
 M-spot location
 Dimensions of element according to profile
 (e.g. thickness, width of strip, notch length, etc.)

Data errors are trapped as far as possible at input time and each value is checked to ensure that it lies within a predetermined 'acceptable' range.

When data entry is complete a final series of checks is made to detect any internal inconsistency and then the dated datafile is saved on disc.

During input, the VDU mimics a pro-forma used by engineers to describe the fuse, and by means of a powerful screen editor, allows the alteration or correction of data. Among other features, this permits the ready creation of new datafiles describing fuses derived by slight modifications of existing designs.

As a consequence of the adoption of a standardised datafile format, each of the applications programs needs to process this data after input into a form suitable for the particular application. Whilst this front-end processing is trivial in some cases, it is very significant in others, notably in the short-circuit program.

TEMPERATURE RISE TEST In the thermal steady-state, heat is generated within the fuse elements due to the passage of current and this heat is lost (i) radially by conduction through the sand and the body and thence by convection and radiation to the surrounding air, and (ii) axially by conduction to the endcaps and thence to the connecting cables and busbars. This complex 3-dimensional heat transfer problem cannot be solved efficiently by numerical solution of the partial differential equations involved and so a semi-analytical solution method has been developed and is described in another paper [1]. It is necessary to take into account the heat generation within the connecting cables and the fuse endcaps to achieve acceptable accuracy.

The temperature-rise program simulates a standard test, so that, according to the fuse rating and type, connecting cables and/or busbars are selected automatically corresponding to the sizes required by the appropriate IEC standard. A simple model of M-spot diffusion is included, so that the likely state of activity of an M-spot (if used) can be estimated. The program gives a simulated test report as output giving the following computed values:-

Cold resistance
 Hot resistance
 Power loss
 mV drop
 End-cap temperature rise
 Body temperature
 Hotspot temperature

plus a series of comments relating to the possibility of melting or M-spot activity. A graph of the temperature distribution along a fuse element can be output if requested.

If the applied current is too high there may be no possible steady-state solution. This condition, along with several others, is trapped by the program and an explanation is output.

Fig. 3 shows typical results which have been obtained using the temperature-rise program. The accuracy achievable at present is discussed in reference (1).

TIME-CURRENT CHARACTERISTIC The purpose of this program is to compute the prearcing time/current characteristic (TCC) of a given fuse design.

The first part of the program calculates the minimum fusing current, which is an asymptote to the TCC. This is achieved by repeated calls of the temperature rise program, according to the following procedure. Starting with the fuse rated current, the test current is increased consecutively by a factor $(1+q)$ until the melting temperature is exceeded. q is then halved and the procedure repeated until the maximum temperature is within 0.1°C of the value required for melting. Since the temperature-rise calculations are very fast, computation of the minimum fusing current is achieved without excessive computing time; $q_0 = 0.1$ gives good results. The computed m.f.c.'s. are very close to those expected from tests, bearing in mind the fact that the 'experimental' value cannot be directly measured, being between the conventional non-fusing current and the conventional fusing current.

The second part of the program calculates points on the TCC, starting from the short-time end, using the decoupled method to represent transient heat loss to the filler [2]. However, to reduce computing time, a simple one-dimensional model is used to represent the fuse elements. The elements are divided axially into a large number of strips and the resulting finite-difference equations are solved using the Crank-Nicholson method to obtain the transient temperature distribution. Use of a one-dimensional representation results in a tridiagonal matrix equation which can be efficiently solved at each time step.

The program outputs pairs of (current/time) values but stops when the time exceeds 10 seconds to save computing time. The remaining part of the curve can be sketched in by hand if required. Fig. 4 shows typical results. If the ratio of full to reduced section of the fuse element exceeds about 4.0 the one-dimensional model is inadequate. In these cases, if desired, the short-circuit program described in the next section can be used to obtain points at the short-time end, at the expense of greatly increased computer time.

SHORT-CIRCUIT TEST A previous paper [3] has described methods for modelling the performance of current-limiting fuses under short-circuit conditions. These methods involve simulation of the transient two-dimensional heating in the elements during the prearcing period, the initial voltage step upon the appearance of arcs, burnback of the unmelted parts of the elements, fusion of the sand surrounding the arcs, which affects the axial arc gradient and the interaction of these processes with

the electric circuit.

The short-circuit program incorporates all these models and again the input/output is arranged as if the user were conducting a test in a high-power short-circuit test laboratory. Thus the user is asked to supply the values of test voltage, prospective current, source type (a.c./d.c.) source circuit power factor (or time constant) and with a.c., the frequency and making angle. The program computes and prints out if desired the complete course of voltage and current transients, indicating the instants at which melting occurs, series arcs merge, arcs burn back to the end-caps and finally the arcs extinguish.

A simulated test report is then output giving the following:-

Prearcing time
 Arcing time
 Total operating time
 Prearcing I^2t
 Arcing I^2t
 Total operating I^2t
 Arcing angle
 Current at start of arcing
 Peak let-through current
 Peak arc voltage
 Total arc energy

Accurate simulation of the prearcing transient requires the use of two-dimensional finite-difference modelling of the thermal and electric fields within the fuse elements. The short-circuit program uses sub-routines after data input to automatically generate the required finite-difference meshes for the different types of element which the program can handle.

Fig. 5 compares predicted values of cut-off current, for fuses of several different types under a variety of source-circuit conditions, with values measured in high-power tests. Similar accuracies are obtained in the computation of prearcing time and total operating time.

DISCUSSION The table below gives a rough comparison of the program sizes and run times (per complete test).

Program	Source code (k bytes)	Data (reals)	Typical C.P.U. time (sec)
data management	25	small	N.A.
temp. rise	24	8000	1
TCC	26	10000	30
short-circuit	30	90000	40

This shows that the heavy computing demands of the short-circuit program

requires the use, at present, of a mainframe computer although this situation may change suddenly with the introduction of 32-bit processors for microcomputers.

Experience with the usage of the programs by design engineers and researchers has shown that the usage can be divided into three categories.

- (1) The programs may be used in parallel with the design and development activity. This type of usage has been limited by the natural uncertainty about the accuracy of the computer simulations, and the restricted number of element profiles which the programs can handle. For example, the short-circuit program requires notches to be identical and uniformly spaced. However, as the accuracy of the program may be increased by the incorporation of improved models and the range of application increased by extending their capability, this class of usage is likely to increase.
- (2) The programs may be used to investigate general aspects of fuse performance, which although possible to determine experimentally would be prohibitively expensive and time consuming. Such investigations have included a study of the variation of arc energy with prospective current and making angle for several different fuse designs.
- (3) The programs are frequently used to supply quick answers to day-to-day problems of the 'what-if' type. For example, if test values are available for a fuse tested at 0.1p.f. it might be required to know how much the arc energy would be reduced if the power factor were raised to 0.2, all other conditions remaining the same. Whilst the absolute accuracy in predicting the value of arc energy may be only $\pm 20\%$, the effect of deviations from a given test condition can be calculated with much higher accuracy. This type of usage has to date probably proved the most useful for the industrial user, since the equipments encountered nowadays in everyday or 'shop-floor' applications are more complex, and sensitive to fault conditions. The versatility of the programs in the suite is a clear advantage when evaluating problems of this nature.

CONCLUSIONS The paper has described the philosophy and design of a suite of programs for simulation of tests on current-limiting power fuses for low-voltage, semi-conductor and high-voltage applications, and some initial experiences have been described.

With the increased availability of cheap computing power and with improved models of the physical processes, use of computer-aided design in this field is bound to increase. The suite described can be extended to include simulations of overcurrent breaking, pulsed loading and cyclic loading tests.

REFERENCES

1. Wilkins, R. "Simulation of fuselink temperature rise tests. Int. Conf. on Electric Fuses and their Applications. Trondheim, 13-15 June 1984.
2. Wilkins, R. and McEwan, P.M. "A decoupled method for predicting time-current characteristics of HRC fuses." Int. Conf. on Electric Fuses and their Applications, Liverpool Polytechnic, 7-9 April 1976.
3. Wilkins, R. and Gnanalingam, S. "Digital simulation of fuse breaking tests." Proc. IEE, 127, part C, No. 6, 1980.

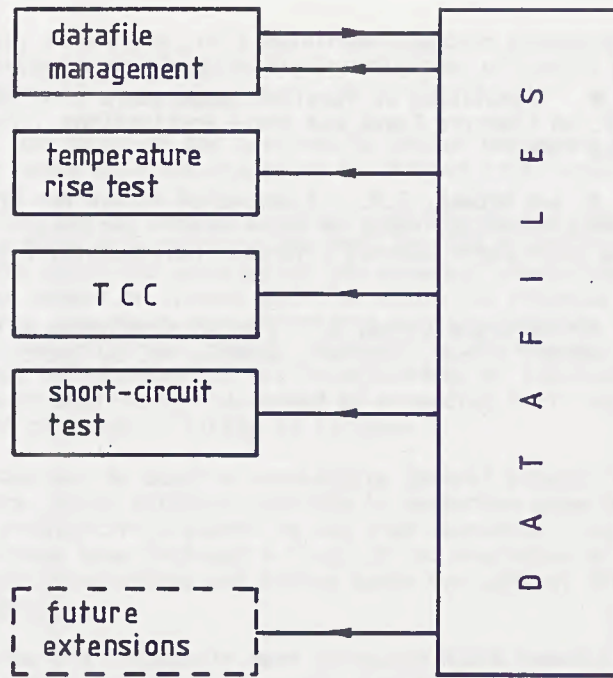


Fig 1. General arrangement

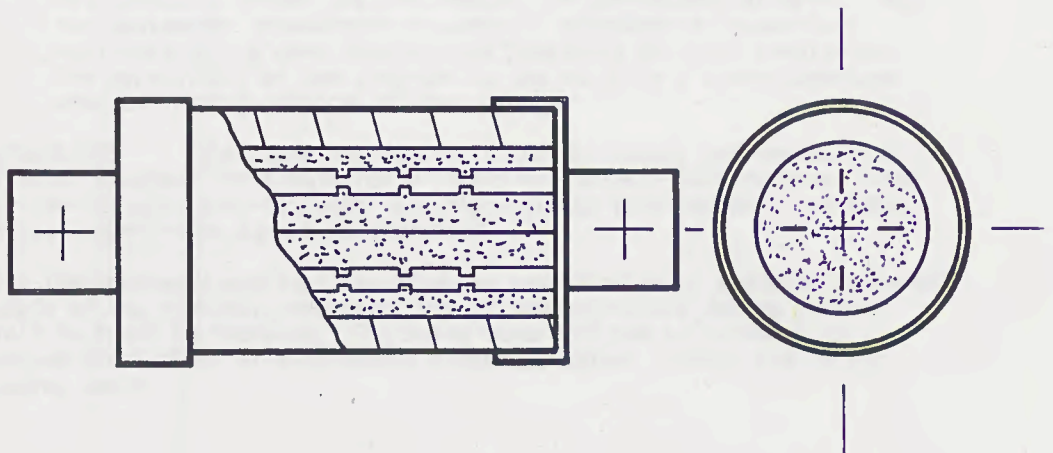


Fig 2. Basic construction

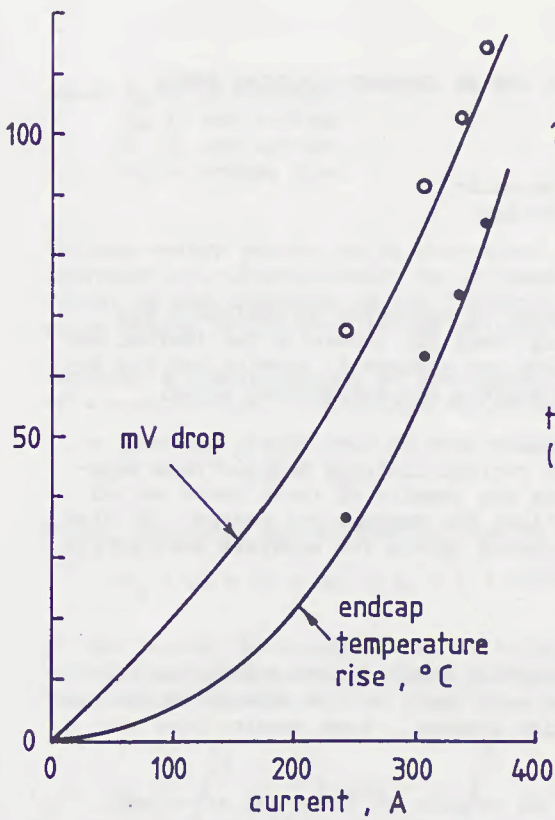


Fig 3. Temperature-rise tests on 315A LV fuse

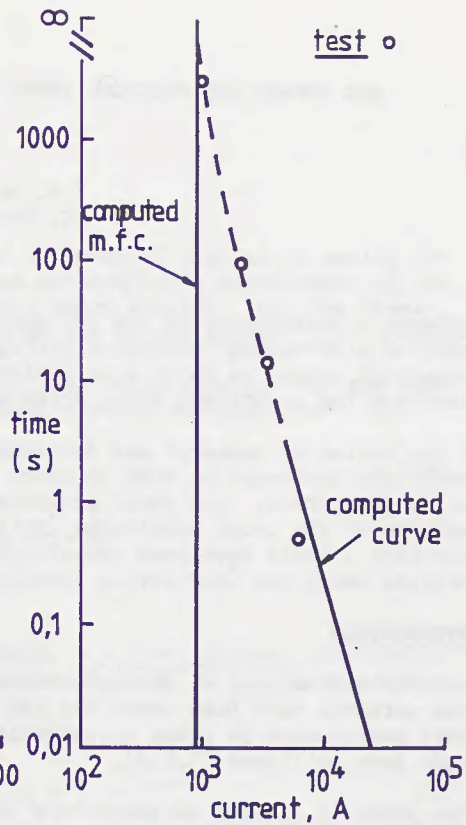


Fig 4. Typical TCC

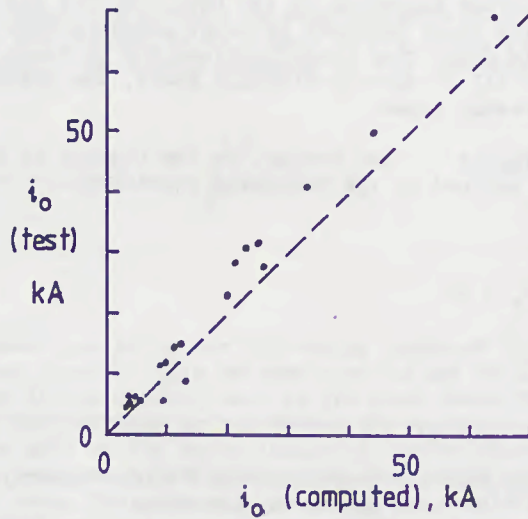


Fig 5. Cut-off currents

ARC ENERGY AND CRITICAL TESTS FOR HV CURRENT-LIMITING FUSES

V.N. Narancic
G. Fecteau

Abstract - Measurement of the arc energy is essential to designers and users of high-voltage current-limiting fuses for assessing the thermal and mechanical stress to which such devices are exposed in service and for determining the conditions under which maximum arc energy will occur.

In the course of research and development work on such fuses, hundreds of tests were performed on 8-kV to 23-kV current-limiting devices from various manufacturers. The paper presents the results of these tests and an analysis of the tests considered critical for maximum arc energy. It also describes a newly developed computer-based system for accurate qualitative analysis which was used during testing.

INTRODUCTION

Research and testing of HV current-limiting fuses intended for distribution networks have been under way for many years with a view to improving their performance in power distribution systems. Some results have already been published [1,2,3].

This paper is limited to describing the results of tests and arc-energy studies on large models made of different metals. Even if present standards do not require measurement of the arc energy, the main purpose of this work was oriented towards defining the conditions giving the maximum arc energy and the maximum stress to which a fuse is exposed in service. The tests were performed according to IEC Publ. 282 [4] and the results are in agreement with those obtained by other investigators [5-8]. Experience has shown, in fact, that specifications for LV fuses are not automatically valid for all HV current-limiting fuses, the differences are explained in the present paper.

Definition of Arc Energy Arc energy, in the context of current-limiting fuses, is defined by the following equation:

$$E_a = \int_0^{t_a} V_a i dt \quad (1)$$

IREQ (Institut de recherche d'Hydro-Québec)
1800 montée Sainte-Julie
Varenes, Québec, Canada
JOL 2P0

where E_a : arc energy
 V_a : arc voltage
 i : arc current
 t_a : arcing time

The arc energy values can be determined by means of digital or analog integrators or, alternatively, by indirect methods (e.g. measurement of the weight or the thickness of the fulgurite) which consider that the dissipated energy is absorbed by the melting of the quartz sand.

Consider a simple circuit of inductance L and resistance R . For the case of arc extinction, the voltage may be expressed by the equation

$$V = Ri + L \frac{di}{dt} + V_a \quad (2)$$

which, following transformation, can be written

$$V_a i dt = (V - Ri) i dt - L i di$$

If the circuit is supplied with DC voltage, $v = V = \text{constant}$, and the current, which at the moment of arc initiation is equal to i_0 , falls to zero, then the arc energy will be

$$E_a = \int_0^{t_a} (V - Ri) i dt - L \int_{i_0}^0 i di = E_s + \frac{L i_0^2}{2} \quad (3)$$

where E_s is the energy received from the source.

If, on the other hand, the circuit is supplied with AC voltage, $v = V \sin \omega t$, and the current in this case is $i = I \sin (\omega t - \phi)$, where ϕ is the phase shift, the energy produced in the half-cycle is:

$$E_a = \int_0^{\frac{T}{2}} (v - Ri) i dt - L \int_0^0 i di = E_s \quad (4)$$

where $\frac{T}{2} = \frac{1}{2f}$;

This equation shows that in AC arc all energy produced in the half-cycle is supplied by the source. This extreme case is not fully applicable to the fuse arc, but it can explain that in the case where the current is long and the arc extinguishes at the moment the current crosses its natural zero, one part or the whole inductive energy flows back into the system. This is evident in tests with long arc, cases of test duty 2. However, in fuse arcs, the phenomena are far more complex, owing to the variable phase shift and the arc voltage, which is temporarily higher than the source voltage; this in turn can influence the energy flow.

The difference between the current i_0 and the peak let-through current is not easy to incorporate, in mathematical form, in either Eq. (3) or Eq. (4) and, according to the authors, should be supplied by the source energy, which depends directly on the path. The calculation of the inductive energy in Table 1 was therefore performed using the value of i_0 .

Since a thorough understanding of arc phenomenon is important for the fuse designer, an investigation was carried out and is reported in this paper.

MEASUREMENT OF THE ARC ENERGY

A large research effort has been devoted to accurate measurement of the arc energy and a special program has even been developed for this purpose (see Appendix 1). In this program, the energy integral Eq. (1) was calculated with a time step of 5 to 20 μ s, the higher of these values being preferred because of the noise picked up by the ultrasensitive instrumentation.

Despite the fact that in realistic terms it is impossible to measure the inductive energy directly, Eq. (3) can be used to calculate a theoretical value, although it is purely hypothetical to consider that all this energy is converted into heat. It was therefore decided to solve the dilemma by measuring the heat developed in the fuse during operation. The calorimetric method used for this purpose was calibrated and found to be sufficiently accurate, to $\pm 2\%$ (Fig. 1).

TESTING AND RESULTS

A series of high-power tests was performed on fuses produced by different manufacturers for comparative purposes. The main purpose of the tests was to measure the arc energy under different circuit conditions, because this information is not given in the manufacturers' literature, and the standards do not prescribe measurement of this parameter. Since adequate quantities of samples for every size of fuse could obviously not be obtained, testing was limited to commercially available distribution fuses. The tests were eventually made on 10- to 100-A fuses designed for voltages of 8 to 23 kV. More than 150 fuses from different manufacturers were subjected to either complete or partial tests but in fact, far more tests were performed on in-house designed fuses made from different metals.

The results of the power tests may be summarized as follows:

- 1 - The closing angle giving the maximum arc energy varies with the prospective-current level. In test duty 2, this angle is approximately $0-10^\circ$ whereas in the higher current range it is near -25° and $40-50^\circ$. Actually it is exceedingly complicated to determine the maximum in the -25° range because, once the energy curve has reached the maximum value, it suddenly drops to its minimum before it even reaches the -30° range (see Fig. 2). At very high prospective currents, namely ≥ 50 kA, the closing angle is over 60° and shows a tendency to increase even further as the current rises.
- 2 - The curve of the arc energy generally rises to a maximum value and then decreases (Fig. 3).

3 - Test duty 2 is well prescribed in the standards.

The test current I_2 usually lies on the point of discontinuity on the energy curve (Fig. 3).

4 - Measurement of the heat developed in the fuse shows that when the arcing process is interrupted by the current crossing its natural zero the heat is less than the total calculated energy. This is frequently the case in test duty 2, when part of the inductive energy flows back into the network (see Table 1, test No. 1, for example). However, in the case of fuse operation with a closing angle in the range of -40° , the total amount of inductive energy is in fact returned because the arc is interrupted, even before the interrupting process is finished, by the approaching voltage and current zero (Table 1, test No. 5 and Fig. 6). Table 1, which gives the results of all tests followed by measurement of the heat developed, shows that in test duty 1 there is generally good agreement between the energy calculated according to Eq. (1) and the measured heat values (see Fig. 7 as an example). Some small differences remain inexplicable, however, as may be seen from tests Nos. 2, 4, 10 and 11.

5 - The calculated values of inductive energy are presented in Fig. 4, from which it can be seen that the maximum inductive energy can, but need not, coincide with the maximum arc energy, even with the test current I_2 .

ANALYSIS OF THE RESULTS

The test results for a silver and a cadmium fuse rated 100 A, 15 kV were presented in an earlier paper [3]. It should be pointed out here, however, that the reported arc energy measurements were in agreement with the mathematical calculations of Lerstrup [5] and Wilkins [6]. According to IREQ's experience, these authors' results well represent the dependence of the arc energy on the prospective current and the ratio of the arc voltage to the peak network voltage. However, their model is highly simplified and does not indicate the point of critical current specified in test duty 2.

The results of the tests performed in the work described here show that the maximum arc energy value depends mainly on the fuse design. HV current-limiting fuses have a lower number of notchings per unit voltage than LV fuses: while a LV fuse can have 10 notchings (N) per kV, this relative number is not applicable to the HV devices owing to limited space and also to the fact that high overvoltages are created by a large number of notchings. The number of notchings also has a considerable influence on the breaking process in the high-current range but much less at lower currents, such as I_2 .

As far as existing fuses are concerned, several silver fuses tested showed a maximum arc energy in the range of 10-20 kA, while other types of fuse have a maximum arc energy reaching the level I_2 . This may be seen in Fig. 4, where the higher curve represents a silver fuse with 3.6 N/kV and the lower dashed curve another silver fuse with 6.3 N/kV. The peak arc voltage of the first was 1.5, and of the second 3.2 times the peak service voltage. It is up to the fuse designer to select the most appropriate

design for the purpose. The arc-energy values of fuses made of other metals lie between the two curves in Fig. 4. Not only is the number of notchings per kilovolt a determining factor for the arc energy, but also other design parameters such as the current density in the notchings, the sand quality, grain size, and compacting. All these parameters explain the wide diversity in the arc energy curves.

Very similar results may be found in the work of Kato *et al.* [7], who reported a maximum arc energy with a prospective current of 10 to 20 kA. Meanwhile the findings of Baxter [8] should also be mentioned. This author reported that the maximum arc energy occurred at a larger prospective current than that corresponding to the maximum inductive energy in the testing of LV current-limiting fuses and, in addition, found that in certain cases (closing angle less than -40°) the inductive energy is higher than the total measured energy. This is in full agreement with conclusions 4 and 5 above.

ADDITIONAL TESTS WITH RESPECT TO THE ARC ENERGY

The aim of every fuse designer is to minimize the arc energy produced in a fuse during the interruption process. The study of parameters influencing the arc energy demands further research so that this section will be limited to describing three different tests performed with the critical current prescribed by the standards (I_2).

a) Influence of circuit parameters on test duty 2

A 30-A cadmium distribution fuse for a voltage level of 15.5 kV under development successfully passed all tests performed. Test duty 2 originally had a short-circuit ratio of 10, in accordance with the relevant standards. In order to find the design limit, the test was repeated under more severe conditions, decreasing the resistance in order to increase the short-circuit ratio to 30. In the latter case, the fuse failed because the current-zero at $t = T$ is delayed by the higher short-circuit ratio, thus causing a higher arc energy; furthermore the recovery voltage is also higher and rises more rapidly.

Two cases of transient recovery voltage are presented on the oscillogram in Fig. 5, where it can be seen that in both cases part of the inductive energy flows back into the system. (This model-fuse was object of the design modification as explained in the following paragraphs. It is presented here merely to illustrate the influence of the circuit parameters on arc energy).

b) Tests with high-speed camera recording

A high-speed camera (5000 frames per second) was used to record the comparative tests of the arc behavior during current interruption in the two critical tests under study. Two fuse models (100 A, 15.5 kV) were therefore prepared using plexiglass tubes with a very thin layer of sand between the fuse elements and the walls. (Plexiglass is not suitable for long-term testing but it proved sufficiently rigid for observation of the first loop).

Test duty 1 (Fig. 8a) was performed with a current of 20 kA and a closing angle of 40° , test duty 2 with a current of 6 kA and a closing angle of 5° . The photographs show that, in the case of the higher current, the arc forms simultaneously all along the strip and is extinguished in less than 200 μ s. In the case of the lower current (Fig. 8b) partial melting occurs and the arc is established only gradually along the strip because of insufficient energy. Under such conditions, the arc duration is considerably longer and it is only when natural current zero occurs that the arc duration is long because of the asymmetry, which represents the "worst" interrupting condition, but a basic difference exists between the two. In case a), at the moment the current reaches zero, the voltage is also at zero and, because of the high current involved, the angle between the voltage and the current is zero. In case b), the current is not very high and the angle between the voltage and the current is consequently fairly wide, which explains the sharp rise in voltage following interruption (see Fig. 5).

These comparative tests led to the conclusion that test duty 2 is very severe, even if the arc energy is not at its maximum, and that knowledge of the prospective current giving the maximum arc energy is essential for determining the maximum thermal and mechanical stresses on current-limiting fuses. The tests confirmed that fuses capable of withstanding such stresses have an infinite interrupting capacity, at least up to 50 kA, which was the maximum level tested.

c) Influence of fuse design on arc energy in test duty 2

Previous tests and oscillograms had indicated that the stress on the fuse in test duty 2 was due mainly to a low prospective current. In order to better understand the nature of this stress, a number of additional tests were performed. For this purpose, an identical fuse was selected from Fig. 5 with the same number of identical notchings but variable spacing. Figure 9 presents the results of tests using five different spacing schemes between the notchings, three equal (cases 1,2,3) and two unequal (cases 4 and 5).

In case 1, the distance was sufficient for successful breaking of a high prospective current but the fuse failed test duty 2, owing to high burn-back in the middle. In case 2, the distance was increased by 25% but was still not sufficient to prevent failure. Finally, with a further increase of 50% (case 3) the distance proved adequate for successful interrupting.

If unequal spacings are used (i.e. longest spacing in the middle, with the pitch slowly decreasing according to the heat distribution along the fuse), interruption is achieved at a lower arc energy. In case 4, the spacing in the middle was 25% longer than at the ends, while in case 5 it was 50% longer; interruption in the latter case was more successful. The reason for this improvement is that the heat was better distributed, which resulted in a greater number of notchings melting simultaneously. The entire test series was performed under identical circuit conditions, proving that an important role is played by fuse design besides the power-system conditions.

Selected spacings proved very useful also in test duty 3, improving the

simultaneous melting in the middle of the fuse, which is usually sufficient for interrupting low currents.

These tests were all performed on low-melting metals (cadmium and zinc alloy) but the results should be valid for any metal if account is taken of the electrothermal properties of the chosen metal. The best proof for the above-mentioned considerations can be seen in Fig. 4. The number of notchings becomes more effective as the current increases because this causes more notchings to melt at the same time. By way of comparison with uniformly notched fuses, the tests revealed that local overheating in a silver fuse with a ceramic housing very often leads to cracks in test duty 2.

CRITICAL TESTS

According to the experience described above, it is possible to conclude that the HV current-limiting fuse faces in fact two critical tests: test duty 2 and the test giving the maximum arc energy.

Selection of the current for test duty 2 is well prescribed in the standards, and the stresses imposed on the fuse during this test are described earlier in this paper. The test with maximum arc energy can be more severe if it is performed with a current close to test duty 2, i.e. if it introduces more energy followed by a sufficiently high voltage jump after breaking. At higher currents, this jump tends to decrease and eventually disappear, and the fuse absorbs the energy without danger of damage, even if the arc energy increases. Test duty 1, in fact, is a mean of verifying the fuse design and assembly. In developing a fuse, it is extremely important to verify the stress imposed by different circuit conditions, but it is up to the designer and the user to decide whether or not more tests should be performed than prescribed.

CONCLUSION

On the basis of many tests on HV current-limiting fuses at IREQ the following conclusions can be drawn:

- HV fuses must not be judged on the same basis as LV fuses: the number of notchings per unit voltage is generally much lower than in LV devices owing to space requirements and permissible overvoltages.
- Test duty 2 intended to verify the interrupting capability in region of the high value of inductive energy does not necessarily produce the maximum arc energy.
- Even if it does not produce the maximum arc energy, test duty 2 provides the strongest stress owing to the long arc and high voltage jump after the arc is extinguished.
- The test with maximum arc energy, if not associated clearly with test duty 1 or 2, is important for the designer but not necessarily for the user.
- The tests show that the shape of the arc energy curve versus fault

current can be influenced essentially by design characteristics, not only by the power system conditions.

- Measurements of the heat developed in the fuse during operation showed good agreement with the time integral of arc voltage and current. In some cases, especially in test duty 2, it was found that all or part of the inductive energy returns to the system. During the research described in this paper many questions and problems were raised with regard to arcing phenomena and further research is required to provide explanations and to find a means of reducing the energy developed during fuse operation.

APPENDIX A

DATA ACQUISITION AND PROCESSING SYSTEM

The high-power laboratory's data acquisition and processing system performs such functions as magnetic data recording, digital conversion and computer processing. During a test, 22 channels bring the data to a magnetic recorder, which acts as a memory between the measuring devices and the computer. Immediately after a test, the analog data is converted into digital form for immediate storage in a large computer. A sophisticated tape-positioning system ensures a high level of efficiency. At the operator's request, curves and results are displayed on CRT screens for consultation, and copies may be obtained using electrostatic plotters.

The telemetering system not only offers several enlargement and zoom facilities but comprises a program library for calculating the integrals of a curve or the product of the two curves, precise aperiodic components, rms values, arc resistance, arc energy, frequency measurements of harmonic content, etc. It is also used for statistical processing. The accuracy and operating speed of the telemetering system are such that it is not necessary to wait for values based on test measurements, so that decisions can be made immediately about the next test program as testing proceeds.

At the present time, the system records every 1- μ s signal and can handle frequencies up to 80 kHz with an error of less than $\pm 1\%$.

Figure 10 shows the CRT screen and tape recorders in the central control room.

ACKNOWLEDGEMENTS

The authors would like to thank the Canadian Electrical Association for authorizing publication of this document, which is part of a development project on current-limiting fuses for distribution networks. They also acknowledge the valuable help of Daniel Maure, a research scientist in IREQ's Thermal Studies Group, in carrying out the calorimetric study and of Lesley Régnier for careful revision of the manuscript.

REFERENCES

- [1] Narancic, V., Braunovic, M., Westrom, A.C. "The Composite Fuse - A New Technology for Current-Limiting Fuses," 7th IEEE/PES Transmis-

- sion and Distribution Conference, April 1-6, 1979. IEEE Publication 79 CM 1399-5-PWR.
- [2] Westrom, A.C., Crooks, W.R., Narancic, V. "Current-Limiting Fuses - A Comparative Evaluation," IEE Transactions, PAS-101, No. 7, 1982, p. 1870.
 - [3] Narancic, V. "Fuse Research at IREQ," Conference Record of International Conference on Distribution Fusing, Canadian Electrical Association, Nov. 2-4, 1981, Montreal.
 - [4] IEC Publ. 282 - Part. 1, 1974, under revision.
 - [5] Lerstrup, K. "The Current-Limiting Fuse with Special Reference to Discrimination and Breaking-Capacity," Ingenioren International, First Edition, Vol. 2, January 1958.
 - [6] Wilkins, R. "Generalized Short-Circuit Characteristics for HV Fuses," Proc. IEE, Vol. 122, No. 11, November 1975.
 - [7] Kato, T., Arai, S., Omori, T. "Burn-Out Test of High-Voltage Current-Limiting Fuses," Electrical Engineering in Japan, Vol. 89, No. 2, 1969, pp. 84-92.
 - [8] Baxter, H.W. "Constants and Closing Angles in Fuse Testing," Electrical Times, July 3, 1958, pp. 3-7.



Fig. 1 Photograph of calorimetric equipment

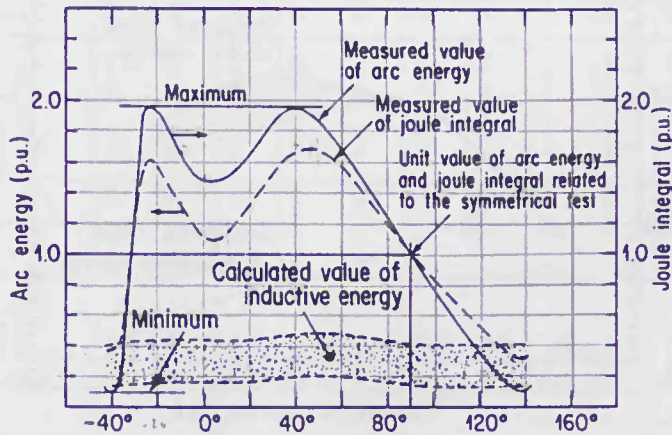


Fig. 2 Arc energy and joule integral for HV current-limiting fuses as a function of the closing angle. The inductive energy varies with the magnitude of the test current.

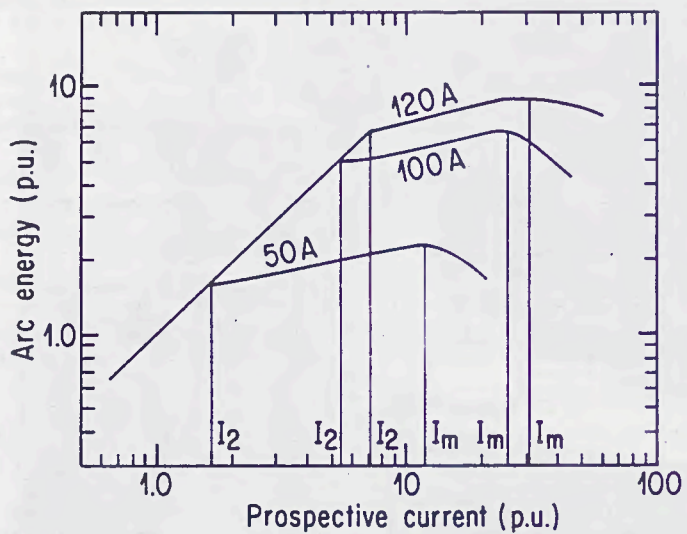


Fig. 3 Arc energy versus prospective current in HV current-limiting fuses designed for a rated current ranging from 50 to 120 A

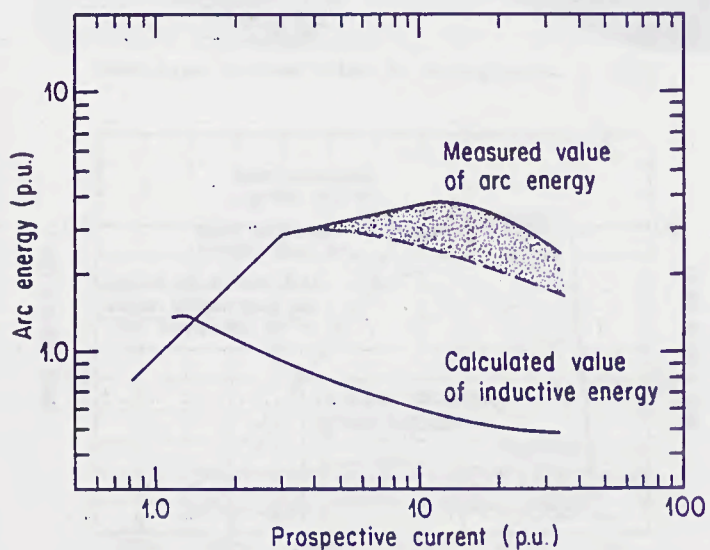


Fig. 4 Measured values of arc energy and calculated values of inductive energy versus prospective current in high-voltage current-limiting fuses

Table 1. Numerical results of tests

Test No.	Fuse maker and metal element	Rating		Circuit parameters			Closing angle (°)	Test duty	Current (A)		Time (ms)		Joule int. $10^3 A^2 s$	Arc energy (kJ)		Remarks
		kV	A	Prosp. current kA	Cos ϕ	$\frac{\bar{X}}{\bar{R}}$			At arc init. I_0	Let-through I_m	Melting	Arcing		VI Heat	$\frac{LiI_0^2}{2}$	
1	Brand 1 Ag	15.5	50	3.8	0.10	10	5.	2	3900	5120	3.5	5.6	98	298	82	Fig. 4
2	Brand 1 Ag	15.5	50	20.0	0.083	12	89.	1	6550	8692	0.57	2.4	85	243	257	Fig. 4
3	Brand 1 Ag	15.5	50	20.0	0.083	12	42.7	1	5969	8287	0.69	4.8	88	325	324	Fig. 4
4	Brand 2 Ag	15.5	100	20.0	0.083	12	43.	1	12400	13200	1.36	4.3	260	585	565	
5	Brand 3 Ag	17.5	100	20.0	0.10	10	-40.	1	5658	5829	1.36	1.42	40	32.3	~30	Fig. 6
6	Brand 4 Ag	17.5	100	20.0	0.10	10	91.	1	7615	10560	0.95	4.5	140	327	315	Fig. 7
7	Brand 5 Cd.	15.5	30	1.65	0.10	10	4.	2	1794	2246	3.19	6.26	20	160	120	Fig. 5
8	Brand 5 Cd.	15.5	30	1.65	0.033	30	8.	2	1684	2660	3.13	6.8	23.6*	181*	-	Fig. 5
9	Brand 5 Cd.	15.5	100	20.0	0.10	10	88.6	1	10418	12480	0.97	3.17	244	425	432	108
10	Brand 5 Cd.	15.5	100	20.0	0.10	10	45.2	1	9800	12200	1.23	5.6	413	790	770	96
11	Brand 5 Cd.	15.5	100	7.0	0.10	10	2.	2	6973	8648	3.33	5.9	268	627	595	142

* Calculated up to first current zero

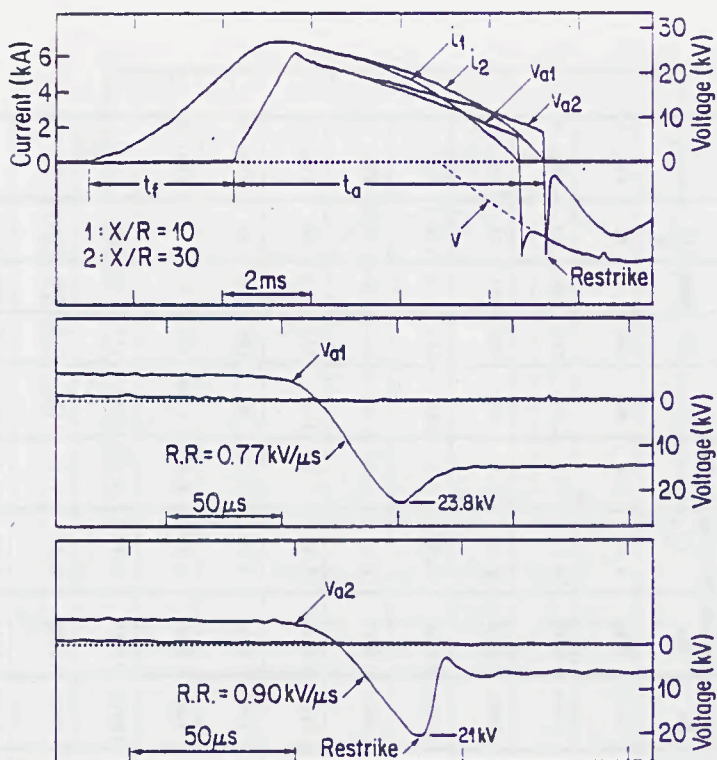


Fig. 5 15.5-kV, 30-A cadmium fuse. Test duty 2 with the same test-circuit parameters except the resistances required to change short-circuit ratio ($x/R = 10$ and 30)

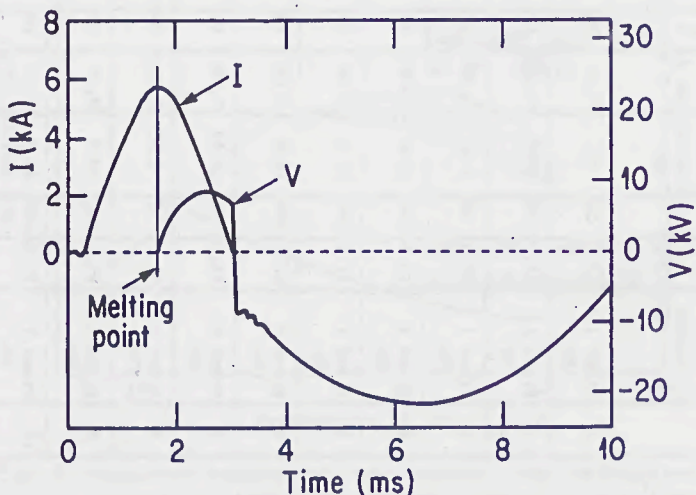


Fig. 6 100-A, 17.5-kV silver fuse. Oscilloscope of a test with a prospective current of 20 kA and closing angle of -40°

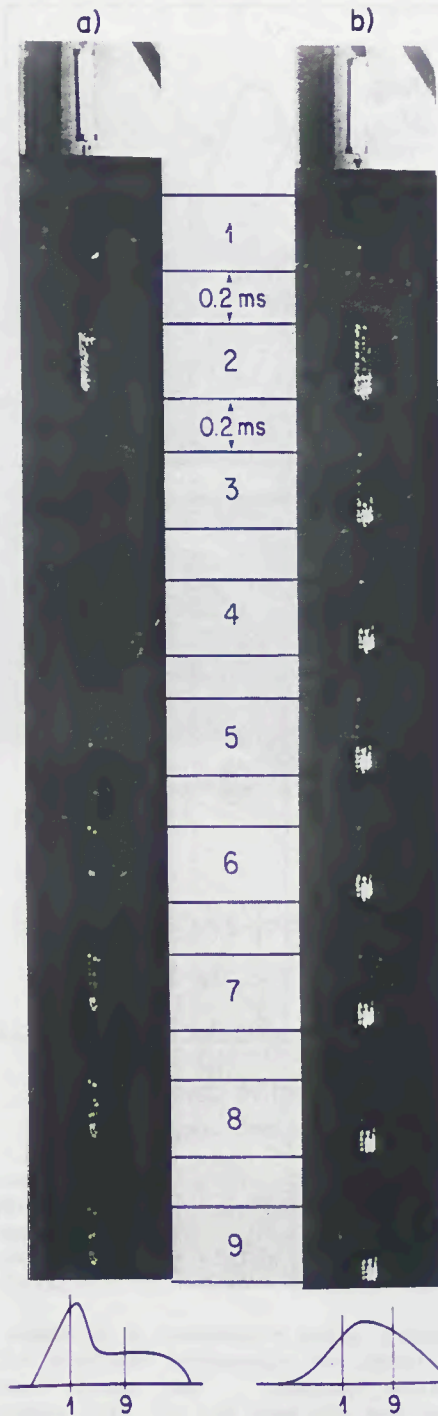


Fig. 8 High-speed camera record of test duties 1 and 2 for a current-limiting cadmium fuse rated 100 A, 15.5 kV (5000 frames per second)

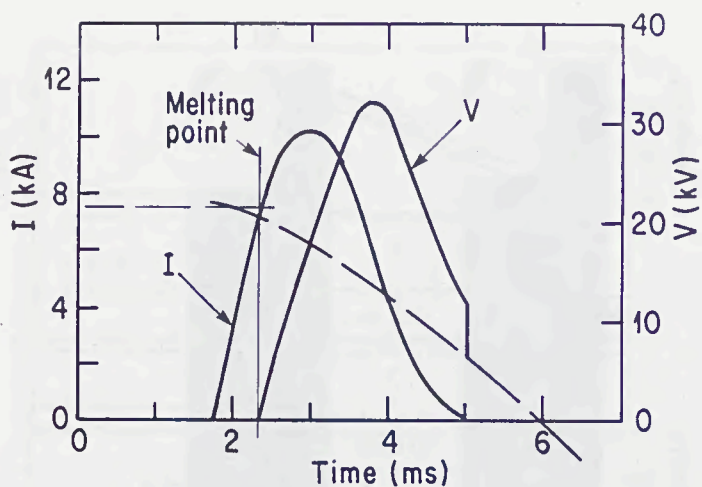
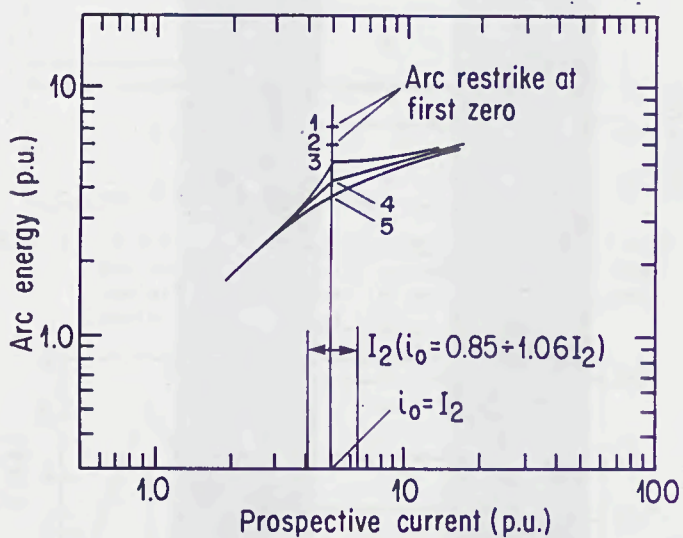


Fig. 7 100-A, 17.5-kV silver fuse. Oscillogram of a test with a prospective current of 20 kA and closing angle of $+90^\circ$



Distance between notchings (in p.u.)

case 1	1	constant
case 2	1.25	constant
case 3	1.50	constant
case 4	1 - 1.25 - 1	variable
case 5	1 - 1.50 - 1	variable

Note: The per-unit value represents a distance sufficiently large for successful breaking of a high prospective current. The total number of notchings was the same for all five cases.

Fig. 9 Arc energy in a HV fuse as a function of its design in test duty 2

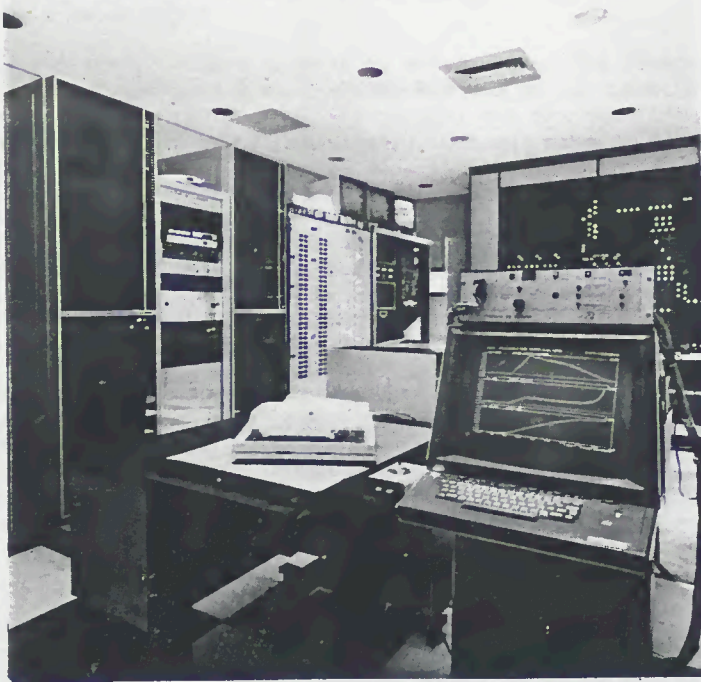


Fig. 10 Photograph of control room with CRT screen and tape recorders in high-power Laboratory.

DETERIORATIONS AND CYCLES TO FAILURE OF
H.V. CURRENT-LIMITING FUSES SUBJECTED TO CYCLIC LOADING

S. Arai

INTRODUCTION Reports stated that there was a possibility that h.v. current-limiting fuses which were made according to old national power fuses standard failed in normal service after running for many years on a high voltage motor circuit. On that opportunity, the investigation about the applications of the fuses to cyclic loading in the field were carried out, and particularly a lot of vital interests concentrated on the deteriorations of the fuses subjected to cyclic loading[1].

It has been known that cyclic pulses or overcurrents of short duration such as motor starting current, inrush magnetizing current of no load transformer, inrush current on energization of a capacitor or capacitor banks and other occasional overcurrents may cause fuse elements to deteriorate. Especially in high voltage circuit, serious trouble may occur when the current-limiting fuse operates under deterioration of elements in normal current conditions.

The method to estimate deteriorated degree or to anticipate the life of failure of elements were required by both the user and the manufacturer in order to avoid accidental and unexpected premature operation of current-limiting fuses subjected to cyclic current. Thus it was intended to investigate the deteriorations and the life of cycles of fuse elements in detail.

A series of tests were undertaken to investigate the deteriorations and cycles to failure about model current-limiting fuses and some consideration was given about the expression of the life of cycles relating to elements subjected to repeating simple pulse current.

TEST SAMPLES AND THEIR TIME/CURRENT CHARACTERISTICS A kind of model current-limiting fuse was employed as test samples for the purpose of investigating cycles to failure and deterioration phenomena of elements subjected to cyclic loading and assessing the effect on the deterioration by the fuse element construction and pulse current waveform, further because of avoiding complex effects on the results of cyclic tests under the influence of different constructions of various kind of type of fuses.

Fig.1 shows a model fuse link. The main components and materials of the model fuse link are a silver ribbon element, granular quartz sand, a normal ceramic barrel and end caps. A single element was stretched in a cylinder

S. Arai is with Tokyo Denki University, Tokyo, JAPAN

barrel filled with quartz sand. The construction of the model fuses was made as simple as possible.

Fig.2 shows the silver ribbon element of model fuses. The dimension of the element of model fuses is 1.5 mm in width and 0.2 mm in thick, it has notches every 8 mm regularly along its length, the minimum width of the notch is 0.8 mm. Some of the elements were bent and others were straight. Fig.2(b) shows the form of the bends. Fuse links with the bent elements have larger electric resistances than those with the straight ones, since the bent elements are longer than the straight ones.

Fig.3 shows the pre-arcing time/current characteristics of the sample model fuses. The fuses with the straight elements are longer pre-arcing time than those with the bent ones at the same prospective current below about 85 A. Pre-arcing Joule integral of the fuses falls under constant region below about 2 msec of pre-arcing time.

LIFE CYCLE TESTS The simple pattern of current was selected as test pulse current. For this test, s-factor is defined by the ratio of the value of pulse current to the current on the pre-arcing characteristics at the same time duration. Thus the s-factor is expressed by following equation

$$S = \frac{I}{I_m} \dots\dots (1)$$

where I is the magnitude of pulse current, I_m is the melting current corresponding to the same pre-arcing time as the pulse duration. The magnitude of pulse current is obtained by multiplying the current on the time/current characteristics of the same time as the pulse duration by the value of s-factor.

Fig.4 shows an example of pulse cycles in the test. The s-factor, pulse duration and current off period when making the tests were selected from the values listed in Table 1. It was taken into account in the selection of pulse duration that the duration of the pulse of 10 sec simulated the motor starting currents and 0.1 sec simulated the transformer magnetizing inrush current. The current off period was determined so that cumulative temperature rise at the center of the barrel surface owing to the repeated pulse kept saturated temperature as low as possible.

Three samples were connected in series in the test circuit and wiring of the test circuit was arranged in reference to JEC-201 temperature rise test[2].

CHARACTERISTICS OF CYCLES TO FAILURE VERSUS VALUE OF S-FACTOR Fig.5 shows the experimental results of cycles to failure versus the value of s-factor for the sample fuses. Experimental results of life cycle tests shows significant difference of number of cycles to failure between fuses with the straight elements and those with the bent ones. Fuses with the straight elements are quite lower cycles to failure than those with the bent ones at the same value of s-factor. For example, for $S = 0.8$ number of cycles to failure of fuses with the bent elements is beyond 10,000, on the other hand that with the straight ones is below 1,000.

Increasing the value of s-factor close to one, cycles to failure of fuses

with the straight elements and those with the bent ones approach different values from one, the former is several tens and the latter is several hundreds.

Number of cycles to failure of fuses with the straight elements is observed relatively much scattering, however that with the bent ones is relatively closely found as observed in Fig.5.

DEFORMATIONS Three samples were mounted in the vertical orientation. A upper end cap was higher temperature rise than a lower one by convection cooling. It is observed that the distribution of fracture positions inclines to the upper portion of a barrel and this inclination is much distinguished for the fuses with the straight elements. It is assumed from these results that the deviations of the distribution of fracture positions concentrated in the upper side of the barrel are effected on the higher temperature deviations from its symmetrical distribution along the length of the fuse link and lower density of filler sand in the portion.

To gain some informations on cyclic fracture, some studies were undertaken about the samples on the cyclic test and after test finished and a fracture element taken out from the barrel.

X-ray photographs of the geometric patterns of the straight elements were taken before, during and after pulse current for one pulse cycle. From these photographs as shown in Fig.6, it is observed that the straight element is straight before a pulse current, bends clearly at two positions during the pulse current and again restores during pulse off period. On the other hand, it is seen that the shape of the bent elements is much the same before, during and after the pulse current. It is confirmed from the above observations that thermal expansion of the element arises owing to heating during pulse duration, compressive stress acts on the element and then as cooling occurs for current off period, the element contracts and may be subjected to tensile stress in the case of occurrence of the plastic deformation.

For the fuses with the straight elements, it is considered that excess strain over the longitudinal compressive strain limit below which the element is held straight acts on the some sections of the element and results in occurrence of local deformation looking like folded or arc shapes at some positions on the element. The same deformed shapes repeat at the same positions every pulse currents. The shapes of deformation resembling folded triangulars were often observed near a upper portion of the barrel on x-ray photographs taken after cyclic test completed. On the other hand, x-ray photographs taken about the fuses with the bent elements show no visible change of shapes of the element during a pulse cycle. It is supposed that thermal expansion of the bent elements by heating distributes evenly along the element and so the strain distribution is uniformly along the element.

In case of the larger value of s-factor than about 0.8 and longer pulse duration than about 10 sec, the pattern of bends of the bent elements deformed gradually in accordance with progressive increasing number of repetitive pulse current, ultimately original bends disappeared and changed into ripples as shown in Fig.7. The cause may be expressed as follows. As the value of s-factor closes to unit and the pulse duration is

longer, the temperature of an element is kept higher for a long time, plastic deformations occurs due to the development of thermal compressive stress depending on high temperature and its long holding time. Cumulative plastic deformation of the element subjected to cyclic loading in high temperature gives rise to the permanent deformation of the elements and the gradual and progressive disappearance of the original bends of the element every repeating pulses.

CRACKS AND FRACTURES The elements taken out from a fuse link after cyclic test completed were inspected by means of x-ray photographic and electron-microscopic examinations. Fig.8 shows cracks formed on a element. Fig.8(a) shows cracks occurred along the polycrystalline grain boundaries and Fig.(b) shows the grown up cracks. The cracks occurred not only at reduced section width of notches but also at the full section width.

Fig.9 shows cracks and their growths on a section of the fractured element. Extended cracks are observed at the full section width under the influence of the prior cold bending work. Two bends and two notches deformed and cracks extended along the borders of bent portions can be seen in a front view of the element corresponding to the side view.

It is observed that some fractures occur at notched portions apart from the minimum cross section and others occur at the full section width. The phenomena of fractures occurred at the positions except the minimum reduced cross section of the element are remarkably different from the melting of elements owing to over current. It is distinctive features for failure of elements subjected to cyclic loading.

It was observed that many fractures occurred during current off period and some fractures occurred during pulse duration. The information of the instant of the fracture happened is given by the precise inspection of the torn surface of elements. The arc burning mark of the torn surface suggests that the fracture of elements happened during pulse current in low test voltage and in the case of no arc mark, fractures happened during current off period.

It has been known that the cause of the phenomena such as occurrence of cracks, growth of cracks and fracture eventually happened on the metal subjected to cyclic loading is the fatigue.

CONSIDERATION OF CYCLES TO FAILURE From the investigations of the elements subjected to cyclic loading under testing and the elements after the test completed, it is observed that cracks are formed on the element, then gradually extend and ultimately lead to failure. It may be concluded that the cause of the failures of elements subjected to cyclic loading are mainly due to the fatigue.

It is stated in the studies of fatigue that the stress-strain loops set up in the constrained elements subjected to repeated expansion and contraction under cyclic pulse current. The steady-state stress-strain loop which settles down in a first few cycles of pulse currents has inelastic strain each cycle.

Manson-Coffin's experimental law gives the following relationship between cycles to fatigue failure and the inelastic strain on the stress-strain

loop within the range of low number of cycles to fatigue failure

$$N^\alpha E_p = C \dots\dots (2)$$

where N is cycles to failure, E_p is the magnitude of the inelastic strain and C is a constant. The constant C depends mainly on material property and temperature. Experimentally α is often taken 0.5, C is derived from the contraction of the area of the wire test specimen obtained from static tensile test.

INELASTIC STRAIN The temperature rise of elements according to the pulse current depends on dissipated energy and the thermal conductivity of fuse link. Providing that an element is constrained completely and no free expansion of the element occurs, thermal strain which is composed of the elastic strain and inelastic strain equals thermal expansion and is expressed as follows

$$E_t = \beta \Delta\theta \dots\dots (3)$$

where E_t is the thermal strain, β is the thermal expansion coefficient, $\Delta\theta$ is temperature rise difference.

Providing that sand fills uniformly a barrel, the straight elements of which temperature rises quite high deform theoretically like sine waves and practically deformations being alike sine waves are often observed in the vicinity of a lower cap. It is considered that sand is rarely filled uniformly in the barrel mounted in vertical orientation. Many experimental results of the fuses with the straight elements reveal that the local deformations of folded shape as a triangular arise in a few positions along an element and the local deformations of arc shapes arise at the reduced section width of an element. On the other hand, supposing from the test results, the strain of the bent elements distributes uniformly together with temperature rise, the deformation of elements occurs evenly along the longitudinal direction of an element.

It is concluded that the local concentrated strain occurred in the straight element amounts to one time or more the thermal strain expressed in Eq.(3). It is assumed that the strains of the bent elements are smaller than the thermal strain expressed Eq.(3) owing to the effect of reducing thermal strain under the influence of uniform distribution of strain and uniform movement of elements.

RELATIONSHIP OF CYCLES TO FAILURE VERSUS S-FACTOR Providing that the straight element is completely constrained by sand filler and end caps, no displacement of the element in sidelong direction occurs, the thermal expansion of the element equals the total strain. It is simply assumed that the temperature rise of the element is proportional to the square value of s-factor throughout the most part of length of the element. The melting point is given when the value of s-factor is equal to unit. Then the temperature rise of the element is given by the function of the value of s-factor as follows

$$\theta = \theta_m S^2 \dots\dots (4)$$

where θ is the temperature rise of the element, θ_m is the temperature rise

of the melting point.

It is assumed that the inelastic strain expressed in Eq.(2) nearly equals the total strain expressed in Eq.(3) in the case of no deformation of the straight elements. As mentioned above, the local deformations were mainly observed in experimental results for the straight elements. It is calculated that the strain in this case increases some multiples of that of the straight element rigidly constrained. On the other hand, in the case of the bent element, its strain is reduced below that of the thermal expansion, since the deformation is evenly distributed along almost all length of the bent element.

Thus the inelastic strain expressed in Eq.(2) is given as follows,

$$E_p = k \beta \theta_m s^2 \dots\dots (5)$$

where k is the factor indicating the proportion of the strain depending on the deformed shape to that of the thermal expansion and may be related to temperature rise and pulse current waveform. Corresponding to the patterns of deformation, k may be classified as follows, $k = 1$ for the straight elements rigidly constrained and not deformed, $k > 1$ for local deformations on the straight elements and $k < 1$ for the bent elements.

Substituting (5) in (2) gives

$$N = (1/\beta \theta_m)^2 (C/k)^2 s^{-4} \dots\dots (6)$$

As temperature of the elements varies between the maximum and the minimum value for a pulse cycle, it is difficult to obtain the appropriately analytical expression about the constant C as some function of the temperature. So the following experimental results are directly used. Fig.10 shows the curve of constant C versus temperature about silver wires obtained experimentally from static tensile test. The constant C depending on temperature rise as shown in Fig.10 is expressed by following equation within the range of temperature between about 400°C and 900°C,

$$C = \mu \theta^{-\gamma} \dots\dots (7)$$

where μ , γ are constant. In the cyclic life test, temperature of the element goes down near ambient temperature every pulse off periods, so introducing (4) and (7) into (6), Eq.(6) reduces to

$$N = (\mu/\beta)^2 \theta_m^{-2(\gamma+1)} k^{-2} s^{-4(\gamma+1)} \dots\dots (8)$$

Substituting (1) in (8), and plotting the results calculated from Eq.(8) on the magnitude of pulse currents on a log-log scale, the linear relation is obtained between cycles to failure and the magnitude of pulse currents. This expression shows the same relationship as obtained previous experimental work [3].

Four curves calculated from Eq.(8) for $k=0.2$, $k=0.6$, $k=1$ and $k=10$ are shown in Fig.5. Data of cycles to failure of the bent elements on log-log scale mostly distribute between two curves of $k=0.2$ and $k=0.6$ and data of the straight elements distribute under the curve of $k=1$. It is observed that the tendency of data distribution for the bent elements coincides nearly with these calculated curves, however the tendency of data

distribution for the straight elements differs from the curve of $k=10$. One reason is considered as follows. The above discussion is based on the assumption that the constant k is constant throughout the range of the test. In practice, it is suggested that the k of the bent elements is almost constant, but the k of the straight elements is appreciably variable according to the test conditions, that is, the strain ranges very wide due to local deformations. As another reason, comparatively low cycles to failure around $s=0.6$ to 0.7 are considered under the influence of quite low value of constant C at the temperature of about 300°C , since the straight elements may still receive strong stress actions until the low value of s -factor.

For the bent elements, strain is reduced below the strain corresponding to the thermal expansion, because of the uniformed distribution of deformation and displacement. This effect is expressed by means of the relation of $k<1$ and the bends of the elements improve the life of cyclic loading.

On the other hand, for the straight elements, thermal expansion concentrates some fixed positions of the element. Strains of these positions increase over the strain equating to thermal expansion, it is expressed by means of the relation $k>1$. It is stated from the relation that local deformations shorten and scatter the life of cyclic loading.

It is expected that in the region of low cycles under about 10^4 cycles Eq. (6) or (8) serves the presumption of number of cycles to failure of current-limiting fuses subjected to cyclic loading.

CONCLUSION Cyclic life tests were carried out for the model current-limiting fuses.

In most cases, the local deformations occur in the straight elements due to thermal expansion.

The bends of the elements disappear and change into ripples as the value of s -factor approaches one and pulse duration is longer.

The process of the occurrence of cracks, their growth and ultimately fracture happening on the elements due to cyclic loading is caused by fatigues.

The expression deduced from Manson-Coffin's law relating to fatigue fracture and the k -constant introduced with respect to deformed shapes is expected to give the estimation of the life of cyclic loading about the same type fuses as model current-limiting fuses with the bent elements in the region of low cyclic failures.

REFERENCES [1] Technical report, (II) No.155, IEEJ, Sept. 1983
[2] Standard of JEC "Power Fuses" JEC-201-1977
[3] G. Stevenson: "Cyclic loading of fuses for the protection of semi-conductors." International Conference on Electric Fuses and their Applications. April 1976

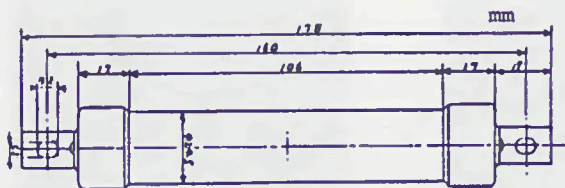


Fig.1 A model fuse link used for life cycles tests



(a) Front view



(b) Side view

Fig.2 A silver ribbon element of the model fuses

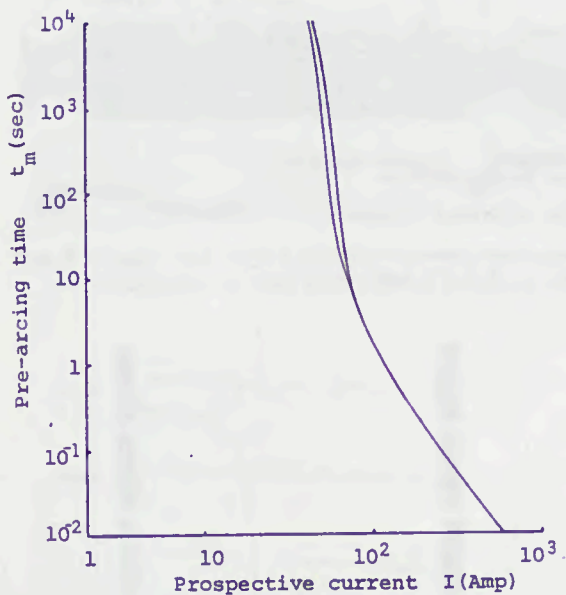


Fig.3 Pre-arcing time/current characteristics of the model fuses

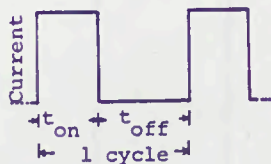


Fig.4 An example of pulse current cycle

		pulse duration t_{on} (sec)			
		0.1	1.0	10	100
S	0.9	60	120	1200	1800
	0.8	60	120	1200	1800
	0.7	60	120	600	1200
	0.6	60	120	600	1200

Table 1 The values of s-factor, pulse durations: t_{on} current off period: t_{off}

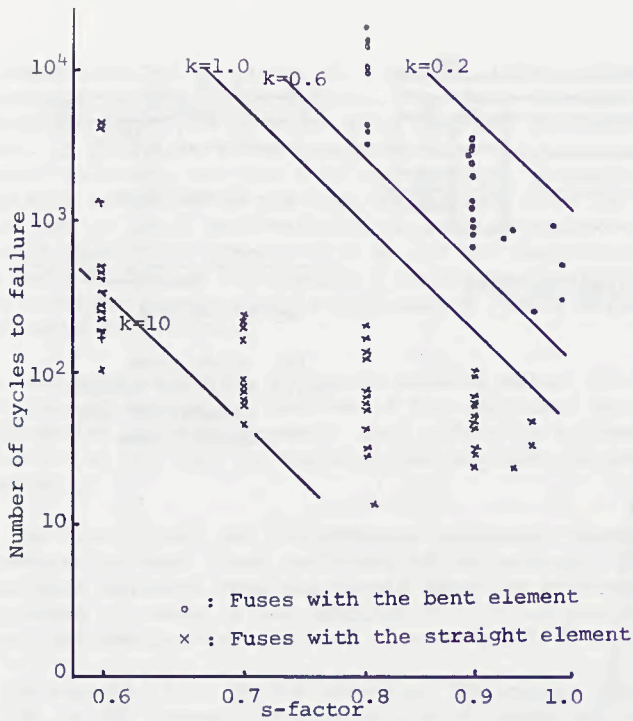


Fig.5 The experimental results of cycles to failure versus the value of s-factor and the curves obtained using Eq. (8)

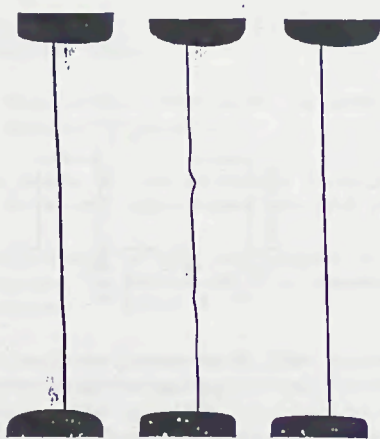


Fig.6 Deformations of the straight element before, during and after pulse current

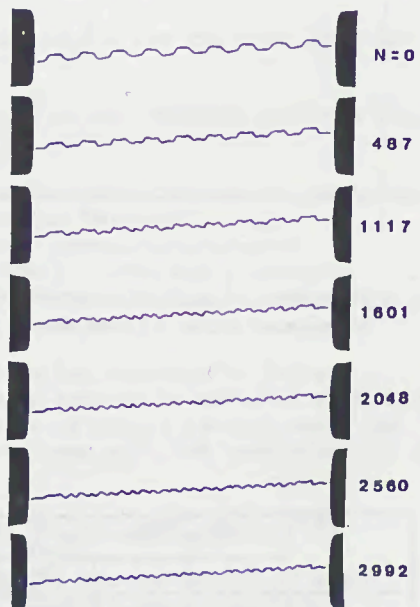
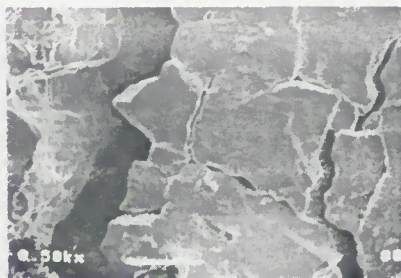


Fig.7 Original bends disappeared and changed into ripples, N is cycles of pulse current



(a) cracks



(b) grown up cracks

Fig.8 Cracks



a front view

a side view

Fig.9 Cracks and their growth at the full section of width under the influence of the prior cold bending work

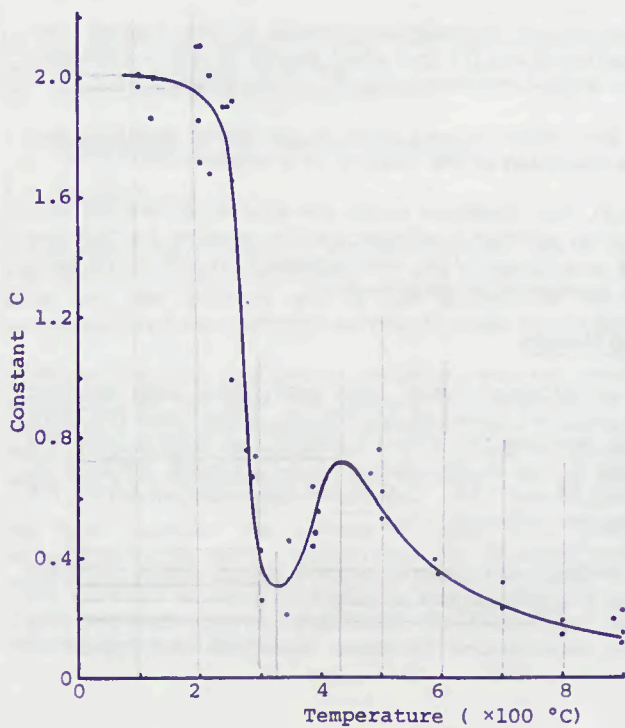


Fig.10 The constant C for silver wire having diameter of 0.7 mm as a function of temperature

THERMAL CONSTANTS OF FILLER AND THEIR INFLUENCE ON THE METALLURGICAL EFFECTS IN FUSE ELEMENTS DURING PULSE DUTY

H W Turner and C Turner

ERA Technology Ltd, Leatherhead, Surrey, UK

1. Introduction

Pulse duty is a form of preloading of a fuselink, which can have an influence on subsequent performance. The importance of pulse duty for miniature fuses has been recognised internationally, as can be seen from the new edition of the IEC miniature fuse specification: IEC 127, now being prepared, which includes tests to ascertain pulse withstand of miniature time-lag fuselinks. These tests consist of 1000 cycles at $10 I_n$ with a duration corresponding to 40% of the pre-arcing I^2t and a repetition rate of 1 pulse per 30 s, followed by one hour at $1.25 I_n$. (I_n = rated current.)

After this test the pre-arcing time at $1.7 I_n$ should be less than 300s. These tests apply to both unfilled and sandfilled miniature fuselinks, and the interval between pulses is normally sufficiently long to make sure that the pulsing has no cumulative effect.

Effects of preloading were considered in an earlier paper (Ref.1), in which it was shown that it was possible to discriminate between temporary and permanent effects.

Pulse duty at a given mean current normally acceptable by the fuselink can result in operation of the fuselink if the I^2t in a short period at the commencement of the pulse exceeds the short-time pre-arcing I^2t of the fuselink (Ref.2).

This paper deals with pulse duty which is very close to the latter situation, but which is insufficient to cause operation of the fuselink on a single pulse.

It has been established (Ref.3), that fuselinks which are sand-filled are far less susceptible to pulse effects than unfilled fuselinks, and the reasons for this are connected with the thermal conditions which are prevalent in the two cases. These thermal conditions are considered in detail below.

2. Experimental Details and Results

Commercial fuselinks of two different types, both sand-filled, with ceramic barrels, were subjected to a series of pulses of dc current. Both types had wire elements, with melting point addition ('M effect'), which was placed near the ends of the elements for type A and in the centre of the element for type B. Two ratings of fuse were used, 3A and 13A. Calculated adiabatic pre-arcing I^2t was considerably different for the different types.

The source of energy for testing with 'square' current pulses was a constant current pulse unit, capable of producing trains of pulses of duration from 0.1 ms to 99.9s, at a fully adjustable duty cycle. The maximum current which could be sustained for 10 ms without deterioration by these fuses was determined by

setting a level at the pre-arcing I^2t and subjecting the fuses to trains of pulses of various values below this level, starting with 50% of the level. The pulses were applied at 10 to 20 ms intervals, so that an estimate of the rate of change of temperature during cooling could be obtained. In general the period 'on' was equal to, or approximately twice the period 'off'. Fig.1 shows typical curves of the change of temperature produced during each pulse and the cooling period for the first ten pulses for equal pulse and cooling periods.

Current and voltage were monitored on a digital oscilloscope, and data stored on floppy disc for further analysis by a dedicated on-line computer. The temperatures were calculated from the resistance ratio of the fuse elements. This is a good means of predicting the proximity to the blowing time of a fuse, and has been used in testing HV fuses at small overcurrent (Ref.4).

X-rays of some of the fuses were taken to determine changes in structure. Structural changes were also investigated by opening up the fuses after test and using an optical microscope. Sections were examined using a scanning electron microscope. The composition of diffused areas was determined by the X-ray emission producing an explanation of the unchanged blowing characteristic even though the metallurgical state was changed after severe pulsing. More details of this aspect of the work are given in Ref.3.

The effects of the thermal constants of the sand filler are such that the fuselinks were capable of accepting single pulses of up to 95% of their 'blowing' current, and rapidly repeated pulses exceeding 70% of their blowing current, without changing their characteristics, and were thus more resistant to the effects of pulsing than the low breaking capacity (unfilled) types previously described in Ref.1.

In the following section a simplified theoretical analysis is presented, which isolates the physical property of the sand which has the biggest effect at different stages of the pulsing process.

3. Importance of the Thermal Constants

3.1 Conductivity

In the above experiments it was seen that the rate of cooling of the fuse element was approximately proportional to the difference in temperature between the wire and the ambient air at the surface of the cartridge (equal to the temperature of the cartridge surface in these experiments).

Although the full equilibrium condition was not reached in these tests, it is interesting to see that the changes in temperature during the pulsing were predictable from the thermal constants of the filler, together with knowledge of the corresponding constants for the element material. The constants involved were the thermal conductivity and diffusivity of the materials.

We first consider the effects of pulse duty upon the fuse element, its temperature rise during pulsing and the equation representing the equilibrium temperature/time relation reached by the element. Assuming no loss of heat, the temperature rise of the element from θ_1 to θ_2 will be given (Ref.1) by the solution of the equation (1):

$$\int_{t_1}^{t_2} i^2 dt = A^2 \frac{dc}{\rho_0 \alpha} \ln \frac{(\theta_2 + \frac{1}{\alpha})}{(\theta_1 + \frac{1}{\alpha})} \quad (1)$$

where

$$\int_{t_1}^{t_2} i^2 dt = \text{the } I^2 t \text{ delivered between times } t_1 \text{ and } t_2$$

θ_1 = temperature of a segment of element cross-section A at time t_1

θ_2 = temperature of a segment of element cross-section A at time t_2

d = density of element material

c = specific heat of element material

ρ_0 = resistivity of element material at 0°C

α = temperature coefficient of resistance of element material averaged over θ_1 to θ_2 .

Thus the I^2t required to raise the temperature from θ_1 to θ_2 may be calculated. The I^2t needed is greater than this amount by the extra I^2t required to make up the losses during the heating process. In the interval between pulses, cooling takes place, and although equilibrium may not yet be reached, it was found possible to calculate the approximate rate of cooling from consideration of steady state conduction, assuming the heat to be conducted out radially. The thermal conductivity K of the sand is approximately equal to that of the barrel in this case, and of the order of $5 \times 10^{-4} \text{ Wmm}^{-1} \text{ K}^{-1}$. Conduction rate is controlled by the equation:

$$\frac{dQ}{dt} = \frac{2 K \pi}{\ln(d_2/d_1)} (\theta_m - 20) \quad (2)$$

Taking the outer temperature of the barrel to be 20°C

where

dQ/dt = rate of loss of heat

d_1 = diameter of the wire (in mm)

d_2 = outer diameter of the barrel (in mm)

θ_m = mean temperature of the wire

But $dQ/dt = \pi/4 \times d_1^2 c_v d\theta/dt$ for each unit length of wire,

where

$$c_v = \text{specific heat per unit volume of the wire}$$

$$d\theta/dt = \text{rate of cooling}$$

For SI units, equation (2) reduces to

$$\frac{d\theta}{dt} = \frac{1.4}{d_1^2 \ln(d_2/d_1)} (\theta_m - 20)$$

$$= K' (\theta_m - 20). \quad (\text{dimensions in mm})$$

Results are shown in Fig.2 for fuselinks of types A and B.

Comparison of experimental and calculated results are given in Table 1.

Table 1

Comparison of calculated cooling constants with experimental results.

External diameter of all fuse barrels = 5.75 mm

Fuselink type and rating	Wire dia mm	K'	
		Calculated	Experimental
A (3A)	0.094	38.5	39.5
B (3A)	0.122	24.4	26
B (13A)	0.33	4.5	6

The thickest wire shows evidence of significant conduction of heat to the end caps. It thus appears that the cooling between pulses is controlled by the conductivity of the filler, particularly for the thinner wires.

3.2 Diffusivity

When the fuse element in sand is subjected to pulses of current at regular intervals, the temperature rises during the current-carrying period, and falls between pulses. Initially, the rise of temperature is considerably higher than the fall, but for currents below the 'run-away' condition, an equilibrium is eventually reached, where the temperature rise during the pulse equals the fall during the off period. This condition is due to the loss of heat into the surrounding sand. The distribution of temperature in the sand can be approximately represented, taking a simplified case of a temperature variation $\Delta\theta$ at the surface of the element of the form $\Delta\theta = \theta_x \cos A$, with the number of cycles per second f , $A = 2\pi ft$, and $dA/dt = 2\pi f$ radians per second. The rate of flow into the sand is dependent on the diffusivity of the sand, κ , which is related to the thermal conductivity, K , the density, ρ and the specific heat c , by:

$$\kappa = \frac{K}{\rho c}$$

the rate of flow can be expressed by the well-known equations:

$$\kappa \frac{d^2\theta}{dx^2} - \frac{d\theta}{dt} = 0 \quad (3)$$

$$\text{or } \kappa \frac{d^2\theta}{dx^2} - \frac{d\theta}{dA} \frac{dA}{dt} = \kappa \frac{d^2\theta}{dx^2} - 2\pi f \frac{d\theta}{dA} = 0 \quad (4)$$

This equation can be solved by taking the constant $\mu = \sqrt{\frac{\pi f}{\kappa}}$ to give

$$\Delta\theta = \theta_x e^{-\mu x} \cos(A - \mu x)$$

For any distance x away from the element in the sand, the temperature variation is from $\theta_x e^{-\mu x}$ to $-\theta_x e^{-\mu x}$, with a lag in temperature of phase angle μx .

Assuming a fluctuation of temperature in the sand of 10% of the fluctuation in the element to be sufficiently low to be able to neglect further effects of the sand, the thickness of sand layer affecting the element surface temperature can be calculated from this formula. For maximum fluctuation at any depth $\cos(A - \mu x) = 1$ and $\Delta\theta = \theta_x e^{-\mu x}$.

$$\text{if } \Delta\theta = 0.1\theta_x, \text{ then } e^{-\mu x} = 0.1 \\ \text{and } \mu x = 2.3$$

$$\text{that is: } x = 2.3 \sqrt{\frac{\kappa}{\pi f}} \quad (\text{mm})$$

The actual diffusivity of the sand surrounding the element is very dependent on the packing factor, the grain size and any impurities or moisture present, so that figures given in the literature may vary by a factor 10 or more.

Taking the following properties for a well-known fuselink:

$$K = 5.10^{-4} \text{ W mm}^{-1} \text{ K}^{-1} \\ C = 1.2 \text{ J g}^{-1} \text{ K}^{-1} \\ \rho = 1.8 \times 10^{-3} \text{ g mm}^{-3}$$

then the diffusivity for closely packed sand is $\kappa = 0.23 \text{ mm}^2 \text{ s}^{-1}$

For $f = 50 \text{ Hz}$ this gives a "depth of penetration": 0.088 mm

This is a measure of the cooling effect of the sand, which cools the surface of the wire during the passage of the pulse and thus can delay the onset of M-effect operation during pulsing. The greater the "depth of penetration", the greater the effect. This local cooling increases with diffusivity of the sand used, "penetration" being approximately proportional to the square root of the diffusivity. The grains in contact with the wire may have a diffusivity which is an order of magnitude greater than the bulk of the filler, the bulk diffusivity being reduced due to the air in the interstices.

The above provides an explanation of the superior performance on pulsing of fuselinks with M-effect in sand compared with similar ratings in unfilled miniature fuselinks (low breaking capacity types).

4. Conclusions

The following conclusions are drawn from the results:

1. The improved resistance to pulsing of sand-filled wire element fuses of low current rating is dependent upon the thermal constants of the filler.
2. The cooling between pulses appears to be determined largely by the thermal conductivity of the filler.
3. The local protective cooling which delays the operation of M-effect, during passage of the pulse, appears to be determined by the diffusivity of the filler.

References

1. Turner, H W and Turner, C : 'Influence of preloading on fuse performance', Fourth International Symposium on Switching Arc Phenomena, Łódź, Poland, 22-24 September 1981. (ERA Report 80-162)
2. Jacks, E : 'High rupturing capacity fuses, design and application of safety in electrical systems', London, E & F N Spon Ltd., 1975.
3. Turner, H W and Turner, C : 'I²t pulses associated with BS1362 fuselinks', ERA Report 81-41; Leatherhead, ERA Technology Ltd., 1981, 'Effect of pulsing on fuses', ERA Report 81-43, Leatherhead, ERA Technology Ltd., 1981.
4. Turner, H W and Turner C : 'Improvements relating to the testing of electric fuses', British Patent No. 117, 817, 1968.

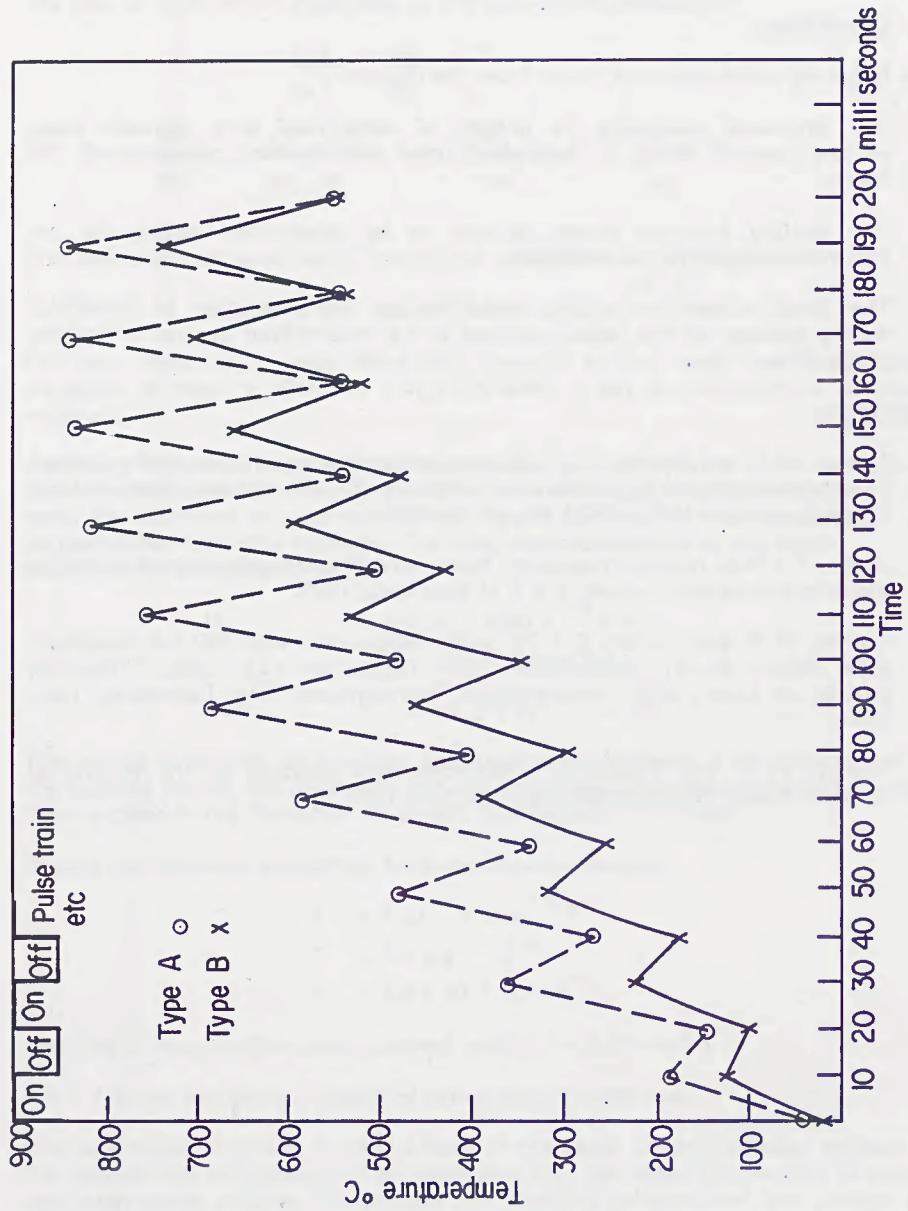


Fig. 1 : Temperature Changes for 3 A Fuselinks, Types A and B. Current Pulse: Type A : 10 A, Type B : 16.7 A

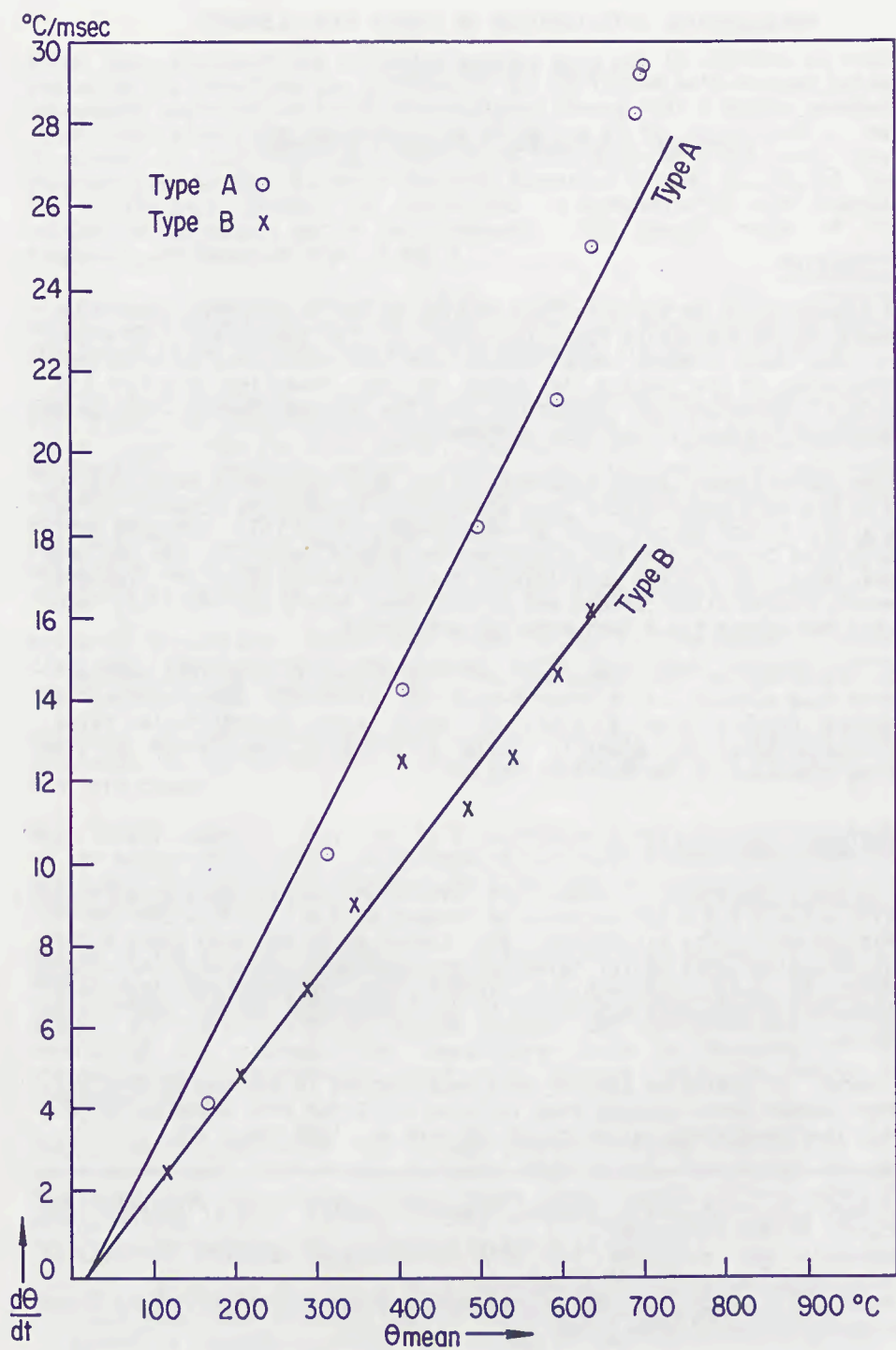


Fig. 2 : Rate of Change of Temperature for 3 A Fuselinks Types A and B

METALLURGICAL DETERIORATION OF COPPER FUSE ELEMENTS
IN HIGH VOLTAGE FUSES

S.Øvland, J.Kulsetås, H.Förster, W.Rondeel

INTRODUCTION

The properties of an electric fuse should, as far as possible, remain unchanged during the entire fuse life-time. It is essential, therefore, that the fuse element metal should have high resistance to oxidation. Furthermore, if the design is based on the so-called M-effect [1], possible intermetallic reactions in the M-spot should not cause significant changes in the fuse performance.

Silver readily meets these demands. It has high resistance to oxidation, and it has been demonstrated that intermetallic reactions between silver and a tin M-spot do not occur at unacceptable rates [2]. Although other metals like copper, zinc and aluminium are widely used in low voltage fuses, most high voltage fuse designs are still based on silver elements. However, rising silver prices and doubts about future availability, have pushed the search for a less precious substitute.

This contribution is concerned with intermetallic reactions between a copper fuse element and a tin M-spot at different temperatures. It contains results from a study of solid state interdiffusion rates, dissolution rates for copper in liquid tin, and a description of the fusing processes in the M-effect region.

EXPERIMENTS AND RESULTS

Solid state reactions. Copper-tin diffusion samples were prepared by fusing a 2.6 x 1.0 x 100 mm piece of Sn onto a 2.6 x 0,135 x 200 mm Cu strip by means of a microtorch. The copper strip had been given a thin (<1µm) silver coating for oxidation protection. Examination of fresh samples by X-ray microanalysis showed that no detectable amounts of intermetallic compounds had formed at the interface during the fusing process.

A number of diffusion samples were heat treated in an oven at four different temperatures ranging from 147°C to 222°C for time spans up to 2800 hrs. The temperature variation in the oven was less than ± 2°C.

S.Øvland is with Norsk Hydro, Research Centre Materials Technology Section, N-3901 Porsgrunn.
J.Kulsetås and H.Forster are with The Norwegian Research Institute of Electricity Supply, N-7034 Trondheim.
W.Rondeel is with A/S Norsk Elektrisk & Brown Boveri, Switchboard and Switchgear Group, N-3700 Skien.

After heat treatment the diffusion samples were cut in sections at right angles to the interface and polished to 0.1 μm finish with diamond paste. Subsequent quantitative X-ray microanalyses showed that a duplex compound layer, with atomic tin concentrations 24.6% and 45.5% respectively, had developed at the interface. This is in accordance with the Cu-Sn phase diagram shown in fig. 1, which predicts formation of the ϵ (Cu_3Sn) and the η' (Cu_6Sn_5) phases. No variations in concentration were detected neither in the metals nor in the compounds. The growth rates of the compounds are shown in figs. 2 and 3.

To check a possible influence of the silver coating, similar diffusion samples were made from uncoated copper strips, and heat treated at 215°C. The growth rates for the intermetallic compounds are shown in fig. 4.

Liquid state reactions. For temperatures exceeding the melting point of tin, 232°C, the diffusion processes simply leads to a dissolution of solid copper into the tin liquid. Dissolution rates were experimentally determined by immersing copper strips into tin melts of different temperatures and copper concentrations. The amount of copper that had been dissolved in a certain period of time, was obtained from the remaining thickness of the copper strip. The temperature of the tin melt was stable when the melt was kept close to its liquidous point, while it decreased by as much as 1.5°C per second for the highest temperatures.

Measured dissolution rates are shown in fig. 5. The amount of copper dissolved from one side of the copper strip has been plotted versus square root of the immersion time.

Analyses of the immersed copper strips show that a thin layer of Cu_3Sn develops at the solid/liquid interface, probably through diffusion of tin into copper.

Most likely copper is dissolved by a continuous growth of the Cu_3Sn layer at the copper side, and a simultaneous dissolution of the compound at the tin side. The thickness of the Cu_3Sn layer was less than 1 μm in all the immersion experiments.

Fusing in the M-effect region. To study the M-effect more closely, a number of fuses with copper fuse elements 2.6 x 0.135 x 520 mm were made. The copper element contained 32 equally spaced constrictions, and had a 2.6 x 1.0 x 5.0 mm tin M-spot placed between two constrictions in the middle of the element. The temperature could be measured by two chromel-alumel thermocouples that were pinched into the M-spot as indicated in fig. 6.

Fusing experiments with low voltage currents ranging from 25 A to 66 A were carried out. For these currents the fusing is caused by the M-effect, and the fusing times range from nearly 3 hrs. down to approximately 17 sec. Careful studies of the M-spot region after current interruption revealed two different patterns of fusing:

- A. The tin M-spot is more or less confined to its original shape and place even after melting, and the copper underneath the tin melt is gradually dissolved until the fusing is completed. Normally the fusing occurs at the edge of the M-spot.

- B. Melted tin flows along the copper strip to a neighbouring constriction, where the narrow copper neck is dissolved into the melt.

Typical M-spot temperature curves for a fusing pattern of type "A", are shown in fig. 6. The temperature increases rather rapidly to the melting point of tin where it slows down considerably due to the melting energy. When the tin is melted, the temperature rise is more or less constant until the temperature starts to escalate just prior to fusing.

In a second series of fusing experiments the current was shunted at different stages in the fusing process between the melting time for tin (t_m) and the total fusing time (t_f). Also in this series the fusing followed pattern "A". Analyses of the M-spot region showed that the copper underneath the tin liquid is gradually dissolved. The dissolution rate is generally higher at the edge of the M-spot. At t_f the dissolution has reached a stage where the current path through solid copper is completely broken, and the current has to flow through the melt. Clearly this causes a run-away effect in the temperature.

It should be noticed that current interruption does not occur when the solid copper strip is broken. Indeed, experiments terminated just prior to fusing showed that the current can flow through the melt even when the copper is completely dissolved 1 to 2 mm to the sides of the M-spot. This proves that final fusing does not occur until the tin-copper melt has reached a temperature at which it has sufficiently low viscosity to flow into the voids between the quartz grains.

DISCUSSION

The annealing experiments have shown that the intermetallic compounds Cu_3Sn and Cu_6Sn_5 develop at the copper-tin interface in an M-spot. The measured thicknesses vary considerably along the interface and even more so between identically heat treated samples. This is due to the fact that the diffusion processes are influenced by a number of statistical parameters like cleanness of the interface, voids in the metals, stress concentrations, etc.

Despite the large spread in the results, figs. 2 to 4 demonstrate that the growth has a parabolic time dependency, at least for long annealing times. It can also be seen that the initial growth rate of Cu_6Sn_5 is considerably higher than the long term growth rate. Cu_3Sn starts to grow after a certain delay time which increases with decreasing temperature. Similar observations were made by Kay and Mackay [3] in a study of tin coatings on copper. The explanation for this is to be found in the phase diagram. Copper is insoluble in solid tin. Diffusion of copper into tin, therefore, immediately leads to the formation of the tin-rich compound Cu_6Sn_5 . Tin, on the other hand, is slightly soluble in copper even at low temperatures (1.3 weight % at 200°C). Hence, diffusion of tin into copper does not lead to formation of Cu_3Sn until the concentration has reached the solubility limit. The time needed to reach this limit naturally increases with decreasing temperature. When the Cu_3Sn compound starts to grow, one would expect the Cu_6Sn_5 growth rate to be reduced since the availability of copper for further growth is

reduced. This is in accordance with our results.

Comparison of figs. 2 and 3 with fig. 4 indicates that the thin silver coating has a very limited effect on the growth of copper-tin compounds. It seems that the growth rate of Cu_3Sn is somewhat higher for the uncoated copper strip. This could, however, equally well be due to differences in residual stresses in the two types of copper strips [3].

Fig. 7 is an Arrhenius plot of the quadratic growth rates obtained from figs. 2 and 3. The experimental values for Cu_3Sn falls reasonably well on a straight line. This is not true for Cu_6Sn_5 . A possible explanation might be the ordering transformation that occurs for this compound at 186°C . The results are, however, too limited to confirm this.

The measured growth rates for Cu_3Sn are in reasonable agreement with those reported by Onishi and Fujibuchi [4], while there are considerable discrepancies for Cu_6Sn_5 , our results showing a much stronger temperature dependency. No satisfactory explanation has been found for this difference.

The time spans needed to complete the transformation of a $50\ \mu\text{m}$ thick copper fuse element to high resistance intermetallic compounds are listed in table 1.

Temp. [$^\circ\text{C}$]	147	182	222
Transf.time	14 years	2.5 years	24 days

Table 1. Transformation times for $50\ \mu\text{m}$ copper.

This demonstrates that to prevent the copper element underneath the M-spot from being transformed into high resistance compounds, the long term service temperature should not exceed approximately 150°C . Short term temperature rise, due to for instance motor starts or inrush currents, does not cause unacceptable deterioration even if the temperature approaches the melting point of tin (232°C). It should be noted that the transformation times for copper are considerably longer than for silver [2].

Dissolution rates for solid copper in liquid tin have proved to be strongly temperature and concentration dependent, as clearly demonstrated in fig. 8. For pure tin melts the dissolution rate follows an Arrhenius type of equation, while it decreases more rapidly with temperature for melted alloys. Again it appears that the corresponding process between silver and tin is markedly faster [5].

From these results one would expect the M-effect for copper to be slower than for silver, as indeed it is. In our experiments the fusing times for copper elements were 3 to 5 times larger than those for corresponding silver elements, ($2.6 \times 0.12 \times 520\ \text{mm}$).

The interrupted fusing experiments have shown that the fusing process

follows one of two different patterns. Surprisingly enough it turned out that the total fusing time is independent of the fusing pattern for a given current. Further it was established that the ratio between the melting time for the M-spot (t_m) and the total fusing time (t_f) very nearly is constant, $t_m/t_f \approx 0.2$, in the M-effect region. One would expect, therefore, that if a fuse element during service has suffered temperatures taking the fusing process close to current interruption, the actual part of the time-current characteristics will be shifted toward shorter times by a factor of almost 5. Clearly this kind of aging is not acceptable, especially not for motor fuses. Frequently occurring service currents should, therefore, not be allowed to bring the fuse element to the melting point of the M-spot.

CONCLUSIONS

Copper fuse elements containing a tin M-spot are gradually aged even at temperatures below the melting point of tin through formation of high resistance intermetallic compounds. The aging rate is, however, acceptably low.

For temperatures exceeding the melting point of tin the aging rate is strongly accelerated and could lead to undesirable changes in the time-current characteristics.

Copper is superior to silver as far as resistance to intermetallic reactions in the M-spot is concerned.

REFERENCES

- [1] Metcalf, A.W (1939), BEAMA J. 44, 109-112.
- [2] Daalder, J.E., Kulsetås, J. (1979), Diffusion Phenomena in Sn-Ag Couples Around and Below the Eutectic Temperature. EFI TR NR. 2526.
- [3] Kay, P.J., Mackay, C.A. (1976), The Growth of Intermetallic Compounds on Common Basis Materials with Tin-Lead Alloys. Trans. Inst. Metal Finishing, 54, 68-74.
- [4] Onishi, M., Fujibuchi, H. (1976), Reaction-Diffusion in the Cu-Sn System. Trans. JIM, 16, 539-547.
- [5] Valle, A. (1980), Thesis. The University of Trondheim, Norwegian Institute of Technology, Physics Department, (in Norwegian).

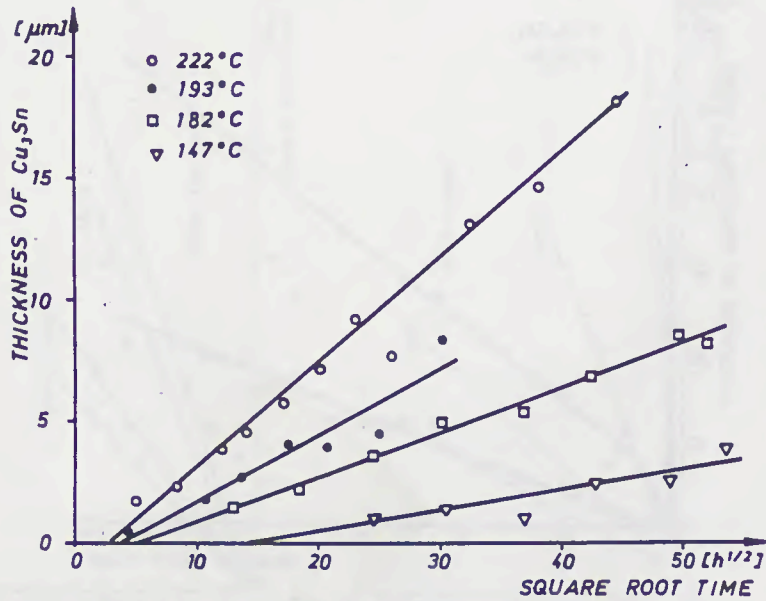
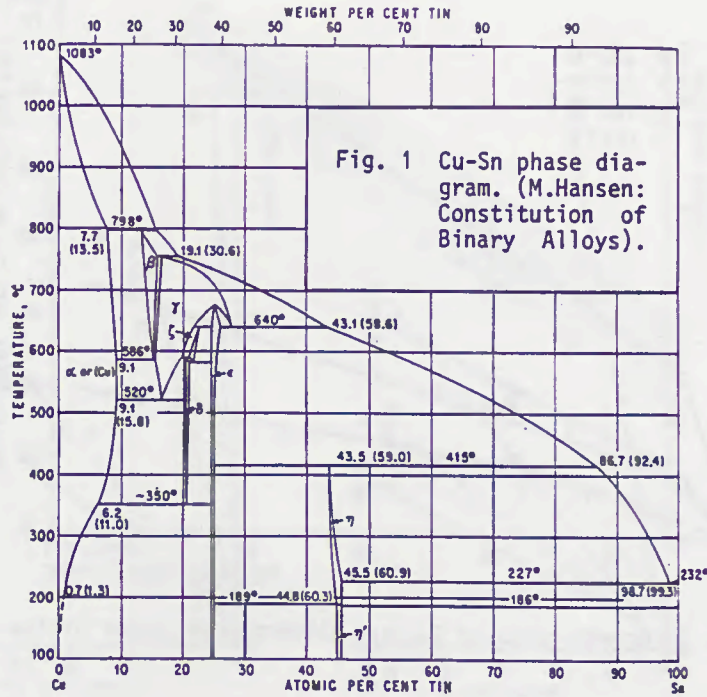


Fig. 2 Growth rates of Cu_3Sn , silverplated copper strips.

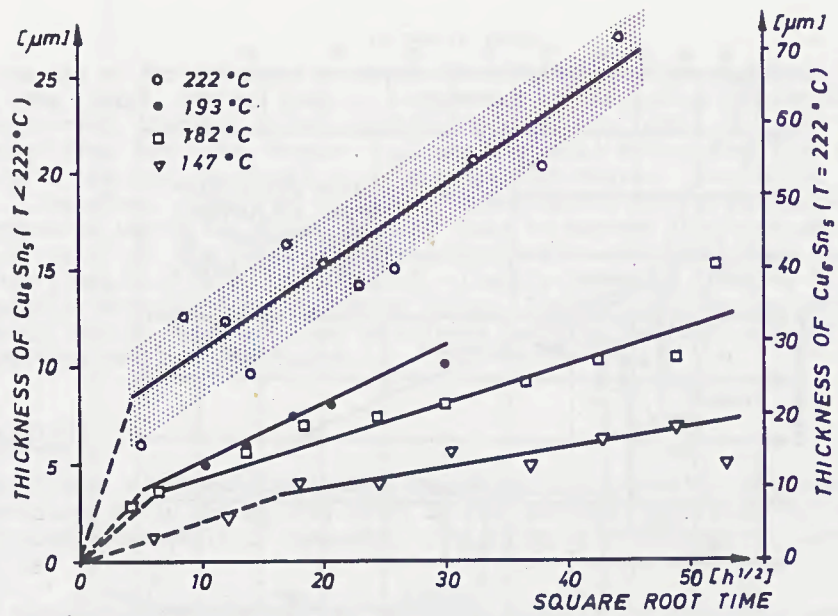


Fig. 3 Growth rates of Cu_6Sn_5 , silverplated copper strips.

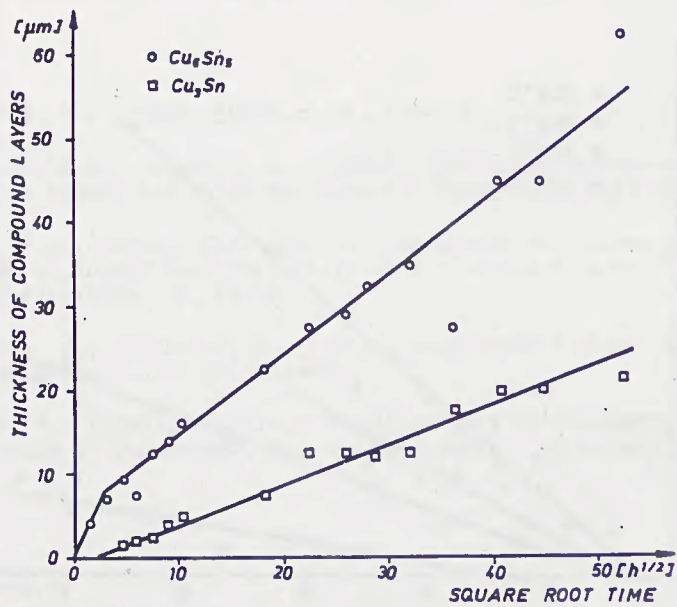


Fig. 4 Growth rates of Cu_3Sn and Cu_6Sn_5 at 215°C , unplated copper strips.

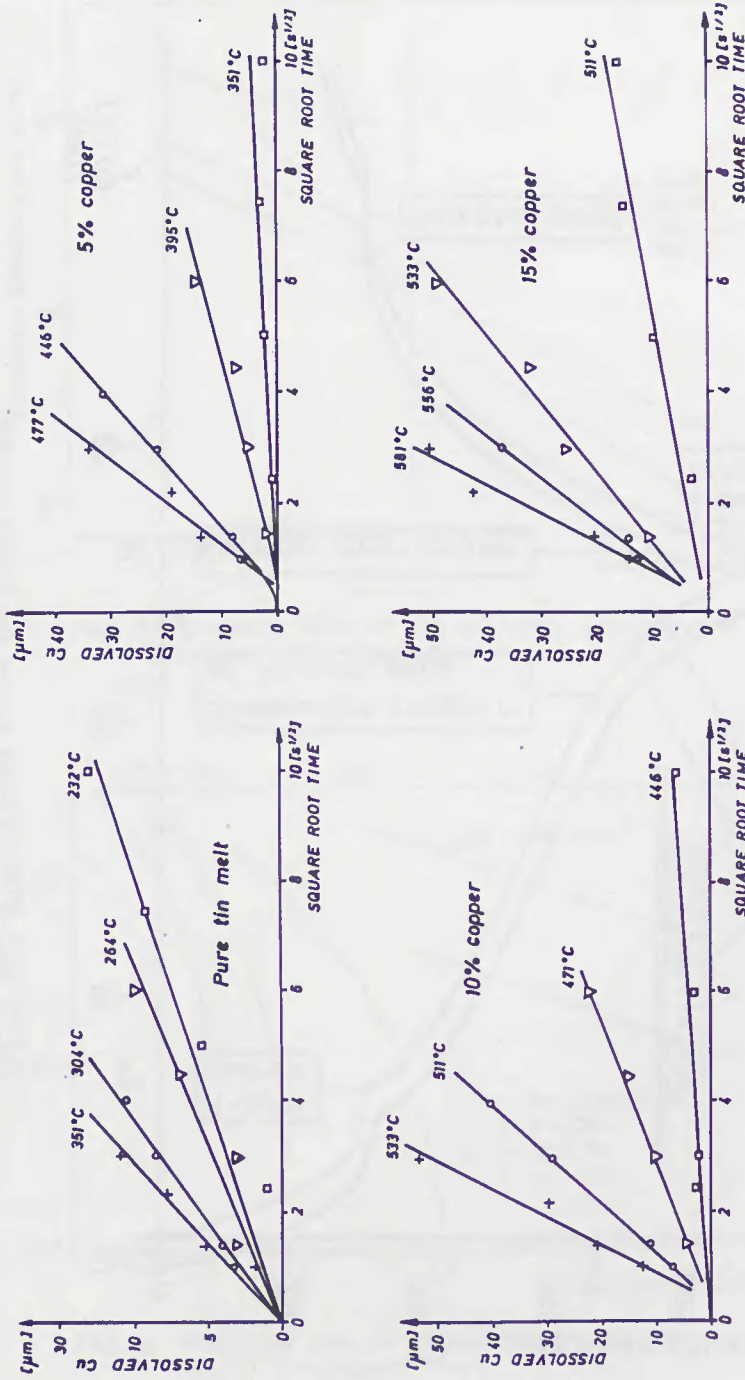


Fig. 5 Dissolution rates for solid copper in liquid tin-copper alloys.

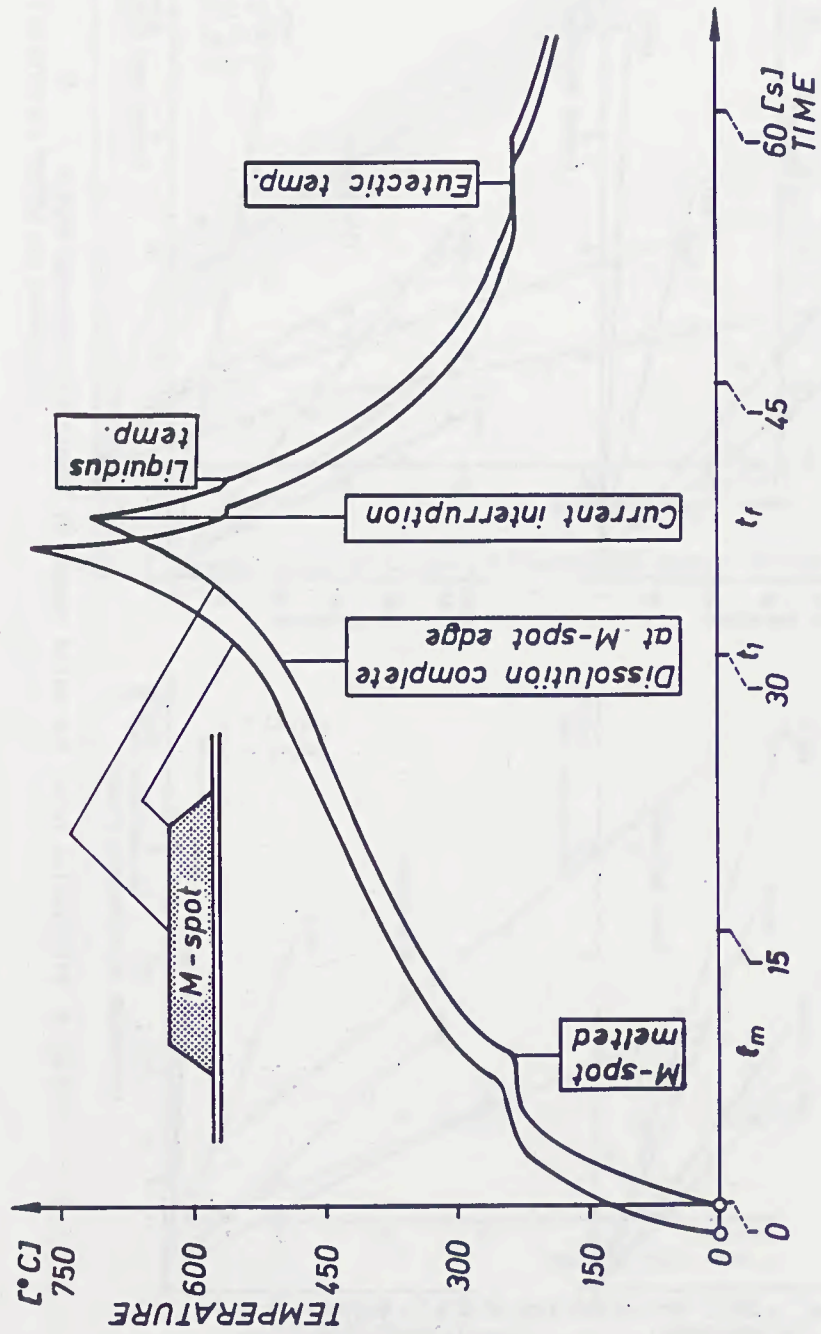


Fig. 6 M-spot temperature during the fusion process.

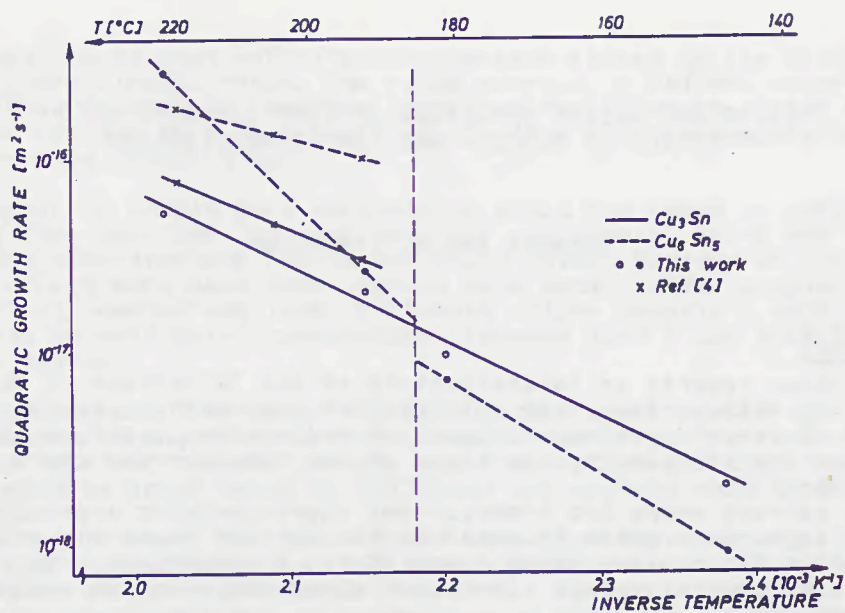


Fig. 7 Arrhenius plot of the quadratic growth rates of intermetallic compounds.

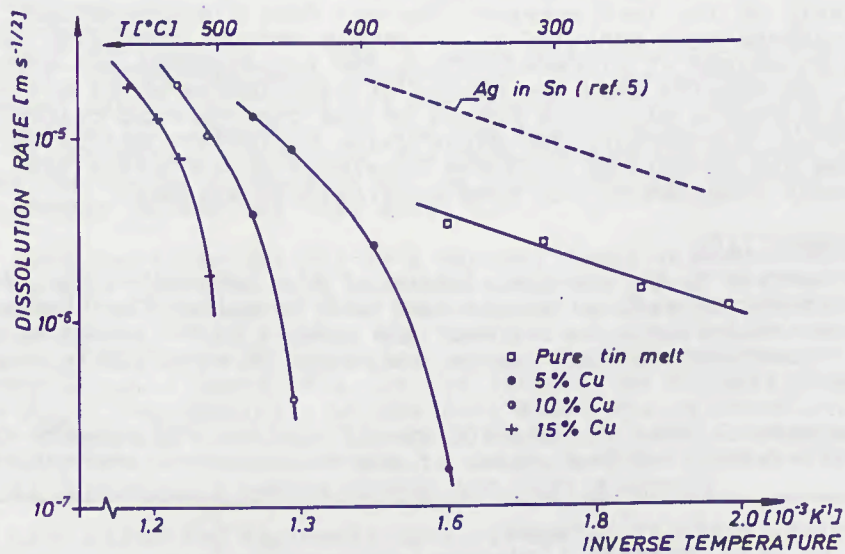


Fig. 8 Arrhenius plot of dissolution rates of copper in liquid tin-copper alloys

FUSING AND AGEING BEHAVIOUR OF FUSE ELEMENTS WITH
"M"-EFFECT AT MEDIUM- AND LONG-TIME OVERLOAD

M. Hofmann and M. Lindmayer

ABSTRACT

This paper reports on investigations of the "M"-effect of fuse elements with various base metal/solder combinations in the range of very-long-time overload and medium-time overload. Two factors are influencing the shape of the time/current characteristics:

- The current where the time/current characteristic approaches the asymptotic shape is equal to the current where the solder reaches the solidus point temperature. A comparison with calculated current values shows good agreement with the measurements.
- In the medium-time range the different fuse elements perform according to the solder's dissolution capability for the base metal. There is no correlation with the solidus point temperature.

In further tests the dissolution behaviour was studied independently of the load current. Various fuse element/solder combinations were annealed in a furnace and the remaining base metal thickness at different times and temperatures was measured. The results show two ranges of dissolution which are in good accordance with both ranges of the time/current characteristics. Furthermore the dissolution capability can be described and calculated with the knowledge of diffusion laws and phase diagrams of the base metal/solder systems.

1. INTRODUCTION

In "M"-effect fuses the dissolution of the base metal (Cu, Ag) by a deposit of soft solder is utilized to adjust the time/current characteristics in the overload range. On the other hand this irreversible effect may be the cause of undesirable ageing.

IEC recommendations /1/ and VDE specifications /2/ require for standard fuses that the shapes of the time/current character-

Dipl.-Ing. Matthias Hofmann
Prof. Dr.-Ing. Manfred Lindmayer
Institut für Elektrische Energieanlagen
Technische Universität Braunschweig
D-3300 Braunschweig, Germany

istics lie between definite time/current values in the overload and short circuit range. The rated current is defined according to these values. The maximum test time for fuses up to 160 A rated current is 1 or 2 hours. No further regulations are made concerning longer times.

In order to obtain more information about the range of very long time overload (between one hour and several days) and of medium time overload (below one hour) investigations of the "M"-effect were made with various base metal/solder combinations at overcurrent load. Different solder materials with different solidus point temperatures between 124° C and 327° C were tested.

At overcurrent load tests the dissolution behaviour is not independent of the load current, because the effective remaining cross section, the resistance, the temperature and thus the dissolution speed mutually influence and enhance each other.

In order to study the dissolution behaviour independently of the load current various fuse element/solder combinations were annealed at different temperatures in a furnace. The dissolution of the base metal in dependence of time and temperature was studied, measuring the remaining base metal thickness by micrographs. The results are compared with diffusion theories and they contribute to explain the ageing behaviour as well as the shape of the time/current characteristics, which had been found by the overload current tests.

2. TEST METHODS

2.1 Test Arrangement Fig. 1 shows the principle of the test circuit. The high-current transformer T2 is connected to the AC power supply (220 V/50 Hz) over contactor K1, variable-ratio transformer T1, contactor K2 and the antiparallel thyristors V1, V2. The secondary circuit of the high-current transformer supplies the series connection of the shunts R1, R2, current transformer T3 and the fuse model E.

The tests were carried out in a current range between 80 A and 130 A, with currents kept constant within ± 1 A by a control circuit. The fuse model E is designed to hold replacable test fuse elements. Fig. 2 shows the basic dimensions of the fuse elements. One edge of the solder deposit is located in the centre of the element, i.e. at the site of the highest temperature ϑ_{\max} . The terminals of the fuse model are watercooled. Their temperature is kept constant at 18° C - 19° C to ensure reproducible random conditions. All tests were carried out with air as surrounding medium around the fuse elements.

The main measuring equipment consists of:

- a. a time counter, which records the fusing time in steps of 20 ms.
- b. an infra-red radiation pyrometer, which allows contactless temperature measurement on the fuse element surface.

c. an x-t-recorder for the fuse element voltage and the temperature of the solder deposit.

2.2 Characteristic Data of Investigated Materials Two base metals were used for the fuse elements:

- Cu
- Ag

Several solder alloys with low, medium and high eutectic temperatures and melting temperature range respectively were chosen:

- Bi/Pb	55,5/44,5	wt. %	124° C
- Bi/Sn	57/43	wt. %	134° C
- Sn/Cd/Zn	70/25/5	wt. %	160° C
- Sn/Cd	80/20	wt. %	177° C - 192° C
- Sn/Pb	60/40	wt. %	183° C
- Sn			232° C
- Pb			327° C

(Data: manufacturers' data and /3/)

2.3 Fusing Tests These tests were carried out in the circuit of fig. 1 with the material combinations of chapter 2.2. For each current and material approximately 5 single trials were carried out. The time t_s until fusing is plotted as an average.

2.4 Dissolution Behaviour Tests The following base metal/solder combinations were exposed to different temperatures in a furnace (base metal + solder):

- Cu + Sn
- Cu + Sn/Pb 60/40
- Ag + Sn
- Ag + Sn/Cd 80/20

The temperature values and the annealing times for the tested fuse elements were:

- 150° C 0 - 20 days
- 200° C 0 - 10 days
- 250° C 0 - 50 hours
- 350° C 0 - 320 minutes
- 480° C 0 - 60 minutes

After each test the fuse elements were cooled down quickly.

Afterwards micrographs were made and the remaining base metal thickness \bar{d} was measured. The dissolution depth \bar{x} is then given by the following equation:

$$\bar{x} = \frac{d_l + d_r}{2} - \bar{d} \quad (1)$$

(see also fig. 3)

3. RESULTS

3.1 Fusing Characteristics at Medium- and Long-Time Overload

Fig. 4 shows the measured time/current characteristics. The time range covered lies between 10 minutes and 7 days. The solid lines connect the measured time/current values. The dashed lines lie outside the range of measurement and represent the shape of curves to be expected by theoretical considerations.

Material symbols with arrows mark the asymptotic current values gained theoretically by assuming that the solidus point (melting point) temperature is just reached there. Arrow symbols within the figure mark current values, where the fuse elements were tested without fusing. In these cases the solder also never became liquid.

It was expected that evident material changes occur only when the solder is liquid. This was confirmed for at least 4 material combinations (Ag + Sn, Cu + Sn, Cu + Sn/Pb 60/40, Cu + Sn/Cd/Zn 70/25/5). For these materials at very long times and for the same base metal (Cu) the asymptotic current values are arranged in the sequence of the solidus temperatures T_s , e.g.:

Cu + Sn/Cd/Zn 70/25/5	($T_s = 160^\circ \text{C}$)	at 85 A,
Cu + Sn/Pb 60/40	($T_s = 183^\circ \text{C}$)	at 90 A,
Cu + Sn	($T_s = 232^\circ \text{C}$)	at 95 A.

As mentioned before these current values can be determined by calculation. For this calculation an equation derived by /4/ is used, which describes the dependence between current I and temperature ϑ_{\max} in the centre:

$$I = \sqrt{\frac{\lambda \cdot \kappa_e}{\alpha_e}} \cdot \frac{2 \cdot b \cdot d}{l} \cdot \arccos \left(\frac{1}{\vartheta_{\max} \cdot \alpha_e + 1} \right) \quad (2)$$

<p>I - current λ - heat conductivity κ_e - electrical conductivity α_e - temperature coefficient of electrical conductivity</p>	<p>b - width of fuse element d - thickness of fuse element l - length of fuse element ϑ_{\max} - maximum temperature at $l/2$</p>
--	---

The conditions for the validity of equation (2) are:

- Heat conduction occurs only within the base metal of the fuse element to the terminals. This is often valid in air.
- Negligible electric current and heat flow occurs through the solder deposit. This condition is nearly fulfilled because the electrical and thermal conductivities of the solder are much smaller than those of the base metal.

If the solidus temperature T_s is taken for ϑ_{\max} and the materials data are inserted, the equation gives the desired current values.

Fig. 5 shows the calculated values, which are compared with the measured currents at which the solders became liquid. The results show good agreement of calculations and measurements.

The comparison of Cu + Sn and Ag + Sn fuse elements shows that the asymptotic course of the Ag + Sn characteristics lies at a higher current (100 A) than that of Cu + Sn (95 A). This effect could be expected because of the better heat conductivity of silver. With higher currents, however, the greater dissolution capability for silver quickly leads to smaller fusing times of Ag + Sn fuse elements in comparison with Cu+Sn.

In view of time/current behaviour and ageing this leads to the following conclusions: From known literature /5/ it could be expected that the diffusion speed is practically negligible in the solid state, and becomes effective only when the solder is liquid. The measurements as well as the calculation basing on this assumption show that the asymptote of the time/current characteristics actually coincides with the current where the solder becomes liquid. At a higher current range the dissolution capability predominates the fusing behaviour.

The influence of solidus temperature and dissolution capability must not coincide. Therefore the consequence is that crossovers between different time/current characteristics do exist.

In practical application the rated current of a fuse is defined at long fusing times according to two values /1, 2/:

- a. the conventional non-fusing current $I_{nf} = 1,3 \cdot I_N$
- b. the conventional fusing current $I_f = 1,6 \cdot I_N$

The characteristics have to run between these angle points. The conventional fusing time is e.g. one hour for fuses up to 63 A rated current.

In order to compare the characteristics of different base metal/solder combinations it is essential to refer all characteristics to the same rated current. Therefore all characteristics have to be modified with known methods like changes of cross-section and/or length.

Fig. 6 shows the results of such an adaptation. All characteristics were fit by multiplying the currents of fig. 4 with a constant in order to run through the point with the conventional time 1 hour and 91,35 A (which is $1,45 \cdot I_N$ of a fuse with $I_N = 63$ A rated current).

It can be recognized that at this point most of the base metal/solder combinations have not reached the asymptotic shape and show fusing after some hours at even lower overcurrents.

This means that at low long-time overloads ageing starts the earlier the more the asymptote lies at lower overcurrents. Especially the fuse elements with solders, which have low solidus temperatures, are expected to be more subject to

ageing, e.g. Cu + Sn/Pb 60/40 is more subject to ageing than Cu + Sn and Ag + Sn. At medium-time overload the specific dissolution behaviour of the materials dominate the time/current behaviour.

3.2 Results Of Dissolution Behaviour Tests Already the newly manufactured fuse elements showed a certain depth of dissolution, referred to as starting dissolution depth. The single starting values of Cu + Sn fuse elements scattered between 0 and 9 μm , those of Cu + Sn/Pb 60/40 fuse elements between 0 and 7 μm . These values are typical for the dissolution by the manufacturing process (soldering). They are plotted at $t = 0$ in the following diagrams.

As results of the annealing tests with Cu+Sn and Cu+Sn/Pb 60/40 fuse elements fig. 7 shows the dissolution depth \bar{x} (see also fig. 3) in dependence of time t with temperature T as parameter.

Generally the dissolution depth increases with higher temperature. In the beginning a fast dissolution occurs, followed by a certain stagnation or saturation after some time.

As long as the test temperatures were lower than the solders' solidus temperatures no progress of the dissolution was detectable. All measured \bar{x} values lied within the starting range even after 20 days of annealing time.

But at $T = 200^\circ\text{C}$ the Sn/Pb 60/40 solder is already liquid whereas the Sn solder is still solid. Cu + Sn/Pb 60/40 shows already an increasing dissolution depth with the time whereas that of Cu + Sn remains still in the starting range. At temperatures above 250°C when both solders are liquid the dissolution depth of Cu + Sn is always greater than that of Cu + Sn/Pb 60/40. Then the curves of the dissolution depth also characterize the fusing behaviour under current load. In fig. 4 above 95 A - the current where both solders are liquid - Cu + Sn shows always a quicker dissolution i.e. the fusing time is smaller than that of Cu + Sn/Pb 60/40. The dissolution capability then rules the fusing behaviour.

The measurements of the annealing tests confirm that both ranges of dissolution are in good accordance with the two ranges of the time/current characteristics.

Theoretically the dissolution capability could be described with the knowledge of diffusion laws and phase diagrams of the base metal/solder systems.

With the special example of Cu + Sn this means:
Diffusion mainly occurs from Cu to Sn /5/.

At temperatures below the solidus temperature this leads to the growth of intermetallic layers at the interface between base metal and solder. The growth rate is so small that it can be neglected in the considered time range.

At temperatures above the solidus point the diffusion speed of copper into tin becomes higher by orders of magnitude /6/. The reverse direction tin into copper is negligible.

Now two effects are responsible for the value of the dissolution depth:

a. The growth of intermetallic layers at the interface. Three intermetallic layers exist in the investigated temperature range /3, 5, 6/, see also fig. 8:

1. δ -phase (Cu₄₁ Sn₁₁)
2. ϵ -phase (Cu₃ Sn)
3. η - or η' -phase (Cu₆ Sn₅)

They were identified in micrographs in the above sequence between the copper base and tin.

b. The dissolution of copper in the liquid solder.

Because the diffusion speed is proportional to the concentration gradient, the dissolution starts with a steep increase at $t = 0$. After some time the concentration of copper in tin approaches a temperature-dependent saturation value which corresponds to the liquidus line in the phase diagram fig. 8, e.g. 1,35 % by weight at 250° C, 4,33 % at 350° C, 13,42 % at 480° C (points marked with circles in fig. 8). When this saturation value is reached no further copper is dissolved by the liquid solder.

Under the assumption that the base metal is dissolved in the liquid tin until saturation and no additional intermetallic layers are formed, and that the dissolution occurs uniformly under the original area of the solder, a theoretical maximum dissolution depth for $t \rightarrow \infty$ can be calculated. The final dissolution depth x_{∞} is only dependent on the saturation concentration $C_S(T)$, the densities ρ_{Sn} and ρ_{Cu} and the height d_{Sn} of the solder deposit. Equation (3) gives the correlation:

$$x_{\infty} = \frac{\rho_{Sn}}{\rho_{Cu}} \cdot d_{Sn} \cdot \frac{C_S(T)}{1 - C_S(T)} \quad (3)$$

- x_{∞} - dissolution depth for $t \rightarrow \infty$
 d_{Sn} - height of new solder deposit
 ρ_{Sn} - density of tin
 ρ_{Cu} - density of copper
 $C_S(T)$ - saturation concentration by weight (depending on temperature) for copper in liquid tin according to liquidus lines.

The horizontal lines 1 in fig. 7 show the values of the maximum dissolution depth according to equation (3). For a more accurate picture also the copper containing intermetallic layers have to be considered. Their thicknesses at the maximum annealing time were measured from micrographs and converted to a copper thickness according to their copper content and added to the value given by equation (3).

The lines 2 show the results.

The measured maximum values and the calculated values show good agreement.

These values were calculated with the solder height of newly manufactured fuse elements. During the annealing time, however, the shape of the solder deposit changes and the area of the interface between deposit and base metal changes e.g. from 4 mm length to about 4,4 mm. If this height reduction to about 90 % of the manufacturing height is taken into account an even much better agreement between calculation and measurement is obtained.

A comparison between the results shows that at higher temperatures (350-480° C) the dissolution of copper in liquid tin until saturation dominates indeed, whereas at lower temperatures the formation of intermetallic layers contributes about 50 % to the total copper consumption.

The lines 3 and 4 in fig. 7 show theoretical results for Cu + Sn/Pb 60/40 fuse elements. In the investigated temperature range the dissolution capability of Pb for Cu is very small. Therefore the lead content of the solder can be considered as a mainly inactive filler, reducing the amount of the active component tin to 60 weight % or 70 volume %. Then the theoretical values of the dissolution depth were calculated by multiplication of the Cu + Sn values from equation (3) with the factor 0,7 according to the solder's tin content by volume.

The measured values confirm this expected tendency, the deviation is, however, greater. A more precise explanation would demand the consideration of the exact system Cu-Sn-Pb.

Further tests were made with fuse elements, where silver was the base metal. The solder materials were Sn and Sn/Cd 80/20. Fig. 9 shows the results.

The starting dissolution depth of Ag fuse elements is greater than that of Cu fuse elements. At higher temperatures the dissolution of the base metal is much stronger with Ag fuse elements. Especially the Ag + Sn fuse elements show sometimes a big scatter of the dissolution depth.

In the temperature range of 250° C to 480° C Ag + Sn always shows a greater dissolution depth in comparison with Ag + Sn/Cd 80/20.

At a temperature $T = 250^{\circ}\text{C}$ the agreement between measured and calculated (see equation (3)) values for both Ag fuse elements is quite good. But at higher temperatures (350°C and 480°C) both solders tend to spread widely across the surface of the base metal. This causes an unpredictable and not very constant reduction of the height of the solder deposit. It leads to inaccuracies in the precalculation of the maximum dissolution depth by using the solder deposit height of newly manufactured fuse elements.

If the solder spreading is suppressed, the calculation is practicable again.

Altogether the saturation effect may also have great influence on the fusing behaviour at low overload currents and long fusing times. In order to achieve fusing in this range, the base metal beneath the solder deposit must be dissolved through the whole thickness. For safe operation the height of the solder deposit should not remain under a certain minimum height which, under the simplified assumptions of equation (3), reads

$$d_{\text{solder}} \geq d_{\text{base}} \cdot \frac{\rho_{\text{base}}}{\rho_{\text{solder}}} \cdot \frac{1 - C_s(T)}{C_s(T)} \quad (4)$$

Otherwise an undesirable stabilization at high temperature levels is possible.

4. SUMMARY

The dissolution behaviour of base metal and solder is the important factor in the overload current range concerning the fusing and ageing behaviour.

Two temperature ranges must be distinguished:

- The temperature of the solder deposit is below the solidus point temperature. The dissolution of base metal is very slow and practically negligible.
- The temperature is greater than the solidus temperature. Then more evident dissolution occurs by growth of inter-metallic layers and dissolution of the base metal in the liquid solder up to saturation. The last effect predominates at higher temperatures.

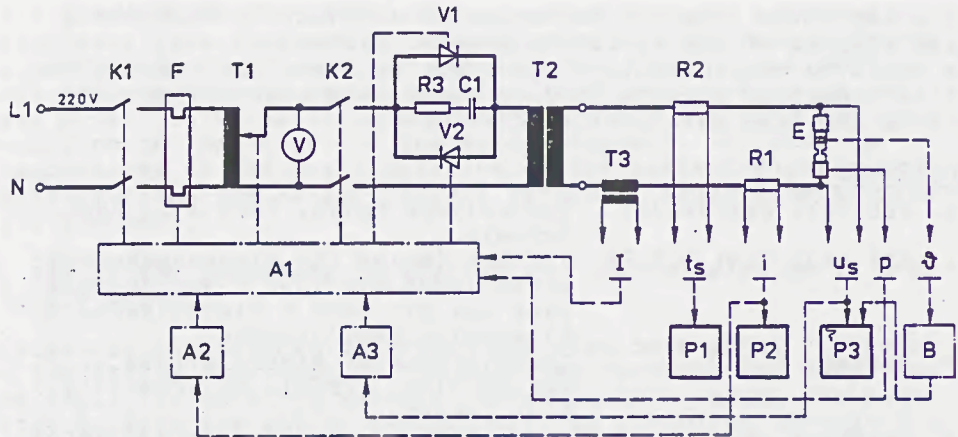
With respect to ageing the results show that fuse elements with solder deposits, which have low solidus temperatures, are more subject to ageing at long-time overload than those, which have higher solidus temperatures.

With respect to fusing characteristics the results show that the asymptotic current values could be estimated by supposing that the solder deposit becomes liquid at these currents. At greater overload currents the fusing behaviour is ruled by the dissolution behaviour. The interpretation of measured dissolution curves at different temperatures shows that characteris-

tic dissolution data can be derived theoretically from the phase diagram of the solder/base metal system. The opposite requirements of good ageing behaviour and desired fusing behaviour have to lead to acceptable compromises concerning the base metal/solder combination.

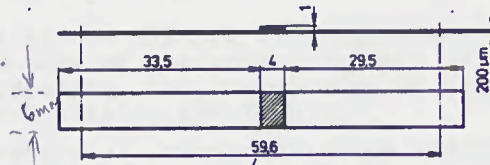
REFERENCES

- /1/ IEC-Publication 269 Low voltage fuses, Part 1-3, Genf, Schweiz.
- /2/ VDE 0636 Teil 1/8.76 VDE-Bestimmung für Niederspannungssicherungen bis 1000 V Wechselspannung und bis 3000 V Gleichspannung, Allgemeine Festlegungen.
- /3/ Hansen, M.: Constitution of Binary Alloys 2nd edition, (1958), Mc Graw-Hill Book Company.
- /4/ Großkopf, R.: Kurze Sicherungsschmelzleiter unter Flüssigkeit zum Schutz von Starkstromanlagen bei Kurzschlüssen. Thesis TU Braunschweig, (1966).
- /5/ Zakraysek, L.: Intermetallic Growth in Tin-Rich Solders, Welding Journal, Research Suppl., (Nov. 1972), p. 536-541.
- /6/ Fidos, H.,
Schreiner, H.: Feuerverzinnung von Kupferschalt-
drähten I+II,
Z. Metallkunde, Bd. 61 (1970)
H. 3, p. 225-228 and H. 4, p. 273-278.



- | | | | |
|----|-------------------------------|--------|-----------------------------|
| A1 | control unit | R3, C1 | thyristor protection |
| A2 | PI-current control | T1 | variable-ratio transformer |
| A3 | limit value contactor | | (22 kVA, 220/0...220 V) |
| B | infra-red radiation pyrometer | T2 | high current transformer |
| E | fuse model | | (40 kVA, 220/8x5 V) |
| F | over-current protection relay | T3 | current transformer |
| K1 | contactor 1 | V1, V2 | thyristors |
| K2 | contactor 2 | | |
| P1 | time counter | I, i | test current |
| P2 | digital voltmeter | p | cooling water pressure |
| P3 | x-t recorder | us | fuse element voltage |
| R1 | shunt for current measurement | ts | fusing time |
| R2 | time counter shunt | phi | temperature of fuse element |

Fig.1 Test circuit



(length between watercooled terminals)

Fig.2 Dimensions of fuse elements

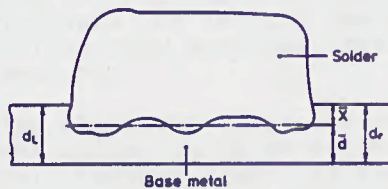


Fig.3 Principle of evaluation of micrographs

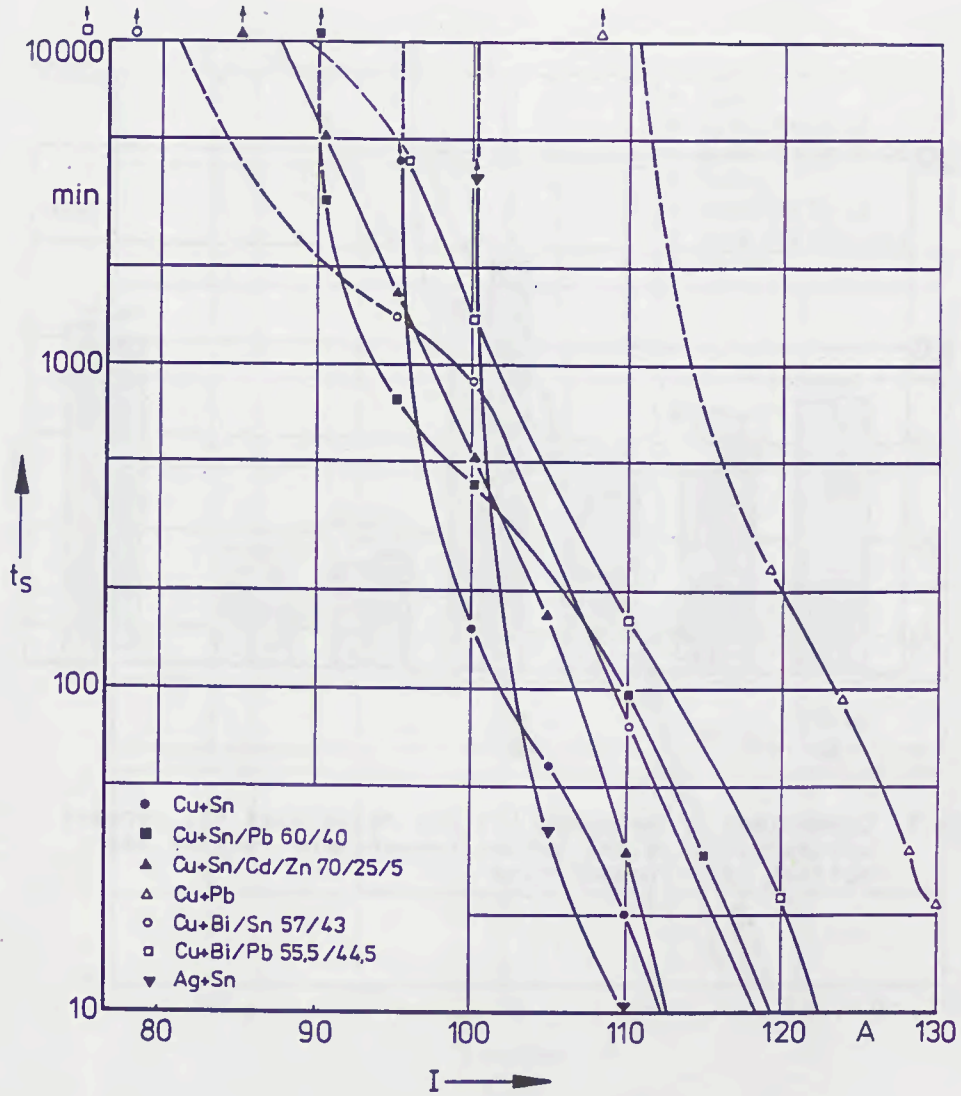


Fig.4 Time/current characteristics at medium- and long-time overload

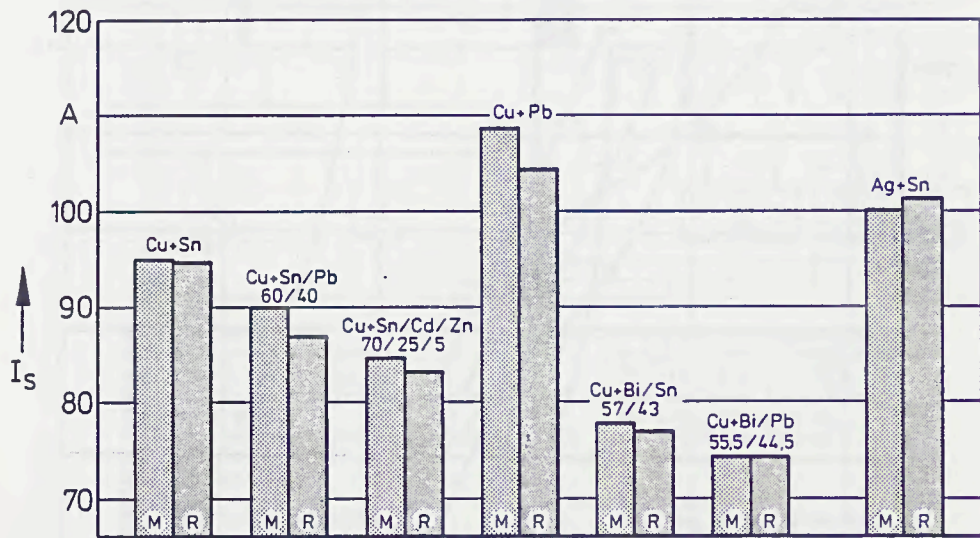


Fig.5 Comparison of measured (M) and calculated (R) current values at which the solder temperature reaches the solidus point temperature

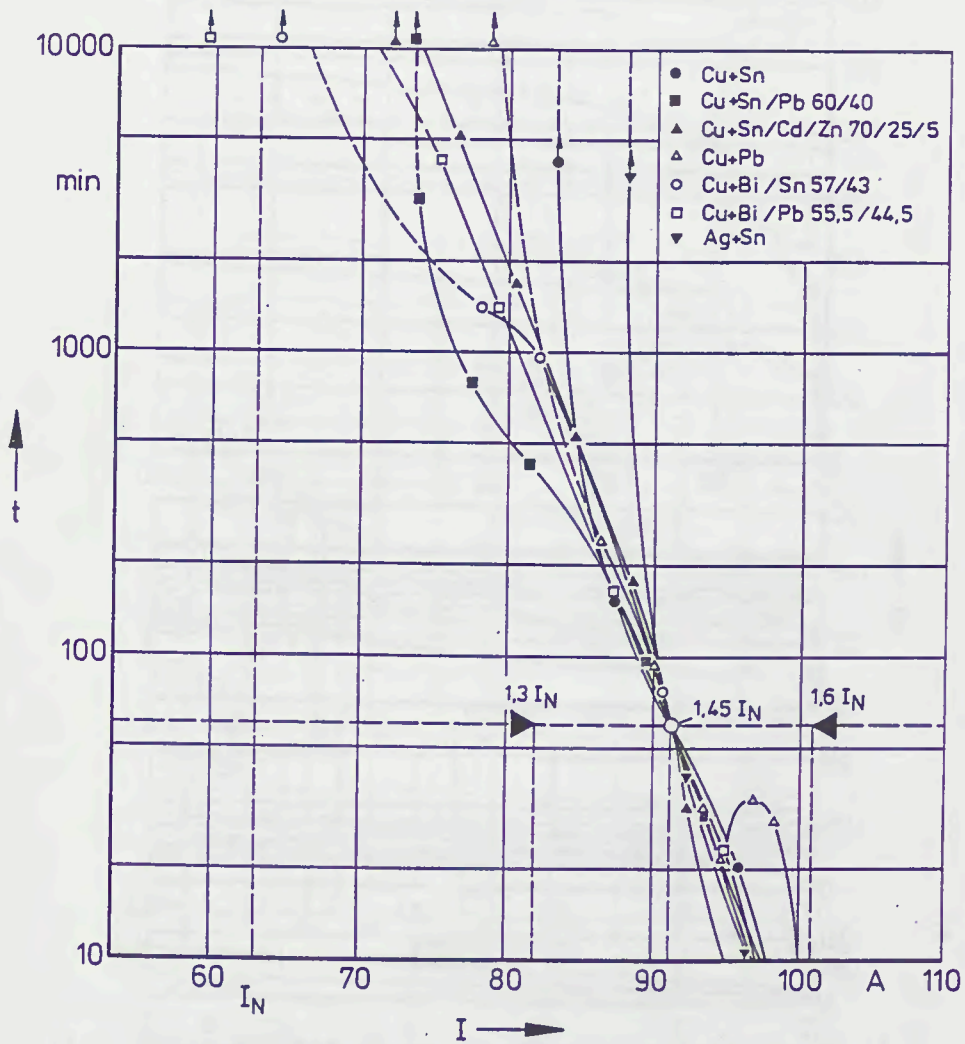


Fig.6 Time/current characteristics with adaptation to the point 60 minutes/ 91 A

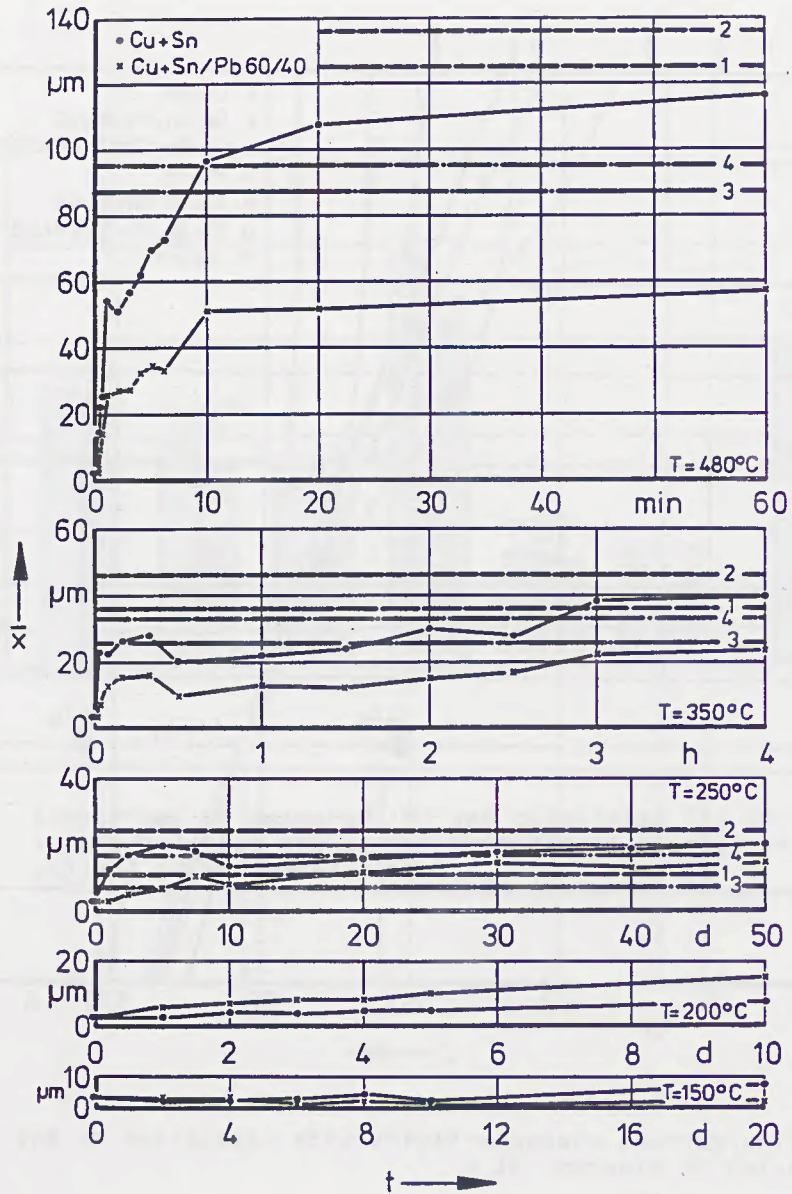


Fig.7 Dissolution depth \bar{x} in dependence of time t with temperature T as parameter for Cu fuse elements
 (Theoretical values for $t \rightarrow \infty$:
 lines 1,3 - without intermetallic layers
 lines 2,4 - with intermetallic layers)

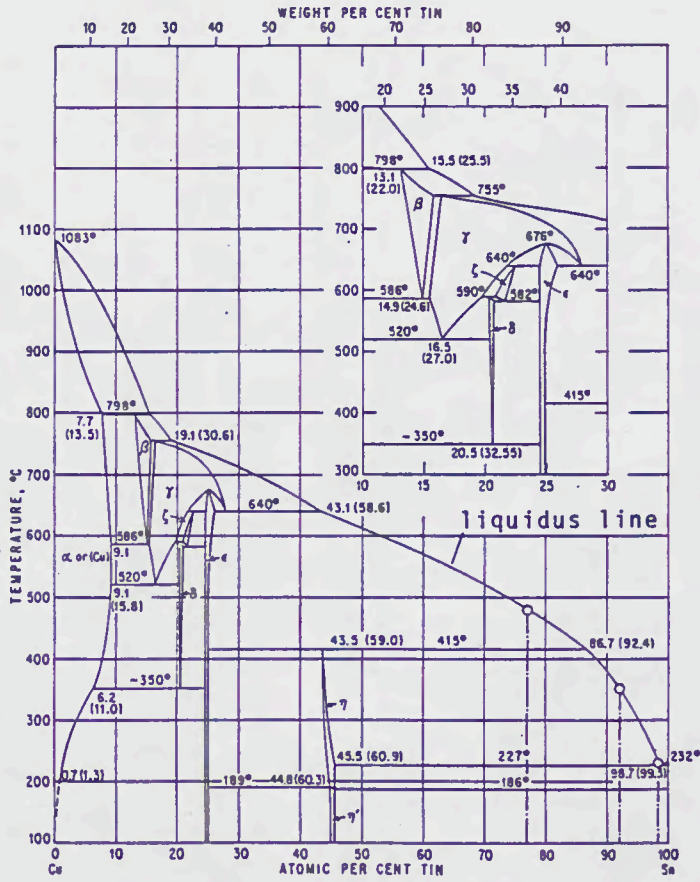


Fig.8 Phase diagram of the Cu-Sn system (from Hansen /3/)

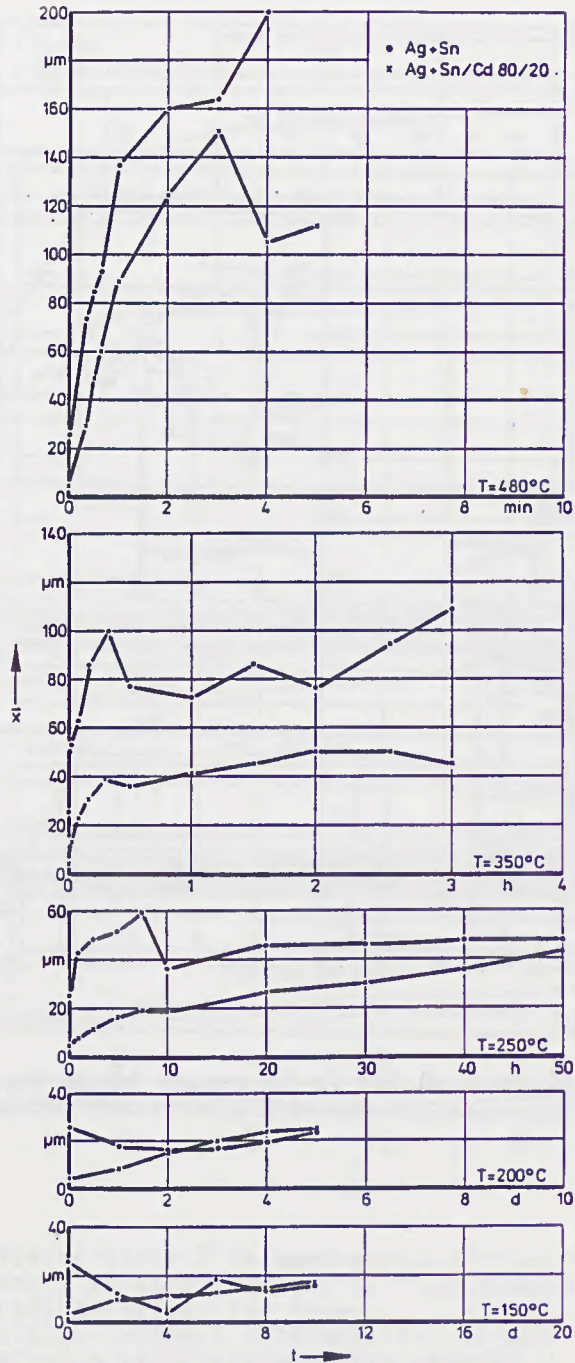


Fig.9 Dissolution depth \bar{x} in dependence of time t with temperature T as parameter for Ag fuse elements

